

Assessment of endosomes as sites of signal transduction in plants during bacterial attack

William John Lennox Heard

**Thesis submitted to the University of East Anglia
for the degree of Doctor of Philosophy**

December 2014

© This copy of the thesis has been supplied on condition that anyone who consults it is understood to recognise that its copyright rests with the author and that use of any information derived there-from must be in accordance with current UK Copyright Law. In addition, any quotation or extract must include full attribution.

Abstract

Endomembranes are integral to cellular function and particularly to plant defence. Environmental signals are perceived and immediate signalling responses are triggered from the PM, but how information is effectively transduced to generate the appropriate responses is less well understood. Furthermore the role of endosomes in implementing these responses is also not well understood. Outstanding questions are the importance of signalling by proteins from locations other than the PM and the relevance this has to overall signal transduction and how do endosomes contribute to defence. The work in this Ph. D. focussed on the understanding the role of endosome localised signalling proteins in response to detection of the bacterial PAMP flagellin and the corresponding proteome changes occurring in endosomes following detection of bacteria as part of defence responses.

To understand and test the role of endosomes in defence I characterised the proteomes of several endomembrane compartments including endosomes with an IP based method. Data obtained through this IP method is biologically relevant and simpler than other methods for preparation of endomembranes for proteomic analysis. The proteomic data was used to accurately predict the localisation of three members of the PRA1 RAB GTPase regulatory family of proteins. Furthermore this data was able to elucidate the differences in RFP-RABF2b/ARA7 and RABF1/ARA6-RFP labelled LE/MVBs and their interaction with the TGN.

Assessment of endosomal proteomes after flagellin treatment reveals a potential role for LE/MVB mediated secretion of flavonols in pathogen defence. Moreover, MPK cascade components were found in endosomal proteomes both before and after flagellin perception. Upon treatment, the flagellin responsive MPKs (MPK3, 4 and 6) were activated at endosomes and putative targets for phosphorylation by these MPKs identified. These data suggest endosomal signalling by MPKs occurs following flg22 treatment. Furthermore endosomal signalling is implicated in LE/MVB formation, cytoskeletal rearrangement and secretion of antimicrobial compounds.

Acknowledgments

I would like to thank my supervisors Drs Alex Jones and Professor Silke Robatzek for the opportunity to work in their labs and for all their help, patience and guidance during my Ph. D. You have both taught me a lot about science and have been excellent mentors.

I would also like to thank Professor Cyril Zipfel and Dr Charles Brearley for critical input and insight into my work.

My special thanks go to the TSL proteomics team of Dr Frank Menke, Dr Paul Derbyshire but especially Dr Jan Sklenar. Jan's excellent handling of the mass spectrometers, attention to detail, extensive experience, intellectual input, and regular philosophical updates made this project possible. Thank you to the Liz Hughes, Neil Stammers and Timothy Wells for all their help with media and growing plants. Thank you also to Drs Dan Maclean and Matthew Moscou for all of their help with the bioinformatics.

Drs Martina Beck, Malick Mbengue, Christine Faulkner, Vardis Ntoukakis, Joe Win, Diane Saunders, Michaela Kopischke, Gildas Bourdais and Ms Heidrun Haweker, I will eternally be in your debt for all the time and wisdom you imparted to me and for making sure I never took myself or research too seriously.

I would like to show my appreciation to the whole Robatzek lab for their critical feedback and assistance, especially Ms Sara Ben Khaled for regular feedback and heated debate. I would also like to thank the Kamoun Lab for looking after me and sharing their lab with me.

I must acknowledge all the TSL students past and present that made my Ph. D. so enjoyable and for putting up with me. Drs Torsten Schultz-Larsen, Thomas Spallek, Simon 'the Captian' Saucet, Sophie Piquerez, Angela Chaparro-Garcia, Oliver Furzer, Laura Masini, and Andrew Dawson, Daniel Couto, Jan Bettgenhauser, thank you.

The occupants of TSL room 2.00 over the years have made my day to day working a real pleasure and my special thanks go to Matthew Smoker, Jodie Pike, Artemis Giannakopoulou, Katrin Werler, Lilliana Cano, Ola Białas, Chi-Hang Wu and Cecile Lorrain.

Good luck to the TSL footballers. It has been a real pleasure to play with all of you.

Thank you to my family: Mary, Julian, Emily and Elizabeth and of course Emily Jamieson for their support, tolerating and indulging me.

Contents

Abstract.....	2
Acknowledgements.....	3
1 Introduction.....	13
1.1 The plant immune system is an excellent model with which to study signalling.....	13
1.1.1 FLS2 is a good model for defence signalling.....	16
1.2 The endomembrane system regulates signalling and defence.....	17
1.2.1 RAB GTPases, tethers and SNAREs regulate endomembrane trafficking.....	18
1.2.2 Endomembranes are altered during plant-pathogen interactions.....	21
1.2.3 Secretion via the TGN mediates pathogen perception and defence responses	
22	
1.2.4 Unconventional secretion allows defence protein secretion to the apoplast ...	25
1.2.5 The endocytic route in defence.....	25
1.2.6 Do endocytic compartments contribute to defence signalling?.....	27
1.3 Methods for protein identification.....	30
1.3.1 Shotgun proteomics for high throughput protein identification.....	30
1.4 Thesis Aims.....	33
2 Experimental procedures.....	35
2.1 Plant material.....	35
2.1.1 Plant growth on soil.....	36
2.1.2 <i>In vitro</i> seedling growth for IP.....	36
2.1.3 <i>In vitro</i> seedling growth for PAMP induced resistance (PIR).....	37
2.2 Plant pathology assays.....	37

2.2.1	Microorganisms used in this study	37
2.2.2	Bacterial cultures	37
2.2.3	Soil grown <i>A. thaliana</i> infection with <i>Pto</i> DC3000.....	37
2.2.4	PIR in <i>In vitro</i> grown <i>A. thaliana</i> infection with <i>Pto</i> DC3000 Lux.....	38
2.2.5	ROS burst assay.....	38
2.3	Molecular biology.....	38
2.3.1	DNA based techniques	38
2.3.2	Protein biochemistry	42
2.4	Cell biology	49
2.4.1	Transient protein expression by particle bombardment.....	49
2.4.2	Sub-cellular protein localisation	50
2.5	Proteome analysis	50
2.5.1	Spectrum matching with MASCOT.....	50
2.5.2	SAINT Analysis.....	51
2.5.3	Proteome definition.....	51
2.5.4	Electronic annotation of identified proteins.....	51
3	Development of a method for the affinity enrichment of proteins associating with endomembrane markers.....	53
3.1	Introduction and objectives	53
3.1.1	Proteomic characterisation of LE/MVBs is the essential first step to understanding the role of LE/MVBs in signalling	53
3.1.2	RABF2b/ARA7 is a good model for studying LE/MVBs	54
3.1.3	Approaches for the preparation of endomembrane compartment proteins for proteomic analysis	55

3.1.4	Statistical methods to identify organelle proteins.....	57
3.1.5	Novel purification techniques for organelle proteomics	57
3.1.6	Markers have significantly aided research into endomembranes	59
3.1.7	Objectives.....	60
3.2	Results.....	60
3.2.1	RFP-RABF2b/ARA7 co-fractionates with the ER and PM on a sucrose gradient 60	
3.2.2	RFP-RABF2b/ARA7 endosomes can be biochemically separated from the cytosol and ER but not the PM.....	61
3.2.3	Immuno-purification gives a significant enrichment of endosome markers with minimal endoplasmic reticulum and plasma membrane contamination	63
3.2.4	Pre-fractionated input to an IP does not reduce contamination with unwanted proteins 65	
3.2.5	Affinity purification of seven different endomembrane compartment markers. 65	
3.2.6	Proteomic analysis reveals a large degree of overlap between proteomes	69
3.2.7	YFP-GOT1 is not amenable to tryptic digests	71
3.2.8	Endomembrane regulators and suspected contaminants found in six or more enrichments	72
3.2.9	This IP approach identifies more proteins transiently associating with endomembranes than identified in other proteomic studies.....	77
3.3	Discussion	78
3.3.1	Endomembrane compartments require extensive biophysical knowledge to purify 78	
3.3.2	Limitations of this IP method.....	79

3.3.3	Affinity purification using marker proteins allows distinction of biophysically similar compartments	80
3.3.4	Affinity purification is a necessary complement to other proteomic methods ..	81
3.3.5	Conclusions and further work.....	81
4	Validation and characterisation of a LE/MVB proteome.....	83
4.1	Introduction and Objectives.....	83
4.1.1	The Golgi has been extensively proteomically characterised and is an ideal bench mark against which to compare proteomic data.....	83
4.1.2	The TGN is a suitable comparison organelle for my LE/MVB proteomic data.	84
4.1.3	The name TGN describes a population of heterogenous endomembrane compartments	84
4.1.4	The TGN is a proteomically diverse population of endomembrane compartments.	85
4.1.5	Higher throughput proteomic approaches are essential to elucidate protein content of the different TGN populations.....	87
4.1.6	The TGN compartments are directed to be secretory vesicles or LE/MVBs ...	89
4.1.7	RAB GTPases dictate compartment identity	89
4.1.8	PRA1 and YIP proteins control the regulatory RAB GTPases	91
4.1.9	LE/MVBs exist as a diverse population	93
4.1.10	Objectives.....	94
4.2	Results.....	94
4.2.1	The proteomic data is not suitable for direct quantitative comparisons between proteomes.....	94

4.2.2	The proteomic data recapitulates known differences between the Golgi and the tonoplast and the similarity between two LE/MVB markers	95
4.2.3	The YFP-GOT1 proteome compares favourably with other published Golgi proteomes.....	96
4.2.4	RFP-RABF2b/ARA7 is more TGN like than expected	97
4.2.5	YFP-RABD2a and RFP-RABF2b/ARA7 define subpopulations of the TGN ...	99
4.2.6	RABF1/ARA6-RFP functional specificity is conferred by 9 unique proteins	99
4.2.7	Canonical RAB GTPase regulators (GDFs) appear in the conventional RAB GTPase proteomes, but not in the atypical RAB RABF1/ARA6-RFP proteome.....	100
4.2.8	Defining a combined LE/MVB proteome	105
4.3	Discussion	106
4.3.1	The proteomic method discriminates between compartments and expands our knowledge of the Golgi.....	107
4.3.2	Localisation of PRA1s.....	107
4.3.3	RFP-RABF2B/ARA7 labels a population of the TGN.....	108
4.3.4	RABF1/ARA6 identity is conferred by a few proteins.....	109
4.3.5	RABF1/ARA6 requires non-canonical GDF machinery to associate with membranes.....	110
4.3.6	A preliminary LE/MVB proteome	111
4.3.7	Conclusions and further work.....	111
5	Characterising flg22-induced proteome changes in Endosomes	113
5.1	Introduction and Objectives.....	113
5.1.1	Endosomes are functionally altered during biotic interactions	113

5.1.2	Quantitative proteomic analysis is essential to understand responses to flg22 treatment.....	116
5.1.3	Detection and quantitation of proteins require different experimental conditions	117
5.1.4	Spectrum counting provides a rough measure of protein abundance.....	118
5.1.5	Mass tagging improves quantitation.....	120
5.1.6	Alternatives to mass spectrometry for protein quantitation	121
5.1.7	Objectives.....	122
5.2	Results.....	122
5.2.1	Spectrum counting is not sufficiently quantitative to decipher flg22 induced proteome changes in RFP-RABF2b/ARA7 labelled endosomes	122
5.2.2	iTRAQ labelling and Q-TOF MS improves confidence in quantitative proteome changes	126
5.2.3	Combined iTRAQ and spectrum counting quantitative data implicates RHM1 in abundance changes in LE/MVBs after flg22 treatment.....	127
5.2.4	Candidate led quantification is necessary to further characterise changes in LE/MVBs following flg22 treatment.....	129
5.2.5	Active MPKs are detected in RFP-RABF2b/ARA7 enrichments after flg22 treatment.....	130
5.2.6	Active MPKs are detected in RABF1/ARA6-RFP enrichments after flg22 treatment.....	131
5.3	Discussion	132
5.3.1	Spectrum counting is unsuitable for thorough quantitative analysis of RFP-RABF2b/ARA7 affinity purifications	132
5.3.2	RHM1 is a positive regulator of immunity	133

5.3.3	Recycling FLS2 is enriched with RFP-RABF2b/ARA7 not RABF1/ARA6-RFP	
		136
5.3.4	Active MPKs are localised to endosomes following flg22 treatment but their role in signalling is still unclear	136
5.3.5	Conclusions and further work.....	137
6	Identifying potential targets for endosome localised MPKs after flg22 treatment	138
6.1	Introduction and Objectives.....	138
6.1.1	Candidate MPK3, 4 and 6 targets have been identified in <i>A. thaliana</i>	138
6.1.2	Extensive phospho-proteomic data has been obtained following flg22 elicitation	139
6.1.3	Objectives.....	140
6.2	Results.....	140
6.2.1	Identification of putative endosome localised MPK targets.....	140
6.2.2	Screening of tDNA insertion lines for defects in PAMP induced resistance ..	142
6.2.3	<i>gtp-1</i> and <i>gtp-2</i> mutants are more resistant to <i>Pto</i> DC3000	145
6.2.4	<i>vln</i> mutants are more susceptible to <i>Pto</i> DC3000	146
6.2.5	VLN3 and GTP have experimentally annotated phosphosites.....	148
6.2.6	VLN3-GFP is not more phosphorylated on serine residues after flg22 treatment	149
6.3	Discussion	150
6.3.1	Several putative targets of endosomal MPK are present in RFP-RABF2b/ARA7	150
6.3.2	GTP regulates plant defence	151
6.3.3	VLN3 may regulate the cytoskeleton in response to flg22.....	152

6.3.4	Conclusions and outlook.....	156
7	Discussion and Outlook	158
7.1	Objectives and achievements	158
7.2	Discussion	159
7.2.1	Immuno-precipitation advances endomembrane proteomics	159
7.2.2	Proteomic dissection is essential to understand the TGN	160
7.2.3	LE/MVBs provide a vehicle through which defence compounds could be secreted	161
7.2.4	VLN3 could provide the mechanism by which the cytoskeleton is remodelled following pathogen attack.....	162
7.2.5	Endosomes function as sites of active signal transduction.....	163
7.2.6	The plasma membrane is the predominant site of FLS2 signal activation	164
7.2.7	Endosomal contribution to signalling.....	165
7.2.8	Outlook	166
7.3	Endosomes as sites of signal transduction during bacterial attack	166
7.3.1	Endosomes could provide spatial information and specificity to flg22 triggered signalling.....	169
7.3.2	Mechanistically signalling from endosomes is more efficient than signalling in the cytosol.....	169
7.3.3	Endosomes can provide the long range transport for MPKs necessary for flg22 induced signalling	170
7.3.4	Signalling from the PM, cytosol and endosomes occurs during bacterial attack	171
8	References	173

Major abbreviations

Bgh: *Blumeria graminis* f. sp. *hordei*

CFP: Cyan fluorescent protein

cfu: colony forming unit

CLSM: Confocal laser scanning microscopy

DNA: Deoxyribonucleic acid

dH₂O: Distilled water

EE: Early endosome

ER: Endoplasmic reticulum

Flg22: 22 amino acid peptide ligand for FLS2

FLS2: Flagellin sensing 2

GFP: Green fluorescent protein

IP: Immunoprecipitation

LC: Liquid chromatography

LE/MVB: Late endosome/Multi-vesicular body

LRR: Leucine rich repeat

MPK: Mitogen activated protein kinase

MS: Mass spectrometry

OD: Optical density

PAMP: Pathogen-associated molecular pattern

PM: Plasma membrane

PRR: Pattern recognition receptor

PTI: PAMP-triggered immunity

Pto: *Pseudomonas syringae* pv *tomato*

RABF1/ARA6: RAB GTPase F1/Arabidopsis RAB GTPase 6

RABF2b/ARA7: RAB GTPase F2b/Arabidopsis RAB GTPase 7

RFP: Red fluorescent proteins and derivatives

RLK: Receptor like kinase

RNA: Ribonucleic acid

SDS-PAGE: Sodium dodecyl sulphate-polyacrylamide gel electrophoresis

SNARE: Soluble N-ethylmaleimide sensitive fusion protein attachment protein receptor

TGN: *trans*-Golgi Network

WT: Wild type

YFP: Yellow fluorescent protein

1 Introduction

Plant cells live in a constantly changing environment. Information about the developmental, biotic and abiotic conditions must be constantly perceived and effectively signalled to produce the appropriate response. If we want to effectively engineer plants to suit the needs of our society, we need to understand how information is perceived by plant cells and how signals are transduced to give an appropriate response.

1.1 The plant immune system is an excellent model with which to study signalling

Plants are constantly interacting with microbes including viruses, bacteria, fungi and oomycetes, as well as nematodes and insects (Agrios 1989). These interactions can be beneficial to the plant, for example by fungi promoting nutrient uptake, or detrimental to plant growth as the microbe parasitizes the plant. The interactions between plant and microbial pathogens can cause a variety of diseases. When a susceptible plant is successfully invaded by a virulent pathogen, this is known as a compatible interaction, and conversely when a plant is resistant through activation of defence mechanisms this is known as an incompatible interaction (avirulent pathogen), reviewed (Jones and Dangl 2006). Furthermore, when all known accessions of a species are resistant to all known accessions of a pathogen species, this is known as non-host resistance from the plant (Mysore and Ryu 2004). Conversely when there are both compatible and incompatible interactions between a plant and a pathogen species, this is known as host resistance (Mysore and Ryu 2004).

One of the major determinants of the outcome of a plant pathogen interaction is the plant immune system. Plants do not have mobile immune cells, as in mammals, but rather most cells are independently able to detect pathogens and elicit an appropriate response. Furthermore all immune receptors are encoded into the plant genome, like mammalian innate immunity (Jones and Dangl 2006). The major steps in plant immune signalling have

been fairly well characterised. Plants have a two layered immune system, of which the first layer is the pattern recognition receptors (PRRs) that detect conserved pathogen associated molecular patterns (PAMPs) (Dodds and Rathjen 2010). PAMPs are conserved molecules produced by potential microbial pathogens and detection of PAMPs by PRRs activates PAMP triggered immunity (PTI) (Jones and Dangl 2006). Pathogens may try and subvert resistance or manipulate other host processes to maximise their growth through the production of intra or extracellular effector proteins. The second layer of immunity utilises intracellular resistance proteins (R proteins) that detect the action of effectors on host processes, reviewed (Dodds and Rathjen 2010). Upon recognition of PAMPs or effectors defence signalling is activated and the plant cell must respond accordingly.

PRRs fall into two general categories; those with a kinase domain or without. All characterised receptors have an extracellular domain, such as a leucine rich repeat (LRR) domain for Brassinosteroid (BR) insensitive 1 (BRI1) or lysine motif (lysM) domains for Chitin elicitor receptor kinase 1 (CERK1) that are involved in ligand perception (Hothorn *et al.* 2011, She *et al.* 2011, Liu *et al.* 2012), two juxtamembrane regions that can have a regulatory role and a single transmembrane domain (TM) (Gómez-Gómez *et al.* 2001, Shiu and Bleecker 2001). Extracellular receptors with an intracellular kinase domain are called Receptor Like Kinases (RLKs) or if they lack the kinase domain are known as Receptor Like Proteins (RLPs) (Shiu and Bleecker 2001). *A. thaliana* potentially has over 610 RLKs which are transmembrane proteins, representing almost 2.5% of protein coding sequences (Shiu and Bleecker 2001). Yet very few (<20) have characterised ligands, or indeed roles within the cell (Monaghan and Zipfel 2012, Butenko *et al.* 2014).

RLKs and RLPs are involved in development, such as Clavata 1 (CLV1), CLV2, Coryne (CRN) (Clark *et al.* 1995, Kayes and Clark 1998, Bleckmann *et al.* 2010), BRI1 (Clouse *et al.* 1996) and Feronia (FER) (Escobar-Restrepo *et al.* 2007, Duan *et al.* 2010), as well as defence (reviewed (Monaghan and Zipfel 2012). Linear pathways are of course, an

oversimplification as there are many examples of cross talk between defence and development; signalling from BRI1 interferes with defence (Albrecht *et al.* 2011, Belkhadir *et al.* 2011, Lozano-Duran *et al.* 2013) and CLV2 signalling is induced by nematodes during parasitism of plants to suppress defence responses by promoting stem cell identity (Chen *et al.* 2014).

RLKs in defence are excellent models with which to study defence signalling. The cognate ligands of several receptors involved in development have been identified such as the CLV3 peptide for CLV1 and CLV2/CRN (Clark *et al.* 1995, Kayes and Clark 1998, Bleckmann *et al.* 2010) and brassinosteroid for BRI1 (Clouse *et al.* 1996). However, the receptors involved in developmental signalling are activated by endogenous signals such as peptides or hormones. This can make control of their signalling for experimental purposes difficult and inhibitor treatments are often necessary to ensure the required synchronicity of signalling required for analysis (Asami *et al.* 2000). As defence signalling is elicited by molecules not produced by the plant, this provides an excellent system with which to study signalling. Responses can be triggered specifically by application of highly purified PAMP. Furthermore the cognate PRRs for several individual PAMPs have been well characterised. The generalised structure of FLS2, BRI1 and EFR with their ligand and co-receptor BAK1 is outlined in Figure 1.1 in comparison with the homodimer of EGFR.

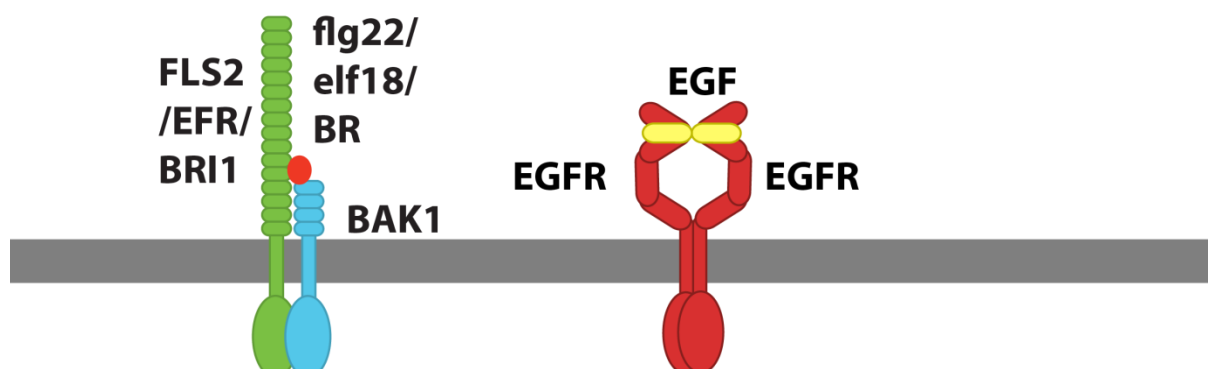


Figure 1.1 Comparison of FLS2/BRI1/EFR and EGFR, adapted from Macho and Zipfel *et al.* 2014

1.1.1 FLS2 is a good model for defence signalling

PRRs are excellent models with which to study signalling. However, *A. thaliana* has a multitude of PRRs that detect PAMPs from bacteria such as Flagellin sensing 2 (FLS2) and Elongation factor Tu receptor (EFR), from fungi - CERK1 whilst other PRRs detect endogenous peptides released by plants upon damage (DAMPs) – Elicitor peptide 1 receptor 1 (PEPR1), PEPR2 or wounding and herbivory associated molecular patterns (WAMPs and HAMPs) reviewed in Monaghan and Zipfel (2012). FLS2 and EFR are LRR-RLKs and as such, show homology to insect Toll receptors or mammalian Toll like receptors (TLRs) (Mogensen 2009) that are also involved in immunity.

PRRs do not function alone in signalling. Many PRRs require a co-receptor or co-regulator to function properly and recruit additional cytoplasmic proteins. For FLS2, EFR, PEPR1 and PEPR2 (amongst others) the five members of the LRR-RLK family of SERKs fulfil this role (Chinchilla *et al.* 2007, Heese *et al.* 2007, Roux *et al.* 2011). The different SERKs exhibit slightly different preferences for the different PRRs but BRI1 associated kinase 1/Somatic embryogenesis receptor kinase 3 (BAK1/SERK3) is the preferred co-receptor for FLS2 (Roux *et al.* 2011). Interestingly BAK1 is also a co-receptor for the developmental RLK BRI1 (Li *et al.* 2002, Nam and Li 2002, Li 2003).

The signalling pathway of FLS2 has been relatively well characterised, making it an excellent model with which to study signal transduction. FLS2 is a membrane localised LRR-RLK that detects the bacterial PAMP flagellin to trigger defence signalling (Gómez-Gómez and Boller 2000, Gómez-Gómez *et al.* 2001). A specific epitope of 22 amino acids (flg22) derived from the flagellin produced by *Pseudomonas aeruginosa* is commonly used experimentally to activate FLS2 (Felix *et al.* 1999, Gómez-Gómez and Boller 2000, Gómez-Gómez *et al.* 2001), trigger defence signalling and ultimately PTI (Zipfel *et al.* 2004). The signalling cascade triggered after FLS2 and BAK1 activation by flg22 initially activates receptor like cytoplasmic kinases (RLCK), which lack a TM, such as *Botrytis* induced kinase (BIK1) (Lu *et*

al. 2010). BIK1 then phosphorylates and activates the enzyme respiratory burst oxidase-D (RBOHD) to generate an extracellular Reactive oxygen species (ROS) burst (Lu *et al.* 2010, Zhang *et al.* 2010, Kadota *et al.* 2014). There is an influx of Ca^{2+} which activates Calcium dependent protein kinases (CDPKs), and two Mitogen activated protein kinase (MPK) cascades are activated. Mitogen-activated protein kinase/extracellular signal-regulated protein kinase (MEK) kinase 1 (MEKK1) activates a cascade of Mitogen-activated protein kinase kinase1/2 (MKK1/2) and MPK4 whilst an unknown MEKK activates a cascade of MKK4/5 and MPK3/6 (Asai *et al.* 2002, Ichimura *et al.* 2006, Nakagami *et al.* 2006, Su *et al.* 2007, Suarez-Rodriguez *et al.* 2007, Gao *et al.* 2008). MPK3, 4 and 6 are activated by phosphorylation upon their activation loop on a conserved TEY motif (Müller *et al.* 2010). MPKs then phosphorylate protein targets to activate mechanisms of defence. Ultimately defence signalling triggers broad spectrum resistance, also known as PTI, through stomatal closure, deposition of callose and secretion of antimicrobial defence compounds to name a few typical responses.

Interestingly, the contribution of FLS2 to immunity was initially believed to be negligible, as plants producing non-functional FLS2 are not more susceptible to infection by the virulent pathogen *Pseudomonas syringae pv tomato (Pto)* DC3000 upon vacuum infiltration (Zipfel *et al.* 2004). However one of the main contributions of FLS2 signalling to immunity is stomatal closure, which prevents bacteria from accessing the apoplast, reviewed (Segonzac and Zipfel 2011). Vacuum infiltration of pathogen bypasses this defence mechanism so the effect of FLS2 signalling is bypassed. When spray inoculation is used, *fls2* mutants are more susceptible to *Pto* DC3000 demonstrating the need for appropriate assays to determine the importance of a proteins, process or signalling pathway (Zipfel *et al.* 2004).

1.2 The endomembrane system regulates signalling and defence

The endomembrane system refers to the collection of interacting membrane compartments within plant cells and provides the primary mechanism by which a cell interacts with the

environment. Endomembranes regulate signalling and mediate defence responses in a variety of ways, the role of endocytosis, secretion and several endomembrane compartments in immunity as well as general cellular function will now be discussed.

1.2.1 RAB GTPases, tethers and SNAREs regulate endomembrane trafficking

To understand the role of endomembranes in immunity we must also understand how endomembranes are controlled. The identity and trafficking of endomembrane compartments is mediated by a variety of proteins. The primary means of compartment recognition is a protein complex consisting of a RAB GTPase, a Soluble N-ethylmaleimide sensitive factor (NSF) attachment protein (SNAP) receptor (SNARE) complex and a tethering factor, reviewed by Uemura and Ueda (2014). These proteins dictate the interactions a compartment can make. RAB GTPases regulate compartment identity by recruiting intra-membrane tethers to link separate endomembrane compartments over a long range, reviewed (Uemura and Ueda 2014). RAB GTPases also recruit SNARE proteins, which promote the direct fusion of membranes once tethering factors have brought them into close contact, reviewed (Uemura and Ueda 2014).

One significant limiting factor in our understanding of endomembranes in immunity is that we do not fully understand the roles of many of the endomembrane regulators. The biochemical function of SNAREs, tethers and RAB GTPases is fairly well characterised, however, the specific time and location in which they act is unclear for many *A. thaliana* regulators. Therefore, a particular regulatory protein may be detected in a defence mutant screen, but it is difficult to relate this phenotype to the process that the protein regulates.

Inferences about function can be made based on homology with better characterised animal or yeast systems but there are significant differences between the regulators in *A. thaliana*, and mammals or yeast due to their evolutionary history. 33 of the 41 mammalian RAB GTPases have no clear ortholog in *A. thaliana* (Rutherford and Moore 2002). All *A.*

thaliana RAB GTPases are orthologs of just eight of the mammalian RAB GTPases, and have been assigned into eight families A-H and each family member assigned a letter and number based on homology e.g. RABG3f (Rutherford and Moore 2002). The major trafficking steps regulated by each RAB GTPase family (A-H) in *A. thaliana* have been characterised but exactly which family member regulates which specific trafficking step under which conditions is unclear (there are eight members of the RABG family in *A. thaliana*) (Rutherford and Moore 2002). Therefore, the main hindrance to work is a lack of knowledge about *A. thaliana* endomembrane regulators and the compartments on which they reside.

The same is true for tethering complexes. All the major endomembrane tethering complex families characterised in yeast and animals are present in *A. thaliana* (Koumandou *et al.* 2007) but their functions have not been extensively studied. Endomembrane tethering factors are divided into two classes. The first class is the single protein tethers such as the Golgins (Latijnhouwers *et al.* 2005, Latijnhouwers *et al.* 2007). The second class is the protein complex tethering factors. There are eight different tethering complexes in *A. thaliana* and they are the Transport Protein Particle 1 (TRAPPI), TRAPP II, Golgi-associated retrograde protein (GARP), Homotypic fusion and vacuole protein sorting (HOPS), Class C core vacuole/endosome tethering (CORVET), Conserved oligomeric Golgi (COG), EXOCYST and Dependence on SLY1-20 (DSL) (Koumandou *et al.* 2007, Peplowska *et al.* 2007, Lachmann *et al.* 2011). There are 24 different orthologs of the mammalian EXO70 subunit (Zhang *et al.* 2010). These differences reduce confidence in the inferences made about the function of endomembrane regulators based on homology and imply that exocytic trafficking, mediated by the EXOCYST requires more complex regulation than in animals or yeast.

In addition to problems caused by lack of homology at the protein level there are also differences in the functioning of the endomembrane system that make inferences difficult. The TGN in mammals functions as an independent organelle from the EE, the TGN regulates secretory traffic to the PM and EE, whereas in plants an independent EE has not

been observed (summarised in Figure 1.2). For example, the TRAPP II complex is needed for secretion to the PM and the forming cell plate (Thellmann *et al.* 2010, Qi *et al.* 2011). However, the lack of an Early endosome (EE) (Viotti *et al.* 2010, Scheuring *et al.* 2011) in plants makes the role of the TRAPP II complex, which tethers the TGN to EE in mammals (Cai *et al.* 2005), impossible to infer from homology alone. The TRAPP II complex component, TRAPP subunit 120 (TRS120), was identified in a TGN proteome with Syntaxin of plants 61 (SYP61) proteome suggesting TRAPP II still mediates trafficking to or from the TGN in *A. thaliana* (Drakakaki *et al.* 2012). Interestingly, in *trs120* and *trs130* mutants (two TRAPP II specific components) the transport of the FM4-64 lipophilic dye is inhibited, as is the recycling of Pin-formed 2 (PIN2) from the Plasma membrane (PM) (Thellmann *et al.* 2010, Qi *et al.* 2011, Qi and Zheng 2011). It therefore appears that TRAPP II regulates secretion from the TGN and endocytosis. The role of a tethering complex in two pathways, in this case secretion and endocytosis has not been described and so is unlikely (Whyte and Munro 2002, Koumandou *et al.* 2007, Bonifacino and Hierro 2011, Lachmann *et al.* 2011, Miller and Ungar 2012). Instead the TRAPP II complex is probably involved in one of these

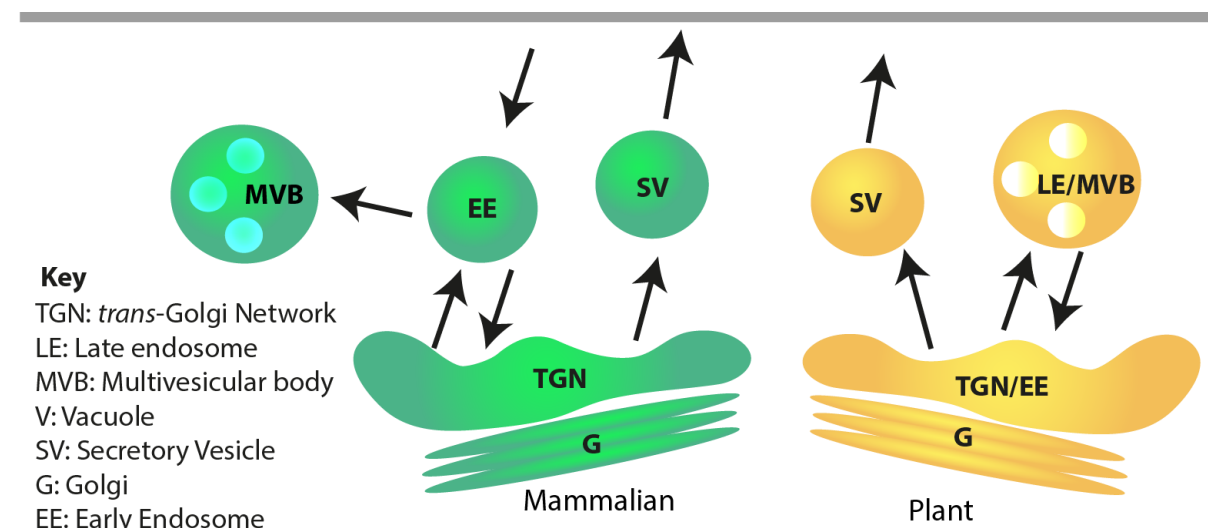


Figure 1.2. Comparison of the mammalian and plant TGN and EE. Adapted from Scheuring *et al.* 2012.

pathways but interference with the TRAPP II complex alters the organelle so that the TGN cannot properly function in either endocytosis or secretion. Supporting the role of the TGN in

secretion is the implication of the TRAPP II complex in activation of the secretion associated RABA family in *A. thaliana* (Qi and Zheng 2011).

1.2.2 Endomembranes are altered during plant-pathogen interactions

Highlighting the importance of endomembranes in defence, pathogens target regulators of the endomembrane system with intracellular effectors. Most of the major classes of endomembrane regulators, including tethers and SNAREs, are suggested targets of pathogen effectors (Mukhtar *et al.* 2011). Endomembranes must be important in defence for pathogens to evolve inhibitory effector proteins. For example the endomembrane regulatory ADP ribosylation factor (ARF)-Guanine exchange factor (GEF) MIN7 is targeted and degraded by the bacterial effector Hrp outer protein M1 (HopM1) to alter secretory traffic (Nomura *et al.* 2006, Nomura *et al.* 2011). Furthermore various drugs now used as inhibitors for endomembrane trafficking were isolated from pathogens. Brefeldin A (BFA) inhibits GNOM function and was isolated from *Eupenicillium brefeldianum* (Misumi *et al.* 1986) whilst wortmannin, which inhibits Phosphoinositide 3-kinase (PI3K) activity was isolated from *Penicillium funiculosum* (Arcaro and Wymann 1993). Yet our knowledge of how these drugs or effectors alter endomembranes is not clear. For example, the exact role of HopM interactor 7 (MIN7) is not clear (Nomura *et al.* 2011) and the function of GNOM was recently re-assessed (Naramoto *et al.* 2014). The importance of secretion in defence responses is also highlighted by the up-regulation of secretory pathway genes following application of the defence hormone Salicylic Acid (SA) (Cheng *et al.* 2008).

The cytoskeleton is another example of regulation of endomembrane trafficking that is altered following pathogen challenge. The actin cytoskeleton is formed of filaments comprised of the multiple monomers of the 10 different actins in the *A. thaliana* genome, reviewed (Ketelaar 2013). Actin is the major filament on which the organelles are anchored and move (Cai *et al.* 2014), thus regulating their movement. Myosin XI, a motor protein that

moves along actin filaments drives the movement of the Endoplasmic reticulum (ER), Golgi, endomembrane vesicles, peroxisomes and mitochondria (Cai *et al.* 2014). These filaments are formed into actin arrays, which are highly dynamic and are altered following biotic and abiotic stress, as extensively reviewed (Staiger *et al.* 2009, Higaki *et al.* 2011, Smertenko and Franklin-Tong 2011). When cells are mechanically stressed by pressure from glass or tungsten needles very highly bundled filament arrays are formed at the site of the stimulus (Hardham *et al.* 2008). Upon removal of the needle, the filament array is disassembled, highlighting the dynamic nature of these formations (Hardham *et al.* 2008). Interestingly, these filament dynamics are reminiscent of the changes that occur during filamentous pathogen infection where the actin cytoskeleton depolymerises and re-bundles underneath the sites of attempted or actual cell penetration (Staiger *et al.* 2009, Higaki *et al.* 2011, Smertenko and Franklin-Tong 2011). Furthermore movement of compartments on the actin cytoskeleton is required for resistance to the fungal pathogen *Blumeria graminis* f. sp. *hordei* (*Bgh*) (Yang *et al.* 2014). There is dynamic actin filament remodelling following challenge with non-filamentous pathogens as well. *Pto* DC3000 infection or application of flg22 to *A. thaliana* induces rapid actin depolymerisation and subsequent remodelling, presumably towards the sites of pathogen detection (Henty-Ridilla *et al.* 2013). The re-orientation of the cytoskeleton probably allows the focal accumulation of organelles around sites of pathogen detection (Yang *et al.* 2014).

Therefore, these regulatory proteins are clearly essential regulators of defence, however to determine how defence is implemented and manipulated by pathogens, we need to know more about endomembranes in general.

1.2.3 Secretion via the TGN mediates pathogen perception and defence responses

Secretion has several specific roles in defence. LRR-RLKs such as FLS2 and BRI1 have signal peptides on their N terminus that cause the mRNA to be directed to the ER for synthesis (Li and Chory 1997, Gómez-Gómez and Boller 2000). FLS2 is synthesised in the

ER and trafficked through the Golgi to the PM (Saijo *et al.* 2009, Haweker *et al.* 2010). En route it is glycosylated and its folding monitored by quality control machinery (Saijo *et al.* 2009, Haweker *et al.* 2010). Strikingly different PRRs have different quality control requirements; protein accumulation of EFR is more affected in ER-Quality control (QC) mutants than FLS2 (Nekrasov *et al.* 2009, Saijo *et al.* 2009, Haweker *et al.* 2010). This is also true for the RLK BRI1, where ER-QC carefully monitors folding of BRI1 (Hong *et al.* 2008, Belkhadir *et al.* 2010). Improperly folded or otherwise defective RLKs are re-directed away from the PM for degradation by ER associated degradation (ERAD) (Su *et al.* 2011). Furthermore the early secretory route, especially the ER, may be the location in which receptor-co-receptor pairs are formed. There are specific pools of BAK1 that are associated with either FLS2 or BRI1, although how these pools of BAK1 are defined is unclear (Albrecht *et al.* 2012). It is likely that the definition of the ultimate role for BAK1, in either FLS2 or BRI1 signalling, occurs during synthesis. Recent evidence has also demonstrated that BRI1-BAK1 partially exists in pre-formed complexes at the PM (Bücherl *et al.* 2013) and for Epidermal growth factor (EGF) receptor (EGFR) in animal systems (Bader *et al.* 2009) and these associations of receptor and co-receptor may form as early as the ER. Interestingly FLS2-BAK1 does not appear to form as closely associated complexes as BRI1-BAK1 before ligand application (Schulze *et al.* 2010, Bücherl *et al.* 2013).

Post-Golgi vesicle traffic plays a major role in plant defence, in addition to the role in secretion of PRRs. The TGN has a myriad of functions including secretion to the PM and cell plate during cell division as well as sorting endocytosed proteins for recycling to the PM or direction to a late endosomal route to the vacuole (Richter *et al.* 2009, Viotti *et al.* 2010). The sorting function of the TGN is similar to the animal EE, leading to the term TGN/EE being commonly used in plant literature (Viotti *et al.* 2010). For simplicity I will only use the term TGN to describe this organelle. After synthesis and glycosylation in the ER and Golgi RLKs are secreted to the PM via the TGN (Rusinova *et al.* 2004, Nekrasov *et al.* 2009, Saijo *et al.* 2009, Haeweker *et al.* 2010, Saijo 2010, Beck *et al.* 2012).

Secretion to the apoplast or cell wall also plays a role in defence. Resistance in *A. thaliana* against *Bgh* is mediated by the SNARE complex of Penetration 1 (PEN1), Soluble SNAP33, Vesicle associated membrane protein 721/722 (VAMP721/722) (Collins *et al.* 2003, Kwon *et al.* 2008). This SNARE complex accumulates at sites of attempted fungal penetration to mediate the exocytosis of cell wall reinforcing compounds. Furthermore, the fungal toxin BFA interferes with the endomembrane regulator GNOM (Geldner *et al.* 2003) and causes altered Golgi and post-Golgi traffic ultimately preventing proper callose deposition (Nielsen *et al.* 2012).

Several tethering complex components are involved in defence related secretion. Recently EXOCYST components EXO70B2 and EXO70H1 were shown to be transcriptionally up regulated following elf18 treatment (Pečenková *et al.* 2011). Furthermore plants deficient in either EXO70B2 or EXO70H1 protein were more susceptible to bacterial and fungal infection (Pečenková *et al.* 2011), probably because of the role of their role in exocytic secretion. To further support this hypothesis, EXO70B2 is targeted for ubiquitination and degradation by the E3 ubiquitin ligase, and negative regulator of PTI, Plant U-box protein (PUB22) (Stegmann *et al.* 2012). Moreover, another EXO70 homolog is involved in Barley penetration resistance to *Bgh* (Ostertag *et al.* 2013). This screen also identified an intra-Golgi tethering complex subunit COG3 in penetration resistance, as well as a homolog of mammalian RAB GTPase 1 (Ostertag *et al.* 2013). These proteins are involved in secretion, but it is unclear from exactly which compartment, reinforcing the importance of secretion in defence and emphasising that more information is needed to fully understand the roles of these proteins.

PEN2 is a peroxisome localised glycosyl hydrolase and its hydrolytic products are required for callose deposition (Bednarek *et al.* 2009, Clay *et al.* 2009). The PEN3 ATP binding cassette (ABC) transporter (Stein *et al.* 2006), localises around papillae and presumably translocates PEN2 produced glucosinolates into the apoplast, as genetics show PEN3 is in a

PEN2 dependent defence pathway (Lipka *et al.* 2005). Peroxisomes traffic to sites of attempted pathogen penetration but PEN3 is also endocytosed into a TGN compartment following PAMP perception (Underwood and Somerville 2013). This endocytosis may be to promote re-localisation of PEN3 to where it is needed and demonstrates that production or activation of a defence protein is not sufficient to mediate resistance, correct localisation is essential.

1.2.4 Unconventional secretion allows defence protein secretion to the apoplast

Other defence related proteins are secreted into the apoplast, such as the Pathogenesis related (PR) proteins, in a Golgi independent manner (Matsushima *et al.* 2002, Watanabe *et al.* 2013). These proteins, which have signal peptides but no transmembrane domains, are produced in the ER and accumulate in ER bodies, ER bodies are spindle like structures formed from the ER that accumulate upon pathogen challenge, wounding or Jasmonic acid (JA) treatment (Matsushima *et al.* 2002). Upon infection of *A. thaliana*, with the fungal pathogen *Colletotrichum gloeosporioides*, ER bodies accumulate and PR proteins are secreted into the apoplast (Watanabe *et al.* 2013). ER bodies have not been observed to directly fuse with the PM, thus it has been postulated that secretion from ER bodies could be through vesicle trafficking directly to the PM. Evidence is, however, lacking for either secretory route (Watanabe *et al.* 2013). Another route of defence related secretion is through direct fusion of the vacuole to the PM, allowing the bulk deposition of vacuolar enzymes into the apoplast to lyse bacteria (Hatsugai *et al.* 2009, Hatsugai and Hara-Nishimura 2010). This form of secretion was observed in a plant-pathogen interaction between *A. thaliana* and *P. syringae* and initiates programmed cell death (Hatsugai *et al.* 2009, Hatsugai and Hara-Nishimura 2010).

1.2.5 The endocytic route in defence

Compartments on the endocytic route also play a role in defence. The endomembrane system mediates traffic from the PM to the vacuole and this is known as the endocytic route. Proteins are endocytosed to the TGN then trafficked to Late endosome/Multivesicular bodies

(LE/MVBs) en route to the vacuole (Viotti *et al.* 2010, Scheuring *et al.* 2011). Endocytic compartments are involved in defence, as demonstrated with the TGN (Section 1.2.2).

LE/MVBs are altered in their function during infection. These compartments were observed to cluster around sites of pathogen penetration (Lu *et al.* 2012, Bozkurt *et al.* 2014). LE/MVBs are also involved in the secretion of defence compounds, although the exact mechanism is unclear. Phenolics and H₂O₂ are produced in LE/MVBs and secreted, presumably through exosomes, to sites of attempted pathogen penetration (An *et al.* 2006, An *et al.* 2006). An open question is exactly how LE/MVBs can be modified from their role as an endocytic compartment to provide this new role in pathogen defence. Answering this question will help us understand how a plant mediates resistance to pathogens.

LE/MVBs may also have a role in maintaining the cell's outer membrane. During infection, filamentous pathogens can produce membrane bound feeding structures or haustoria inside the host cell. The plant must then expand the size of its outer membrane to prevent cell lysis. The extra haustorial membrane, the plant derived membrane surrounding a haustoria, is different from the PM in terms of protein content (Lu *et al.* 2012), suggesting it is not formed only as an extension of the PM. It may be that the redirection of LE/MVBs towards haustoria is part of the mechanism by which the cell membrane is expanded to accommodate the pathogen and prevent cell lysis (Bozkurt *et al.* 2014).

The endocytic route also regulates defence signalling. RLK abundance at the PM is regulated by endocytosis. FLS2 is constitutively recycled between the TGN and the PM (Beck *et al.* 2012) and BRI1 displays a constitutive PM and endosomal localisation (Ruscinova *et al.* 2004). Interestingly, upon flg22 treatment FLS2 is redirected into a late endosomal pathway and co-localises with the LE/MVB markers RAB GTPase F1/Arabidopsis Rab GTPase 6 (RABF1/ARA6) -RFP and RFP-RABF2b/ARA7 (Beck *et al.* 2012). These observations have led to the suggestions that endocytosis of FLS2 may be

relevant for the propagation of signalling (Raikhel and Hicks 2007, Geldner and Robatzek 2008, Irani and Russinova 2009), however direct evidence is lacking. In contrast, the sensitivity of cells to flg22 is mediated by endocytosis of the receptor (Smith *et al.* 2014). FLS2 activation and endocytosis through a late endocytic route that leads to a de-sensitised period after FLS2 activation (Smith *et al.* 2014). Subsequent secretion of receptor allows re-sensitisation of the cell to flg22 by receptor replenishment (Smith *et al.* 2014). Redirection of endocytosed FLS2 into a late endosomal pathway leads to receptor degradation (Beck *et al.* 2012, Smith *et al.* 2014).

One mechanism by which FLS2 is directed for endocytosis to a late endosomal pathway is through receptor ubiquitination. FLS2 is ubiquitinated by the PUB E3 ligases PUB12 and PUB13 and subsequently degraded, presumably in the vacuole, although the proteasome has also been implicated (Lu *et al.* 2011). Supporting the role of receptor endocytosis into a late endosomal pathway in negative regulation of signalling, in *A. thaliana* plants lacking PUB12/13 display elevated immune responses (Lu *et al.* 2011). These mutants do, however hyper-accumulate SA, which could also explain this phenotype (Lu *et al.* 2011).

1.2.6 Do endocytic compartments contribute to defence signalling?

The question has been posed several times in the literature about whether endosomes can function as sites of signal transduction during RLK signalling (Raikhel and Hicks 2007, Geldner and Robatzek 2008, Bar and Avni 2014) in a phenomenon referred to as endosomal signalling. As FLS2 signalling has been extensively investigated, it is an excellent model with which to study endosomal signalling in plants. Endosomal signalling was first suggested for the mammalian EGFR where it was observed that downstream signalling components, including MPKs, were localised to EEs (Vieira *et al.* 1996). It has since been demonstrated that the endosomal localisation of EGFR activated MPKs is required for their full activation (Teis *et al.* 2002, Nada *et al.* 2009). Furthermore, after EGF treatment of HeLa cells, the endocytosed EGFR receptor is trafficked to the perinuclear region with the transcription

factor Adapter protein containing PH domain 1 (APPL1) then alters transcription (Miaczynska *et al.* 2004). There are numerous other examples of endosome localised proteins contributing to overall receptor signal transduction including for the Neuronal growth factor (NGF) receptor tropomyosin-related kinase A (TrkA). The transcription factor APPL1 is again trafficked via endosomes to the nucleus following application of NGF and endocytosis of the activated receptor, TrkA in human PC12 cells (Varsano *et al.* 2006). APPL1 then recruits a G-protein regulator and both are trafficked to the perinuclear region of the cell to dissociate and promote TrkA signalling (Lin *et al.* 2006, Varsano *et al.* 2006) by nucleosome remodelling (Miaczynska *et al.* 2004).

There have also been numerous studies investigating the importance of receptor endocytosis in signal transduction. Inhibition of receptor endocytosis can either lead to enhanced or reduced MPK activation (Vieira *et al.* 1996, Miaczynska *et al.* 2004, Purvanov *et al.* 2010, Brankatschk *et al.* 2012, Sousa *et al.* 2012). The most convincing study to date utilises multiple mutants that limit EGFR trafficking to different endocytic compartments and microarrays to transcriptionally profile the response (Brankatschk *et al.* 2012). From this study it is clear that the majority of EGFR regulated genes are controlled from the PM whilst a subset of genes do not respond when endocytic trafficking is altered. It must be noted here, however, that the sum of EGFR signalling is not MPK activation and transcriptional reprogramming, other changes occur within cells including cytoskeletal remodelling (Balbis and Posner 2010). Therefore studying solely MPK activation or gene activation cannot determine the total importance of endosomes in signalling.

An important distinction must be made here between two hypotheses relating endosomal signalling and are directly relevant to studying endosomal signalling with FLS2. The first is “Do any proteins in the FLS2 signalling pathway signal from endosomes?”. The second is “Is signalling from endosomes relevant to the overall cell response to flg22?”. These two hypotheses are linked but the second requires the first to be true. Therefore, to answer the

question of endosomal function in signalling during bacteria attack, the first hypothesis must be tested before the second can be tested properly. Exactly how endosomes contribute to signalling must be determined (if at all) before the contribution of endosomal signalling proteins can be determined, otherwise the wrong responses may be monitored. Therefore, until the direct functions of endosomal signalling are determined, the relevance of endosomal signalling proteins in FLS2 signalling cannot be determined. Interesting parallels between the relevance of endosomes as sites of signal transduction and the importance of FLS2 in defence against pathogens can be drawn. FLS2 was initially thought to have a negligible contribution to plant defence (Section 1.1.1) because an inappropriate assay was used to test relevance. As the role of endosomes in FLS2 signal transduction is unknown, the importance of endosomes to signalling overall cannot be tested yet.

Therefore to determine whether endosomes can contribute to signalling, and test the first hypothesis, the proteins localised to endosomes must be determined. It is unlikely that the endocytosed FLS2 is signalling directly from LE/MVBs as it was demonstrated that FLS2 is localised to intraluminal vesicles of LE/MVBs (Spallek *et al.* 2013). Numerous other signalling proteins have, however, been localised to endosomes or the endomembrane system. The MPKKK Enhanced disease resistance 1 (EDR1) that functions in negative regulation of immunity localises to endosomes (Gu and Innes 2011). Furthermore MPK4 has been localised to microtubules and is essential for the formation of the cell plate, whilst MPK6 localises to the TGN (Beck *et al.* 2011). Both of these kinases are flg22 responsive, but their endosome localisation has not been tested for its relevance in FLS2 induced signalling. Furthermore MPK6 co-fractionates with FLS2 following flg22 treatment (Müller *et al.* 2010). Demonstrating MPKs localise to endosomes is not conclusive evidence for endosomal signalling; the MPKs must be localised to the cytosolic face of the LE/MVB. Before testing the relevance of endosomes to signalling, the proteomes of different endosomes must be elucidated. Thus, only when the role of endosomes in signalling has

been established and can be correctly monitored, can the overall importance of endosomes in signalling be defined.

Therefore, to understand signalling and plant defence, we also need to understand endomembranes and their proteomes. Furthermore significant advances could be made with good quality endomembrane proteomic data.

1.3 Methods for protein identification

There are numerous methods with which to identify proteins in a sample and they can generally be divided into biased and unbiased approaches. Biased approaches require defined proteins of interest or candidates, and their presence can be tested with specific antibodies raised against the protein or against a tag fused to the protein candidate. When assessing the presence of a protein in a subcellular compartment confocal laser scanning microscopy (CLSM) can also be used. Here the localisation of proteins can be inferred from living cells by the emission of light from a recombinant protein fused to a fluorescent protein tag. Proteins such as GFP or RFP absorb light at one wavelength (395 and 584 nm respectively) and emit it at another (509 and 687 nm respectively), allowing the spatial localisation of proteins to be inferred (Tsien 1998, Campbell *et al.* 2002).

1.3.1 Shotgun proteomics for high throughput protein identification

The principal method for unbiased high throughput identification of proteins is with a mass spectrometer (MS) in what is known as shotgun proteomics (Aebersold and Mann 2003). Here, proteins in a sample are detected in an identity independent manner with a MS. There are multiple different types of MS and several will be used in this study.

MS analysis of complex protein mixtures requires several experimental steps. In most cases samples must be separated by fractionation, even purified endomembranes or Co-Immunoprecipitations (CoIPs) (Steen and Mann 2004). This can be achieved in a variety of ways at either the protein or peptide level. The overall aim of separation of complex samples

is to concentrate the eventual individual peptides and to allow the instrument time to analyse them (Steen and Mann 2004). Whilst there is no 'correct' way to fractionate a sample as methods depend on experimental aims and amount of protein available, there are a few common techniques. The protein sample can be fractionated with SDS-PAGE after denaturation, most commonly for protein separation (Aebersold and Mann 2003). Protein migration is predominantly influenced by size during Sodium dodecyl sulphate (SDS)-Polyacrylamide gel electrophoresis (PAGE), but folding or modification also influence migration time. For example FLS2 migrates much more slowly during SDS-PAGE than would be predicted from its size alone, as glycosylation of the LRR further reduces motility (Haweker *et al.* 2010). Other methods to separate proteins are native electrophoresis, in which proteins are not denatured, or isoelectric focussing, in which molecules migrate based on their charge in a pH gradient (Aebersold and Mann 2003). The gels are subsequently sliced into sections and the proteins cleaved into peptides with a protease, for example trypsin.

Alternatively liquid chromatography can be used to fractionate samples. These techniques can separate at either the protein (followed by cleavage to peptides) or at the peptide level. Reverse phase chromatography and strong cation exchange (SCX) chromatography are commonly used (and in this thesis). In both of these techniques species are allowed to bind to a chromatography column then a gradient is applied to the column: acetonitrile for reverse phase or strong cation solution is passed over the column for SCX, and peptides eluted. Peptides are therefore sorted based on their hydrophobicity (reverse phase) or charge (SCX). The elution from an Liquid chromatography (LC) column can then be pooled into fractions for further fractionation with another technique. Alternatively the elution from an LC column can be directly injected into the MS if volatile salts are used in the ion exchange.

For the principal MS used in this thesis, we used SDS PAGE to fractionate protein mixtures before tryptic digestion to peptides. The peptides were fractionated by reverse phase LC and

are sprayed directly into the MS, an Linear trap quadrupole (LTQ)-Orbitrap XL (Orbitrap), using a voltage differential to generate gas phase ions to be measured. Measurement occurs in the Orbitrap by the radial oscillation of ions (ideally peptides but contaminants such as ionic detergents will also be detected) and calculating mass/charge (m/z) ratios from the frequency of the oscillations of the all ions (Hu *et al.* 2005). Intact peptide (precursors) can then be isolated with Fourier transformation to derive the individual ion overlapping patterns. The instrument measures m/z ratios of ions in milli-seconds to generate a m/z by intensity spectrum. Species intensity is measured in the Orbitrap to generate MS1 spectrum (Hu *et al.* 2005). The top 5 most abundant species are selected for collision induced dissociation (CID). In CID, species are accelerated and allowed to collide with neutral molecules (He) and fragment to form ions (Steen and Mann 2004). These ions are then trapped in the ion trap and scanned over an m/z range to generate MS/MS or MS2 data. The combination of m/z measurements from one CID event in an MS2 is referred to as a spectrum and the spectrum can be matched to the predicted fragmentation of peptides from a known protein set, for example the TAIR10 annotated *A. thaliana* genome. Thus the presence of a peptide in a sample can be inferred as the best match for a spectrum obtained (Steen and Mann 2004). The presence of a protein is subsequently inferred from the presence of its constituent peptides in a sample (Steen and Mann 2004). Therefore a peptide or a protein is never truly identified but matched to a spectrum, however, I will use the term identified for confidence in a spectrum match of over 95% and identification of two peptides for a protein to be identified. The software MASCOT (www.matrixscience.com) is the most commonly used software to match spectra to peptides. The strength of a match relies on the difference between observed and predicted m/z ratios for the database proteins and is adversely affected by the presence of non-matched spectra (Perkins *et al.* 1999).

The data obtained via Orbitrap benefits from high resolution and mass accuracy (Hu *et al.* 2005). High resolution refers to the discriminatory power of a MS to distinguish between species with similar m/z ratios (Steen and Mann 2004). Mass accuracy refers to the ability of

a MS to measure the correct mass of a species and is calculated as difference in the theoretical m/z and the measured m/z .

As an alternative to the Orbitrap a Q-time of flight (TOF) can be used (Aebersold and Mann 2003). These MS measure the m/z ratios of species by measuring their TOF after acceleration through an electric field. With the same kinetic energy, the velocities of species depend only on their m/z ratio therefore the m/z ratio of species can be measured. Low m/z species taking longer to reach the target than high m/z species. Q-TOFs, including the Synapt G2 used in this thesis, has less sensitivity than the Orbitrap but greater linearity, dynamic range and acquisition times (Hu *et al.* 2005).

1.4 Thesis Aims

Endosomes have frequently been implicated as sites of signal transduction however direct evidence is lacking. Several recent studies have demonstrated that endosomal signalling does not contribute significantly to the signalling of BR11. In order to determine the contribution of endosomal signalling to the overall cell response to flg22 good quality proteomic data on endosomes is needed. Using this data the potential role of endosomes in signalling can be investigated. Changes in the endosomal proteome need to be quantified after flg22 treatment and signalling proteins in endosomes identified. Only then can the activity of proteins signalling from endosomes be monitored. Furthermore proteomic data from endosomes and how they change following flg22 treatment will allow for a greater understanding of plant cell defence responses in general.

Thus to determine the contribution of endosomes to signalling during bacterial attack I set several aims:

1. Establish the proteomes of LE/MVBs.
2. Determine LE/MVB proteome changes relevant to FLS2-induced signalling.
3. Investigate endosome localised proteins involved in immune signalling.

4. Examine the relevance of endosome-localised pools of signalling proteins to the overall cellular response to flg22.

2 Experimental procedures

2.1 Plant material

Name	AGI	Details	Reference
UBQ10::YFP		Col-0	(Ueda <i>et al.</i> 2004)
UBQ10::mCherry		Col-0	(Ueda <i>et al.</i> 2004)
UBQ10::RFP-RABF2b/ARA7	AT4G19640	Col-0	(Ueda <i>et al.</i> 2004)
UBQ10::RABF1/ARA6	AT3G54840	Col-0	(Ueda <i>et al.</i> 2004)
UBQ10::YFP-RAG3f	AT3G18820	Col-0	(Geldner <i>et al.</i> 2009)
UBQ10::YFP-GOT1	AT3G03180	Col-0	(Geldner <i>et al.</i> 2009)
UBQ10::YFP-VAMP711	AT4G32150	Col-0	(Geldner <i>et al.</i> 2009)
UBQ10::YFP-RABD2a/ARA5	AT1G02130	Col-0	(Geldner <i>et al.</i> 2009)
35s::CLC2-GFP	AT2G40060	Ws-2	(Geldner <i>et al.</i> 2009)
pVNL3::VNL3-GFP	AT3G57410	<i>vln3</i> /Col-0	(Bao <i>et al.</i> 2012)
UDP	AT3G29360	SALK_098492C	Alonso <i>et al.</i> 2003
KING1	AT3G48530	SALK_074554	Alonso <i>et al.</i> 2003
KING1	AT3G48530	SAIL_679_E05	Alonso <i>et al.</i> 2003
EIF3C	AT3G56150	SALK_015933C	Alonso <i>et al.</i> 2003
VLN3	AT3G57410	SALK_078340C	Alonso <i>et al.</i> 2003
VLN3	AT3G57410	SALK_117097C	Alonso <i>et al.</i> 2003
WD40	AT3G63460	SALK_035921C	Alonso <i>et al.</i> 2003
ALDH3F1	AT4G36250	SALK_045231C	Alonso <i>et al.</i> 2003
ACT-TK	AT4G38470	SALK_112195C	Alonso <i>et al.</i> 2003
ACT-TK	AT4G38470	SALK_113076C	Alonso <i>et al.</i> 2003
SNX2B	AT5G07120	SALK_087925C	Alonso <i>et al.</i> 2003
SNX2B	AT5G07120	SALK_054621C	Alonso <i>et al.</i> 2003

HMZ	AT5G18230	SALK_037715C	Alonso <i>et al.</i> 2003
EIF3B-1	AT5G27640	SALK_107766C	Alonso <i>et al.</i> 2003
GTP binding	AT5G46070	SALK_016366C	Alonso <i>et al.</i> 2003
rhm1-2	AT1G78570		(Diet <i>et al.</i> 2006)
rhm1-1	AT1G78570		(Diet <i>et al.</i> 2006)
vln2,3	AT2G41740, AT3G57410		(van der Honing <i>et al.</i> 2012)
vln2	AT2G41740		(van der Honing <i>et al.</i> 2012)
vln3	AT3G57410		(van der Honing <i>et al.</i> 2012)

2.1.1 Plant growth on soil

A.thaliana seeds were sown on F2 compost. Seedlings were grown in a growth chamber under controlled conditions: 21-23°C; 10 h light / 14 h dark; 75% humidity for *A. thaliana*. Two weeks old mature seedlings were individually transferred to fresh pots filled with compost mix for *A.thaliana* (F2 compost supplemented with grit and systemic insecticide INTERCEPT). Plants were grown in the same conditions as for seedlings as mentioned above.

2.1.2 *In vitro* seedling growth for IP

A. thaliana seeds were surface-sterilized for 12 hours in a sealed chamber by chlorine gas (produced by mixing 8 ml of 8 M HCl with 200 ml of bleach). 5 x 0.1 g of *A.thaliana* seed for all constructs were grown in 5 x sterile 250 ml conical flasks with 200 ml of Murashige and Skoog medium at 22 °C, 16 hours light, shaken at 120 rpm for 8 days.

2.1.2.1 Elicitation of *in vitro* grown seedlings with flg22

A solution of 20 µM flg22 was prepared and 10 ml added to each flask of *A. thaliana* seedlings with mixing via shaking and mild vacuum was applied for 90 s, followed by slow

release of vacuum over 3 min. At the annotated time following flg22 application seedlings were filtered using miracloth (Millipore) and frozen on liquid nitrogen.

2.1.3 *In vitro* seedling growth for PAMP induced resistance (PIR)

A. thaliana seeds were surface-sterilized for 12 hours in a sealed chamber by chlorine gas (produced by mixing 8 ml of 8 M HCl with 200 ml of bleach). Seeds for each construct were grown on solid Murashige and Skoog medium at 22 °C, 16 hours light for 6 days then transplanted into 96 well plates with 100 µl of ½ Murashige and Skoog medium and grown for a further 4 days at 22 °C, 16 hours light, shaken at 120 rpm.

2.2 Plant pathology assays

2.2.1 Microorganisms used in this study

Species	Pathovar	Designation	Details
<i>Escherichia coli</i>		TOP10	For Gateway cloning
<i>Agrobacterium tumefaciens</i>		GV3101	For transient expression of proteins in <i>N.benthamiana</i>
<i>Pseudomonas syringae</i>	Tomato	DC3000	
<i>Pseudomonas syringae</i>	Tomato	Lux DC3000	

2.2.2 Bacterial cultures

Each bacterial strain was grown on solid or in liquid L medium (For 1 L: 10 g tryptone, 5 g NaCl, 1 g glucose, 5 g yeast extract, pH 7.0; for solid medium, 10 g agar was included) with the appropriate antibiotics. *E. coli* strains were grown in an incubator at 37°C, *P. syringae* and *A. tumefaciens* strains at 28°C.

2.2.3 Soil grown *A. thaliana* infection with *Pto* DC3000.

P. syringae strains were streaked on fresh selective media and grown for (28 °C) 24 to 48 h. Bacteria were scraped from the plates and resuspended in H₂O. OD₆₀₀ was measured and

adjusted to 0.02. 0.04% (v/v) Silvet was added and bacteria solution sprayed onto the *A. thaliana* leaves, axial and abaxial surfaces.

2.2.3.1 Estimation of *Pto* DC3000 growth

3 *A. thaliana* leaf disks (each sample equalling 1 cm²) were collected 3 days after inoculation with bacteria (OD₆₀₀ = 0.001, 5x10⁵cfu/mL) and then ground in water. Serial dilutions (10⁻², 10⁻³, 10⁻⁴ and 10⁻⁵) were then spotted on selective media. After 2 days incubation, bacterial colonies were counted according to the dilution spot and normalized in cfu/cm² of plant leaf.

2.2.4 PIR in *In vitro* grown *A. thaliana* infection with *Pto* DC3000 Lux

A. thaliana seedlings were treated with 1 μm flg22, 24 hours after transplantation from solid to liquid medium in 96 well plates. *Pto*DC3000 Lux was streaked on fresh selective media and grown for (28 °C) 24 to 48 h. Bacteria were scraped from the plates and re-suspended in 10 mM MgCl₂. OD₆₀₀ was measured and adjusted to 0.2. After 48 hours of growth in liquid medium *A. thaliana* seedlings were inoculated with bacteria to a final OD₆₀₀ of 0.02

2.2.4.1 Estimation of *Pto* DC3000Lux growth

After two days of growth, photons emitted from plates were measured over 2.5 min with an ICCD photon counting camera (Photek).

2.2.5 ROS burst assay

16 leaf discs (No. 1 cork borer – 3.8 mm diameter) were harvested from soil grown plants and incubated in dH₂O overnight in the dark. The water was removed and replaced with 100 μl of 20 μM luminol (Sigma-Aldrich), 1 μg of horseradish peroxidase (Sigma-Aldrich) and 100 nM of flg22. Light emission was immediately recorded with an ICCD photon counting camera (Photek).

2.3 Molecular biology

2.3.1 DNA based techniques

2.3.1.1 List of selective chemicals used in this study

Selective Chemical	Stock Concentration	Working dilution
--------------------	---------------------	------------------

Kanamycin	50 mg/ml in water	50 µg/ml
Spectinomycin	50 mg/ml in water	50 µg/ml
Streptomycin	50 mg/ml in water	50 µg/ml

2.3.1.2 List of plasmids used in this study

Construct	Insert	Backbone	Type of vector	Reference
UBQ10::YFP- PRA1.B1	PRA1.B1 coding sequence	pUBQ10::YFP-N (Grefen <i>et al.</i> 2010)	Binary vector	This study
UBQ10::YFP- PRA1.B2	PRA1.B2 coding sequence	pUBQ10::YFP-N (Grefen <i>et al.</i> 2010)	Binary vector	This study
UBQ10::YFP- PRA1.F1	PRA1.F1 coding sequence	pUBQ10::YFP-N (Grefen <i>et al.</i> 2010)	Binary vector	This study
UBQ10::RFP- PRA1.B1	PRA1.B1 coding sequence	pUBQ10::RFP-N (Grefen <i>et al.</i> 2010)	Binary vector	This study
UBQ10::RFP- PRA1.B2	PRA1.B2 coding sequence	pUBQ10::RFP-N (Grefen <i>et al.</i> 2010)	Binary vector	This study
UBQ10::RFP- PRA1.F1	PRA1.F1 coding sequence	pUBQ10::RFP-N (Grefen <i>et al.</i> 2010)	Binary vector	This study

2.3.1.3 Plant genomic DNA extraction

The Chelex 100 (Biorad) chelating resin diluted 1:10 in distilled H₂O was used for quick DNA extraction and genotyping reactions. *A. thaliana* leaf disks sampled using a N⁰1 cork borer. The leaf disc was placed in 100 µl in Chelex suspension and disrupted with a pipette tip. The mixture was vortexed briefly, incubated at 95 °C for 5 min and centrifuged at 13 000 rpm for 1 min. 5 µl of supernatant was used per PCR reaction.

2.3.1.4 Polymerase chain reaction

PCRs were performed with 10 – 100 ng DNA as template in 25 µl final volume. Each reaction contained 1x PCR TAQ buffer or Phusion buffer, 0.2 mM dNTPs, 5 U/µl Taq DNA

polymerase (NEB) or 2.5 U/μl Phusion high-fidelity DNA polymerase (NEB), 10 μM of each primer. PCR was performed with successive cycles in a thermocycler (DNA engine PTC225, MJ Research). The temperatures and length of each temperature step were optimised to primers and length of product desired.

2.3.1.5 Plant RNA extraction and cDNA production

Plant tissue was collected in Eppendorf tubes, frozen in liquid nitrogen and ground to a fine powder using a rotating drill (pre-chilled in liquid nitrogen). 900 μl of TriReagent (Sigma) was added and the mixture incubated for 5 min at room temperature. 100 μl of Bromo-chloropropane was added, tubes agitated by flicking then centrifuged at 10 000 g for 20 min at 4 °C. The supernatant was then transferred into a new Eppendorf tube and 400 μL of isopropanol was added to the solution followed by centrifugation at 10 000 g for 20 min. The supernatant was discarded and the pellet washed with 70% ethanol. Ethanol was removed and the pellet air dried for 5 min. The RNA was re-suspended in RNase-free water and DNase treated according to the DNase I RNase-free protocol (Roche). 10% SDS and proteinase K were added to the RNA and the solution incubated for 15 min at 42 °C. RNA was then purified using the RNeasy MinElute cleanup kit (Qiagen) and eluted in RNase-free water. Total RNA was quantified with a Nanodrop (Thermo Scientific).

2.3.1.6 DNA electrophoresis

Presence and length of DNA fragments after PCR were confirmed using electrophoresis. PCR products were mixed with 6x loading dye and in gels containing 1-2% agarose diluted in TAE and ethidium bromide. DNA migration was tested in an electrophoresis tank filled with TAE buffer applied with 100 V for 10-30 minutes. Fragment length was estimated using the 1 kb DNA ladder (40 ng/μl from NEB) loaded on the same gel. DNA was visualised by exposing the gel to UV light in a UV transilluminator from BIO-RAD.

2.3.1.7 Purification of DNA from agarose gel

DNA bands of interest were visualised and excised on a UV table using a scalpel blade. The fragments were purified using QIAquick Spin columns (Qiagen). The DNA was either stored at -20 °C or used directly.

2.3.1.8 Gateway® cloning from cDNA

Coding sequences were amplified from cDNA by PCR into pENTR/D/TOPO entry vectors according to the protocol supplied by Invitrogen. Vectors were then transformed into chemically competent TOP10 cells by heat shock. Positive clones were confirmed by colony PCR and plasmid sequencing. Genes of interest were then transferred into expression vectors using the LR clonase II enzyme. The LR reaction was carried out using the protocol outlined by the manufacturer. In short, 150 ng of entry vector and 150 ng of destination vector were mixed with 1 µl of LR clonase II enzyme mix. Samples were vortexed quickly and incubated for 1 h at 25 °C. The reaction was then halted by addition of 0.5 µl of proteinase K to the mixtures and the reactions incubated at 37 °C for 10 mins. 1 µl of the LR reaction was then transformed into chemically competent TOP10 cells.

2.3.1.9 Transformation of chemically competent *E.coli*

TOP10 *E.coli* were transformed with 250 ng of purified plasmid DNA or 1 µl of LR/gateway reaction. 50 µl of chemically competent cells were incubated in a 1.5 ml Eppendorf tube on ice for 30 min followed by a 30 s incubation at 40 °C. 250 µl of L media was added and the bacteria incubated at 37 °C for 60 min and bacteria plated on selective media.

2.3.1.10 Transformation of electro-competent *A. tumafasciens*

A. tumafasciens (GV3101) were transformed with 250 ng of purified plasmid DNA. 50 µl of chemically competent cells were thawed directly from -80 °C stock on ice. Cells were mixed with DNA and inserted into a pre-chilled electroporation cuvette with 1 mm gap. A Gene Pulser Xcell (BIO-RAD) cell porator was used for electroporation with these following conditions: voltage = 1800 V, capacitance = 25 µF, resistance = 200 Ω. 250 µl of L media

was added and the bacteria incubated at 28 °C for 60 min and bacteria plated on selective media.

2.3.1.11 Colony PCR

To recover transformants following cloning with colony PCR, individual colonies were picked with a tip and a smear inserted into each PCR reaction tube. PCR reaction followed the PCR protocol to confirm specific gene/product. Colonies with the correct DNA fragments were allowed to grow overnight in 10 ml selective L media.

2.3.1.12 Plasmid purification

Transformed bacteria were pelleted after overnight culture with a single 10 min x 1000 g centrifugation step. Plasmid was purified using the QIAprep Spin Miniprep Kit, Qiagen. Plasmid was eluted in 50 µl dH₂O, quantified with nanodrop and stored at -20 °C. Correct sequence of the DNA insert was confirmed with sequencing performed by the GATC Biotech company (<http://www.gatc-biotech.com/en/index.html>).

2.3.2 Protein biochemistry

2.3.2.1 BCA protein quantification assay

Protein solutions were diluted with dH₂O to between 0.5 and 2 mg/ml of protein. 160 µl of 4% CuSO₄ (w/v) was added to 8 ml of bicinchoronic acid (BCA) solution (Sigma). 100 µl of solution was added to wells of a clear plastic 96 well plate with 20 µl of protein solution. Solutions of Bovine serum albumin (BSA) at 0.5, 1, 1.5 and 2 mg/ml were prepared as standards. All solutions were measured in triplicate and the mean average taken. The plate was then incubated at 37 °C for 30 min and absorbance at 562 nm measured with a plate reader (Varioskan Flash - Thermofisher).

2.3.2.2 List of protein extraction buffers used

	Base Buffer	Sucrose gradient buffer	IP buffer	Phosphorylation IP Buffer
Na-HEPES	150 mM, pH 7.5	150 mM, pH 7.5	150 mM, pH 7.5	150 mM, pH 7.5

Sucrose	17.5% (w/v)	15-60% (w/v)	17.5% (w/v)	17.5% (w/v)
EDTA	10 mM	10 mM	10 mM	10 mM
EGTA	10 mM	10 mM	10 mM	10 mM
KCl	7.5 mM	7.5 mM	7.5 mM	7.5 mM
DTT	10 mM	10 mM	10 mM	10 mM
IGEPAL CA-630	-	-	0.01% (v/v)	0.01 or 0.1% (v/v)
Protease inhibitors	1% (v/v)	1% (v/v)	1% (v/v)	1% (v/v)
NaMo	-	-	-	1 mM
NaF	-	-	-	25 mM
Calyculin A	-	-	-	1 nM
PVPP	0.5% (w/v)	0.5% (w/v)	0.5% (w/v)	0.5% (w/v)

2.3.2.3 Plant protein extraction

Plant tissue was frozen in liquid nitrogen and ground with a pestle and mortar to powder, 30-50 g of total fresh weight was then used. Base buffer was added 2 ml to 1 g of fresh weight tissue was added. Homogenate was then filtered through one layer of miracloth (Millipore). All subsequent steps occurred on ice or at 4 °C

2.3.2.4 Sucrose gradient fractionation

Microsomes were prepared from a plant protein extract. The homogenate was centrifuged once at 6000 g for 10 min, the supernatant taken and centrifuged at 10 000 g for 20 min. Then the supernatant was centrifuged for 1 hour at 100 000 g and the pellet was taken as the microsome. The microsome was then re-suspended in 2 ml of sucrose gradient buffer with 25% sucrose and quantified to determine protein content. A 6 step sucrose gradient (30-55%) was prepared in a 12 ml ultracentrifuge tube (Sorvall), 1.71 ml of gradient buffer were overlaid in 5% steps. 9 mg of protein from the 25% sucrose (sucrose gradient buffer)

with re-suspended microsome was then overlaid on top of the 30% sucrose fraction to fill the tube. The gradient was centrifuged at 100 000 g for 18 hours and 1 ml fractions collected from the top of the gradient by pipetting. Protein concentration in each fraction was quantified by BCA assay.

2.3.2.5 3 step sucrose cushion fractionation

Plant protein was extracted in base buffer with 15% sucrose. The homogenate was layered onto a 2 step sucrose gradient in a 5 ml ultracentrifuge tube (Sorvall). 1.5 ml of sucrose gradient buffer (35% sucrose) was layered onto a 1.5 ml sucrose gradient buffer (45% sucrose) layer. Then 2 ml of plant protein homogenate was layered on top to fill the tube. The gradient was centrifuged for 1 hour at 100 000g. The gradient was extracted as two fractions per step and the interface layers by pipetting from the top. Protein concentration was then quantified with BCA.

2.3.2.6 Sucrose cushion fractionation for immunoprecipitation

Plant protein from 3 flasks of 8 day old *A. thaliana* seedlings was extracted in base buffer with 15% sucrose. The homogenate was layered onto a 2 step sucrose gradient in 6 x 35 ml ultracentrifuge tubes (Sorvall). 5 ml of sucrose gradient buffer (35% sucrose) was layered onto a 5 ml sucrose gradient buffer (45% sucrose) layer. Then 25 ml of plant protein homogenate was layered on top to fill the tube. The gradient was centrifuged for 1 hour at 100 000g. The 15% sucrose layer was extracted by pipetting and discarded. The 35% sucrose layer was then extracted with a pipette and diluted 1:1 with IP buffer with 0.02% IGEPAL CA-630.

2.3.2.7 Immunoprecipitation

Eight day old seedlings, from 3 x 250 ml conical flasks, were frozen in liquid nitrogen and ground with a pestle and mortar to powder, 30-50 g of total fresh weight was then used. Protein extraction buffer (150 mM Na-HEPES pH7.5, 10 mM EDTA, 10 mM EGTA, 17.5% (w/v) sucrose, 7.5 mM KCl, 0.01% (v/v) Igepal CA-630, 10 mM DTT (Dithiothreitol), 1% (v/v) Protease inhibitors (Sigma), 0.5% (v/v) PVPP (polyvinylpyrrolidone) at 2 ml to 1 g of

fresh weight tissue was added. All subsequent steps were performed at 4 °C. Protein concentration was determined with BCA assay. Homogenate was filtered through two layers of miracloth and centrifuged at 6000 g for 20 min. 20 µl of chromotek GFP or RFP trap sepharose beads (as appropriate) were added per 50 ml homogenate and incubated for 3 hours with shaking. The homogenate was then centrifuged at 500 g for 5 min and the supernatant discarded. The bead slurry was washed 5 times with fresh pre-chilled extraction buffer (no PVPP or protease inhibitors) with 3 min incubation. The slurry was collected after the last wash and protein eluted with incubation at 95 °C for 10 min in 2x SDS-PAGE loading buffer and taken for either LC-MS/MS or Western blotting.

2.3.2.8 SDS-PAGE and immunoblotting

10% poly-acrylamide SDS-gels were run at 100/200 V and proteins electroblotted onto Polyvinylidene fluoride (PVDF) membranes at 250 mA (Biorad). Membranes were rinsed in Tris buffered saline (TBS) and blocked in 5% (w/v) non-fat milk powder in TBS 0.1% tween (TBST) (w/v) for 1 hour. Primary antibodies were diluted in 0.5% (w/v) non-fat milk (unless otherwise stated in Table 2.2), TBST to the following concentrations and incubated at room temperature for 1 hour. Membranes were washed three times in TBST before 1 hour incubation with secondary antibodies. Signals were visualized using chemiluminescent substrate (Lumigen ECL, GE Healthcare) and GE healthcare Image Quant LAS 3000.

2.3.2.8.1 List of antibodies used

Antibody	Working stock	Manufacturer	Species
α-AHA1 (H ⁺ ATPase 1)	1:2 000	Agrisera AS07 260	Rabbit
α-BIP2 (luminal binding protein)	1:2 000	Agrisera AS09 614	Chicken
α-RbcL (Rubisco Large Subunit)	1:10 000	Agrisera AS03 037	Rabbit
α-COX2 (Cytochrome Oxidase 2)	1:5 000	Cytochrome Oxidase 2	Rabbit
α-RFP	1:10 000	Abcam ab34771	Rabbit
α-FLS2	1:5 000	Purified by Eurogentec	Rabbit
α-pERK (p44/42 MAPK)	1:1 000 (3% BSA)	Cell signalling #9102	Rabbit

α -SEC21	1:2 000	Agrisera AS08 327	Rabbit
α -HSP70 (Heat shock protein 70)	1:5 000	Agrisera AS08 371	Rabbit
α -GFP	1:4 000	Life Tech A-11122	Rabbit
α -pS	1:1 000 (3% Gelatin)	Invitrogen 61-8100	Rabbit
α -Rabbit IgG- HRP	1:10 000	Sigma A6154	Goat
α -Chicken IgG- HRP	1:10 000	Agrisera AS09 603	Goat

2.3.2.9 Tryptic protein digestion from gel

Affinity purified proteins were separated on 4-20% Tris-Glycine nUView pre-cast gradient gels (NuSep) and proteins stained with Simply Blue™ Safe Stain (Invitrogen). The SDS-PAGE gels were cut into 7 slices per affinity purification. Gel slices were washed for 30 min with 50% ACN/ 25 mM ammonium bicarbonate (ABC) at 37 °C, twice. Then 100% ACN was added for 10 mins and the liquid removed. 10 mM DTT in 50 mM ABC was added to cover the gel pieces for 30 min at 56°C shaking and the supernatant removed. 55mM iodoacetamide in ABC (in the dark) was applied for 20 min. The gel pieces were washed twice for 15 min with 50% ACN/ 25 mM ABC and dehydrated with 100% ACN for 10 mins. 1µg of trypsin, 46 mM ABC, 5% ACN was applied at 37 °C overnight and the supernatant removed and retained. The gel pieces were washed three times by addition of 50% ACN, 5% formic acid and sonicated for 10 min and the wash supernatants were then pooled with previous supernatants. The supernatants containing the peptides were then dehydrated to dryness.

2.3.2.10 In solution tryptic protein digestion

Following IP performed with the following modifications. An additional wash step was added of 3 min in dH₂O at 4 °C. Proteins were eluted from the IP beads with 100 µl of 0.1% TFA in dH₂O followed by centrifugation for 1 min at 500 g. The supernatant was collected and the elution, centrifugation repeated four more times, the collective washes were pooled and dehydrated to dryness in a speedvac (MiniVac Duoconcentrator). Protein was then re-solubilised in 8 M urea. 50 µM DTT in 55 mM Triethylammonium bicarbonate (TEAB) was

added and the solution incubated for 1 hour at room temperature followed by 100 mM iodoacetamide in 55 mM TEAB incubated in the dark for 1 hour. 0.3 µg of trypsin was added and incubated at 37 °C overnight. 1 µl acetic acid in 55 mM TEAB was added to halt the digestion. The peptides were then dehydrated to dryness in a speedvac (MiniVac Duoconcentrator). LC-Orbitrap analysis of peptide solutions

An Orbitrap (ThermoFisher Scientific) and a nanoflow-Ultra high performance liquid chromatography (UHPLC) system (nanoAcquity, Waters Corp.) was used to analyse peptide solutions. The generated peptides dissolved in 2% acetonitrile, 0.2% trifluoroacetic acid were applied to a reverse phase trap column (Symmetry C18, 5 µm, 180 µm x 20 mm, Waters Corp.) connected to an analytical column (BEH 130 C18, 1.7 µm, 75 µm x 250 mm, Waters Corp.) in vented configuration using nano-T coupling union. Peptides were eluted in a gradient of 3-40 % acetonitrile in 0.1 % formic (solvent B) acid over 50 min followed by gradient of 40-60 % B over 3 min at a flow rate of 250 nL min⁻¹ at 40°C. The MS was operated in positive ion mode with nano-electrospray ion source with ID 0.02mm fused silica emitter (New Objective). Voltage +2kV was applied via platinum wire held in PEEK T-shaped coupling union. Transfer capillary temperature was set to 200 °C, no sheath gas, and the focusing voltages in factory default setting were used. The Orbitrap, MS scan resolution of 60,000 at 400 m/z, range 300 to 2000 m/z was used, and automatic gain control (AGC) target was set to 1000000 counts, and maximum inject time to 1 000 ms. In the LTQ, MS2 spectra were triggered with data dependent acquisition method for the 5 most intense ions. The threshold for CID was above 1000 counts, normal scan rate, AGC accumulation target was set to 30 000 counts, and maximum inject time to 150ms. A data dependent algorithm was used to collect as many tandem spectra as possible from all masses detected in master scan in the Orbitrap. For the latter, Orbitrap pre-scan functionality, isolation width 2 m/z and collision energy set to 35% were used. The selected ions were then fragmented in the ion trap using CID. Dynamic exclusion was enabled

allowing for 1 repeat only, with a 60 s exclusion time, and maximal size of dynamic exclusion list 500 items. Chromatography function to trigger an MS2 event close to the peak summit was used with correlation set to 0.9, and expected peak width 7s. Charge state screening enabled allowed only higher than 2+ charge states to be selected for MS2 fragmentation.

2.3.2.11 iTRAQ labelling of peptides

Briefly, peptides were digested with trypsin in 50mM triethylammoniumbicarbonate buffer, after reduction with DTT and carbamidomethylation with iodoacetamide. 35µl of the digest was mixed with ethanolic solution of iTRAQ reagent, and incubated for 2 hours at RT. Samples were labelled using 4-plex iTRAQ labelling kit (AB Sciex Ltd., USA). Individual samples labelled the unique isotopic labels were combined, and evaporated to dryness in vacuum concentrator.

2.3.2.12 Strong cation exchange chromatography

Peptides were separated by two dimensional liquid chromatography. In the first dimension we used Strong cation-exchange chromatography (SCX) on 1 x 150mm PolySULFOETHYL A™ (PolyLC Inc., USA) column. Mobile phase composition was 20mM potassium phosphate pH2.7 with 20% Acetonitrile in the solvent A, and with 0.5M potassium chloride in the solvent B. Sample was dissolved in the solvent A, and injected on the column on U3000 (Thermo, USA) liquid chromatograph. When UV detector response (214nm) stabilized, 40min gradient elution with fractionation (1min/fraction at 60µl/min) started. Fractions were evaporated and dissolved in 0.1%TFA and 2%Acetonitrile for second dimension of LC separation.

2.3.2.13 MS analysis of iTRAQ labelled peptides

Samples were analysed by LC-MS/MS in data dependent mode on a Synapt G2 mass spectrometer (Waters) coupled to a nanoAcquity UPLC system (Waters Ltd, Manchester, UK). Peptides were trapped using a pre-column (Symmetry C18, 5µm, 180 µm x 20 mm, Waters Ltd) which was then switched in-line to an analytical column (BEH C18, 1.7 µm, 75 µm x 250 mm, Waters Ltd) for separation. Peptides were eluted with a gradient of 3-40%

acetonitrile in water/0.1% formic acid at a rate of 0.75% min⁻¹ with a flow rate of 250 nL min⁻¹. The column was connected to a 10 µm SilicaTip™ nanospray emitter (New Objective, Woburn, MA, USA) for infusion into the mass spectrometer. Glu-Fibrinogen peptide (1 pmole µl⁻¹, Sigma-Aldrich) was infused at 0.5 µl min⁻¹ as a lock mass for recalibration and measured every 30 s. The mass spectrometer was controlled by the Masslynx 4.1 software (Waters) and operated in positive DDA and sensitivity mode with capillary voltage of 3 kV, cone voltage of 40 V. Scan time was 0.5 s over the range of 350-1800 m/z for full scans. MS2 was performed on the top 5 peptides per full scan (charge stages 2-4 +) and triggered by ion intensities above a threshold of 7000. Scan time was 1 s for the MS2 scan, and a charged stage dependent collision energy optimised for iTRAQ labelled peptides was applied in the trap cell.

Peaklist (pk1) files were generated in ProteinLynx Global Server 2.5.2 (Waters) and used for protein identification and relative iTRAQ quantitation by a database search. The search and the quantitation were performed using an in-house Mascot Server 2.4 (Matrixscience, London, UK) on a TAIR protein database. The Mascot searches and quantification has been summarized in Scaffold-PTM (Proteome Software Inc., USA). Data was exported to excel for quantitative comparisons.

2.4 Cell biology

2.4.1 Transient protein expression by particle bombardment

pUBQ10::YFP or pUBQ10::RFP-PRA1.B1/PRA1.B2/PRA1.F1 were coated onto 1 µm gold particles and bombarded into 4- to 5-week-old leaves of pUBQ10::RFP-RABF2b/ARA7, pUBQ10::YFP-GOT1 and pUBQ10::RABF1/ARA6-RFP using a Bio-Rad Biolistic PDS-1000/He particle delivery system. Bombardment sites were imaged 16 hours after bombardment by confocal microscopy. Data were collected from at least two independent bombardment events and 5 independent plants.

2.4.2 Sub-cellular protein localisation

Confocal laser microscopy was performed using the laser point scanning microscope Leica SP5. YFP was excited using the 514-nm argon laser, and fluorescence emissions were captured between 520 and 550 nm for YFP. RFP was excited at 561 nm, and emission was taken between 580 and 620 nm. The sequential scan mode was used for simultaneously imaging of YFP/RFP. Images were processed using the LeicaLite and Adobe Photoshop CS4 software packages. Images are maximum projections of a consecutive series of multiple Z planes 1 μm apart. Pearson's Rank correlations were calculated using voxel intensity in the YFP and RFP channels with the software Imaris.

2.5 Proteome analysis

2.5.1 Spectrum matching with MASCOT

Peak lists in format of Mascot generic files (.mgf files) were prepared from raw data using Proteome Discoverer v1.2 (ThermoFisher Scientific). Peak picking settings were as follows: m/z range set to 300-5000, minimum number of peaks in a spectrum was set to 1, S/N threshold for Orbitrap spectra set to 1.5, and automatic treatment of unrecognized charge states was used. Peak lists were searched on Mascot server v.2.4.1 (Matrix Science) against TAIR (version 10) database with GFP, RFP and common contaminants such as keratin added. Only tryptic peptides, were permitted with up to 2 possible miscleavages and charge states +2, +3, +4, were allowed in the search. The following modifications were included in the search: oxidized methionine (variable), carbamidomethylated cysteine (static). Data were searched with a monoisotopic precursor and fragment ions mass tolerance 10ppm and 0.8Da respectively. Mascot results were combined in Scaffold v. 4 (Proteome Software) and exported in Excel (Microsoft Office). Peptide identifications were accepted if they could be established at greater than 95.0% probability by the Peptide Prophet algorithm (Searle 2010) with Scaffold delta-mass correction.

2.5.2 SAINT Analysis

Protein identifications and total spectrum counts were exported from Scaffold and the fold enrichment over control samples (containing fluorescent protein baits) was calculated using SaintExpress (Teo *et al.* 2014). Default settings were used, where all three replicates counted equally and we did not use any known interaction information to weight interaction probabilities. Proteins were considered to be statically enriched if the SaintExpress probability score was greater or equal to 0.8 in keeping with recommendations (Teo *et al.* 2014, Choi *et al.* 2011). At least three controls of mCherry, YFP and Col-0 enrichments were used.

2.5.3 Proteome definition

A finalised list of proteins identified in each proteome was created according to the following criteria: A minimum of two unique peptides were required to identify a protein and identifications were classified into three groups. Group 1 proteins have spectrum matches in the affinity enrichments and none in the controls in two or more replicate affinity purifications. Group 2 proteins have spectrum matches in both control and affinity enrichments but have at least two times more spectrum matches in the affinity purifications than in the control in two or more replicates. Group 3 proteins have spectrum matches in only one out of three replicates affinity purifications and so have only weak evidence supporting their assignment to a proteome and are reported for completeness. I present proteins in groups 1 and 2 for each affinity purification bait as being identified in that proteome. The Sungear diagram was generated in virtual plant (Poultney *et al.* 2007). Venn diagrams were produced in R (File S1).

2.5.4 Electronic annotation of identified proteins

To identify transmembrane domains and putative signal peptides in our proteomic data I parsed a bulk download of protein data from Swiss-Prot and pTREMBL (http://web.expasy.org/docs/swiss-prot_guideline.html) using the Perl script (File S2). I also extracted protein name information and number of transmembrane domains from TAIR10 by

direct download of proteins with transmembrane domains from (<http://www.arabidopsis.org/> and <http://www.uniprot.org>). Transmembrane domain information from TAIR10 was used preferentially to that from Swiss-Prot, and protein records from the manually curated Swiss-Prot preferentially to data from electronically annotated pTREMBL. Data was then amalgamated with information of acylaton (Hemsley *et al.* 2013) and comparison to published proteomic data(Dunkley *et al.* 2006, Sadowski *et al.* 2008, Drakakaki *et al.* 2012, Nikolovski *et al.* 2012, Parsons *et al.* 2013, Groen *et al.* 2014) in Excel.

3 Development of a method for the affinity enrichment of proteins associating with endomembrane markers.

Acknowledgements: All LC-MS/MS analysis was performed by Dr Jan Sklenar, analysis of data generated through LC-MS/MS analysis was partially analysed by Dr Jan Sklenar and partially by William Heard. SAINT analysis was performed by Dr Alex Jones. All other techniques were performed by William Heard. Sections 3.2.3, 3.2.5, 3.2.6, 3.2.7, 3.2.8, 3.2.9 contain data submitted in a paper to Molecular and cellular proteomics.

3.1 Introduction and objectives

3.1.1 Proteomic characterisation of LE/MVBs is the essential first step to understanding the role of LE/MVBs in signalling

Endomembranes are integral to cellular function, as demonstrated by the severe developmental phenotypes that frequently occur in mutants lacking endomembrane regulators, for examples see Mayer *et al.* 1993; Assaad *et al.* 2004; Cai *et al.* 2005; Gendre *et al.* 2013[166]. Yet our knowledge of the plant endomembrane system, and the proteins both regulating and trafficking through it, is limited because of lack of study and low homology to mammalian and yeast systems (discussed in Section 1.2.1).

Great advances have been made in localising proteins to endomembrane compartments, using confocal and electron microscopy. More recently, excellent progress has been made in the plant field with characterising the proteomes of the ER, the vacuole, PM, mitochondria and chloroplasts, and smaller vesicle-like compartments such as peroxisomes and Golgi (Carter *et al.* 2004, Kleffmann *et al.* 2004, Dunkley *et al.* 2006, Eubel *et al.* 2007, Jaquinod *et al.* 2007, Schmidt *et al.* 2007, Eubel *et al.* 2008, Ito *et al.* 2010, Drakakaki *et al.* 2012, Elmore *et al.* 2012, Nikolovski *et al.* 2012, Parsons *et al.* 2012, Groen *et al.* 2014). However, basic proteomic data is minimal for compartments such as LE/MVBs in plants.

The innovative use of proteomic data has led to discoveries that would otherwise not have been possible. For example, using proteomic data of the Golgi and structure-based homology analysis, Nikolovski and colleagues (Nikolovski *et al.* 2012) could identify 12 previously uncharacterised Golgi glycosyltransferase (GT) families. This revealed that there could be up to 30% more GTs in plants than previously estimated. Furthermore it highlights the importance of organelle proteomics in deciphering the biochemical functionality of a compartment.

To better understand the wider functions of LE/MVBs within a cell, we first need a proteome of these compartments. Therefore, my first objective was to develop a method to allow proteomic analysis of LE/MVBs.

3.1.2 RABF2b/ARA7 is a good model for studying LE/MVBs

The term LE/MVB represents a group of endomembrane compartments comprised of membranes and proteins on the endocytic route to the lysosome, or the vacuole in plants (Alberts *et al.* 2008). The identity of a LE/MVB is dictated by the presence of RAB GTPases on the cytosolic face of the membrane that regulate its protein and lipid composition (Saito and Ueda 2009). In plants, late endosome identity is conferred by the RAB5 GTPase family, RABF1/ARA6, RABF2b/ARA7 and RABF2a/RHA1 (Ueda *et al.* 2001, Rutherford and Moore 2002, Lee *et al.* 2004, Ueda *et al.* 2004), and the RAB7 GTPase family, RABG1, RABG2 and RABG3a-f (Rutherford and Moore 2002, Geldner *et al.* 2009). RAB7 family GTPases also have a role at the tonoplast membrane (Nielsen *et al.* 2008). Amongst the LE/MVB population there is a clear distinction between RAB5 and RAB7 labelled structures (Bottanelli *et al.* 2012). The RAB5 family label the earlier 'late' endosome and as the endosome matures, the RAB7 family GTPases are brought onto the membrane by RAB5 family GTPases and their effectors (Cui *et al.* 2014, Lawrence *et al.* 2014). The RAB7 family

GTPases, through the action of their effectors, then prevent association of the RAB5 family GTPases, following the RAB cascade hypothesis (Markgraf *et al.* 2007).

In addition to the distinction between the RAB5 and RAB7 family GTPase labelled endosomes, it is clear that there is diversity between RAB5 family GTPase labelled endosomes. The different RAB5 family GTPases are expressed in different tissues, but they are also functionally distinct (Ueda *et al.* 2004, Ebine *et al.* 2011). Several cargos of the endocytic route pass through these endosome populations and this highlights the functional differences between them. The RLK FLS2 co-localises with both RFP-RABF2b/ARA7 and RABF1/ARA6-RFP after ligand induced endocytosis, but displays up to 90% co-localisation with RFP-RABF2b/ARA7, and only up to 60% co-localisation with RABF1/ARA6-RFP (Beck *et al.* 2012). Similarly, peak co-localisation of FLS2-GFP with RFP-RABF2b/ARA7 occurs at 30 minutes of ligand treatment, whereas for RABF1/ARA6-RFP co-localisation is delayed to 60 minutes of flg22 induced endocytosis (Beck *et al.* 2012).

Despite these differences in functionality of endosomes, for this study I followed the assumption that compartments would be sufficiently biophysically and biochemically similar that RFP-RABF2b/ARA7 endosomes could be used as a model to optimise the protocol for endosome enrichment for proteomic analysis.

3.1.3 Approaches for the preparation of endomembrane compartment proteins for proteomic analysis

Historically the preparation of endomembrane compartments for proteomic analysis has made extensive use of the biophysical properties of a compartment. One of the most common methods for the enrichment of endomembranes for proteomic analysis is in the enrichment of microsomes. This method helps define proteins associating with membranes, reviewed Abas and Luschnig (2010). Microsomes are commonly defined as the membrane fraction spun down at 100,000g from a post-mitochondrial fraction (De Duve 1971, Dallner

1974). This includes a mixture of the endomembrane organelles of the cells studied (varying by species), but predominantly vesicles derived from lysed ER (reviewed in (Abas and Luschnig 2010). Microsome preparations rely on the greater density of endomembrane organelles than the extraction buffer in which they are suspended. Therefore upon a centrifugation (usually ultra-centrifugation of >100 000 g) step, they are pelleted and form a microsome fraction (Abas and Luschnig 2010). Typically there is also a single pre-clearing step to remove unwanted organelles and cell debris e.g. cell walls, nuclei (Abas and Luschnig 2010). There is a subsequent stronger centrifugation step which can be varied depending on the cells analysed. This is a relatively crude preparation, as the aim is to pellet all endomembranes, and compartment specific (amongst the microsome organelles) protein localisation cannot be determined. Furthermore, the microsomal fraction is frequently very difficult to re-suspend, due to the ultracentrifugation steps, and frequently organelles are damaged by the required agitation to re-suspend the microsomal pellet (Abas and Luschnig 2010).

To provide greater organelle resolution to the identification of proteins than a microsomal fractionation, methods of organelle preparation for proteomic analysis were improved, exploiting differences in compartment properties. Endomembrane compartments have different biophysical properties. Different densities and surface charge from lipid composition, protein content and shape provide the opportunity to selectively isolate or enrich compartments using their different biophysical properties. Centrifugation in varying densities of extraction media (often sucrose but other media have been used more recently) allowed the proteomic characterisation of a variety of endomembrane compartments including animal clathrin coated vesicles and synaptic vesicles (reviewed (Castle 2001). Whilst this approach has been successful in some cases, difficulties have been encountered in isolating pure organelles, especially for delicate compartments and those with significant similarities in biophysical properties to other organelles (Dunkley *et al.* 2004, Sadowski *et al.* 2008, Groen and Lilley 2010, Nikolovski *et al.* 2012). This has stimulated the development of

novel approaches employing statistical methods to extract data against a background of noise, circumventing the need for purification entirely.

3.1.4 Statistical methods to identify organelle proteins

Statistical approaches include the Localization of Organelle Proteins by Isotope Tagging (LOPIT) technique (Dunkley *et al.* 2004, Dunkley *et al.* 2006, Sadowski *et al.* 2008, Nikolovski *et al.* 2012) or protein correlation profiling (PCP) (Foster *et al.* 2006). Both techniques assess the co-migration of proteins down a density gradient after centrifugation with known marker proteins from a specified organelle but use different methods for protein quantitation. A protein that co-migrates with a marker protein for a specific organelle is then assigned to that compartment proteome. For these techniques, good quality marker proteins and careful statistical analysis is essential, but specific compartment purification is not. When there were insufficient marker proteins known for an organelle, IP of a known marker (Vacuolar H⁺ ATPase-A1 - VHA-A1) was used to preliminarily characterise the proteome of the plant TGN/EE to allow successful analysis with LOPIT (Groen *et al.* 2013).

3.1.5 Novel purification techniques for organelle proteomics

To improve purity of isolated organelles and as an alternative to density gradient centrifugation, surface charge properties can be used to isolate membrane structures such as the PM (Widell *et al.* 1982, Lund and Fuglsang 2012). In these studies, aqueous polymer solutions are used to separate the membrane structures based on hydrophobicity, a property defined by phospholipid composition etc. (Schindler and Nothwang 2006). The PM is preferentially enriched in the hydrophobic top phase comprised of the aqueous polymer PEG, rather than the lower phase of the aqueous polymer solution of dextran (Schindler and Nothwang 2006). Surface charge was also used in addition to migration in density medium to great effect by Parsons *et al.* 2012 for enrichment and proteomic analysis of the Golgi. Here, an electrical current was applied to a Golgi enriched fraction obtained by sucrose gradient separation to further purify the Golgi. This purification method allowed proteomic

analysis of the plant Golgi and led to elucidation of Apyrase 1(ATAPY1)'s novel function as an NDPase in the Golgi (Parsons *et al.* 2012).

An analogous approach uses the protein identity of a compartment to selectively enrich for the organelle, whereby an affinity binding protein and a corresponding target associated with the membrane of choice are used to target and precipitate the organelle. This can be described as IP of an organelle. The organelle properties (usually density with agarose beads or magnetism with iron beads) of an organelle are changed through binding to a bead through an antibody. The organelle can then be more easily precipitated from solution. This technique has been used to enrich mitochondria (Hornig-Do *et al.* 2009) and even cell line specific nuclei (Deal and Henikoff 2011). Furthermore the technique was more recently established for endomembrane organelles in animals (Morciano *et al.* 2005, Steuble *et al.* 2010) and then plants (Drakakaki *et al.* 2012) to prepare intact CFP-SYP61 labelled TGN vesicles. All of these techniques could be used individually or in combination to enrich LE/MVBs for proteomic analysis.

These IP techniques can yield intact compartments, or at least membrane structures resembling the desired organelles, as determined by electron microscopy (Morciano *et al.* 2005, Steuble *et al.* 2010, Drakakaki *et al.* 2012). It is not necessary, however, to isolate intact compartments to define an organellar proteome. IP of PM membranes from animal cell cultures, obviously disrupts the normal structure of the organelle (as the PM is broken) (Zhang *et al.* 2006) or indeed any enrichment of the PM (Benschop *et al.* 2007, Nühse *et al.* 2007, Tang *et al.* 2008, Keinath *et al.* 2010). Yet biologically relevant proteomic data was obtained through these methods. As long as the protein target is suitably localised and important in the functioning of an organelle, IP will enrich for proteins associating with the target and so localising to the organelle, as demonstrated by IP of VHA-A1 for the description of the TGN proteome (Groen *et al.* 2014). In a similar approach to Groen *et al.* 2014, Fujiwara *et al.* (2014) utilised an IP based method to assess the interactome of

SNAREs. As several SNAREs have defined localisations within the cell, this methodology allows for inference of the proteomes of the compartment to which the SNARE localises (Fujiwara *et al.* 2014). For this approach to be successful, careful choice of marker proteins as IP targets is essential.

3.1.6 Markers have significantly aided research into endomembranes

Marker proteins have proven essential to our understanding of the endomembrane system; identification of diagnostic residents of a compartment allow the definition of that compartment microscopically, biochemically or biophysically. Such markers usually have putative or defined regulatory or structural roles within a compartment. I selected markers that meet these criteria for this study: Golgi transport 1 (GOT1) has a putative role in uncoating Coat protein 2 (COPII) vesicles and is located at the Golgi (Conchon *et al.* 1999, Lorente-Rodríguez *et al.* 2009)); VAMP711 (vacuolar SNARE) marks the tonoplast (Geldner *et al.* 2009); RABD2a/ARA5 (RAB GTPase) labels the secretory route from the Golgi to the TGN to post Golgi vesicles; Clathrin light chain 2 (CLC2) is an integral component of clathrin coated structures trafficking from the PM and the TGN/EE. To label endosomal compartments, RABF2b/ARA7 and RABF1/ARA6 (both RAB 5 GTPases) are used as LE/MVB markers, whilst RABG3f (RAB 7 GTPase) labels both the LE/MVB and tonoplast. Collectively, these markers act as a powerful suite of tools to assess diverse endomembrane organelles.

None of these markers have been tested for complementation. Without this data, it cannot be concluded as to whether the compartments labelled are biologically relevant. These markers are, however, frequently used for co-localisation studies and so proteomic data obtained using these markers is useful as it directly applies to the markers used, rather than the represented biological compartments. Furthermore, these markers are being expressed under a constitutive promoter. The UBG10 promoter expresses to lower levels than the 35s promoter but there is still overexpression (Grefen *et al.* 2010). This can also result in

artefacts, for example overexpression of RAB GTPases results in enlargement of the labelled compartments (Spallek *et al.* 2013).

3.1.7 Objectives

In order to meet my overall aims of assessing the role of endosomes in signal transduction, I required proteomic data for endosomes. Therefore, in this chapter, I aim to develop a method to suitably enrich endosome proteins, using RABF2b/ARA7 initially as a marker, and expanding to other endosome markers. Then I will utilise this method to proteomically characterise other endomembrane compartments.

3.2 Results

3.2.1 RFP-RABF2b/ARA7 co-fractionates with the ER and PM on a sucrose gradient

In order to biophysically characterise the RFP-RABF2b/ARA7 endosomes in relation to other endomembrane compartments, I tested their migration on a sucrose gradient. Microsomes were prepared, re-suspended in 25% sucrose gradient buffer, quantified with BCA assay and 9 mg of protein was layered on a sucrose gradient (30-55% sucrose) and centrifuged at 100 000 g x 18 hrs. I collected 12, 1 ml fractions from the bottom of the gradient, and took 12.5 µl of each fraction with 6 µg of microsomal and cytosolic protein for SDS-PAGE. Distribution of RFP-RABF2b/ARA7 endosomes, PM, ER, chloroplasts/cytosol and Golgi vesicles was then assessed with immunoblot using αRFP, αFLS2/αAHA1, αBIP2, αRbcL and αSEC21 respectively (Figure 3.1). RFP-RABF2b/ARA7 co-fractionated partially with the PM, ER and cytosol. However, the majority of the RFP-RABF2b/ARA7 appears in lighter fractions of around 35% sucrose, whilst the majority of the ER and PM were found in the denser fractions of >40% sucrose.

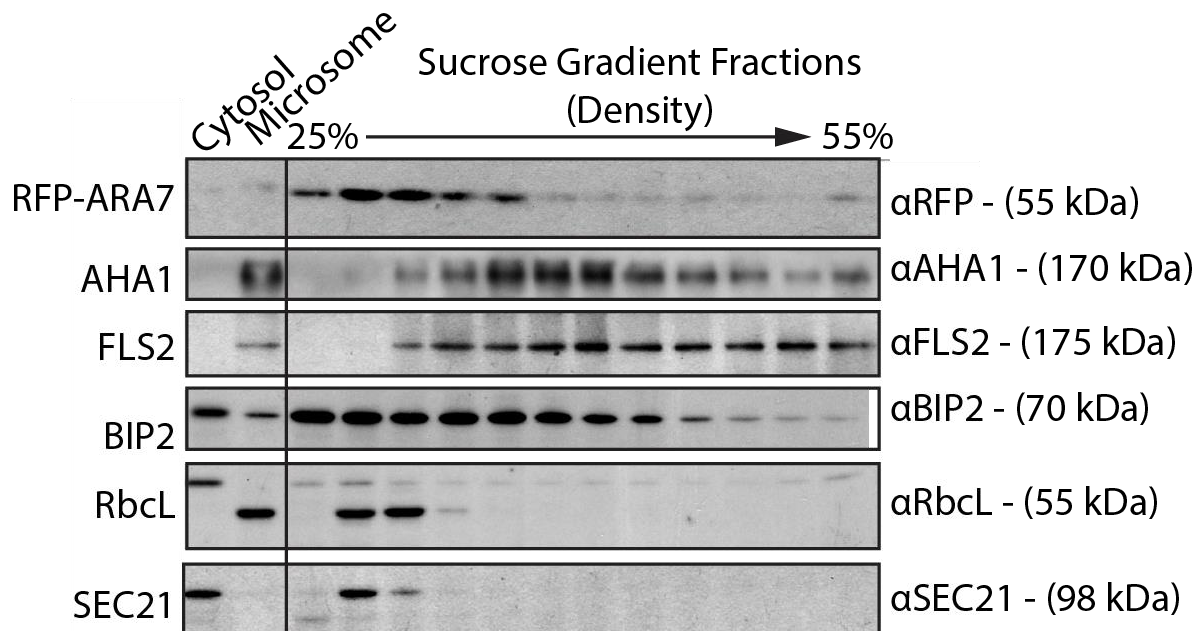


Figure 3.1. Co-fractionation of organelles on a sucrose gradient. A microsome fraction from *A. thaliana* stably expressing RFP-RABF2b/ARA7, was fractionated on a 25-55% sucrose gradient followed by immunoblot, along with total microsomal and cytosolic fractions with α RFP, BIP2, Sec21, FLS2, RbcL, AHA1 as indicated.

3.2.2 RFP-RABF2b/ARA7 endosomes can be biochemically separated from the cytosol and ER but not the PM

Using the knowledge of ER, PM and RFP-RABF2b/ARA7 migration in sucrose gradients, I developed a modified microsome production protocol to deplete ER, cytosol and PM from the RFP-RABF2b/ARA7 enriched microsome. A crude extract of protein was prepared from *A. thaliana* expressing RFP-RABF2b/ARA7 in 15% sucrose gradient buffer and loaded onto a 35%, 45% stepped sucrose gradient and centrifuged at 100 000 g x 1 hr. I used a single step purification strategy, rather than a two-step microsome preparation, for simplicity, and to avoid the need for re-suspension of the microsomal pellet.

Fractions were collected from the 15%, 35%, 45% sucrose steps and from the interfaces, and 12.5 μ l analysed with SDS-PAGE and immunoblot (Figure 3.2). I tested for abundance of RFP-RABF2b/ARA7, PM, ER, cytosol and Golgi vesicles using α RFP, α FLS2/ α AHA1, α BIP2, α HSP70 and α SEC21 respectively. The majority of the RFP-RABF2b/ARA7 was

detected in the 35% fraction and the associated interfaces. In addition, there was a depletion of ER in the 35% and interface fractions, however, the PM was also predominantly detected in the 35% fraction. Therefore I concluded it was unlikely that I could achieve a pure fraction of RFP-RABF2b/ARA7 labelled endosomes using biophysical properties alone.

The identification of BIP2 (a soluble ER marker protein) only in the most dense pellet of the gradient also demonstrates that this method of tissue lysis (pestle and mortar grinding on liquid nitrogen) can yield intact organelles. If the ER was broken, then BIP2 should be identified in the predominantly cytosolic top 15% fraction, which it is not (Figure 3.2). As the ER's structure is substantially more elaborate than those of vesicular endosomes, it is likely that the LE/MVBs are intact as well.

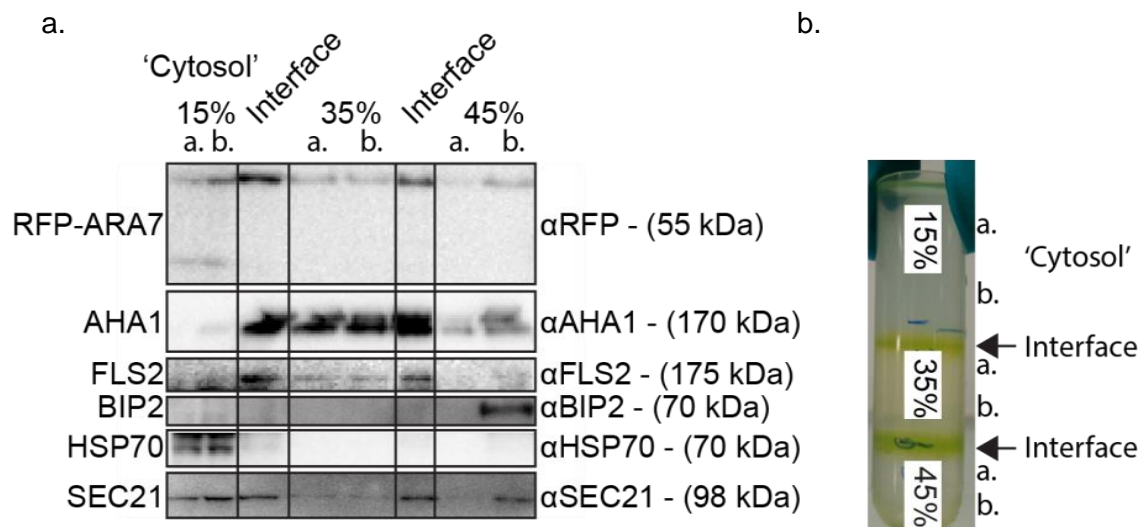


Figure 3.2.A 3 step sucrose gradient to remove cytosol and ER from crude extract. A crude extract (in 15% sucrose) from *A. thaliana* stably expressing RFP-RABF2b/ARA7, was fractionated on two 35%-45% sucrose steps followed by immunoblot with α RFP, BIP2, Sec21, FLS2, Hsp70, AHA1 as indicated. b. is a photograph of the resulting gradient after centrifugation. Percentages represent sucrose concentration (w/v).

3.2.3 Immuno-purification gives a significant enrichment of endosome markers with minimal endoplasmic reticulum and plasma membrane contamination

To test whether I could use IP of RFP to enrich for RFP-RABF2b/ARA7, and associating proteins, whilst depleting other contaminating organelles, I analysed a variety of IP buffers with different additives. IPs of RFP-RABF2b/ARA7 and Col-0 as a control were analysed with SDS-PAGE and colloidal Coomassie stain (Figure 3.3). Visual inspection shows that an addition of 0.01% (v/v) IGEPAL CA-630 yields a good enrichment of RFP-RABF2b/ARA7, and other proteins, with the least contamination in the control lane. This concentration of IGEPAL CA-630 was used as it is below the critical micelle concentration 0.29 mM or 0.0179%, v/v (Piercenet.com) of this detergent and so should prevent the lysis of membrane structures.

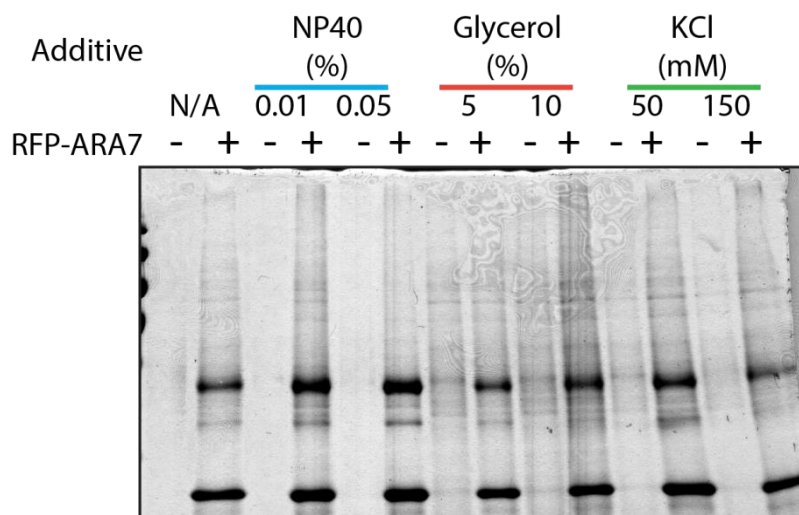


Figure 3.3. SDS-PAGE comparison of immune-purifications with different additives. Total extracts from *A. thaliana*, stably expressing RFP-RABF2b/ARA7 were subjected to immuno-affinity enrichment of RFP followed by SDS-PAGE and coomassie stain.

To further interrogate the level of contamination of our IP protocol, I used IP of RFP and YFP to enrich RFP-RABF2b/ARA7 (IP - RFP) and a LE/MVB/tonoplast marker YFP-RABG3f (IP - YFP) from *A. thaliana* expressing the relevant fusion proteins and Col-0 as a control. 10% of

the IP in each case was used for SDS-PAGE and immunoblot for RFP-RABF2b/ARA7, RABG3f and markers for the ER, Mitochondria, chloroplasts/cytosol and PM (α RFP, α GFP, α ER, α COXII, α RbcL and α AHA1 respectively).

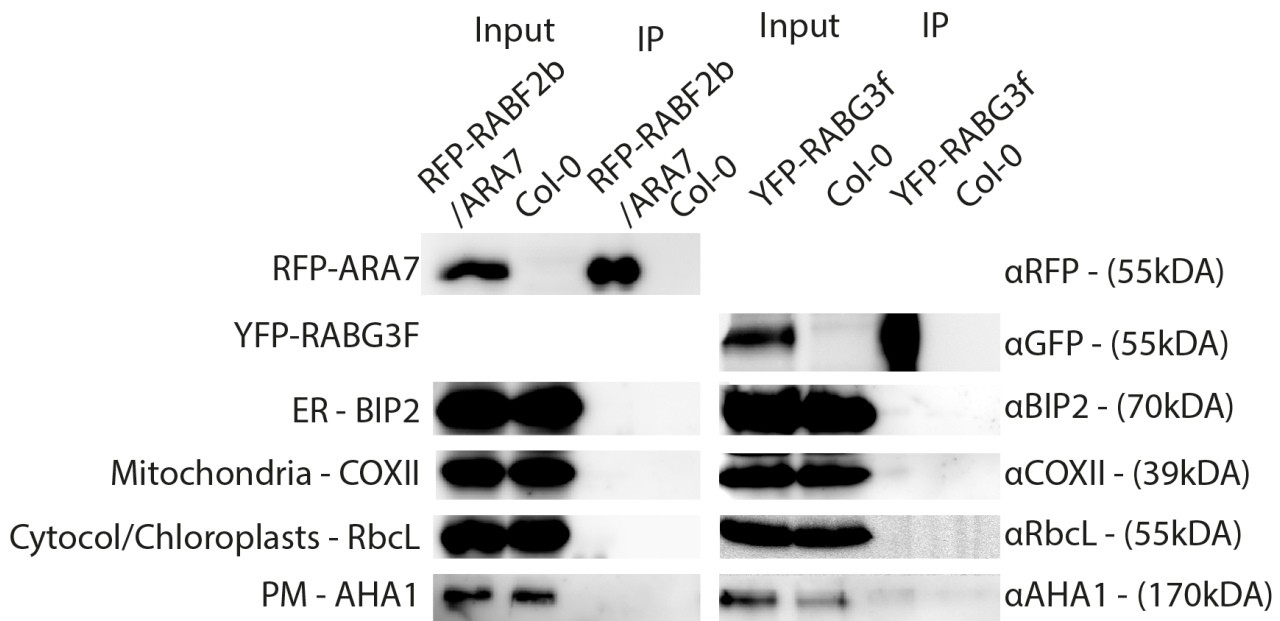


Figure 3.4. Immunoblotting of RFP-RABF2b/ARA7 and YFP-RABG3f enrichments to determine organelle contamination. Total protein extracts, from *A. thaliana* Col-0 or stably expressing RFP-RABF2b/ARA7 or YFP-RABG3f, were subjected to immunoaffinity enrichment of RFP or YFP followed by immunoblot with α RFP, GFP, BIP2, COXII, RbcL, AHA1 as indicated.

Whilst all organelles could be easily detected in the inputs of Col-0, RFP-RABF2b/ARA7 and YFP-RABG3f (Figure 3.4), they could not be detected with this system in the IPs. Whilst these immunoblots demonstrate that the endosome marker alone can be enriched with IP, I was unable to assess the co-enrichment of other known associating proteins, e.g. Vacuolar protein sorting 9a (VPS9a), VAMP727, Suppressor of K⁺ Transport Growth Defect1 (SKD1) for RABF2b/ARA7, as no suitable antibodies could be obtained. However, based on this data, I concluded that a good enrichment of an endosomal marker can be achieved with IP and a much greater depletion of contaminating organelles, compared to using sucrose gradients alone.

3.2.4 Pre-fractionated input to an IP does not reduce contamination with unwanted proteins

To determine whether RABF2b/ARA7 associating proteins could be co enriched with our IP method I performed IP of YFP-RABF2b/ARA7 (Col-0 seedlings as a control) from a crude extract followed by SDS-PAGE fractionation, tryptic digest and LC-MS/MS. Strikingly undesirable organelle proteins (e.g. from the ER and cytosol) could be detected, even though they were not detected with immunoblot. Therefore, I also performed IP of GFP from a fractionated input from the 35% and interface fractions (Figure 3.2) of Col-0 and YFP-RABF2b/ARA7 expressing seedlings followed by SDS-PAGE fractionation, tryptic digest and LC-MS/MS. A brief summary of the MS data is presented in Figure 3.5. Known RABF2b/ARA7 proteome proteins are detected in both IPs from crude and a fractionated input (Figure 3.5a). The fractionated IP yielded a smaller percentage of spectra assigned to RABF2b/ARA7 proteome proteins and a larger percentage of spectra assigned to ER proteins. Furthermore there were roughly equal numbers of spectra assigned to keratin, trypsin and ribosomes (I assumed these to be contaminants) in the IPs from crude and fractionated inputs. Therefore I surmised that there was no benefit to IP from a pre-fractionated sample and all further IPs are from crude extract. Furthermore, the contaminating proteins examined with Figure 3.5 are present at similar abundances in both Col-0 control and YFP-RABF2b/ARA7 IPs, therefore are likely to be sticking to the affinity beads. This demonstrates the need for good controls when using this protocol for organelle proteomics.

3.2.5 Affinity purification of seven different endomembrane compartment markers

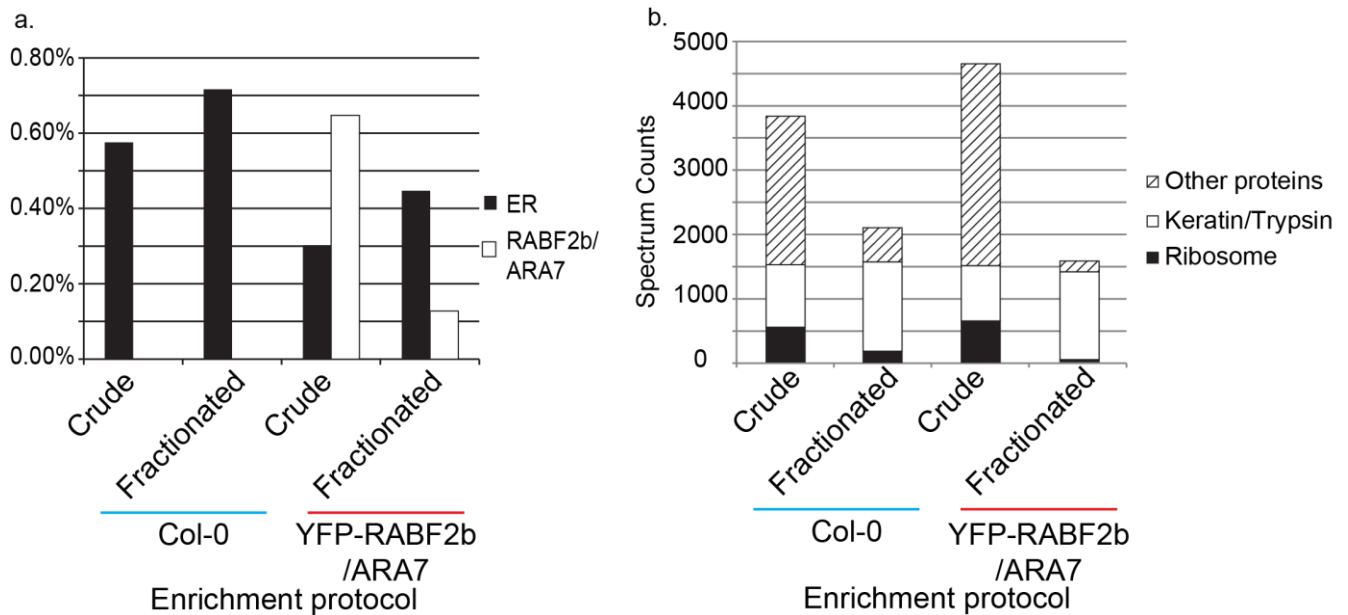


Figure 3.5. MS assessment of pre-fractionation on levels of contaminating proteins in IP of YFP-RABF2b/ARA7. Crude extracts of proteins from *A.thaliana* stably expressing YFP-ARA7 were subjected immuno-affinity enrichment of YFP, run on SDS-PAGE, tryptically digested and subsequently analysed with LC-MS/MS. A. Comparison of percentage of total spectra assigned to the ER or RABF2b/ARA7 endosomes in affinity enrichments of YFP-RABF2b/ARA7 from *A. thaliana*. B. Comparison of total number of spectra assigned keratin/trypsin, ribosomal proteins and other proteins.

To provide adequate controls for my survey of endosomal proteomes, I chose seven endomembrane marker proteins for numerous different endomembrane organelles (Figure 3.6a). Details of the marker proteins, their mammalian and yeast homologs are presented in Table 3.1 and in Section 3.1.6. All of these markers were under the control of constitutive promoters to ensure expression in all plant tissues - UBQ10 (Ueda *et al.* 2001, Ueda *et al.* 2004, Grefen *et al.* 2010) or 35s for CLC2-GFP (Konopka *et al.* 2008). Expression of protein markers was confirmed in leaf epidermal cells using CLSM (Figure 3.6b). RFP-RABF2b/ARA7, YFP-RABF2b/ARA7, RABF1/ARA6-RFP, YFP-RABD2a/ARA5, CLC2-GFP and YFP-GOT1 localise predominantly to motile cytoplasmic structures. YFP-RABG3f localises to both cytoplasmic structures and a membrane resembling the tonoplast. YFP-VAMP711 localises to a membrane structure resembling the tonoplast. These data are

in accordance with their reported localisations (Ueda *et al.* 2001, Ueda *et al.* 2004, Konopka *et al.* 2008, Geldner *et al.* 2009).

ATG	<i>A.thaliana</i>	Mammals	<i>S.cerevisiae</i>	<i>S.pombe</i>	Construct	Localisation
AT3G18820	RABG3f	RAB7	YPT7	YPT7	YFP-RabG3f	Vac/LE/MVB
AT4G19640	ARA7/RABF2b	RAB5	YPT51/52/53	YPT5	RFP-RABF2b/ARA7	LE/MVB
AT3G54840	ARA6/RABF1	RAB22			RABF1/ARA6-RFP	LE/MVB
AT1G02130	ARA5/RABD2a	RAB1	YPT1	YPT1	YFP-RABD2a/ARA5	Golgi/TGN/SV
AT4G32150	VAMP711	VAMP7	YKT6	sec22	YFP-VAMP711	Vac
AT2G40060	CLC2	CLTB	CLC1	CLC	CLC2-GFP	CCV
AT3G03180	GOT1	GOT1A	GOT1p	GOT1	YFP-GOT1	Golgi

Table 3.1. Affinity purification baits and their homologs in Mammals and Yeasts.

ATG numbers and *A.thaliana* short names are from TAIR. Homologs were identified from published works.

To evaluate the proteomes of the various endomembrane compartments, I utilised the IP approach detailed above (Section 3.2.3) for the affinity purification of endomembrane markers (Figure 3.6) canonical of several endomembrane compartments. For this, crude protein extracts from sterile grown *A. thaliana* seedlings stably expressing the different endomembrane markers listed (YFP-RABG3f, YFP-GOT1, YFP-VAMP711, YFP-RABD2a/ARA5, CLC-GFP, RFP-RABF2b/ARA7, RABF1/ARA6-RFP) above were subjected to IP for YFP/RFP/GFP as appropriate, proteins fractionated by SDS-PAGE, gel slices tryptically digested, and analysed with LC-MS/MS. The IP, SDS-PAGE, digestion and LC-MS/MS (Orbitrap XL) analysis for each protein was repeated three times. Supplemental controls were also added using IP of YFP and mCherry, digested in solution and analysed with an Orbitrap Fusion.

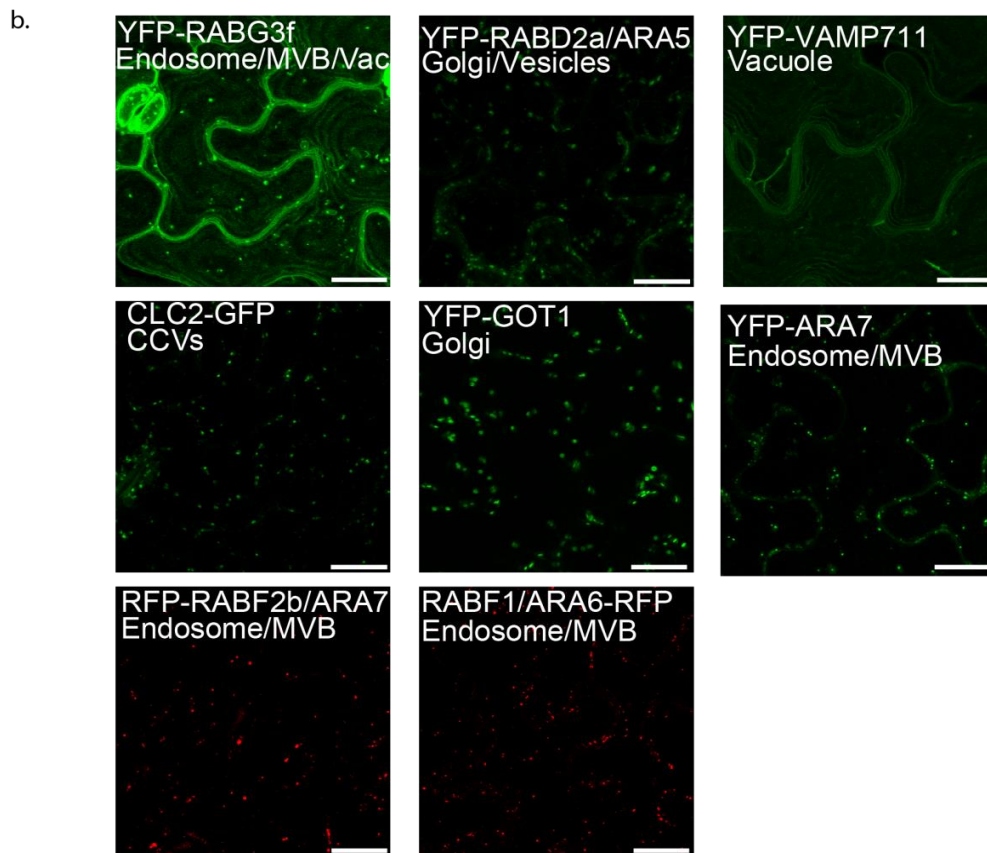
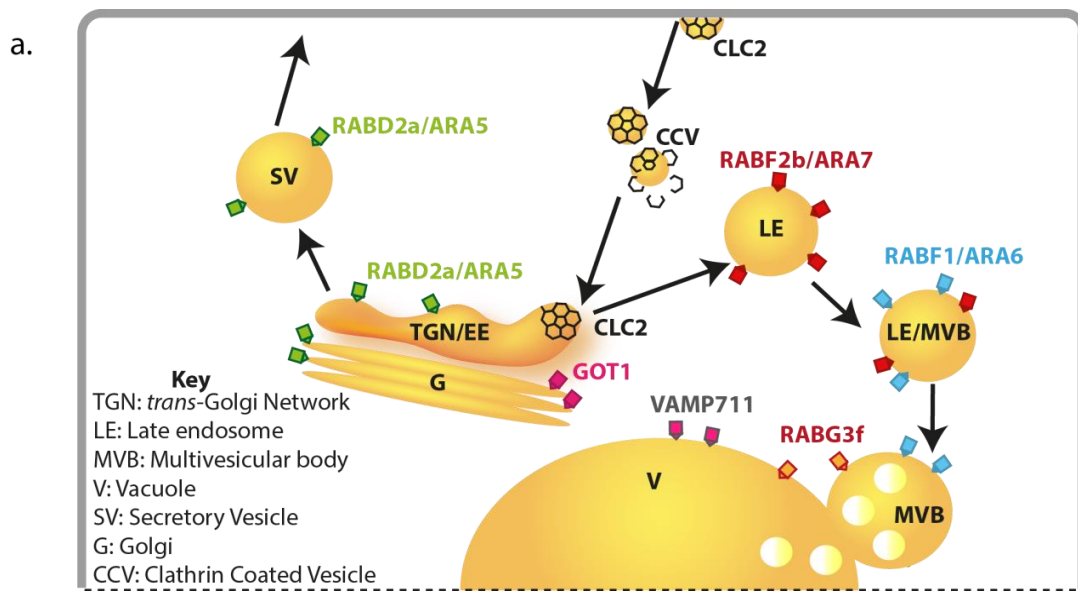


Figure 3.6. Endomembrane targets. a. Schematic overview of the endomembrane marker proteins used in this study and their localisations. RABD2a/ARA5 – post-Golgi/Golgi/TGN/Secretory vesicles (SV), RABF1/ARA6 – LE/MVBs, RABF2b/ARA7 – LE/MVBs, CLC2 – Clathrin Coated Vesicles, GOT1 – Golgi, RABG3f – LE/MVB/Vacuole, VAMP711 – Vacuole. b. Localisation of fluorescent-tagged marker proteins. Standard confocal micrographs of leaf epidermal cells of *A. thaliana* transgenic plants stably expressing the indicated recombinant proteins. Scale bars 10 μ M. Pattern of localisation was observed in all 8 of 8 images per genotype. References: pUBQ10:YFP-RabG3f, YFP-RABD2a/ARA5, YFP-VAMP711, YFP-Got1 [11], RABF1/ARA6-RFP, RFP-RABF2b/ARA7 (provided by K. Schumacher, Heidelberg, Germany), p35S:CLC-GFP (provided by S. Bednarek, Madison WI, USA).

	Total number of proteins	Number of unique proteins	% previously identified	% membrane associated
YFP-RABD2a/ARA5	120	22	18%	34%
RABF1/ARA6-RFP	63	9	14%	33%
RFP-RABF2b/ARA7	279	121	43%	33%
CLC2-GFP	49	15	31%	24%
YFP-GOT1	62	30	48%	77%
YFP-RABG3f	136	42	31%	22%
YFP-VAMP711	51	12	24%	41%

Table 3.2. Numbers of proteins identified in affinity purifications. Proteins that were identified in and unique to (according to criteria in materials and methods) each affinity purification. Percentage of proteins identified in selected previous proteomic studies was calculated from whether a protein was identified in Nikolovski et al. 2012, Parsons et al. 2012, Sadowski et al. 2008, Dunkley et al. 2006, Drakakaki et al. 2012. Percentage of proteins with membrane associations was calculated using annotations from Uniprot (<http://www.uniprot.org>) and TAIR (<http://www.arabidopsis.org/>) as described in the materials and methods.

3.2.6 Proteomic analysis reveals a large degree of overlap between proteomes

To determine whether the proteomic data from all 21 IPs was suitable for further analysis, I examined the combined dataset. Using LC-MS/MS we identified a total of 159903 peptides corresponding to 2526 proteins; the respective proteins, peptides and spectrum counts for each affinity based purification are listed in Table S1. The reproducibility of the identification of each protein, using analysis by SAINT (Choi *et al.* 2011) Table S2. Proteins were accepted as enriched by a specific affinity bait if the protein was identified in at least two of three replicate affinity purifications. This criterion substantially reduced the total number of accepted proteins to 433 (Table 3.2). Most proteins were identified from RFP-RABF2b/ARA7 affinity-purifications, with 279 proteins assigned. This bait also had the highest number of unique proteins assigned to its proteome; 121. The CLC2-GFP proteome had the smallest number of total proteins, 49, of which 15 were unique to that bait (Table 3.2).

To visualise the differences and commonalities in the seven affinity enrichments I used the Sungear tool from Virtual plant (Poultney *et al.* 2007) (Figure3.7). The CLC2-GFP and YFP-VAMP711 proteomes are clearly distinct from the other proteome. There are also substantial pair wise and collective overlaps between the RFP-RABF2b/ARA7, RABF1/ARA6-RFP and YFP-RABG3f. However, complex comparisons between all groups can be drawn, therefore, in addition to the analysis below, the full set of proteins associated with each group in the Sungear diagram can be explored using filters in Table S3.

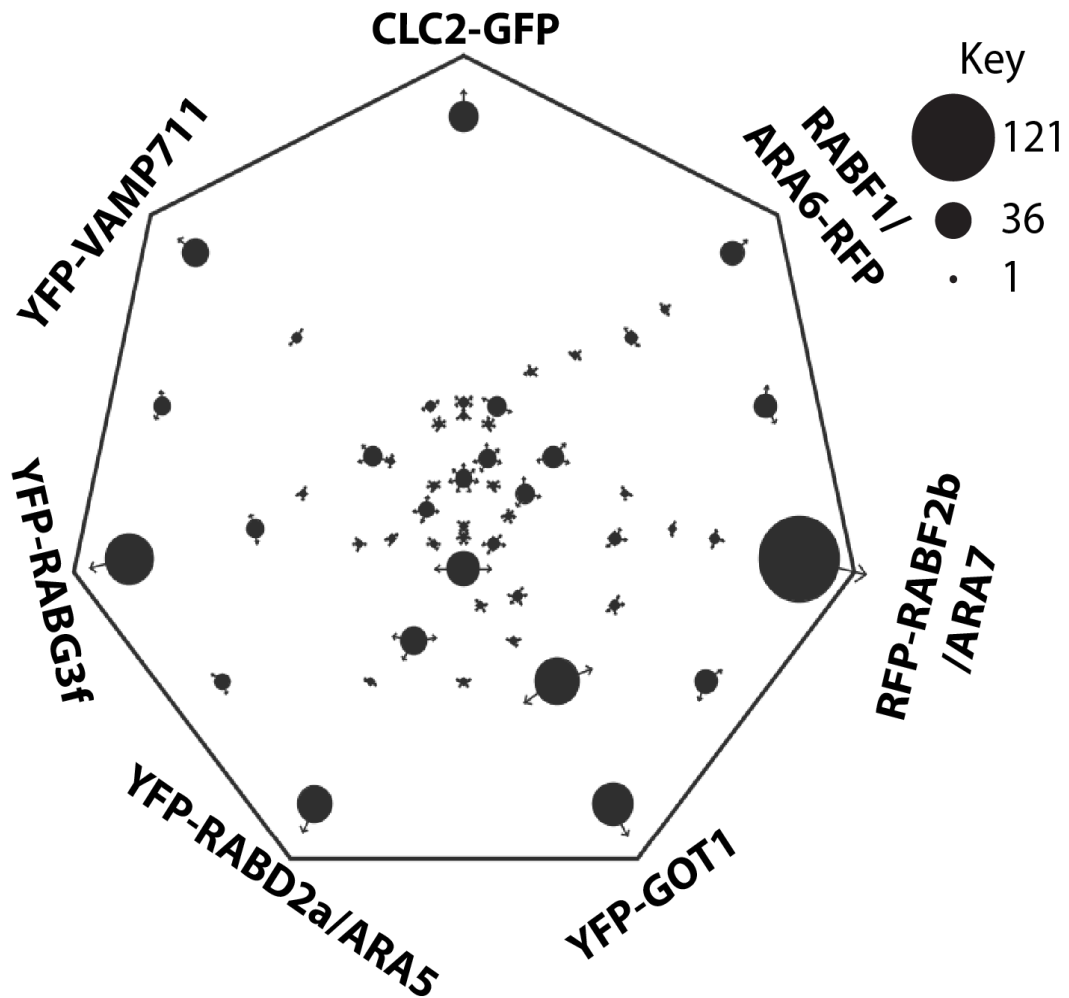


Figure 3.7. Sungear diagram of proteins assigned to the different proteomes. Sungear diagrams generated in virtual plant (<http://virtualplant-prod.bio.nyu.edu/cgi-bin/sungear/index.cgi>) (Poultney et al. 2007). Groups of proteins are indicated by the black dots, with a size proportional to the number of proteins in the group. The arrows on each dot point to the proteome assignment of a group of proteins. Enrichments were performed three times for each bait, proteins were accepted when they were more than two times more abundant, or unique to, the marker enrichment compared to the control.

3.2.7 YFP-GOT1 is not amenable to tryptic digests

All affinity purifications had many assigned spectra to the relevant fluorescent protein tag and most have assigned spectra to the target protein in the corresponding enrichment

ATG	Group	Short name	YFP-RABD2a/ARA5	RABF1/ARA6-RFP	RFP-RABF2b/ARA7	CLC2-GFP	YFP-GOT1	YFP-RABG3f	YFP-VAMP711
AT5G22780	CCV	Adaptin α 2	NS	NS	11	NS	NS	A	A
AT2G25430		ECA4	NS	NS	NS	73	A	43	NS
AT4G32285		CAP1	NS	NS	60	NS	A	A	A
AT3G11130		CHC1	NS	NS	NS	29	NS	NS	NS
AT3G08530		CHC2	NS	NS	NS	60	NS	A	A
AT2G20760		CLC1	A	NS	NS	18	A	A	A
AT2G40060		CLC2	NS	NS	A	110	NS	A	A
AT4G33650		DRP3A	8	NS	10	7	NS	NS	NS
AT1G10290		DRP2A	NS	NS	NS	NS	NS	NS	3
AT4G34660		SH3PH	A	A	NS	40	A	A	A
AT1G52360		Coatomer	Coatomer β ' (SEC27p)	5	4	10	NS	NS	7
AT4G31480	Coatomer β (SEC26p)		NS	A	A	NS	A	11	NS
AT4G31490	Coatomer β (SEC26p)		NS	NS	13	NS	NS	A	A
AT1G62020	Coatomer α (RET1p)		16	16	21	NS	NS	12	7
AT2G21390	Coatomer α (RET1p)		6	7	9	NS	NS	6	NS
AT5G05010	Coatomer δ (RET2p)		10	NS	10	NS	NS	NS	NS
AT3G63460	SEC31B		8	6	10	NS	NS	NS	NS
AT5G16300	COG	COG1/VPS51	33	NS	120	NS	NS	NS	NS
AT4G24840		COG2	NS	NS	37	NS	NS	NS	A
AT1G67930		COG5	NS	NS	20	A	NS	A	A
AT5G51430		COG7	27	NS	50	NS	A	NS	NS
AT5G11980		COG8	30	NS	47	NS	NS	NS	A

AT2G27600	ESCRT	VPS4	NS	NS	7	A	NS	8	A
AT5G03540	EXOCYST	EXO70A1	NS	NS	60	NS	A	NS	A
AT5G59730		EXO70H7	NS	NS	30	NS	A	A	A
AT5G49830		EXO84B/VPS51	NS	NS	40	NS	NS	23	NS
AT5G12370		SEC10	9	NS	12	NS	NS	NS	NS
AT1G47550		SEC3A	NS	NS	NS	NS	NS	33	NS
AT1G76850		SEC5A	NS	NS	107	NS	NS	NS	NS
AT3G10380		SEC8	20	12	29	10	NS	12	NS
AT4G02030		GARP	VPS51	NS	NS	8	NS	A	NS
AT1G71270	VPS52		33	40	50	40	NS	37	NS
AT1G50500	VPS53		37	NS	87	NS	NS	60	NS
AT4G19490	VPS54		15	NS	46	NS	NS	NS	NS
AT3G60860	GEF	BIG2	24	NS	60	NS	A	NS	NS
AT1G01960		BIG3	15	NS	33	8	NS	9	NS
AT3G43300		BIG5/MIN7	16	NS	23	NS	NS	11	NS
AT1G13980		GNOM	53	NS	97	NS	NS	NS	A
AT2G01470		SEC12	NS	NS	NS	A	NS	NS	33
AT1G16920	GTPase	AtRABA1b	7	NS	5	NS	NS	NS	NS
AT4G18800		AtRABA1d	NS	NS	33	NS	NS	NS	117
AT3G46830		AtRABA2c	14	NS	NS	A	NS	38	NS
AT4G17170		AtRABB1c	NS	NS	NS	NS	NS	6	4
AT1G43890		AtRABC1	NS	12	NS	NS	NS	7	A
AT3G11730		AtRABD1	A	NS	NS	NS	NS	30	NS
AT1G02130		AtRABD2a	56	NS	NS	NS	NS	NS	NS
AT5G47200		AtRABD2b	NS	NS	10	NS	NS	11	7
AT3G54840		AtRABF1	NS	195	NS	NS	A	NS	A
AT4G19640		AtRABF2b	100	272	2330	NS	NS	76	NS
AT3G18820		AtRABG3f	NS	NS	NS	A	NS	120	9
AT2G44610		AtRABH1b	NS	NS	NS	NS	NS	6	NS

AT3G56110	RAB regulator	AtPRA1.B1	NS	A	117	A	53	NS	A
AT2G40380		AtPRA1.B2	NS	A	NS	A	60	NS	A
AT2G38360		AtPRA1.B4	NS	NS	110	A	NS	NS	NS
AT2G44100		GDI1	NS	A	57	A	A	657	A
AT3G59920		GDI2	NS	A	NS	A	A	177	A
AT3G19770		VPS9a	A	NS	130	A	A	A	A
AT4G30260		YIP4b	62	NS	104	A	A	NS	NS
AT3G05280		YIP5b	80	A	NS	A	NS	NS	60
AT1G75850		Retromer	VPS35A	NS	A	NS	A	A	40
AT2G17790	VPS35B		NS	NS	NS	A	A	43	A
AT5G06140	SNX1		NS	NS	53	NS	A	NS	NS
AT2G45200	SNARE	GOS12	NS	A	A	NS	40	A	A
AT4G04910		NSF	70	NS	113	NS	70	NS	93
AT3G05710		SYP43	NS	A	23	A	A	A	NS
AT1G16240		SYP51	NS	NS	NS	A	A	NS	53
AT4G32150		VAMP711	A	NS	NS	A	NS	A	1713
AT1G04750		VAMP721	A	A	A	A	A	A	167
AT2G33120		VAMP722	33	9	16	NS	6	18	A
AT3G54300		VAMP727	NS	NS	40	A	A	A	A
AT3G27530	Tether	GC6	NS	NS	17	NS	NS	NS	A
AT1G21630	TPLATE complex	EH2	NS	NS	NS	20	A	A	A
AT2G07360		TASH3	8	NS	6	5	A	A	NS
AT5G57460		TML	23	NS	NS	NS	A	A	A
AT3G01780		TPLATE	NS	7	10	NS	NS	NS	NS
AT3G50590		TWD40-1	6	NS	8	NS	NS	A	A
AT5G24710		TWD40-2	NS	NS	NS	10	A	NS	A
AT5G11040	TRAPP	TRS120	NS	23	NS	A	A	NS	NS
AT5G16280		TRS85	417	NS	NS	A	NS	53	NS
AT3G52850	VSR	VSR1	NS	NS	52	A	NS	A	NS

AT2G14740	VSR3	A	A	A	A	A	A	47
AT2G14720	VSR4	NS	NS	147	A	A	NS	A

Table 3.3. Endomembrane regulators identified in affinity purifications. Summed spectrum counts (over each replicate) of each affinity purification. Cells are highlighted when the protein was significantly enriched (using the SAINT analysis described in materials and methods) in an affinity purification. If a protein was absent in an IP it is annotated as A, if a protein was detected but not significantly enriched it is annotated as NS. Annotations for inclusion in a complex were manually curated from literature (Vernoud *et al.* 2003, Uemura *et al.* 2004, Latijnhouwers *et al.* 2005, Masclaux *et al.* 2005, Latijnhouwers *et al.* 2007, Robinson *et al.* 2007, Alvim Kamei *et al.* 2008, Geldner *et al.* 2009, Schellmann and Pimpl 2009, Thellmann *et al.* 2010, Zhang *et al.* 2010, Chen *et al.* 2011, Shahriari *et al.* 2011, Gendre *et al.* 2013, Gadeyne *et al.* 2014).

3.2.9 This IP approach identifies more proteins transiently associating with endomembranes than identified in other proteomic studies

To compare the proteomes defined in this study with those of other published proteomic studies, I compiled a database of proteins identified in six proteomic studies. These are: the CFP-SYP61 proteome (TGN/EE) (Drakakaki *et al.* 2012), VHA-a1-GFP (TGN/EE) (Groen *et al.* 2014), ER, Golgi, Mitochondria/Plastid, PM, Vacuole (Nikolovski *et al.* 2012), Golgi (Parsons *et al.* 2012), ER, Golgi, Mitochondria/Plastid/PM/Vacuole (combined from (Dunkley *et al.* 2006, Sadowski *et al.* 2008)). For each of the proteins identified in all studies I curated the annotations from the Uniprot database (<http://www.uniprot.org>) and the TAIR10 database (<http://www.arabidopsis.org>). Using this data, I extended the analysis to include predicted transmembrane domains and membrane associated modifications (Table 3.2, Table S3). Overall, I identified 64 proteins with one transmembrane domain and 58 with multiple transmembrane domains, 12 proteins with membrane association lipid modifications (these were predominantly RAB GTPase proteins of various classes that are commonly prenylated), and a diverse set of 63 potentially S-acylated proteins (Table S3). The remaining 63% of our dataset did not have any membrane association motifs. This suggests that my IP method preferentially enriches for proteins transiently associating with compartments, when compared to other methods.

The proportions of proteins in each proteome with membrane association motifs varied across the enrichments; YFP-GOT1 had the greatest at 77%, whilst YFP-RABG3f has the smallest proportion of membrane-associated proteins, 22% (Table 3.2). The proportion of YFP-GOT1 membrane associated proteins is comparable to specific Golgi or TGN/EE proteomic studies such as 77% (Drakakaki *et al.* 2012) or 65% (Parsons *et al.* 2012). That the other affinity baits, such as RFP-RABF2b/ARA7 endosomes, show a lower proportion of membrane associated proteins is likely to be a consequence of the choice of bait protein for IP and my methodology.

The lower proportion (compared to Drakakaki *et al.* 2012 and Parsons *et al.* 2012) of membrane associated proteins in my proteomic dataset raises the possibility that this approach identifies more proteins with transient membrane interactions, such as vesicle coats (e.g. COPI and COPII), motor proteins (e.g. myosins), and endomembrane tethers (Table 3.3), cargo proteins. This is to be expected with my choice of baits, which are regulators that affect cytosolic protein recruitment, e.g. RAB GTPases. In addition this protocol does not contain long centrifugation steps or carbonate washes, as used in other protocols. Both of these steps will reduce the number of transiently associating proteins identified in the enrichment and may explain why I observe an enhanced number of these proteins using this IP method.

3.3 Discussion

I have developed a methodology for the purification of endomembrane compartments that share biophysical and biochemical characteristics in a single cell. Targeted IP of marker proteins allows for distinct proteomic characterisation of these compartments. The proteomic data produced with this method is relatively free from contaminating organelle markers and enhances the number of peripherally associated proteins relative to other methods. Thus, the data obtained by application of this method provides a valuable list of candidate proteins associated with the function and regulation of each organelle. Using these lists as a starting point, in depth analysis and predictions will validate the specificity of the data and provide the framework for comprehensive proteomic characterisation of endomembrane proteomes.

3.3.1 Endomembrane compartments require extensive biophysical knowledge to purify

The preliminary work presented in Section 3.2.1 and 3.2.2 (Figures 3.1 and 3.2) demonstrates that RFP-RABF2b/ARA7 labelled endosomes cannot be purified by density gradient centrifugation alone. It is likely that this principle applies to most endosomal compartments. Therefore I concluded that an alternative approach was necessary to achieve

our aims of a simple, broadly applicable, high throughput method to provide an insight into these, largely uncharacterised, proteomes.

I made use of extensive in department experience (Schwessinger *et al.* 2011, Kadota *et al.* 2014) and literature survey of IP methods to develop a protocol for the selective IP of marker proteins; affinity purification of proteins associating with the diagnostic marker proteins for given endomembrane compartments. The use of 0.01% IGEPAL CA-630 as an additive to the extraction buffer reduces the non-specific binding of proteins to the beads (Figure 3.3) and this is true for YFP tagged RAB GTPases (YFP-RABG3f) as well as RFP-RABF2b/ARA7. In addition, IP directly from a crude extraction of proteins is the best compromise between relevant protein yield and purity.

3.3.2 Limitations of this IP method

In this method I did not remove the cytoplasm prior to IP. Not removing the cytosol from the extraction procedure will change the nature of the enrichment. IP of RAB GTPases will extract proteins interacting with the bait whilst it is in the cytosol as well as on membranes. However, current knowledge of RAB GTPases suggests that, with the exception of RAB activation suppressors (GDP dissociation inhibitors - GDIs) (Saito and Ueda 2009), they have minimal interaction with other proteins in the cytosol while in their inactive state. Following this assumption, both GDIs and RAB activators are identified in my proteomic data. Therefore, on balance, the benefits yielded by reduced contamination in the fractions, and the increased yield and speed of the preparation, I determined that this method was suitable for further analysis of endosome, and other endomembrane compartment, proteomes.

One principal question is whether intact compartments can be enriched with this method. Whilst not relevant to the aims of this thesis, as discussed in section 3.1.5, this is a pertinent question. Extracting plant membranes after lysis of cells with a pestle and mortar and liquid

nitrogen can be optimised to not lyse the ER (Section 3.2.2). This optimised method was used to all subsequent IPs. Detergents are also an additive that can cause membrane lysis. The major contrast between my IP method and those used for IP of transmembrane proteins or cytosolic proteins is the concentration of detergent used. For IP of PM resident proteins, high concentrations of detergent (for IGEPAL CA-630 >1%) are necessary to cause mycelle formation of the lipids and so extract the protein from the membrane (Schwessinger *et al.* 2011, Kadota *et al.* 2014). The detergent concentration used in this study (0.01% IGEPAL CA-630) does not lyse membranes as it is below the Critical mycelle concentration (CMC) for IGEPAL CA-630. Therefore it is likely that endomembrane compartments are intact. However, the large number of proteins identified that transiently interact with membranes is likely to reduce the numbers of potential cargos detected. Therefore, whilst compartments are likely to be intact, cargos are less likely to be detected.

3.3.3 Affinity purification using marker proteins allows distinction of biophysically similar compartments

RABF2b/ARA7 and RABG3f label multiple compartments. Whilst RABF2b/ARA7 is usually used as a marker for LE/MVBs it has been localised to the endocytic route from the TGN to the vacuole depending on expression levels (Lee *et al.* 2004, Ueda *et al.* 2004 and conference communication Carine de Marcos Lousa). Similarly RABG3f clearly labels both the tonoplast and an endosomal population (Geldner *et al.* 2009). Thus, it is possible that by extracting membranes by IP of RAB GTPases that compartment specificity will be difficult to define. However, by using multiple markers for endosomes, comparisons can be made between compartments to allocate proteins to specific compartments. Accordingly, a more detailed, compartment specific comparison is detailed in Chapter 4.

This approach allows dissection of trafficking routes that are biophysically very similar but known to be functionally different. For example, RABF2b/ARA7 and RABF1/ARA6 label partially overlapping but functionally distinct endosome populations (Ueda *et al.* 2004,

Ebineet *et al.* 2011). Hence, data generated from this IP method has the potential to be incredibly useful for the scientific community to elucidate highly overlapping and similar, but distinct endomembrane compartments such as the TGN/EE, endosomes and ER-Golgi traffic. The distinctions between highly overlapping compartments and organelles will be explored in Chapter 4.

3.3.4 Affinity purification is a necessary complement to other proteomic methods

The differences between proteomic datasets derived from affinity purification and those from other methods of enrichment/isolation mean there are subtle, but important differences in the conclusions that can be made from the data, as discussed above. Both approaches are useful and have been combined with great success to characterise the proteome of the TGN/EE, reviewed (Groen *et al.* 2013). Therefore, I emphasise that data generated from this method is a starting point to help initially characterise the proteome of the labelled compartments, not a definitive proteome in itself. Data generated from this approach will be useful to my further work and the community. The data can be used to make inferences about compartment function (as will be explored in Chapter 4). Furthermore proteins identified in this study could be used as organelle markers for CLSM or to optimise large scale organelle proteomic studies such as PCP or LOPIT (Dunkley *et al.* 2004, Foster *et al.* 2006) as was demonstrated recently (Groen *et al.* 2013). Whilst this approach is not unique as demonstrated by Groen *et al.* 2014 and Fujiwara *et al.* 2014, who also use IP based methods. This is the first method to utilise RAB GTPases.

3.3.5 Conclusions and further work

I developed a method that allows for the enrichment of proteins associating with an endomembrane compartment marker, and thus the given compartment. This method is applicable to numerous different endomembrane compartments, regardless of biophysical properties. My ultimate objective is to elucidate the role of endosomes in signalling in the context of pathogen induced endocytosis. For this I must assess the proteomes of multiple

endosome populations and the methodology I have established and the dataset from Section 3.2.6 is an excellent starting place.

4 Validation and characterisation of a LE/MVB proteome

All techniques were performed by William Heard. Sections 4.2.2-4.2.7 contain data submitted in a paper to Molecular and Cellular Proteomics.

4.1 Introduction and Objectives

The quality of proteomic data rests on the discriminatory power of the methods used for protein extraction and purification. Any dataset acquired by a novel method requires validation to determine whether it is representative of the intended target. Thus, this chapter addresses the biological relevance of the data obtained in Section 3.2.6 with the particular aim of characterising a LE/MVB proteome in accordance with my overall aims of elucidating the role of LE/MVBs in signalling.

4.1.1 The Golgi has been extensively proteomically characterised and is an ideal bench mark against which to compare proteomic data

The Golgi is perhaps the best proteomically characterised endomembrane organelle in plants (as discussed in Sections 3.1.4 and 3.2.9) and has been successfully analysed using a variety of techniques (Dunkley *et al.* 2004, Dunkley *et al.* 2006, Sadowski *et al.* 2008, Nikolovski *et al.* 2012, Parsons *et al.* 2012). The extensive proteomic knowledge of the Golgi, makes it an ideal standard against which to compare my proteomic data. Attempts to purify the Golgi were unsuccessful with density gradient centrifugation alone, however the LOPIT technique was used to identify Golgi resident proteins (Dunkley *et al.* 2004, Dunkley *et al.* 2006, Sadowski *et al.* 2008, Nikolovski *et al.* 2012). Each of these studies used slightly different gradients or statistical analyses to identify novel proteins and provide new insights into the plant Golgi. Furthermore, surface charge was used in addition to migration in density medium to great effect by Parsons *et al.* 2012 for enrichment and further proteomic analysis of the Golgi (Section 3.1.5). Interestingly, the similarity of proteomic data obtained is very closely linked to the method used to obtain it. The proteomes generated from LOPIT analysis are more similar to each other than to those obtained by affinity purification or

surface charge purification, highlighting the need for combined approaches to elucidate proteomes (Parsons *et al.* 2013). All of these studies contribute to our knowledge of the Golgi and provide unique insights into its proteome (reviewed Parsons *et al.* 2013).

4.1.2 The TGN is a suitable comparison organelle for my LE/MVB proteomic data

The TGN is a multi-functional organelle within the cell, and is defined by its association with the Golgi *in planta* (Gendre *et al.* 2014). The TGN in plants is formed from the most *trans*-Golgi cisternae (Staehelin and Kang 2008, Kang *et al.* 2011), and has been implicated in secretion to the PM, secretion to the cell plate, endocytic trafficking and trafficking to the vacuole (reviewed Gendre *et al.* 2014). One specific role for the TGN in endocytic trafficking is in the formation of LE/MVBs (Scheuring *et al.* 2011). The term TGN/EE is commonly used in plant literature but this is based on a long standing and incorrect assumption that TGN will always act as an EE. As I will explore later not all TGN acts an EE and so the term is misleading. I will therefore use only TGN.

To date there are no published LE/MVB proteomes against which to compare my RFP-RABF2b/ARA7, RABF1/ARA6-RFP and YFP-RABG3f data. Therefore, proteomic data from the TGN compartment could be compared against my LE/MVB marker proteomes to assess the quality of the dataset. LE/MVBs are on the endocytic route along with the TGN. Moreover, the interaction between LE/MVBs and the TGN has been partially characterised. Current knowledge of the nature of the interaction between LE/MVBs and the TGN will now be explored.

4.1.3 The name TGN describes a population of heterogenous endomembrane compartments

Although the TGN is typically regarded as one organelle, not all of the TGN is involved in all of the functions ascribed to the TGN. The TGN is a name for a population of morphologically distinct endomembrane structures, and it is not a homogeneous organelle. Determining which of these populations are directly involved in the formation of LE/MVBs is essential to

further understand the endocytic route. Initially a TGN will be closely associated with the rest of the Golgi and is known as Golgi Associated-TGN (GA-TGN) (Kang 2011, Kang *et al.* 2011). As a TGN matures it associates less with the Golgi until it becomes a Golgi Independent (GI-TGN) (Uemura *et al.* 2014). This process is known as “cisternal peeling” and is accompanied by a decrease in TGN size(Kang 2011, Kang *et al.* 2011). A GA-TGN is around 30% smaller than the most *trans*-Golgi cisternae, and a GI-TGN is smaller still(Kang 2011, Kang *et al.* 2011). As there are striking morphological differences between the GA and GI-TGN (Kang *et al.* 2011), they must proteomically differ to some extent. Interestingly, however, there are no proteins that have been defined as GA or GI-TGN specific. There are, however, defined proteomically different populations of the TGN (reviewed Gendre *et al.* 2014).

4.1.4 The TGN is a proteomically diverse population of endomembrane compartments.

There are two broad populations of the TGN, one labelled with VHA-A1/SYP61/SYP43, and one labelled with RABA2a/RABA1b/VAMP721 (Chow *et al.* 2008, Asaoka *et al.* 2012, Feraru *et al.* 2012). These two populations are generally overlapping but partially distinct. Furthermore, these populations within the TGN are functionally specialised. TGN populations labelled with different markers show demonstrably different biological characteristics. The functionality of different TGN populations has been investigated with two drugs. Endosidin 1(ES1) stabilises the actin cytoskeleton (Toth *et al.* 2012) and the drug Concanamycin A (Conc A) interferes with the function of vacuolar ATPases, especially the TGN localised VHA-A1 and so disrupts MVB formation(Scheuring *et al.* 2011). ES1 specifically disrupts the VHA1-A1 and SYP61 compartments labelled TGN but not the TGN compartments labelled by SYP41 (Robert *et al.* 2008). These data support the hypothesis that there are at least two different populations of TGN compartments (Figure 4.1).

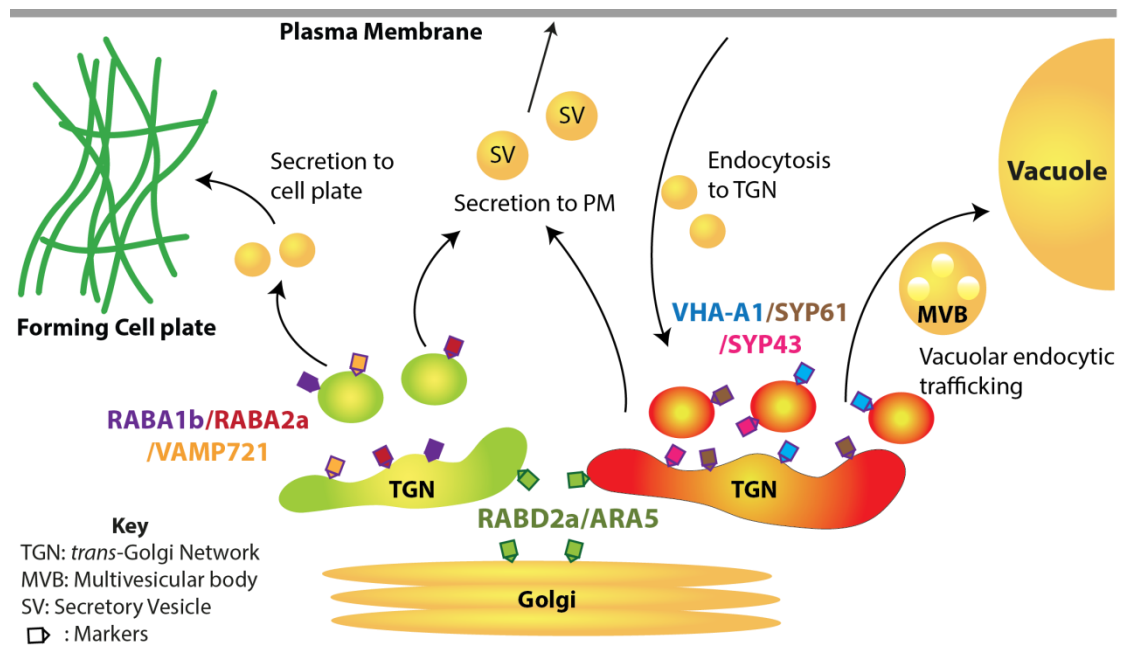


Figure 4.1. TGN populations and their functions. Schematic overview of the TGN populations, their protein markers and the principal biological functions in which they are involved. VHA-A1, SYP61 and SYP43 label one TGN population that is principally involved in secretion to the PM, endocytosis to the TGN and to the Vacuole. The RABA1b/RABA2a/VAMP721 labelled TGN is predominantly involved in secretion to the cell plate and to the PM. These populations are not totally distinct but exhibit a preference in biological function. Adapted from Gendre et al. 2014.

In addition to drugs, fluorescent endocytic tracer dyes, such as FM4-64, can be used to elucidate the involvement of different populations of the TGN in endocytosis. The SYP61/VHA-A1 labelled TGN are the principal TGN population involved in endocytosis. SYP61/VHA-A1 labelled TGN show extensive labelling with the endocytic tracer dye FM4-64 (Zouhar *et al.* 2009), whilst RABA2a labelled TGN do not (Chow *et al.* 2008). Transiently expressed *atSYP61* in *N. benthamiana* co-localises with endocytosed *atFLS2* (Choi *et al.* 2013), presumably at the TGN although the localisation of *atSYP61* in *N. benthamiana* has not been characterised. Furthermore, other RAB GTPases, such as RABD2a/ARA5 localise to the Golgi as well as compartments labelled by FM4-64 (Geldner *et al.* 2009). The Golgi apparatus is not usually labelled by FM4-64 except after very long exposure. This, therefore,

suggests that RABD2a/ARA5 labels some non-Golgi structures, likely to be the TGN, as well as the Golgi, although this has not been conclusively demonstrated.

Generally the VHA1-A1/SYP61/SYP43 labelled TGN has been implicated in secretion to the PM, endocytic trafficking and trafficking to the vacuole (Gendre *et al.* 2014). The RABA2a/RABA1b/VAMP721 TGN are thought to be involved in secretion to the cell plate and the PM (Gendre *et al.* 2014). The generalised roles of the two TGN populations are summarised in Figure 4.1. It is clear that these populations have different characteristics and Gendre *et al.* (2014) suggest that two populations is the minimum for the TGN, however properly defining them has proven difficult.

4.1.5 Higher throughput proteomic approaches are essential to elucidate protein content of the different TGN populations

One of the principal problems in with our understanding of the TGN has been throughput. Microscopy limits the throughput of proteins that can be studied at one time, studies of three or more proteins simultaneously are rare. Therefore, for example, the relationship between VHA1-A1, SYP61, SYP43 and the Golgi cannot be compared simultaneously in one experiment. Instead complicated relationships must be analysed in a pairwise manner, dramatically inflating the work required. Furthermore, microscopy is inherently biased to the proteins selected for study. The work in defining GA and GI-TGN was performed using the SYP43 and VHA-A1 TGN marker proteins (Uemura *et al.* 2014). Therefore the localisation of other TGN markers to GA or GI-TGN has not been tested. Perhaps the RABA2a/RABA1b/VAMP721 labelled TGN is only GA or GI. This is unlikely, but must be tested.

Proteomic approaches have started to be used to understand the TGN as a higher throughput method for studying protein localisation. One recent study analysed the VHA-A1 labelled TGN. In this study, IP of the VHA-A1 marker was used to preliminarily characterise

the TGN proteome, followed by LOPIT (Groen *et al.* 2014). As expected, the IP of VHA-A1 identified SYP61 but not the VAMP721 marker. In addition, the other TGN population markers RABA1b/RABA2a were not identified. Although, no RAB GTPases were detected at all presumably due to the use of carbonate washes to remove peripheral membrane proteins. Strikingly, LE/MVB marker proteins such as the SNARE VAMP727 and LE/MVB RAB5 regulator VPS9a were also identified. This suggests a strong link between the VHA-A1 labelled TGN and LE/MVBs due to the presence of respective markers associating with VHA-A1.

Proteomic analysis of the TGN using IP of the SYP61 marker protein identified numerous secreted cargos, confirming the role of the SYP61 labelled TGN in secretion to the PM (Drakakaki *et al.* 2012). Moreover, a plethora of other TGN markers were also identified including RABA2a, RABA1b, VHA-A1 and Echidna (ECH). The latter has since been developed as a TGN marker and is implicated in secretion to the PM and cell plate (Gendre *et al.* 2011, Drakakaki *et al.* 2012, Boutté *et al.* 2013, Gendre *et al.* 2013). Interestingly, VAMP721 was identified, no LE/MVB regulators were found. This suggests that the VHA-A1 labelled TGN is more closely associated to LE/MVBs than the SYP61 labelled TGN.

Additional genetic evidence supports the division between VHA-A1 and SYP61 labelled TGN. In *ech* mutants (a TGN marker closely associating with SYP61) Auxin resistant 1 (AUX1) secretion is inhibited (Boutté *et al.* 2013). By contrast, VHA-A1 functionality is not required for AUX1 localisation as Conc A does not inhibit AUX1 secretion (Brux *et al.* 2008). These data suggest further functional division between the SYP61 and VHA-A1 labelled TGN and support the hypothesis that VHA-A1 labelled TGN more closely interacts with MVBs than SYP61 labelled TGN. Whilst these markers may be on the same compartment, the compartment is likely to be subdivided. Exactly how similar the SYP61 and VHA-A1 labelled TGN are, and how they interact with LE/MVBs are crucial questions in our understanding of the TGN-LE/MVB interaction.

4.1.6 The TGN compartments are directed to be secretory vesicles or LE/MVBs

The relationship between the TGN and the LE/MVB is complex. The ultimate fate of a TGN compartment is hypothesised to be the depletion of membrane, by vesicle budding, until the compartment breaks up to form yet more secretory vesicles (Kang 2011, Kang *et al.* 2011, Scheuring *et al.* 2011). This is certainly the fate of some TGN compartments, but relies on the assumption of no membrane replenishment. It was demonstrated that GFP-SYP43 recovers in the GA-TGN after photobleaching, showing that membrane replenishment occurs in the GA-TGN at least (Scheuring *et al.* 2011, Uemura *et al.* 2014). Perhaps GI-TGN are unable to replenish membrane and so are condemned to be depleted and form SVs (Kang 2011, Kang *et al.* 2011). LE/MVBs are also generated from TGN bodies (Scheuring *et al.* 2011). LE/MVB formation is distinct from the production of SVs and is a maturation process, whereby a portion of a TGN body is altered in identity to an LE/MVB. So there is clearly a bifurcation in the fate of the TGN between an ultimately secretory vesicle fate and an LE/MVB fate.

Entire TGN compartments could be destined to be either LE/MVBs or secretory vesicles. Alternatively, it could be that there are distinct subdomains within each TGN body that have different fates. This mechanism has been shown for the grouping of cargos into specific regions of the TGN for onward transport (reviewed Surma *et al.* 2012; Gendre *et al.* 2014) and is supported by the observations of subdomains of VHA-A1 and SYP61 within a TGN compartment (Robert *et al.* 2008).

4.1.7 RAB GTPases dictate compartment identity

To understand the process, by which compartment identity is modified from one to another, we need to understand the mechanisms by which the compartment identity regulators are regulated themselves. The principal regulators of compartment identity are the RAB GTPases. RAB GTPases are molecular switches that are active when GTP bound (membrane bound) and inactive when GDP bound (cytosolic), (Saito and Ueda 2009). RAB

GTPases recruit proteins (RAB effectors) to a membrane to alter or reinforce an identity on the endomembrane structure (Saito and Ueda 2009).

RAB effectors implement compartment identity directly. Some, such as the mammalian RAB5 effector Early endosome associated 1 (EEA1), are tethering factors that direct the interactions a compartment has with other organelles over a long range (Christoforidis *et al.* 1999). Alternatively, RAB effectors can be SNAREs that mediate inter-compartment interactions over a shorter range (SNAREs mediate membrane fusion). Syntaxin 13 is another RAB5 effector and together with EEA1 drives endosome fusion in mammals (McBride *et al.* 1999). Another well characterised role of RAB effectors is facilitating the maturation of a compartment from one identity to another in a RAB cascade. For example, the *A.thaliana* RAB5 GTPases recruit the Monensin sensitivity 1 (MON1)-Calcium caffeine zinc sensitivity 1 (CCZ1) complex, activators of RAB7s, to LE/MVBs (Cui *et al.* 2014, Lawrence *et al.* 2014). MON1-CCZ1 activate RAB7s on LE/MVBs and promote a more vacuole like identity, which in turn pushes off the RAB5 GTPases (Bottanelli *et al.* 2012). Thus the RAB cascade promotes compartment maturation in the late endocytic route.

The process of MVB formation starts at the TGN and so there must be TGN membranes with partial LE/MVB identity. Whilst RAB GTPases may dictate overall compartment identity, the MVB membrane structures are generated by the ESCRT machinery. The Endosomal sorting complexes required for transport (ESCRT) components (ESCRT-0, ESCRT-I, ESCRT-II and ESCRT-III) act sequentially to induce intraluminal vesicle formation (reviewed Hurley 2008). Plants do not have clear homologs of the recognised animal ESCRT-0, but the Ton1 recruiting motif 33 like (TOL) proteins and FYVE domain protein required for endosomal sorting 1 (FREE1) were recently shown to fulfil a similar role in higher plants (Korbei *et al.* 2013, Gao *et al.* 2014). ESCRT-0 is now commonly used as a term for the ESCRT-0 function and not solely for the homologs of the animal ESCRT-0.

Together with the ESCRT machinery, other LE/MVB identity specifiers such as the RAB5 GTPases (RABF1/ARA6, RABF2a/RHA1 and RABF2b/ARA7) are likely to be present on the TGN to specify LE/MVB identity. RAB GTPases regulate membrane identity by recruiting proteins (RAB effectors) to the membranes on which they are located (Saito and Ueda 2009). Upon Conc A treatment, LE/MVB identity proteins (RABF1/ARA6 and RABF2b/ARA7) accumulate on the TGN, displaying strong co-localisation with SYP61 and VHA-A1 (Scheuring *et al.* 2011). This data supports the observation that RAB5 GTPases are present on the TGN/EE membranes as does low level co-localisation with the TGN marker VHA-A1 (Ueda *et al.* 2004).

Furthermore, RFP-RABF2b/ARA7 is frequently cited in literature as a LE/MVB marker, however initial characterisation of this protein suggested a partially early endosome function as well. Assessing the similarity between the published TGN proteomes and the RFP-RABF2b/ARA7 proteome will help elucidate the role of RABF2b/ARA7 within the cell.

4.1.8 PRA1 and YIP proteins control the regulatory RAB GTPases

RAB GTPases regulate the identity of a membrane but, as mentioned above, they are controlled in several ways themselves (Summarised in Figure 4.2). They are poor GTPases and require a GAP to hydrolyse GTP and be inactivated, and a GEF to switch the GDP for GTP and be activated, (reviewed Saito and Ueda 2009). The CCZ1-MON1 complex acts as a GEF for RAB7 GTPases whilst VPS9a acts as a GEF for RAB5 GTPases. RAB GTPases have an additional layer of regulation, by altering their affinity for membranes. All RAB GTPases have a hydrophobic membrane association modification, which is usually prenylation on one or more conserved cysteine residues on their C-terminus (Saito and Ueda 2009). In *A. thaliana* there are three proteins that bind this prenylation motif and so prevent the RAB from associating with the membrane, (reviewed Saito and Ueda 2009). As membrane association is a pre-requisite for RAB GTPase activation by exchange of GDP for GTP, these proteins are known as GDP dissociation inhibitors (GDIs)- GDI, GDI1 and GDI2

(Ueda *et al.* 1996, Žárský *et al.* 1997). The GDIs are removed and the RAB GTPase associates with the membrane via the function of a GDI dissociation Factor (GDF) (Sivars *et al.* 2003, Chen and Collins 2005, Kano *et al.* 2009, Lorente-Rodríguez *et al.* 2009). The homologs of yeast GDFs in *A.thaliana* are the Ypt Interacting protein (YIP) and Prenylated Rab GTPase acceptor 1 (PRA1) family (Alvim Kamei *et al.* 2008, Gendre *et al.* 2013).

There is clearly tight regulation of RAB GTPase activity, especially through GDF/GDI activity.

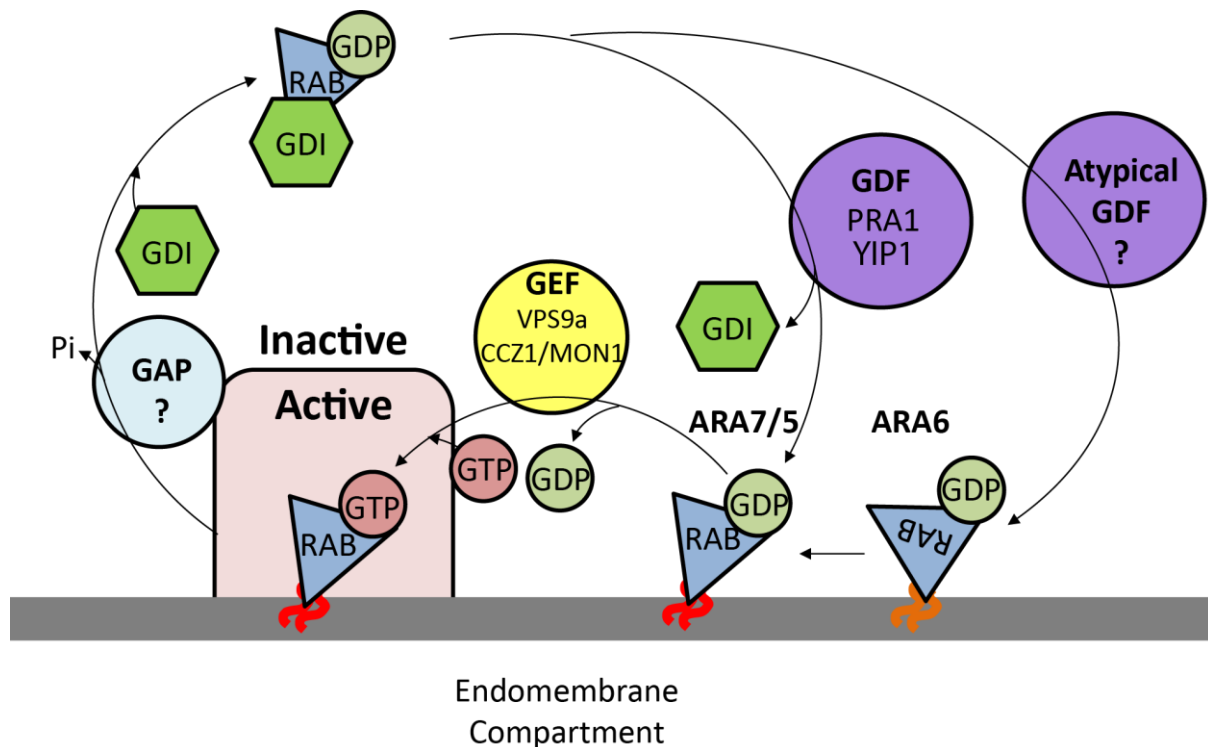


Figure 4.2.Regulation of RAB GTPases.Known and suspected RAB GTPase regulators are detailed. VPS9a is the regulator of the RAB5 GTPases (Goh *et al.* 2007) and the CCZ1/MON1 dimer is the GEF for RAB7 GTPases (Cui *et al.* 2014, Lawrence *et al.* 2014). The PRA1 and YIP1 family have been implicated as GDFs (Alvim Kamei *et al.* 2008, Gendre *et al.* 2013).

In *A. thaliana*, there has been a radiation of the PRA1 and YIP1 proteins into two families of GDFs, 19 in the PRA1 family and seven in the YIP family (Alvim Kamei *et al.* 2008, Gendre *et al.* 2013). The PRA1 family are co-expressed with RAB GTPases and a few select members have been localised to a variety of endomembrane compartments (Alvim Kamei *et al.* 2008). With so many different GDFs (compared to the three GDIs) it is likely that they

dictate the membranes with which a RAB GTPase associates. One pressing question is, therefore, where do these GDFs localise *in planta*?

Intriguingly the plant unique RAB GTPase RABF1/ARA6, associates with membranes by N-myristoylation and lacks the C-terminal cysteine motif for prenylation, (Ueda *et al.* 2001). As GDIs bind to RAB GTPases through the C-terminal prenylation modification, it remains open whether GDIs can bind to RABF1/ARA6. Whilst RABF1/ARA6 binding to membranes is not reduced in single *gdi1* mutants, the association of GDIs to RABF1/ARA6 has not been investigated directly (Ueda *et al.* 2001). Furthermore, it remains unknown how RABF1/ARA6 is directed to the appropriate membranes. The GEF for RABF1/ARA6 is VPS9a (Goh *et al.* 2007), but literature knowledge of RAB GTPases indicates GEFs function downstream of membrane association of a RAB GTPase. Therefore it is still unknown whether RABF1/ARA6 associates with canonical GDFs to promote association with the correct membranes.

4.1.9 LE/MVBs exist as a diverse population

RABF1/ARA6 and RABF2b/ARA7 labelled LE/MVBs are distinct. RABF2b/ARA7 LE/MVBs are more susceptible to application of the drug BFA than RABF1/ARA6 LE/MVBs (Ueda *et al.* 2004). Furthermore, RABF2b/ARA7 co-localises to a greater extent with the SNARE VAMP727 whilst RABF1/ARA6 co-localises to a greater extent with the SNAREs SYP21 and SYP22 (Ueda *et al.* 2004). The two populations of RAB GTPases also have different biological functions. Mutant *rabf2b/ara7* and *rabf2a/rha1* exaggerate the developmental phenotype of *syp22-1* knock out plants, while *rabf1/ara6* loss of function mutants suppress the *syp22-1* phenotype (Ebine *et al.* 2011, Ebine *et al.* 2012). Also, RABF1/ARA6 has been implicated in salt stress tolerance and *rabf1/ara6* mutants accumulate more Flowering Locus T (FLT), whereas in both cases, RABF2b/ARA7 is not involved (Ebine *et al.* 2012). These data demonstrate that whilst the RAB5 GTPases label morphologically similar compartments, they have very different biological functions. These differences must relate to

differences at the proteome level too. It will be interesting to determine which tethering factors or other RAB effectors are RABF1/ARA6 or RABF2b/ARA7 specific.

4.1.10 Objectives

My objectives for this chapter are to provide independent experimental evidence to test the biological significance of my proteomic data by comparison with literature and validate the predicted localisation (based on my proteomic data) of PRA1.B1, PRA1.B2 and PRA1.F1 (GDF) proteins with CLSM. The analysis of GDFs will help elucidate the functional specificity of these proteins and how RAB GTPases are generally regulated. Secondly, I can use these data to make inferences about the biology of the endomembrane system. My comparisons between the LE/MVB proteomes and the TGN will also be used to make inferences about the interaction between the TGN and LE/MVBs. These experiments and comparisons will dictate whether this data can be used for further study of endosomes and their roles in signalling.

4.2 Results

4.2.1 The proteomic data is not suitable for direct quantitative comparisons between proteomes

The efficiency of the IP method (Section 3.2.6) to enrich for proteins associating with an endomembrane marker varied according to the bait protein used. Whilst input protein was carefully balanced (after quantification with BCA assay to ensure equal input into the IP) the yield of bait proteins and co-enriched proteins varied between marker protein bait (Table S3). Therefore conclusions made by numbers of proteins identified or quantity of protein identified in each IP must be made with caution. I can, however, make conclusions about the identity of proteins that are identified with each bait, but analyses need to reflect the relative number of proteins in each proteome.

4.2.2 The proteomic data recapitulates known differences between the Golgi and the tonoplast and the similarity between two LE/MVB markers

In order to confirm the power of my IP method (Section 3.2.6) to discriminate between compartments, I tested whether known biological differences between compartments (the tonoplast and the Golgi) were reflected in the data. A comparison between the YFP-GOT1 (Golgi) and the YFP-VAMP711 (tonoplast) proteomes revealed a modest overlap of 46 proteins (Figure 4.3a). In order to test the significance of this overlap, I tested the H_0 of independent assignment of proteins between the two proteomes with a χ^2 analysis. Based on these data, the H_0 cannot be rejected ($P \sim 0.5$), demonstrating that proteomic data obtained with this method can discriminate between the Golgi and the tonoplast.

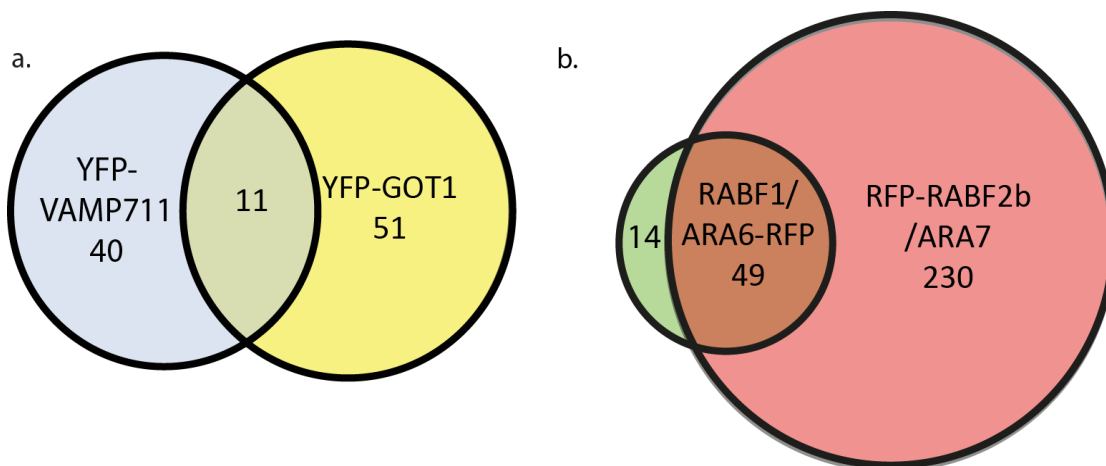


Figure 4.3. Venn diagrams comparing the proteins assigned to different endomembrane proteomes. The number in each area of the Venn diagram indicates number of proteins assigned to the proteome or proteomes indicated.
a. Comparison of the YFP- GOT1 (Golgi) and the YFP-VAMP711 (Tonoplast).
b. Comparison of the RFP-RABF2b/ARA7 (LE/MVB) and RABF1/ARA6-RFP (LE/MVB).

In order to test whether the proteomic data obtained with this method could also recapitulate a published biological similarity, I compared the RFP-RABF2b/ARA7 (LE/MVB) proteome to the RABF1/ARA6-RFP (LE/MVB) proteome (Figure 4.3b). These two populations of endosomes display a significant overlap of 182 proteins. The H_0 of independent assignment of proteins between the two proteomes can be rejected with a χ^2 analysis ($P < 0.005$).

Therefore I am confident that my proteomic data reflects published biological similarities and differences between proteomes.

4.2.3 The YFP-GOT1 proteome compares favourably with other published Golgi proteomes

To establish the biological relevance of my dataset, relative to literature, I compared the YFP-GOT1 enrichment with the TGN and well characterised Golgi proteomic data (from different methodologies outlined in section 3.2.9) and displayed the results with a Venn diagram (Figure 4.4). The comparison revealed a large number of proteins known to be associated with Golgi: 63 of the 152 proteins in the YFP-GOT1 proteome were previously identified in Golgi proteomic analyses (Figure 4.4, Table S3). These include Golgi-localised enzyme complexes such as galacturonosyltransferases (AT2G20810, AT2G38650,

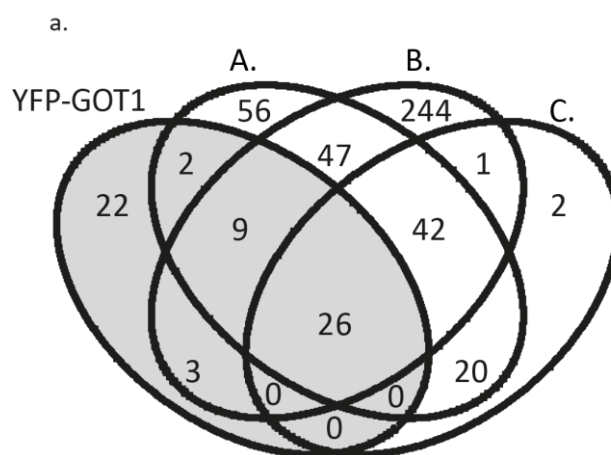


Figure 4.4. Venn diagrams comparing the proteins assigned to YFP-GOT1 (Golgi) with published endomembrane proteomes. The number in each area of the Venn diagram indicate number of proteins assigned to the proteome or proteomes indicated. Venn diagram comparisons of YFP-GOT1 (Golgi) proteomes. Proteomes are A - Nikolovski et al. 2012, B - Parsons et al. 2012, C - Sadowski et al. 2008/Dunkley et al. 2006. Grey area highlights my data.

AT3G02350, AT3G25140, AT3G61130), xylose synthase (AT2G47650) and xylose transferases (KKT5, AT1G74380; XYLT, AT5G55500) and two UDP-D-glucuronate 4-

epimerase 6 (GAE1, AT3G23820; GAE6, AT4G30440). These enzymes were also identified by Parsons *et al.* (2012) and Nikolovski *et al.* (2012) but not observed in the CFP-SYP61 affinity purification (Drakakaki *et al.* 2012). Of the remaining YFP-GOT1 proteins, 24 are predicted to have Golgi, ER-Golgi interface or PM/extracellular localisations and 33 predicted to be cytosolic (SUBA3). The high overlap between my YFP-GOT1 proteome and the published data supports the hypothesis that this method enriches Golgi proteins and proteins trafficking through the Golgi.

4.2.4 RFP-RABF2b/ARA7 is more TGN like than expected

Whilst there is no published LE/MVB proteome, there are two published TGN proteomes that can be used for comparison with my LE/MVB proteomes. Therefore, to assess the biological relevance of my LE/MVB marker proteomes (RFP-RABF2b/ARA7, YFP-RABG3f, RABF1/ARA6-RFP), I compared the RFP-RABF2b/ARA7 proteome to the TGN, utilising the published proteomic data from VHA-A1-GFP IPs (Groen *et al.* 2014) (Figure 4.5a).

30% of RFP-RABF2b/ARA7-labelled bodies co-localises with VHA-A1-GFP (personal communication, Beck and Robatzek) and around 20% of VHA-A1-GFP labelled bodies co-localises with RFP-RABF2b/ARA7 (Dettmer *et al.* 2006). Thus, I expected that there would be an overlap of between 20-30% of proteins from the RFP-RABF2b/ARA7 proteome and that of the VHA-A1-GFP proteome. Strikingly, we can accept the conservative H_0 of 30% overlap (χ^2 $p < 0.005$). This unexpected similarity between the RFP-RABFb/ARA7 and the VHA-A1 proteomes suggests that RABF2b/ARA7 interacts closely with VHA-A1. Whilst the overlap between RFP-RABF2b/ARA7 is significant at 30% overlap, it should still be noted that only 20 proteins of 279 in the RFP-RABF2b/ARA7 proteome are shared with the VHA-A1 proteome. Therefore, these two compartments are still largely independent, they associate more than the CLSM data would suggest. As a contrast, I compared the RABF1/ARA6 proteome to the VHA-A1 proteome and both a H_0 of independent assignment

and 30% overlap can be rejected (χ^2 $p < 0.005$). Further supporting the observations that RABF1/ARA6 is more different from VHA-A1 labelled TGN than RABF2b/ARA7.

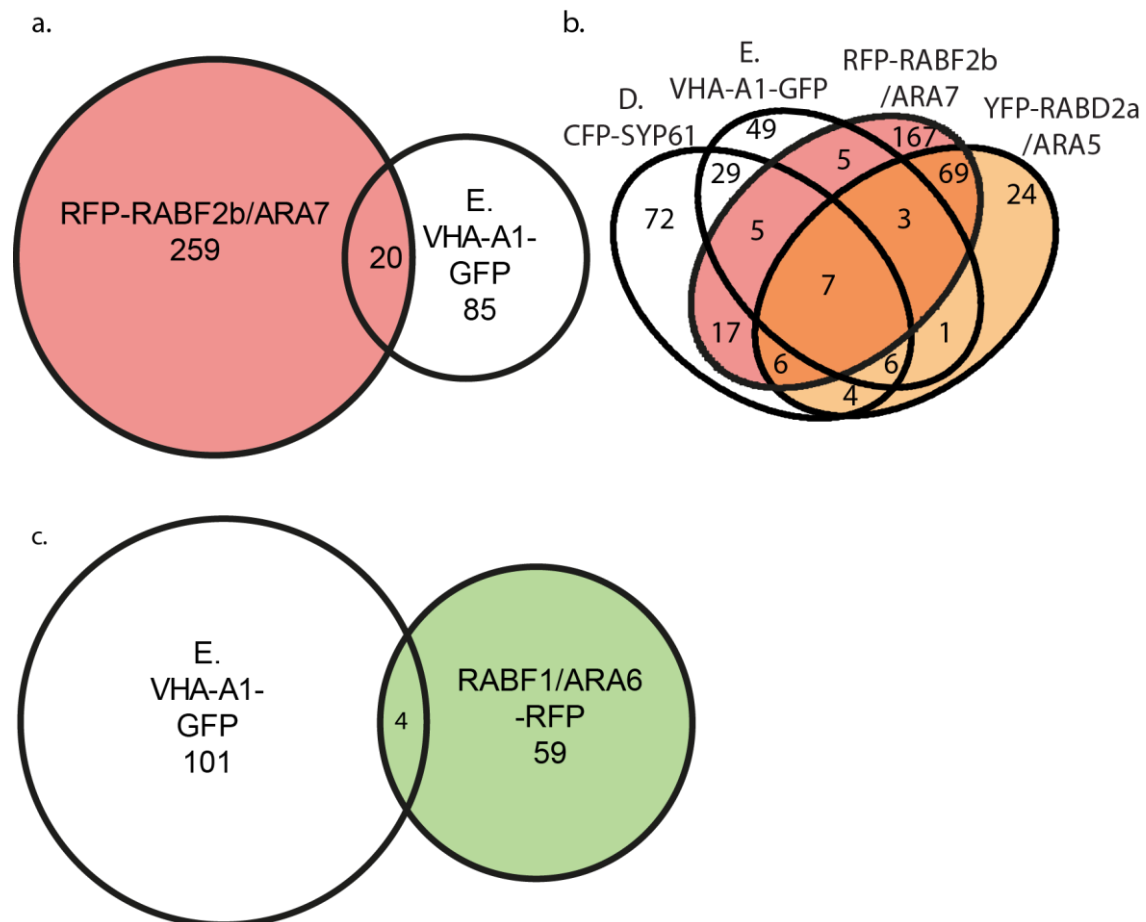


Figure 4.5. Venn diagram comparison of RFP-RABF2b/ARA7, YFP-RABD2a/ARA5 and VHA-A1-GFP IPs. a. Venn diagrams comparing proteins assigned to RFP-RABF2b/ARA7 and VHA-A1-GFP. The number in each area of the Venn diagram indicates number of proteins assigned to the proteome or proteomes indicated. b. Venn diagram comparing the proteins assigned to the YFP-RABD2a/ARA5 (Golgi/TGN/EE) and the RFP-RABF2b/ARA7 (LE/MVB) with published TGN/EE proteomes. The number in each area of the Venn diagram indicate number of proteins assigned to the proteome or proteomes indicated. Proteomes are: D - Drakakaki et al. 2012., E – Groen et al. 2014.

Within the 20 protein overlap were several known TGN markers and residents: YIP4b (AT4G30260) (Gendre *et al.* 2013), VHA-A1 (AT2G28520) (Dettmer *et al.* 2006), and SYP43 (AT3G05710) (Uemura *et al.* 2004) as well as the known RABF2b/ARA7 endosome resident SNARE VAMP727 (Ueda *et al.* 2004). These results further demonstrate the modest

biological overlap between the TGN and LE/MVB and further support the relatedness of these compartments and their proteomic interactions. It also provides evidence that RFP-RABF2b/ARA7 labelled LE/MVBs form directly from a TGN subdomain labelled with VHA-A1SYP61 was not identified in my LE/MVB marker proteomes, perhaps suggesting it labels a different subdomain of the TGN. However, lack detection does not mean SYP61 is absent. Instead it is more likely that in these experiments, it was below the limit of detection.

4.2.5 YFP-RABD2a and RFP-RABF2b/ARA7 define subpopulations of the TGN

To further examine TGN proteomes, I compared YFP-RABD2a/ARA5 enriched proteins with RFP-RABF2b/ARA7, and with the published CFP-SYP61 and VHA-a1-GFP proteomes (Figure 4.5b). YFP-RABD2a/ARA5 is localised throughout the TGN in punctate structures that are sensitive to BFA and co-localise with FM4-64 and VHA-a1 (Geldner *et al.* 2009; Pinheiro *et al.* 2009). This RAB GTPase also has a role in regulating ER to Golgi traffic (Geldner *et al.* 2009, Pinheiro *et al.* 2009). Of the 120 proteins assigned to the YFP-RABD2a/ARA5 proteome, there was substantial overlap with RFP-RABF2b/ARA7 (85 proteins) and, to a lesser extent, with CFP-SYP61 (23 proteins) and VHA-a1-GFP (17 proteins) enrichments (Figure 4.5b, Table S3). I did not identify VHA-a1 in the YFP-RABD2a/ARA5 enrichment. Six proteins are common to CFP-SYP61, VHA-a1-GFP and YFP-RABD2a/ARA5 enrichments but were not shared with RFP-RABF2b/ARA7, these include TRS85 (AT5G16280), YIP5b (AT3G05280) and a SCAMP family protein (Secretory Carrier Membrane protein, AT1G32050) suggesting spatial distinction within the TGN between YFP-RABD2a/ARA5 and RFP-RABF2b/ARA7.

4.2.6 RABF1/ARA6-RFP functional specificity is conferred by 9 unique proteins

One striking observation, as discussed in Section 4.2.2, is that the proteomes of RFP-RABF2b/ARA7 and RABF1/ARA6-RFP are very similar with an overlap of 49 proteins (Figure 4.3b). This overlap is significantly different from what would be expected if these proteins were independently assigned (Section 4.2.2). It is consistent with RABF2b/ARA7 and RABF1/ARA6 labelling compartments within the same endocytic route (Ueda *et al.* 2001,

Lee *et al.* 2004) There is also a much smaller proportion of unique RABF1/ARA6-RFP proteins than would be expected if proteins were independently assigned to the two proteomes. Only 14 proteins are not detected in the RFP-RABF2b/ARA7 proteome and of these, just 9 proteins are unique to RABF1/ARA6-RFP across my entire dataset. Surprisingly, there were no RABF1/ARA6 unique SNAREs or tethering factors identified.

One substantial difference between the RFP-RABF2b/ARA7 and RABF1/ARA6-RFP endosomes was the presence of numerous TGN localised proteins in the RFP-RABF2b/ARA7 but not RABF1/ARA6-RFP proteomes (Table S3). These TGN localised proteins are SYP43 (AT3G05710) and (Chow *et al.* 2008, Saito and Ueda 2009, Feraru *et al.* 2012). This observation provides additional supporting evidence to the notion that RFP-RABF2b/ARA7 labels a sub population/sub compartment of the TGN.

4.2.7 Canonical RAB GTPase regulators (GDFs) appear in the conventional RAB GTPase proteomes, but not in the atypical RAB RABF1/ARA6-RFP proteome

To test whether my proteomic data could be used to predict the localisation of a protein, I examined three members of the PRA1 family of proteins. The PRA1 family is a protein family

	PRA1.B1	PRA1.B2	PRA1.F1
RFP-RABF2b/ARA7	Identified	n.i.	n.i.
RABF1/ARA6-RFP	n.i.	n.i.	n.i.
YFP-GOT1	Identified	Identified	n.i.
YFP-RABD2a/ARA5	Identified	n.i.	n.i.

Table 4.1. Predicted localisation of PRA1 proteins based on my proteomic data. Proteins identified in the enrichments of RFP-RABF2b/ARA7, RABF1/ARA6-RFP, YFP-GOT1 and YFP-RABD2a/ARA5 were predicted to co-localise. When proteins were not identified in a particular condition, n.i. is used.

of potential regulators of RAB GTPases of which several were identified in my proteomic

data. I focused on localising PRA1.B1(AT3G56110), PRA1.B2 (AT2G40380) and PRA1.F1 (AT1G17700). PRA1.F1 is included as a negative control that was not in the proteomic data (Table 4.1). Some PRA1 family members have been localised (including PRA1.F1) with transient expression of fluorescent protein fusions in tobacco leaf epidermal cells (Alvim Kamei *et al.* 2008), but the identity of PRA1.B1 and PRA1.B2 labelled compartments in *A.thaliana* are unknown. These chosen proteins have varied and overlapping predicted localizations. I therefore co-expressed PRA1.B1, PRA1.B2 and PRA1.F1 using particle bombardment with either a YFP or RFP tag in plants stably expressing a YFP-GOT1, YFP-RABD2a/ARA5, RFP-RABF2b/ARA7, RABF1/ARA6-RFP in *A. thaliana* leaf epidermal cells to test whether their predicted localisations.

When YFP-PRA1.B1 was transiently co-expressed with stable RFP-RABF2b/ARA7 by particle bombardment (Figure 4.6), it co-labels a sub population of RFP-RABF2b/ARA7 bodies. There are however, independent RFP-RABF2b/ARA7 and YFP-PRA1.B1 structures. Furthermore, I often observed a tight association between RFP-RABF2b/ARA7 and YFP-PRA1.B2 and YFP-PRA1.F1 but rarely co-labelling of the same compartments. This is in agreement with the predictions I made from the proteomic data.

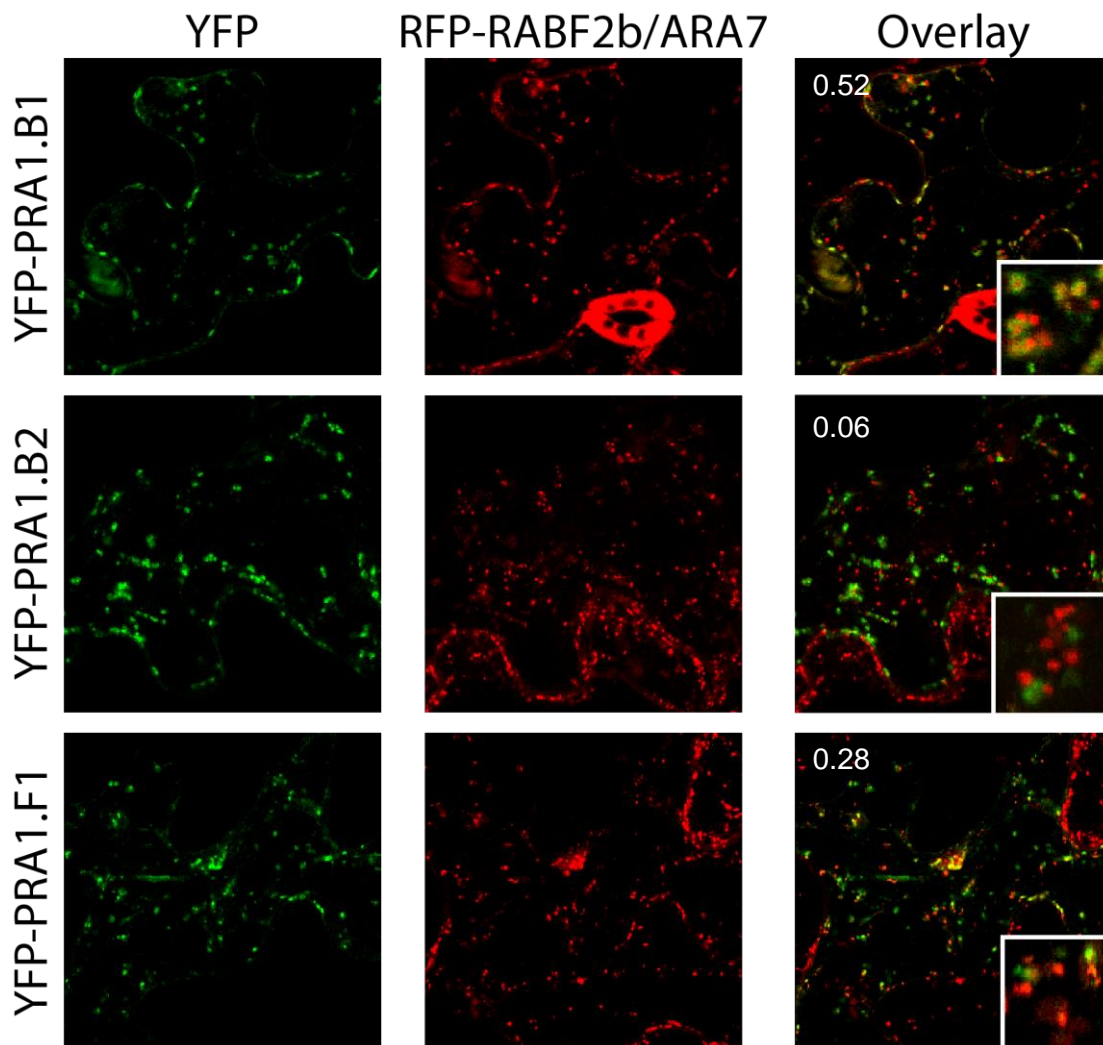


Figure 4.6. Co-localisation of YFP-PRA1 family members with RFP-RABF2b/ARA7 (LE/MVB). Standard confocal micrographs of leaf epidermis of the indicated *A.thaliana* transgenic plants stably expressing UBQ10::RFP-RABF2b/ARA7, transiently transformed using particle bombardment, expressing fluorescent tagged PRA1 family members. Insets show an enlarged section of each image.

RABF1/ARA6-RFP was not predicted to co-localise with any of the PRA1 proteins and live cell imaging confirmed these predictions (Figure 4.7). Neither YFP-PRA1.B1, YFP-PRA1.B2 nor YFP-PRA1.F1 co-labelled RABF1/ARA6-RFP positive structures. However, there was often a tight association between compartments, but rarely co-labelling.

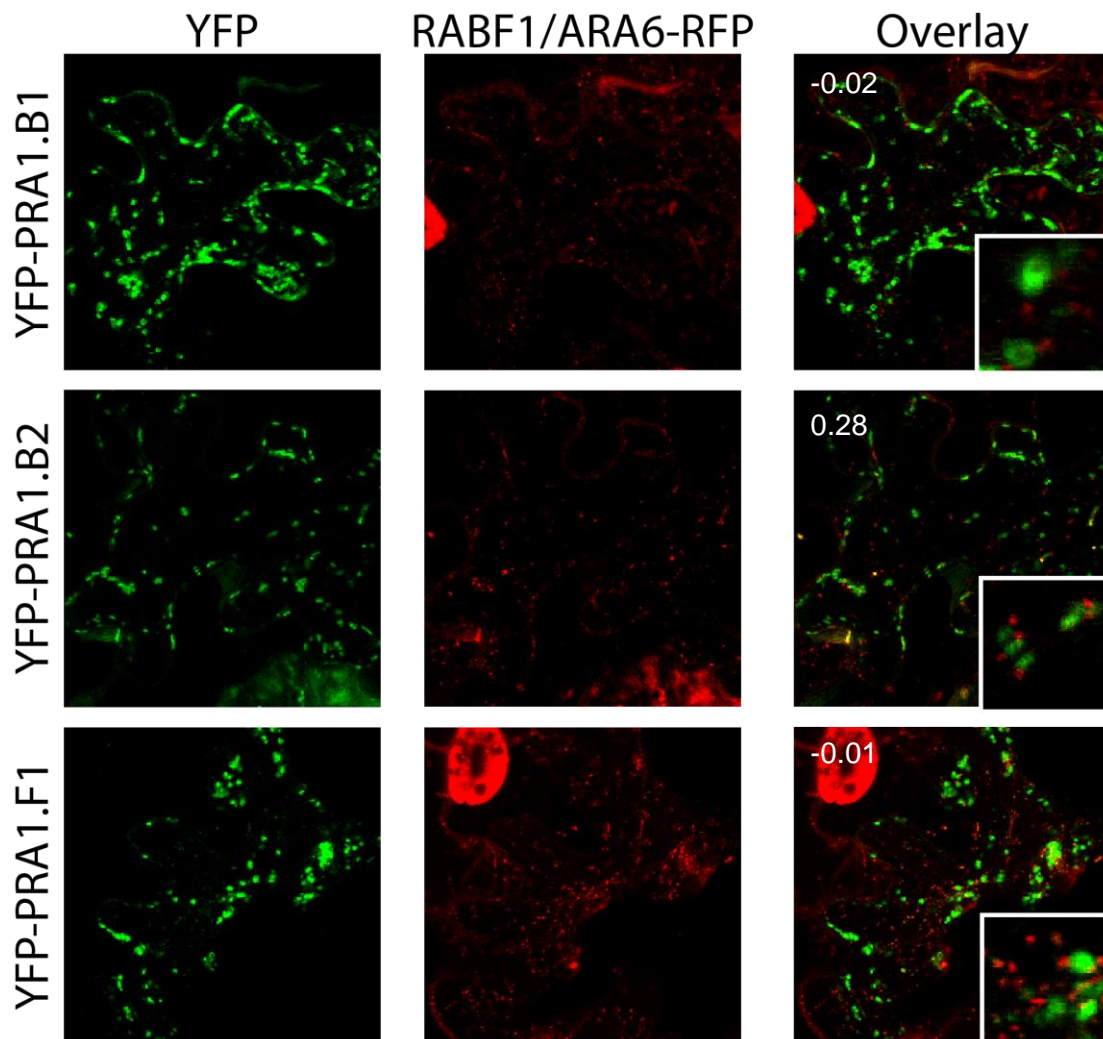


Figure 4.7. Co-localisation of YFP-PRA1 family members with RABF1/ARA6-RFP (LE/MVB). Standard confocal micrographs of leaf epidermis of the indicated *A.thaliana* transgenic plants stably expressing UBQ10::RABF1/ARA6-RFP, transiently transformed using particle bombardment, expressing fluorescent tagged PRA1 family members. Insets show an enlarged section of each image.

I predicted that YFP-GOT1 would co-localise with RFP-PRA1.B1 and RFP-PRA1.B2. This was confirmed with live cell imaging (Figure 4.8). YFP-GOT1 labelled halo like cytoplasmic membrane structures, typical of a Golgi marker and both RFP-PRA1.B1 and RFP-PRA1.B2 labelled small regions within these rings, suggesting that they partially localise to sub regions within the Golgi. PRA1.F1 conversely, did not localise to YFP-GOT1 structures.

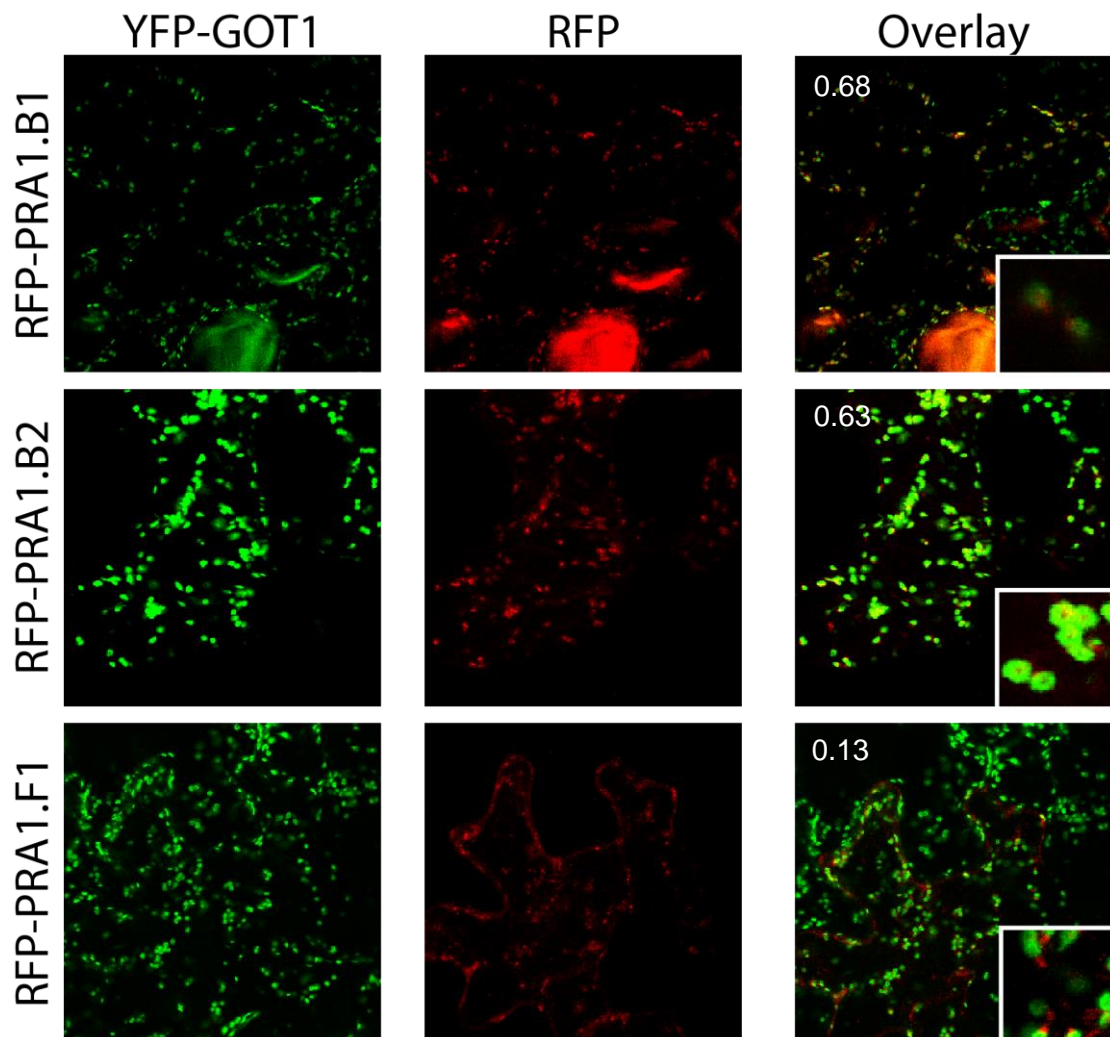


Figure 4.8. Co-localisation of RFP-PRA1 family members with YFP-GOT1.

Standard confocal micrographs of leaf epidermis of the indicated *A.thaliana* transgenic plants stably expressing UBQ10::YFP-GOT1, transiently transformed using particle bombardment, expressing fluorescent tagged PRA1 family members. Insets show an enlarged section of each image.

Intriguingly, I observed that RFP-PRA1.B1, RFP-PRA1.B2 and RFP-PRA1.F1 co-localise to some extent with YFP-RABD2a/ARA5 (Figure 4.9). This is a deviation from the predicted co-localisation of only RFP-PRA1.B1 with YFP-RABD2a/ARA5. Overall, however, the co-localisation of PRA1 family proteins with the target organelle markers used for IP are in agreement with the predictions of protein localisation derived from the proteomic data.

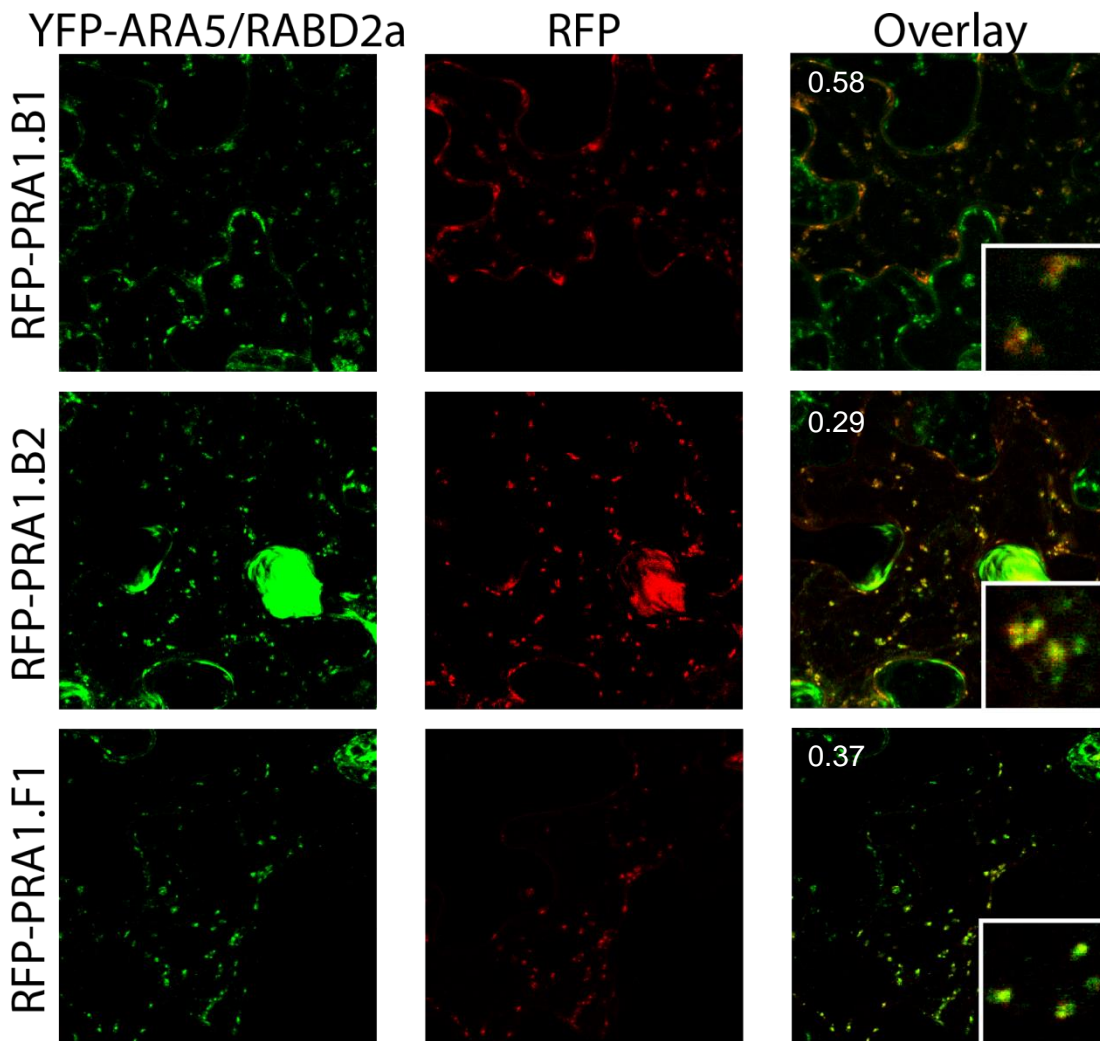


Figure 4.9. Co-localisation of RFP-PRA1 family members with YFP-RABD2a/ARA5. Standard confocal micrographs of leaf epidermis of the indicated *A.thaliana* transgenic plants stably expressing UBQ10::YFP-RABD2a/ARA5, transiently transformed using particle bombardment, expressing fluorescent tagged PRA1 family members. Insets show an enlarged section of each image.

4.2.8 Defining a combined LE/MVB proteome

As my proteomic data compared well with literature and could be used to predict protein localisation I am confident that it is largely accurate and representative. Therefore, to achieve my aim of producing a putative LE/MVB proteome, I combined my YFP-RABG3f, RFP-RABF2b/ARA7 and RABF1/ARA6 proteomes and compared them to my control proteomes (YFP-RABD2a/ARA5, YFP-GOT1 and CLC2-GFP (Figure 4.10). I did not include

YFP-VAMP711 as a control proteome since proteins that were present in the LE/MVB could conceivably be identified in the YFP-VAMP711 proteome, considering the tight association between these compartments. This is irrespective of known biological differences between the LE/MVBs (as demonstrated by my proteomic data). I considered proteins identified in the overlap between all the LE/MVB markers and not the control markers to be represent a 'core' endosomal proteome. The proteins identified in one LE/MVB marker proteome and not the control proteomes were considered a 'peripheral' endosomal proteome. Combined they should form a suitable proteome for LE/MVBs for further work to assess the role of any LE/MVB population is signalling.

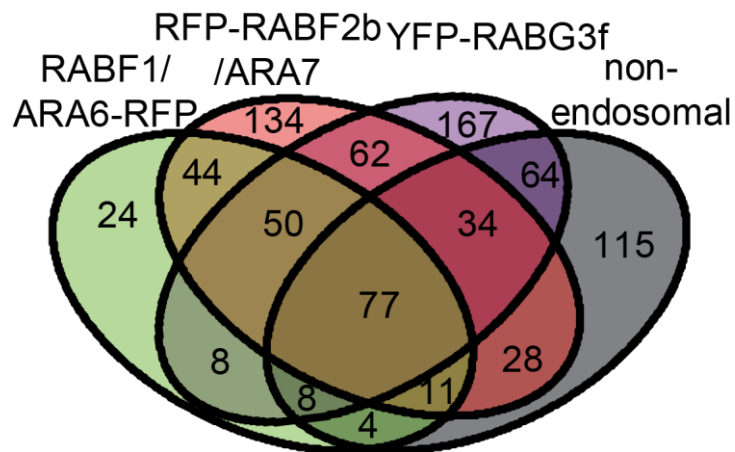


Figure 4.10. Estimating the LE/MVB proteome with Venn diagram comparison of RFP-RABF2b/ARA7, YFP-RABG3f, RABF1/ARA6-RFP and non-endosomal proteomes. The number in each area of the Venn diagram indicates number of proteins assigned to the proteome or proteomes indicated. The non-endosomal segment is the combination of the control proteomes (YFP-RABD2a/ARA5, YFP-GOT1 and CLC2-GFP).

4.3 Discussion

In this chapter I demonstrated that my proteomic dataset is consistent with and contributes to knowledge of several endomembrane compartments. I also elucidated the function of

several endomembrane regulators, whilst confirming predicted localisations made from the proteomic with an analogous technique. Finally, I also demonstrate that my proteomic data can be used to produce a putative LE/MVB proteome.

4.3.1 The proteomic method discriminates between compartments and expands our knowledge of the Golgi

My proteomic dataset reflects biological differences between defined endomembrane compartments. This IP based method can proteomically discriminate between the Golgi and the tonoplast as the proteins identified in the IPs of the Golgi and tonoplast markers were different (Section 4.2.2). Furthermore, my YFP-GOT1 proteomic data accurately identifies Golgi localised proteins. These data validate my method and allow me to make further biological inferences using my data.

4.3.2 Localisation of PRA1s

The proteins of the PRA1 family exhibit a varied distribution within the cell. PRA1.B2 is a Golgi localised GDF. PRA1.B1 has a much broader localisation along the secretory route of the Golgi and TGN as well as localisation to LE/MVBs with RFP-RABF2b/ARA7. PRA1.F1's cellular localisation is not defined. RFP-PRA1.F1 co-localises with YFP-RABD2a/ARA5, which does not conform to my predictions from the MS data. This observation highlights the difficulty in inferring absence from MS data. Alternatively it may be that this is the correct localisation for RFP-PRA1.F1 in *A. thaliana* leaf epidermal cells, but in the majority of plant cell types, they do not co-localise and therefore, this small pool of PRA1.F1 cannot be detected in my YFP-RABD2a/ARA5 enrichments, which represent an average of all plant cell types.

In contradiction to my results (that RABF2b/ARA7 and PRA1.F1 do not co-localise) a previous study reports co-localisation between RFP-RABF2b/ARA7 and PRA1.F1-GFP (Alvim Kamei *et al.* 2008). This contradiction could reflect differences in the systems used for expression. Whilst I utilised the native system of *A. thaliana* with stable expression of the

RAB GTPases, Alvim Kamei and colleagues use *N. tabaccum* and transient expression of both PRA1.F1 and RFP-RABF2b/ARA7. For example, *atFLS2* co-localises with *atSYP61* but not *atVHA-A1* upon flg22 treatment in *N. benthamiana* (Choi *et al.* 2013), but the reverse is true in *A. thaliana* (Beck and Robatzek, personal communication). In addition, it has been demonstrated that RAB GTPases as markers are very sensitive to protein levels (Spallek *et al.* 2013). This suggests that localisation of RAB GTPases in particular in a heterologous system should be treated with caution.

4.3.3 RFP-RABF2B/ARA7 labels a population of the TGN

The TGN is known to not only have distinct sub-compartments, but also be divided into the two populations of SYP43/SYP61/VHA-A1 and RABA1b/RABA2a/VAMP721 (reviewed Gendre *et al.* 2014). The presence of different TGN localised proteins in the RFP-RABF2b/ARA7 proteome and that of the YFP-RABD2a/ARA5 proteome demonstrates that these two RAB GTPases label different populations of the TGN. Due to the number of TGN marker proteins, but not SYP61, in the RFP-RABF2b/ARA7 proteome, I suggest that RFP-RABF2b/ARA7 mainly labels one population of VHA-A1 positive TGN that is also SYP61 independent. This would be the most parsimonious explanation of my approach identifying TGN markers in the RFP-RABF2b/ARA7 proteome. It is possible that these TGN mature into LE/MVBs and this is triggered by the action of RABF2b/ARA7. Moreover, this data suggests that some VHA-A1 TGN are at least partially independent of SYP61. It may be that VHA-A1 is enriched in a sub-domain of the same TGN body with SYP61, however this cannot be resolved with my data. A model of the VHA-A1/SYP61/SYP43 function and sub-compartmentalisation based on these data is presented in Figure 4.11.

The similarity between the RFP-RABF2b/ARA7 proteome and the published TGN proteomes, suggests that whilst RABF2b/ARA7 is frequently cited as an exclusive LE/MVB marker (Dettmer *et al.* 2006, Robert *et al.* 2008, Gendre *et al.* 2014), it also labels the TGN as initially suggested (Ueda *et al.* 2001, Ueda *et al.* 2004).

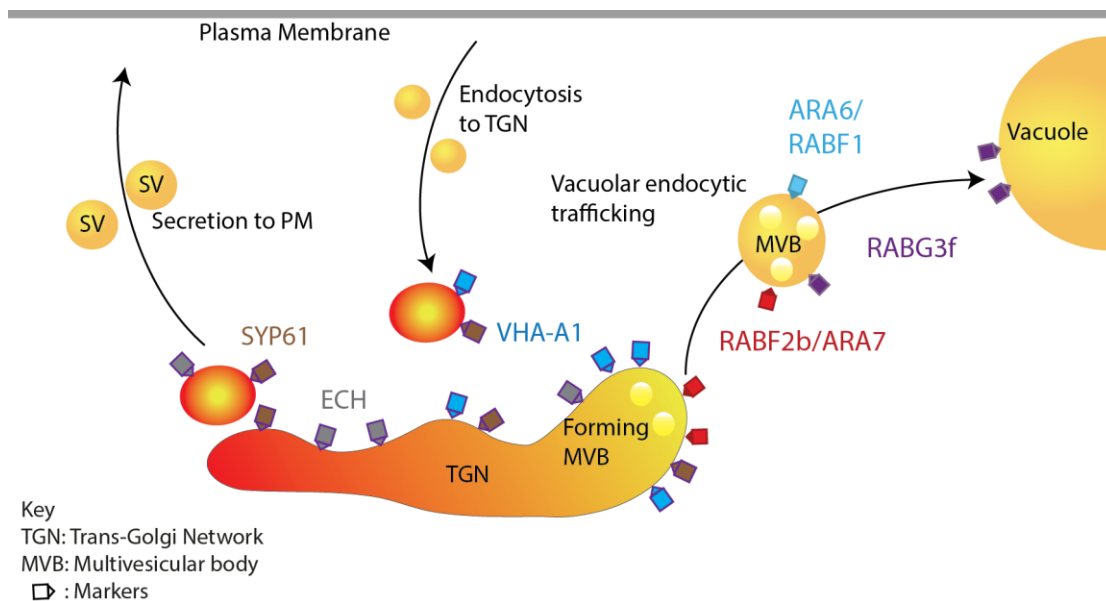


Figure 4.11. Model of functional division within the TGN. The SYP61/ECH labelled TGN subdomains are preferentially involved in the secretion of proteins to the PM, whilst VHA-A1 labelled TGN subdomains are predominantly associated with MVBs. These are presented as subdomains, but could be interacting populations. The LE/MVB specifier RABF2b/ARA7 localises to the VHA-A1 labelled TGN and induces LE/MVB identity in these compartments.

4.3.4 RABF1/ARA6 identity is conferred by a few proteins

Using my proteomic data, I could confirm that the RFP-RABF2b/ARA7 and the RABF1/ARA6-RFP proteomes show significant similarity. It is particularly interesting that the RABF1/ARA6-RFP proteome has so few unique proteins compared to the RFP-RABF2b/ARA7 (Section 4.2.2). RAB GTPases need to recruit effector proteins to confer the unique functionality to a compartment. According to my dataset, there are few proteins that could confer such unique function to RABF1/ARA6 labelled LE/MVBs. The lack of unique SNAREs or tethering factors in the RABF1/ARA6 proteome is striking and raises the question of how the unique properties of RABF1/ARA6 LE/MVBs are conferred. It is therefore likely that a lack of RABF2b/ARA7 identifying proteins and quantitative differences in protein levels confer the unique RABF1/ARA6 identity to endosomes.

This data also raises the question of how RABF1/ARA6 LE/MVBs form as no TGN markers were identified in this proteome. RABF1/ARA6 LE/MVBs must mature from RABF2b/ARA7 endosomes or form directly from another structure such as the PM (Ebine *et al.* 2011). That the proteins identified with RABF1/ARA6-RFP are nearly a subset of RFP-RABF2b/ARA7 accords with observations that a RABF2b/ARA7 endosome population matures into the RABF1/ARA6 endosomes on the endocytic route (Ueda *et al.* 2004, Ebine *et al.* 2011). An alternative explanation is that this method of discovery LC-MS/MS analysis does not provide sufficient quantitative data to resolve any differences in protein abundance between the RFP-RABF2b/ARA7 and RABF1/ARA6-RFP proteomes.

There are however a few RAB GTPase effector candidates. Perhaps the most likely RABF1/ARA6 specific effector protein is Guanylate binding protein (AT5G46070). Homologous proteins are implicated in endomembrane trafficking and pathogen defence in mammalian systems but the exact role is unclear (Britzen-Laurent *et al.* 2010, Vestal and Jeyaratnam 2011). Most of the other 9 other RABF1/ARA6-RFP unique proteins are poorly characterised, so whilst they may be RABF1/ARA6 effectors their function cannot yet be inferred.

4.3.5 RABF1/ARA6 requires non-canonical GDF machinery to associate with membranes.

Numerous canonical GDFs were found in the combined proteomic analysis, with at least one member of the PRA1 or YIP1 family identified with each RAB GTPase studied, except for RABF1/ARA6. This conforms to the hypothesis that RABF1/ARA6 uses different GDF machinery to all other RAB GTPases, as it lacks a C terminal palmitoylation site. No tested GDFs co-localised, with CLSM, with RABF1/ARA6 labelled compartments. Nevertheless, RABF1/ARA6 must still need GDF machinery to bring it onto the correct membranes, as it cycles between a membrane and cytosol localisation (Ueda *et al.* 2004). Therefore, I

postulate that RABF1/ARA6 requires non-canonical GDF machinery; as yet we cannot identify any of these non-canonical GDFs.

4.3.6 A preliminary LE/MVB proteome

Utilising my proteomic dataset, I estimated a preliminary LE/MVB specific proteome. This proteome can be defined as the proteins identified in the RFP-RABF2b/ARA7, YFP-RABG3f, RABF1/ARA6-RFP proteomes but not the YFP-RABD2a, YFP-GOT1 or CLC2-GFP proteomes (Section 4.2.9). This estimation of the proteome is deliberately conservative, to remove proteins commonly found in endomembrane compartments. Despite this, my estimation cannot be a conclusive LE/MVB proteome. As demonstrated in Section 4.2.3 and (reviewed Parsons *et al.* 2013), multiple techniques are needed to definitively confirm an organelle proteome. The proteome put forward here is only a starting point for the further examination of LE/MVBs.

With regards to my overall aims of assessing the role of LE/MVBs in signalling, I identified MKK2 and MKK5 in my LE/MVB proteomes. MKK5 was identified with the RABF1/ARA6-RFP proteome and MKK2 was identified with the YFP-RABG3f proteome. MAPK cascade components localising to the endomembrane system is not unprecedented. MPK6 was identified in proteomic studies of the TGN (Muller and Beck *et al.* 2011), whilst MPK4 was identified on microtubules (Beck and Muller *et al.* 2011) and these localisations are relevant to their role in cell division. Furthermore, a MAPKKK (EDR1) is recruited to the TGN by Keep on going (KEG) (Gu *et al.* 2011). The identification of MKKs is particularly relevant to my overall aims of testing the role of LE/MVBs in defence signalling as MKK2 and 5 are components of the MPK cascade downstream of FLS2. The relevance of MKKs in LE/MVB proteomes will be explored in Chapter 5.

4.3.7 Conclusions and further work

The proteomic data obtained through my IP method is biologically relevant. In this chapter it was essential to establish a method suitable for LE/MVB enrichment with the analogous

technique of CLSM. This method is faster than the previous methods discussed and requires minimal knowledge of the target compartment's biophysical properties. Therefore this method is generally applicable and will be incredibly useful to the community. Strikingly, MPK cascade components were identified in the LE/MVB proteomes, suggesting that defence signalling may occur from this compartment. Now the endosomal proteome can be assessed for functionality and changes after bacterial attack. This will be explored in Chapter 5.

5 Characterising flg22-induced proteome changes in Endosomes

5.1 Introduction and Objectives

To further interrogate the role of LE/MVBs in the plant cell's response to bacterial attack and their involvement in signalling, I needed to assess proteome changes in LE/MVBs following flg22 treatment. If LE/MVBs are important in immune signalling or indeed any part of the response to pathogens, it should be reflected by a proteomic change in LE/MVBs following flg22 treatment.

5.1.1 Endosomes are functionally altered during biotic interactions

Endomembranes dictate the outcome of biotic infections. The TGN, which can act as an early endosome, has a well characterised role in secretion (as discussed in Chapter 4). During biotic interactions defence proteins such as PR1, C14 (Wang *et al.* 2005, Bozkurt *et al.* 2011) are secreted via the TGN and secretion is up regulated following defence activation with SA (Wang *et al.* 2005, Wang and Dong 2011). Moreover PMR4/GSL5, the principal enzyme involved in callose deposition upon biotic stress and wounding (Jacobs *et al.* 2003, Nishimura *et al.* 2003, Luna *et al.* 2011), is recycled constitutively through the TGN (Drakakaki *et al.* 2012, Ellinger *et al.* 2013). Whilst the TGN has an undoubtedly significant and highly relevant role in defence, I will focus on the less well understood role of LE/MVBs in biotic interactions.

LE/MVBs exhibit altered function during plant-pathogen interactions. Substantial work has focused on the role of LE/MVBs in resistance to filamentous fungal and oomycete pathogens reviewed by Voigt (2014). Whilst bacteria are not filamentous pathogens, but ideally grow in the apoplast, defence responses to both types of pathogen share similarities that will be explored here. One example is callose deposition, which is thought to provide a mechanical barrier to penetration of the cell wall by pathogens, yet also occurs during bacterial infection

(Voigt 2014). Whilst both defence against bacteria and filamentous pathogens share similarities, there are also marked differences. For example defence against bacteria requires SYP132 but not PEN1, whilst defence against filamentous pathogens requires PEN1 but not SYP132 (Collins *et al.* 2003, Kalde *et al.* 2007, Kwon *et al.* 2008)

LE/MVBs are altered in both movement and function following pathogen attack. Various endomembranes, including LE/MVBs, cluster around sites of attempted or actual pathogen penetration of host cells (An *et al.* 2006, An *et al.* 2006, Böhlenius *et al.* 2010, Lu *et al.* 2012). This altered localisation demonstrates a significant rearrangement in the usual movements of LE/MVBs. LE/MVBs are also involved in a novel route of secretion during the interaction of *N. benthamiana* and the plant pathogen *P. infestans* (Bozkurt *et al.* 2014). Here FLS2, which is trafficked through the late endocytic route after flg22 treatment, is directed from LE/MVBs to the haustoria. A haustorium is the main site of interaction between the plant cells and the pathogen. These examples clearly demonstrate altered movement of LE/MVBs during plant-pathogen interactions.

LE/MVBs also have a role in limiting progression of pathogen infection. LE/MVBs are involved in callose deposition (Meyer *et al.* 2009). RABF1/ARA6 labelled LE/MVBs were proposed as the origin of exosomes for the secretion of callose to form papillae in a GNOM dependent fashion (Nielsen *et al.* 2012). Another proposed function for LE/MVBs is through delivery of defence compounds to the apoplast via exosomes. For example, during infection of *Hordeum vulgare* L. (barley) by the powdery mildew fungus *Bgh*, LE/MVBs provide the secretion route for phenolics and H₂O₂ (An *et al.* 2006). Furthermore, the LE/MVB localised ARFA1b/c is required for Required for MLO-Specified 2 (ROR2) mediated penetration resistance through callose deposition in the *H. vulgare* and *Bgh* interaction (Böhlenius *et al.* 2010). Although this implicates LE/MVBs in callose deposition, their exact role is unclear (Böhlenius *et al.* 2010).

LE/MVBs are clearly important in the delivery of defence compounds and antimicrobials to the extracellular space to inhibit pathogen growth. One class of defence compounds that may be involved in defence against pathogens are the class of flavonoids known as flavonols. Flavonols are phenolic compounds and have roles in many processes including UV protection, pathogen defence and auxin transport (Treutter 2006). Several flavonols have been shown to have antimicrobial properties and are used as biopesticides (Cespedes *et al.* 2014, de Lima *et al.* 2014). Flavonols are also found in strategic locations within plants ready for deployment (reviewed in Treutter 2006). It may be that these flavonols are present in LE/MVBs ready for exosome mediated secretion during pathogen infection, although evidence about their localisation is lacking.

The altered function of LE/MVBs in defence must be dictated to some extent by proteome changes. The proteins that regulate compartment identity, like the RAB effectors that control the interactions of a compartment, are probably altered in abundance during defence. It is likely that tethering factors and SNARE proteins change in abundance, allowing the LE/MVB to interact with novel compartments, such as the PM or EHM, for secretion. VAMP721/VAMP722 protein levels are stabilised following flg22 treatment demonstrating that the SNARE complement of some compartments must be altered although the exact nature of the VAMP721/VAMP722 compartments is unclear (Yun *et al.* 2013, Yun *et al.* 2013). In addition defence proteins may be re-directed to LE/MVBs for degradation or for further signalling. Therefore these changes could be detected with proteomic analysis of LE/MVBs after flg22 treatment. Assessing these RFP-RABF2b/ARA7 proteome changes with IP after flg22 treatment could also help elucidate the role of LE/MVBs in defence against bacteria and against filamentous pathogens.

5.1.2 Quantitative proteomic analysis is essential to understand responses to flg22 treatment

In order to understand the specific roles of LE/MVBs during pathogen infection, we must first examine how their proteomes change during the course of a biotic interaction. Quantitative proteomics is an incredibly powerful tool that allows the abundance changes of proteins following a stimulus to be measured. This approach has several advantages over changes quantified by transcriptome and translome data. For example, quantitative proteomics allows measurement of protein levels directly, unlike transcriptome or translome data. Furthermore, proteomic techniques can also be used to measure changes in protein modifications and changes that occur before transcriptional change, something unattainable with RNA based techniques.

Quantitative proteomic analysis has proven very successful in determining changes in the abundance of proteins during biotic interactions. The rapid interactions of PRRs with other proteins, such as FLS2 and EFR following ligand perception, have been extensively characterised using IP and LC-MS/MS (Heese *et al.* 2007, Lu *et al.* 2010, Roux *et al.* 2011, Kadota *et al.* 2014). This approach led to the discovery of the interaction of FLS2/EFR with the co-receptor BAK1 (Heese *et al.* 2007, Roux *et al.* 2011) and downstream targets RBOHD and BIK (Lu *et al.* 2010, Kadota *et al.* 2014), which helped develop our understanding of PAMP perception and PRR signalling.

Subcellular fractionation can also provide a spatial aspect to the proteomic data so quantitative changes can be localised within the cell. Extensive quantitative proteomic analysis was performed on the PM after activation of defence via the R protein Resistance to *P. syringae* 2 (RPS2) (Elmore *et al.* 2012). Activation of RPS2 is triggered upon the degradation of the PM associated protein RPM1 interacting protein 4 (RIN4) by avirulence Resistance to *Pseudomonas syringae* pv tomato 2 (avrRpt2) (Mackey *et al.* 2003). Therefore, RPS2 can be activated inducibly by application of DEX to plants transformed with avrRpt2

under a DEX inducible promoter. This study used a label free analysis (which will be expanded upon later) to quantify relative changes in proteins between treated and untreated conditions. Interestingly, the PRRs (PEPR1, Wall associated kinase - WAK1) were more abundant at the PM following defence activation (Elmore *et al.* 2012). Other downstream components of the PRRs, e.g. RBOHD and BIK1, were also increased in abundance at the PM following RPS2 activation (Elmore *et al.* 2012). The PM has also been analysed for quantitative changes following flg22 treatment (Benschop *et al.* 2007, Nühse *et al.* 2007) revealing phosphorylation on several endomembrane regulators. Another study assessed detergent resistant membranes from PM preparations to identify quantitative changes at the PM following flg22 treatment (Keinath *et al.* 2010). A similar approach of PM enrichment with two phase partitioning has also been used successfully in studying non-PRR RLKs such as BRI1 to identify proteins in its signalling pathway such as the Brassinosteroid-Signalling kinases (BSKs) (Tang *et al.* 2008, Tang *et al.* 2010).

Overall, these quantitative techniques allowed the characterisation of proteins that change in abundance at the PM following flg22 treatment. Yet, there are no published studies assessing the quantitative changes occurring at LE/MVBs following flg22 treatment. Using my IP approach at various times following flg22 elicitation could allow characterisation of proteome changes at LE/MVBs and further our understanding of the role of LE/MVBs in defence. Choosing the correct techniques for quantitation are essential.

5.1.3 Detection and quantitation of proteins require different experimental conditions

Measuring abundance changes in proteins between two conditions requires a different experimental approach to determining presence or absence of proteins. Proteins must be sufficiently abundant to be detected in all the conditions examined to be reliably quantified (Bantscheff *et al.* 2007). This is due to the high level of stochasticity inherent in detection of low abundance peptides (Bantscheff *et al.* 2007). Moreover more data is required to

accurately gauge levels of a protein than is required to simply determine presence. Therefore proteins need to be at a higher abundance in a sample for reliable quantification (limit of quantification) than they do for detection (limit of detection) (Steen and Mann 2004). Abundance here does not just necessarily mean absolute abundance but also relative abundance within a sample as most mass spectrometers work by sampling the most abundant MS1 spectra for MS2 analysis.

There are multiple techniques for quantification of proteins that are detected in a sample analysed with MS/MS. Methods for quantitation can be generally divided into those that use stable isotope labelling and label free techniques. I will focus on techniques for relative quantification within an experiment, rather than absolute quantification, as I only need to compare IPs over time.

5.1.4 Spectrum counting provides a rough measure of protein abundance

The most straightforward to perform method of quantitation from mass spectrometric data is by spectrum counting. Spectrum counting is a label free approach, in which MS2 spectra are counted and used to infer abundance of the protein from whose peptides they are matched. Quantitation by spectrum counting was used to great effect in Heese *et al.* 2007 and Roux *et al.* 2011. Thereby a rough measure of abundance was determined. This approach is appealing for the simplicity of data acquisition and does not require expensive chemical labels (as required for a labelling analysis). It is also controversial as spectrum counting does not measure any direct physical property of a peptide and assumes a linear response of each peptide from protein (Bantscheff *et al.* 2007). As the number of spectra counted for each peptide is so dependent on the properties of the individual peptides, it requires multiple spectra from multiple peptides to be analysed to provide accurate quantitation (Bantscheff *et al.* 2007). The major confounding factors to accurate quantitation with spectrum counting are the protein coverage and number of spectra needed and the necessity of separate MS analysis as peptides from multiple conditions are indistinguishable (Russell and Lilley 2012).

Old *et al.* demonstrate that the number of spectra required to determine a fold change increases exponentially with decreasing magnitude of the change (Old *et al.* 2005). Four spectra are required to detect a threefold change whereas 15 are required to detect a twofold change (Old *et al.* 2005).

Despite these issues, spectrum counting is frequently used and can reflect protein abundance changes (Old *et al.* 2005). Accuracy of measurement of protein abundance can be further improved by using the Protein Abundance Index (PAI) (Rappsilber *et al.* 2002). PAI is calculated by dividing the number of observed peptides by the number of possible tryptic peptides from a protein (Rappsilber *et al.* 2002). Thus, PAI allows the number of peptides detected to be scaled to the number of possible peptides generated by a given protein, thereby facilitating comparisons from protein to protein. PAI is useful for comparing abundance across proteins, but in my case of comparing the same protein across multiple conditions, PAI is not necessary.

An analogous technique for label free quantitation of proteins is by generating Extracted Ion Chromatograms (XICs). Here, the ion chromatograms from the precursor peptides fragmented in an LC-MS/MS run are extracted to give a signal intensity over time plot for each peptide (Bondarenko *et al.* 2002). This can then be used to infer protein abundance from abundance of the constituent peptides as peak area increases linearly with protein abundance (Bondarenko *et al.* 2002). Comparing the intensity of XICs, however, requires strong reproducibility from each LC-MS run to allow peaks areas to be overlaid for comparison and quantitation (Bondarenko *et al.* 2002).

One last method of label free quantitation with a mass spectrometer uses a candidate led approach. This technique is known as Multiple Reaction Monitoring (MRM) (Kirkpatrick *et al.* 2005). The reactions that are monitored here are transitions of a peptide as it is fragmented in a triple quadrupole to allow quantitation against a synthetic peptide or for relative

quantification based on intensity (Kirkpatrick *et al.* 2005). Triple quadrupoles are utilised to maximise specificity. Here only peptides with the correct m/z ratio are selected by the first quadrupole for fragmentation by the second quadrupole and detection in the third quadrupole. This allows for the required purification for accurate quantification of peptides as retention time, peptide mass, and fragment mass combine to effectively eliminate ambiguity (Wolf-Yadlin *et al.* 2007).

5.1.5 Mass tagging improves quantitation

The alternative approach to label free quantitation with MS is to use labelling, usually with stable isotopes. Ultimately peptides from the experimental conditions to be analysed are labelled with isotopically different (and so different mass) tags. Therefore the differently labelled peptides can be analysed together but differentiated upon analysis.

The isotopes can be integrated in the growing organism by feeding with the different isotopes, either ^2H , ^{15}N , ^{13}C or ^{18}O (Bantscheff *et al.* 2007). One particularly popular method is to use Stable Isotope Labelling with Amino Acids in Cell Culture (SILAC) (Ong *et al.* 2002) and has been used successfully in plants (Gruhler *et al.* 2005). One population of cell culture is fed $^{13}\text{C}_6$ arginine so that arginine containing peptides from this population will be mass shifted compared to the other population of cell culture. The SILAC technique therefore labels the proteins as they are being synthesised. Metabolic labelling, however, is only really feasible in cell culture, as multiple generations need to be grown exclusively on the isotopic media, and so in many cases is prohibitively expensive (Bantscheff *et al.* 2007).

Alternatively, the labels can be added to the peptides after biosynthesis. These approaches rely on the biochemical modification of peptides, usually on reactive amine groups (Bantscheff *et al.* 2007). A peptide is sequenced using MS/MS and the abundance of a peptide is inferred by the intensity of a reporter ion that dissociates from the rest of the tagged peptide during CID and generation of MS2 spectra (Bantscheff *et al.* 2007). The

favoured target sites for labelling are cysteines and lysines as these have particularly reactive side chains (Bantscheff *et al.* 2007). Initial work developed the isotope-coded affinity tag (ICAT) technique, using variably deuterated biotin tags to label cysteines (Gygi *et al.* 1999). Obviously peptides without cysteines are therefore unlabelled, limiting this approach. Isobaric tag for relative and absolute quantitation (iTRAQ) was developed as an alternative mass tagging approach (Ross *et al.* 2004). iTRAQ labels both lysine residues and the N terminus of peptides, drastically increasing applicability as most peptides will be labelled (Ross *et al.* 2004). This technique has been used very successfully for plant endomembrane proteomics as part of LOPIT (Dunkley *et al.* 2004, Dunkley *et al.* 2006, Nühse *et al.* 2007, Sadowski *et al.* 2008, Nikolovski *et al.* 2012, Groen *et al.* 2013).

Taken together mass tagging approaches allow for quantitation of peptides in all samples (as samples are combined for analysis) and fractionating combined peptides from each condition reduces variability (Berg *et al.* 2006). Therefore they should lead to a more reproducible measure of protein quantitation in a sample than with label free analysis.

5.1.6 Alternatives to mass spectrometry for protein quantitation

Mass spectrometric approaches are not always the most appropriate for assessing protein abundance or PTM abundance in samples. If the proteins of interest can be identified or predicted, and commercial antibodies are available, then immunoblot allows for a more direct and simpler measurement of abundance. Immunoblot and MRM require prior knowledge of the proteome and will inevitably bias the proteins investigated towards those already known to function in the process studied. MRM and antibody based approaches do, however, have the advantage of being relatively complexity independent. As there is no perfect technique for protein quantification multiple approaches should be used to triangulate the answer of which proteins are altered in abundance or modified following a stimulus.

5.1.7 Objectives

To characterise the changes in the proteomes of LE/MVBs during pathogen attack, using the PAMP flg22 and IP of RFP-RABF2b/ARA7 (as a proxy for LE/MVBs). I will initially use the unbiased approach of shotgun proteomics and quantification with spectrum counting and iTRAQ. A candidate based approach of western blot will also be used to investigate proteome changes in specific target proteins.

5.2 Results

Acknowledgements: iTRAQ labelling and all LC-MS/MS analysis was performed by Dr Jan Sklenar, analysis of data generated through LC-MS/MS analysis was partially analysed by Dr Jan Sklenar and partially by William Heard. All other techniques were performed by William Heard.

5.2.1 Spectrum counting is not sufficiently quantitative to decipher flg22 induced proteome changes in RFP-RABF2b/ARA7 labelled endosomes

In order to identify changes in the LE/MVB proteome following pathogen attack I utilised the IP approach (Section 3.2.5) on liquid grown seedlings expressing the RFP-RABF2b/ARA7 marker at 0, 15 and 60 min after flg22 treatment with an additional control of Col-0. These time points were chosen as 15 min is at the peak of cytosolic MPK activation and 60 is after most MPKs have been activated. Gel lanes were sliced, excised (as shown in Figure 5.1) and the proteins tryptically digested and analysed with LC-MS/MS.

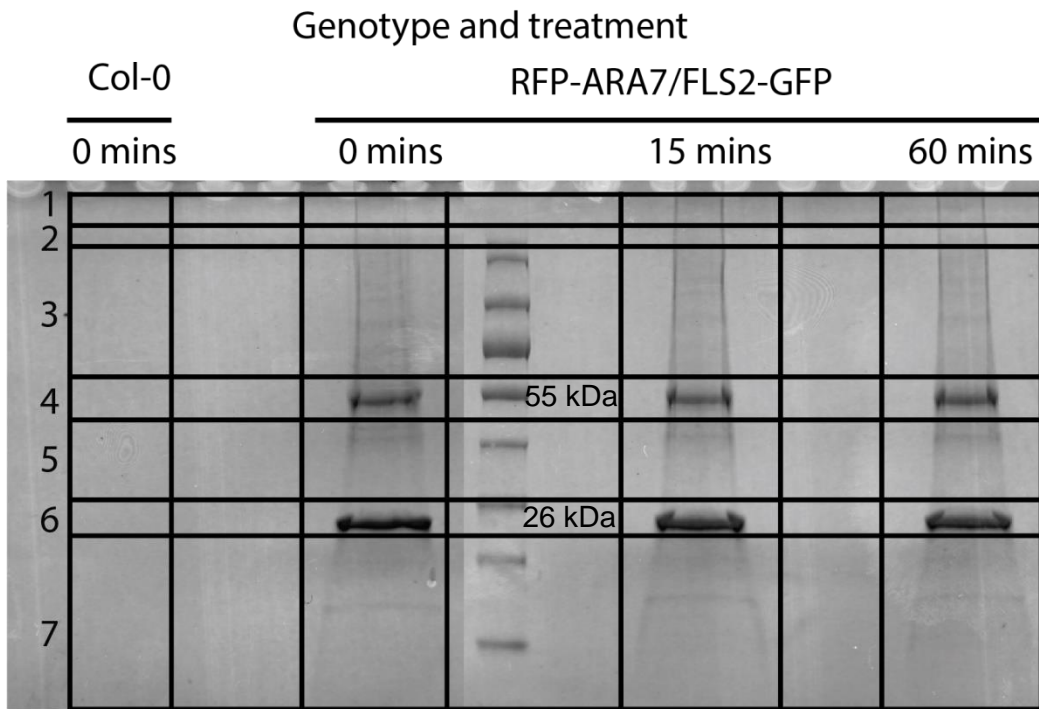


Figure 5.1. SDS-PAGE separation and excision of bands for tryptic digestion of IPs RFP-RABF2b/ARA7 after flg22 treatment. 1 g of protein (in solution) was extracted from sterile grown *A.thaliana* seedlings stably expressing both RFP-RABF2b/ARA7 and FLS2-GFP at 0, 15 and 60 minutes of flg22 treatment. 100% of each IP was used for SDS-PAGE. Proteins were visualised with Colloidal Coomassie (Instant Blue – Invitrogen). Gel lanes were excised as indicated into seven slices. Representative gel of three replicates.

Using this approach 1216 proteins were identified over three replicates. Proteins equally abundant (determined by spectrum counting) in the control (Col-0) conditions were eliminated from further analysis. Proteins were grouped based on their changes at times (15 or 60 min) after flg22 treatment relative to untreated RFP-RABF2b/ARA7 IPs. If a protein was not present at one time point it was regarded simply as increased or decreased, otherwise a log₂ ratio is calculated for protein abundance at 15 or 60 min flg22 relative to the untreated control. The numbers of proteins changing (by over twofold or with an incalculable increase due to missing values) in each repetition is displayed in Figure 5.2. There were 50 and 36 proteins that displayed a greater than twofold change at 15 min and 60 min, respectively, relative to untreated.

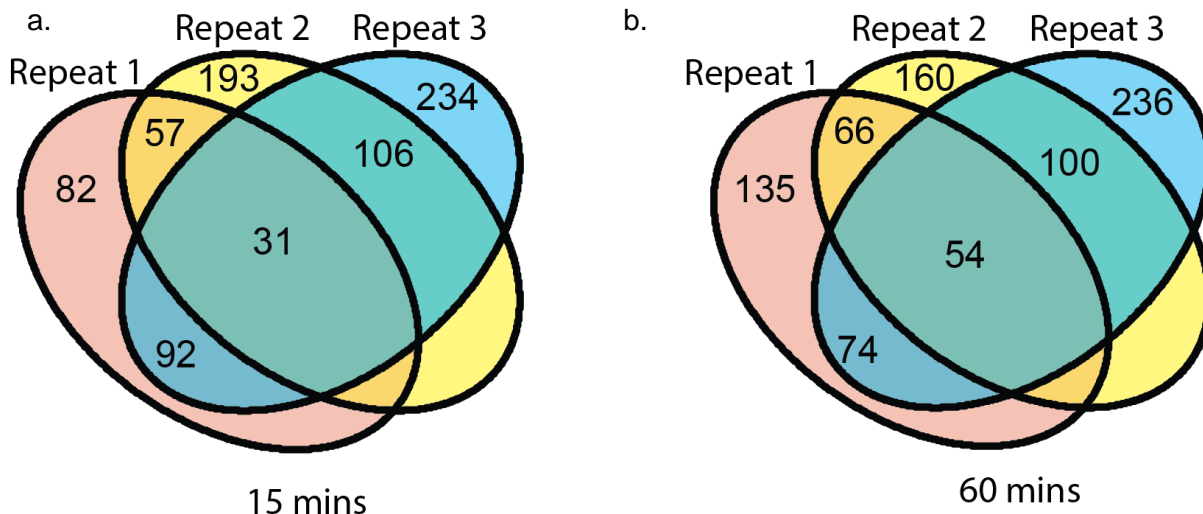


Figure 5.2. Venn diagram comparison of proteins that change in the RFP-RABF2b/ARA7 proteomes following flg22 treatment. a. Venn diagram comparing the proteins assigned to the RFP-RABF2b/ARA7 (LE/MVB) proteome with a greater than two fold change relative to untreated samples following 15 minutes of flg22 treatment. The numbers in each area of the Venn diagram indicate number of proteins assigned to the proteome or proteomes indicated. b. Venn diagram comparing the proteins assigned to the RFP-RABF2b/ARA7 (LE/MVB) proteome with a greater than two fold change relative to untreated samples following 60 minutes of flg22 treatment. The numbers in each area of the Venn diagram indicate number of proteins assigned to the proteome or proteomes indicated.

To test for the consistency in protein changes (up or down relative to time 0) I visualised the proteins with twofold or greater changes at one time point in all three replicates using a heat map (Figure 5.3). Proteins were grouped depending on their changes at the two time points and surprisingly, only 20 of the 80 proteins displayed a consistent directional change (the same directional change in all three experiments relative to untreated). Of the proteins with consistent changes, all have a missing value in one of the time points, and <5 spectra when they are detected (Table S5). This reduces confidence in the conclusion that these proteins really do change in abundance after flg22 treatment, as they are on the limit of detection, and so subject to the inherent stochasticity involved in quantitation by spectrum counting (Section 5.1.4). Also 3 of the 20 proteins have inconsistent changes between different replicates at the other time point, again reducing my confidence in this method for

determining protein quantification. This dataset is useful but, for the above reasons, needs to be tested with an analogous technique to confirm for change in protein abundance.

	15	15	15	60	60	60	iTRAQ
AT1G05240	up	up	up	null	up	null	
AT1G20330	up	up	up	null	null	null	
AT2G05830	up	up	up	null	up	null	
AT2G44120	1	up	up	0	up	up	
AT4G16390	up	1	1	null	1.321928	1.321928	
AT5G51430	up	1	up	up	1.222392	null	
AT1G09620	null	up	null	up	up	up	
AT1G70940	null	up	up	up	up	up	
AT1G74470	null	0	2	up	1.321928	1.584963	
AT1G76850	null	up	down	up	up	1.584963	
AT1G78570	up	null	1.584963	up	up	1	Up at 60 mins
AT2G20360	null	null	up	up	up	up	
AT2G26890	null	up	-0.58496	up	up	1.415037	
AT3G58500	null	null	up	up	up	up	
AT4G25080	null	1	0	up	1	1.321928	
AT5G13530	null	up	up	up	up	up	
AT5G59730	null	null	null	up	up	up	
AT2G39990	down	1	up	1	0.807355	up	
AT3G52140	-0.22239	-0.41504	0.485427	-1.80735	-1.41504	down	
AT4G12060	down	down	-1	down	down	-1	
AT1G06950	0	up	0.678072	down	up	2	
AT1G09430	-2	-0.41504	up	down	-1	up	
AT1G09630	up	-1	down	null	-1	0	
AT1G10200	down	up	up	down	up	up	
AT1G18270	down	up	2	1.584963	up	0	
AT1G20200	-1	up	-0.73697	down	up	down	
AT1G22530	-1	2.321928	1.099536	-2	0.415037	1.440573	
AT1G43800	up	0	up	up	down	up	
AT1G44170	0.321928	up	up	-1	up	up	
AT1G49340	null	down	0.321928	up	down	down	
AT1G55860	down	2	1	0.36257	1	0.263034	
AT1G57660	-1	0	up	1	-1.58496	up	
AT1G64090	up	up	down	null	null	down	
AT1G67930	down	up	up	1	up	null	
AT1G70320	down	up	down	0	null	0.584963	
AT1G72560	down	up	null	down	up	up	
AT2G17930	null	down	null	up	down	up	
AT2G26250	-1.80735	1.321928	-1	down	1.321928	0	
AT2G28900	down	null	null	down	up	up	
AT2G32920	-0.73697	1.584963	up	down	1.584963	up	
AT2G34460	-0.58496	-1.32193	up	down	-1.32193	up	
AT2G34560	down	null	up	down	up	up	
AT2G36360	down	1.321928	1.584963	down	1.321928	2	
AT2G37620	up	1	up	null	1	null	
AT2G41840	down	down	up	down	-0.41504	null	
AT2G44610	0	-1.22239	up	down	-1.22239	up	
AT2G45770	1	-0.41504	up	1	down	up	
AT2G46280	down	1.584963	up	down	0.584963	up	
AT2G47240	up	up	down	null	up	0.584963	
AT3G04870	down	1	0.415037	down	down	1	
AT3G05040	null	down	0.584963	up	down	-1	
AT3G05280	down	0.584963	up	down	down	up	
AT3G07690	down	null	up	down	up	up	
AT3G09740	down	down	up	down	0	null	
AT3G18000	-1.45943	0	1.584963	down	down	1	
AT3G27530	down	up	0.584963	down	up	down	
AT3G49910	up	up	down	up	null	0.584963	
AT3G57290	-1.48543	1	0.678072	-2.80735	1.415037	1.137504	
AT3G62830	0.584963	up	1	down	up	down	
AT4G01800	-1.41504	1	-1	down	1.415037	1.807355	
AT4G02030	up	up	0	up	up	down	

AT4G10060	down	up	down	down	up	-0.58496	
AT4G18480	0	-0.41504	up	down	-1	up	
AT4G31850	null	0.415037	up	up	-1.16993	up	
AT4G36440	up	down	up	null	0.415037	up	
AT4G38540	down	0.736966	up	down	1.415037	up	
AT4G39200	null	down	up	up	-1	up	
AT5G01010	0	down	up	down	down	up	
AT5G02960	null	down	null	up	down	up	
AT5G03540	up	1	down	up	0	down	Down at 15 mins
AT5G06140	0	up	0.321928	down	up	1.169925	
AT5G09900	0.652077	2	1.321928	-1.80735	2	2.321928	
AT5G13710	-1	1	up	0.807355	1	up	
AT5G15450	-0.58496	up	0	down	up	down	
AT5G22800	down	up	up	down	up	up	
AT5G41950	0	0	0	1	1	down	
AT5G42650	-1.32193	0.584963	down	-1.73697	1.5025	1	
AT5G49830	down	0	null	down	-1.32193	up	
AT5G61780	-1.80735	2.169925	-0.67807	down	2.459432	1.247928	
ATCG00770	up	-1	up	up	-0.67807	null	

Figure 5.3. Heat map of protein abundance changes in RFP-RABF2b/ARA7 IPs following flg22 treatment. Log₂ ratios of spectrum counts of proteins are shown at the indicated time of flg22 treatment relative to the respective control (RFP-RABF2b/ARA7 and no flg22 treatment). Only proteins with log₂ ratios greater than ± 1 consistently in one time point are shown. If there is a missing value in one time point, no ratio could be calculated and “Up” is used if a protein was only detected at that time after flg22 treatment. “Down” is used if a protein is not identified at the indicated time after flg22 treatment, but was in the IP before flg22 treatment. Data from three replicates is shown. Quantitative data from one iTRAQ replicate is shown in the final column. Only proteins with log₂ ratios greater than ± 0.5 in one time point are shown with the corresponding direction of change. Colours indicate direction and magnitude of the change relative to unelicited RFP-RABF2b/ARA7 IPs, red indicates an increase in abundance relative to 0 min and green indicates a decrease in abundance relative to 0 min.

5.2.2 iTRAQ labelling and Q-TOF MS improves confidence in quantitative proteome changes

To improve my confidence in quantification of proteins in RFP-RABF2b/ARA7 enrichments that change after flg22 treatment, I utilised the analogous quantification technique of mass labelling to assess protein amounts. I performed IP of RFP-RABF2b/ARA7 in a RFP-RABF2b/ARA7, FLS2-GFP background at 0, 15, 30 and 60 min of flg22 treatment with only one repetition (due to time limitations and technical problems with subsequent iTRAQ repetitions). The proteins were digested and analysed with the iTRAQ Q-TOF protocol. Whilst

there is a substantial reduction in the number of proteins identified in one repetition of the iTRAQ mass labelling and analysis with LC-Q-TOF (compared to the spectrum counting LC-Orbitrap data), I could improve the number of proteins identified as suitable for reliable quantification (Figure 5.4). The definition of proteins that can be reliably quantified with spectrum counting is deliberately generous (identified with >5 spectra in one time point in a replicate). Even using these criteria, mass labelling with iTRAQ still yields a superior number

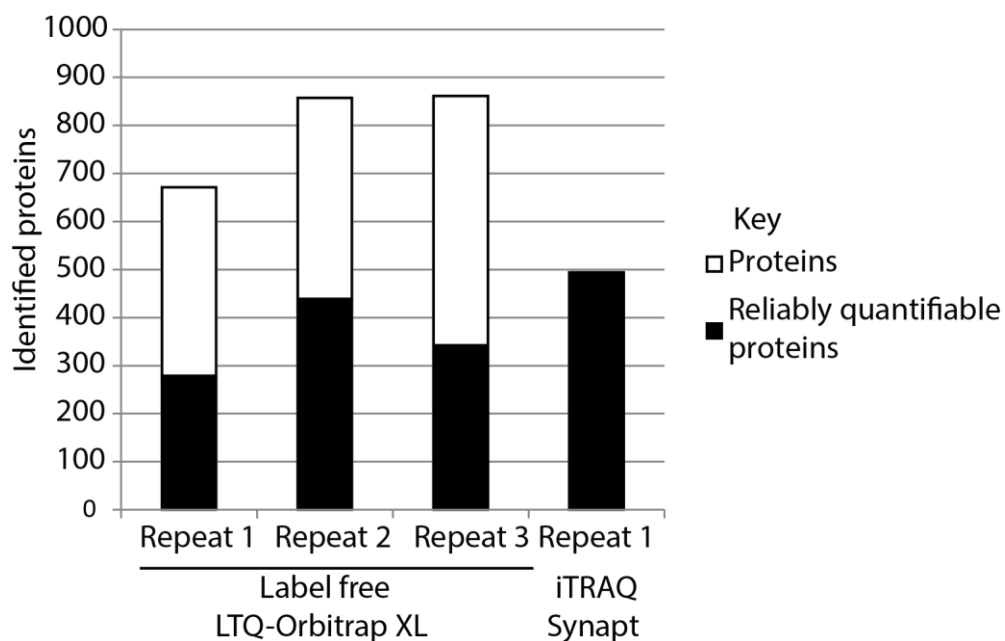


Figure 5.4. Proteins identified and proteins that might be quantified in both Orbitrap and Synapt repeats. Columns represent total proteins that were identified in each of the MS runs indicated (combining all proteins identified in RFP-RABF2b/ARA7 IPs at each time point after flg22 but not present in Col-0 controls). Proteins are deemed as reliably quantifiable if they are identified in all conditions, except Col-0 control, in one IP repeat. of quantifiable proteins.

5.2.3 Combined iTRAQ and spectrum counting quantitative data implicates RHM1 in abundance changes in LE/MVBs after flg22 treatment

To determine whether any of the proteins with suspected abundance changes in RFP-RABF2b/ARA7 affinity purifications following flg22 treatment were reproducible with analogous techniques of quantification, I compared my spectrum counting and iTRAQ

quantification datasets (Figure 5.5). As only two proteins were changed by more than twofold compared to unelicited in the iTRAQ dataset, I allowed proteins with >1.5 fold change to be

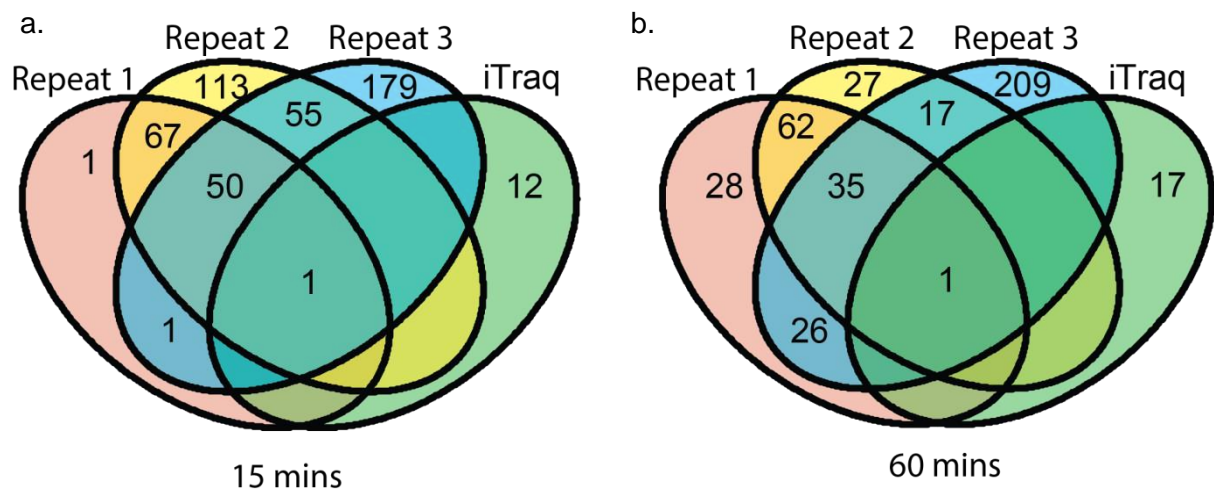


Figure 5.5. Venn diagram comparison of proteins that change in the RFP-RABF2b/ARA7 proteomes following flg22 treatment including iTRAQ data. a. Venn diagram comparing the proteins assigned to the RFP-RABF2b/ARA7 (LE/MVB) proteome with a greater than two fold change relative to untreated samples following 15 minutes of flg22 treatment. The numbers in each area of the Venn diagram indicate the number of proteins assigned to the proteome or proteomes indicated. b. Venn diagram comparing the proteins assigned to the RFP-RABF2b/ARA7 (LE/MVB) proteome with a greater than two fold change relative to untreated samples following 60 minutes of flg22 treatment. The numbers in each area of the Venn diagram indicate number of proteins assigned to the proteome or proteomes indicated. If there were no proteins in the overlap, the region has been left blank.

included. However, there was only one protein with a consistent abundance change in all three spectrum counting quantification repetitions and the iTRAQ quantification experiment at the same time points. This protein, Rhamnose synthase 1 (RHM1 - AT1G78570), is consistently more abundant in the RFP-RABF2b/ARA7 enrichments after 60 min flg22 treatment (Figure 5.3 and Figure 5.5). It is therefore a very strong candidate for further study.

To gain first insights into the potential role of RHM1 in the plant response to pathogens, I obtained *rol1-1* mutants. These mutants carry a point mutation causing a premature stop codon in the coding sequence of RHM1 (Diet *et al.* 2006, Ringli *et al.* 2008). I tested *rol1-*

1mutants for altered susceptibility to spray inoculated *Pto* DC3000. The *rol1-1* mutant displayed enhanced susceptibility to *Pto* DC3000 (Figure 5.6), suggesting a role for RHM1 in

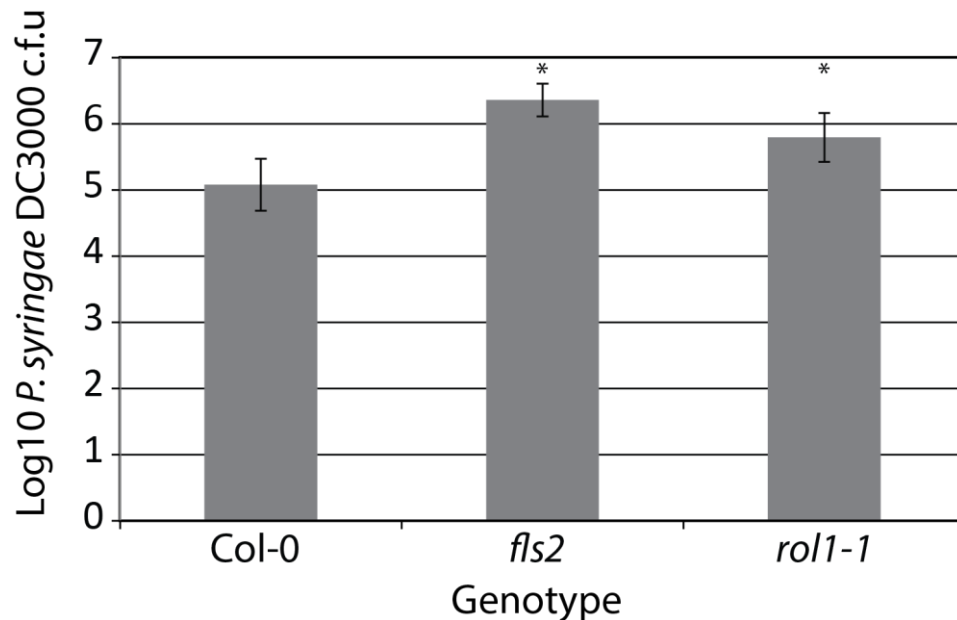


Figure 5.6. *rol1-1* mutants are more susceptible to spray inoculated *P.syringae* DC3000 than Col-0. 4 weeks old mutants were spray inoculated with the virulent pathogen *P.syringae* DC3000. Columns represent estimated bacterial growth 3 days post infection. Error bars represent the standard deviation. * denotes a significant difference (Student's t test) from Col-0, $p < 0.05$. Graph shows data from 3 biological replicates.

resistance to bacteria.

5.2.4 Candidate led quantification is necessary to further characterise changes in LE/MVBs following flg22 treatment

To further characterise proteomic changes in LE/MVBs I utilised a candidate led approach focussing on known components of the FLS2 signalling pathway – FLS2 and MPK3, 4 and 6. FLS2 was chosen as it is endocytosed following flg22 treatment (Robatzek *et al.* 2006). The MPKs were chosen as both MKK2 and MKK5 were identified in the combined LE/MVB proteome (Section 4.2.9). These MKKs are signalling components downstream of FLS2 signalling (Mészáros *et al.* 2006, Brader *et al.* 2007, Gao *et al.* 2008) and reviewed

(CristinaRodriguez *et al.* 2010). Identification of these MKKs at LE/MVBs indicates that the downstream MPKs may also be present at LE/MVBs.

5.2.5 Active MPKs are detected in RFP-RABF2b/ARA7 enrichments after flg22 treatment

To test for the presence of signalling components (FLS2 or MPK3,4 or 6) in LE/MVB marker IPs, I performed IP of RFP-RABF2b/ARA7 on sterile grown seedlings stably expressing RFP-RABF2b/ARA7 and FLS2-GFP, following flg22 treatment at 0, 15, 30, 60 and 90 min flg22 treatment. RFP-RABF2b/ARA7 was enriched in the IP and this was independent of flg22 treatment (Figure 5.7). Strikingly, FLS2-GFP was detected in unelicited samples. This is surprising as FLS2-GFP and RFP-RABF2b/ARA7 exhibit maximum co-localisation between 20 and 40 min of flg22 treatment (Beck *et al.* 2012). Suggesting FLS2 is trafficked

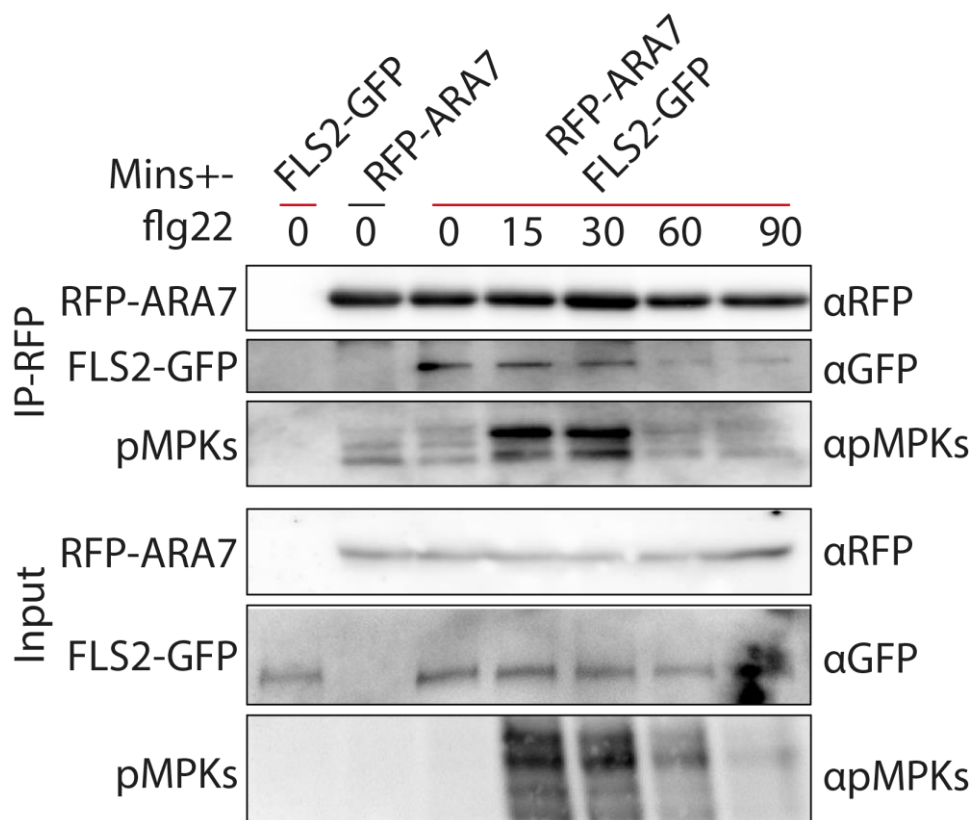


Figure 5.7. Immunoblotting of RFP-RABF2b/ARA7 IPs after flg22 treatment to assess the abundance of FLS2 and active MPKs. RFP-RABF2b/ARA7 was subjected to IP after flg22 treatment, separated on SDS-PAGE and subjected to immunoblot with αGFP, αRFP and αpMPK as indicated. Representative blot of three replicates.

from this compartment at this time or internalised into intraluminal vesicles. Furthermore the downstream kinases of MKK2 and MKK5, MPK3, 4 and 6, are present and phosphorylated in RFP-RABF2b/ARA7 affinity purifications following flg22 treatment (Figure 5.7). This suggests that RFP-RABF2b/ARA7 labelled LE/MVBs function as sites of signal transduction.

5.2.6 Active MPKs are detected in RABF1/ARA6-RFP enrichments after flg22 treatment

To test whether active MPKs and FLS2 are present in another LE/MVB marker proteome, I performed IP of RABF1/ARA6-RFP on sterile grown seedlings stably expressing RABF1/ARA6-RFP and FLS2-GFP, following flg22 treatment. I could not detect FLS2-GFP in IP of RABF1/ARA6-RFP. By contrast, active MPK 3, 4 and 6 were identified in IPs of

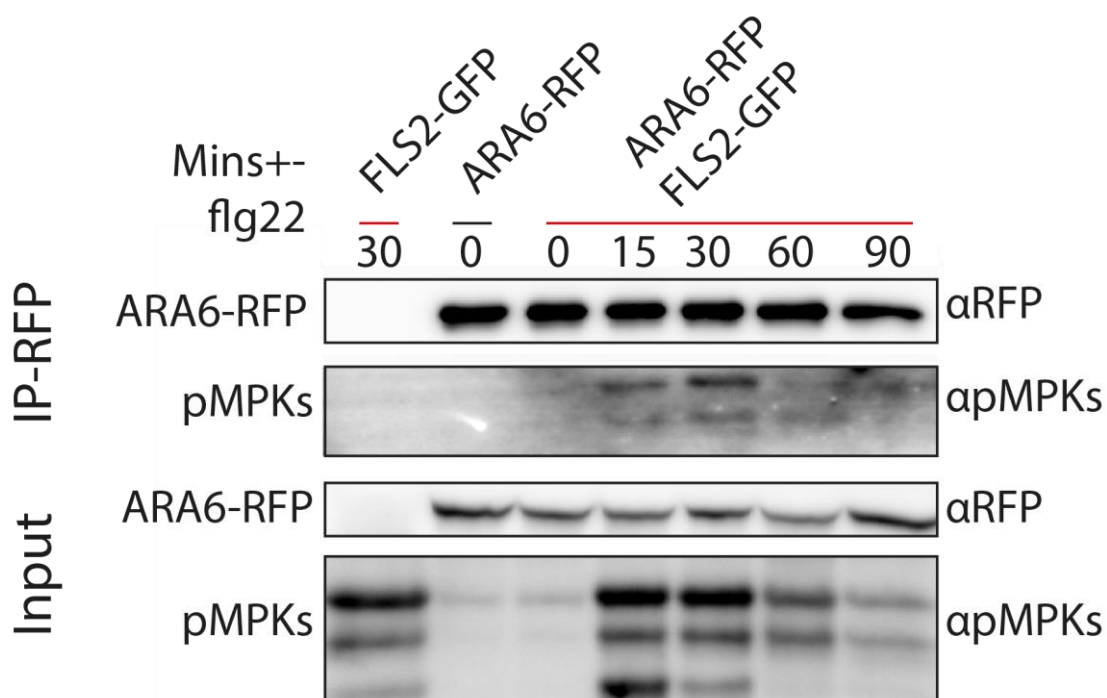


Figure 5.8. Immunoblotting of RABF1/ARA6-RFP IPs after flg22 treatment to assess the abundance of FLS2 and active MPKs. RABF1/ARA6-RFP was subjected to IP after flg22 treatment, separated on SDS-PAGE and subjected to immunoblot with α RFP and α pMPK as indicated. Representative blot of three replicates.

RABF1/ARA6-RFP enrichments with immunoblot (Figure 5.8), demonstrating that active

MPKs are probably present at all RAB5 GTPase labelled LE/MVBs in *A. thaliana*. Furthermore, as MKK5 was identified in the YFP-RABG3f proteome it is likely that this is also the case for RAB7 GTPase labelled LE/MVBs as well.

5.3 Discussion

In this chapter I demonstrated that RHM1 is a positive regulator of immunity and probably functions at LE/MVBs. A biased, candidate led approach revealed that, not only are signalling components present at endosomes, but they are also active. This data is intriguing, but needs further analysis to determine whether the LE/MVB localised MPKs contribute to flg22 induced signalling.

5.3.1 Spectrum counting is unsuitable for thorough quantitative analysis of RFP-RABF2b/ARA7 affinity purifications

Quantification using spectrum counting identified 20 proteins consistently changed in abundance in the RFP-RABF2b/ARA7 proteome after flg22 treatment with limited confidence. However, I was unable to consistently detect (at any time point) proteins such as FLS2 (Section 5.2.4). The experimental design is one of the primary limitations of quantification by spectrum counting. Russell and Lilley (2012) demonstrate that the stage at which data is combined is the principal component of technical variation. Experiments are most technically variable when peptides are combined after lyophilisation to be analysed in one LC-MS/MS run (Russell and Lilley 2012). As in my experiments data was only combined after LC-MS/MS, it is unsurprising that there is high variation within and between experiments. Options to compensate for this technical variation would be to scale quantitative values to an internal standard (such as RFP-RABF2b/ARA7 or an exogenous non-*A. thaliana* protein). Using an internal standard is limited, however, as the standard must be present in all gel slices, as each gel slice is individually processed. Therefore, there were no appropriate internal standard proteins to be used in my experiments even though input quantity of RFP-RABF2b/ARA7 was normalised during SDS-PAGE (Figure 5.1). Thus,

instead of repeating these experiments I decided to analyse these proteins using an orthologous technique.

The addition of the iTRAQ experimental analysis adds confidence to the conclusions of quantitative changes after flg22 treatment. The methodology used for the iTRAQ experiments meant that all peptides from one time point were digested simultaneously. Therefore, RFP-RABF2b/ARA7 could be used as an internal standard between IP conditions and experiments to compensate for variability introduced at digestion stages. Furthermore peptides from each experimental condition are combined after iTRAQ labelling, so at least are analysed in the same LC-Q-TOF run. Utilising these two quantitative datasets, only one protein could be reproducibly identified as changing in abundance following flg22 treatment in all experiments.

Therefore, further work will include using a more sensitive mass spectrometer to analyse IPs of RFP-RABF2b/ARA7 after flg22 treatment. Peptides need to be digestion in solution to allow an internal RFP-RABF2b/ARA7 standard to be used to normalise abundances between conditions. Subsequent separation at the peptide level should help minimise variation based on individual sample handling compared to separation at the protein level with SDS-PAGE and lane slicing. Without labelling, the peptides cannot be analysed in a single LC-MS/MS run. However the department has recently purchased an Orbitrap Fusion and this more sensitive mass spectrometer should increase the number of spectra assigned to each protein and so bring more proteins above the limit of quantification. Thus the combination of an internal standard and the more sensitive mass spectrometer should yield better quantitative data.

5.3.2 RHM1 is a positive regulator of immunity

The combined spectrum counting and iTRAQ quantitation indicates RHM1 increases by over 1.5 fold in abundance in RFP-RABF2b/ARA7 LE/MVBs following 60 min of flg22 treatment.

Furthermore the non-functional *rol1-1* allele is more susceptible to the virulent pathogen *PtoDC3000*. I focussed my study on *rol1-1* as this allele is non-functional and has fewer pleiotropic effects than the reported gain of function *rol1-2* allele (Diet *et al.* 2006). Confirmation of the abundance changes of RHM1 in LE/MVBs after flg22 treatment, using an analogous technique is also necessary. As is thorough characterisation of other PAMP induced responses is essential to ensure that the enhanced susceptibility is not due to off target effects, affecting receptor abundance or SA levels for example

The role of RHM1 in *A. thaliana* has not been well characterised. RHM1 functions by converting UDP-D-Glc to UDP-L-Rha in *planta* (Reiter and Vanzin 2001), however the full implications of this function are unknown. Two *rol1* mutants were identified, one carries a premature stop codon in the coding sequence (*rol1-1*) and one carries a point mutation (R283K) in the coding sequence (*rol1-2*) (Diet *et al.* 2006). Both of these mutations lead to a decrease in the dehydratase activity of the expressed product. The *rol1-2* allele has a more severe developmental phenotype, however, than the *rol1-1* allele and this was suggested to be from pleiotropic effects of this point mutation (Diet *et al.* 2006).

Based on my quantitative data RHM1 is recruited to LE/MVBs following flg22 treatment. The reason for this recruitment is unclear, but there are three conflicting hypotheses. RHM1 could modify pectin for secretion through exosomes and alter the pectin matrix to help strengthen the cell wall and so prevent pathogen penetration. There is a reduction in rhamnogalacturonan I and II (RGI and RGII) levels in the *rol1* mutants (Diet *et al.* 2006). RGI and RGII with homogalacturonan (HGA) form the pectin matrix of the cell wall, and RGI is thought to regulate cell wall porosity (Ridley *et al.* 2001). There is, however, limited evidence of pectin following pathogen challenge, making this hypothesis unlikely.

Alternatively the altered flavonol composition could affect constitutive defence responses. *rol1* mutants display altered leaf phenotypes due to altered flavonol biosynthesis (Kuhn *et*

*al.*2011). Furthermore the *rol1* leaf phenotype is partially due to altered auxin accumulation in leaves and partially through an unknown mechanism (Ringli *et al.* 2008, Kuhn *et al.* 2011). Flavonol accumulation affects the functioning of the actin cytoskeleton (Ringli *et al.* 2008, Kuhn *et al.* 2011) and a properly functioning actin cytoskeleton is important for secretion and stomatal immunity. As my data suggests an increase in RHM1 at LE/MVBs following flg22 treatment this hypothesis is unlikely. The enhanced flavonol phenotype in *rol1* mutants is constitutive and so does not explain the altered localisation of RHM1 following flg22 treatment.

The third hypothesis for the observed enhanced susceptibility of the *rol1* mutants is that RHM1 may be recruited to LE/MVBs following flg22 treatment to produce additional flavonols for secretion and defence. The *rol1* mutants display altered flavonol accumulation and altered leaf and stomatal morphology (Diet *et al.* 2006, Ringli *et al.* 2008, Kuhn *et al.* 2011). *rol1* mutants contain strongly reduced amounts of flavonols glycosylated with multiple rhamnose units, while flavonols with single rhamnose units are often more abundant in *rol1* mutants (Ringli *et al.* 2008). In roots there is a decrease in overall flavonol content of 25% in both *rol1* mutants and an increase by 30% (*rol1-1*) and 10% (*rol1-2*) in shoots (Ringli *et al.* 2008). It may be that these flavonols are produced in LE/MVBs ready for exosome mediated secretion during pathogen infection. Several flavonols have been shown to have antimicrobial properties and have been used as biopesticides (Cespedes *et al.* 2014, de Lima *et al.* 2014) but no role have been demonstrated in PTI. Flavonols modified with multiple rhamnose subunits could contribute to defence against microbial pathogens and are secreted after synthesis at LE/MVBs. This is the most likely explanation, but whether secretion of flavonols is affected in *rol1-1* mutants both before and after flg22 treatment needs to be tested.

5.3.3 Recycling FLS2 is enriched with RFP-RABF2b/ARA7 not RABF1/ARA6-RFP

One striking observation from my data is that FLS2-GFP can be found in IPs of RFP-RABF2b/ARA7 before flg22 treatment and it decreases in abundance from 30 min. FLS2 constitutively recycles through partially RFP-RABF2b/ARA7 positive compartments identified after BFA treatment (Beck *et al.* 2012) and these are enriched in my IPs. Furthermore, the decrease in abundance of FLS2-GFP in the RFP-RABF2b/ARA7 proteome after 30 minutes of flg22 could reflect FLS2 being trafficked from the compartment further on in the late endocytic route. This contrasts with CLSM data from Beck *et al.* (2012) showing that FLS2-GFP maintains a high level of co-localisation with RFP-RABF2b/ARA7 after 30 minutes of flg22 treatment. This observed difference could be due to the different tissues being examined (whole seedlings compared to leaf epidermis) or due to the different age and growth the seedlings examined. Alternatively this IP method could preferentially enrich for proteins on the exterior of the LE/MVB and during this timeframe FLS2 is moved into the intraluminal vesicles of LE/MVBs (Spallek *et al.* 2013) resulting in less FLS2-GFP detected even though it is present in the compartment. As FLS2-GFP does not co-localise to the same extent with RABF1/ARA6-RFP as with RFP-RABF2b/ARA7 (Beck *et al.* 2012), it is unsurprising it is not detected in the RABF1/ARA6-RFP IPs.

5.3.4 Active MPKs are localised to endosomes following flg22 treatment but their role in signalling is still unclear

Active MPKs can be enriched with the two RAB5 GTPases (RABF2b/ARA7 and RABF1/ARA6) as well as with RABG3f. The most parsimonious explanation is that MPKs are constitutively localised to LE/MVBs. MKK2 and 5 were identified in my proteomic analysis of LE/MVBs without flg22 treatment. Furthermore MPKs have been localised to the TGN and the endomembrane system or cytoskeleton in several studies (Müller *et al.* 2010, Beck *et al.* 2011, Gu and Innes 2011). Therefore, even without direct localisation data, my postulation that MPKs are present at LE/MVBs constitutively is sound, but not conclusive.

This data demonstrates that signalling components are active, in a biochemical sense, at LE/MVBs following flg22 treatment. To support the biological significance of MPK activation at endosomes, substrates should also be present at this location. This data is essential for conclusions to be made, as an alternative interpretation of the presence of phosphorylated MPKs in LE/MVBs following flg22 treatment is that they are en route for degradation (with FLS2) and no longer play a role in signalling.

5.3.5 Conclusions and further work

RHM1 is increased in abundance at LE/MVBs and is a positive regulator of PTI. The role of RHM1 in the resistance of *A. thaliana* to *Pto* DC3000 will be further explored, but not in this thesis. The principal conclusion from this chapter, however, is that active MPKs are present at LE/MVBs following flg22 treatment. My attempts to determine the biological significance of LE/MVB localised active MPK3,4 and 6 will be explored in Chapter 6.

6 Identifying potential targets for endosome localised MPKs after flg22 treatment

6.1 Introduction and Objectives

As demonstrated in Chapter 5 active MPKs have been identified in LE/MVB proteomes. The next question to be addressed is whether these endosome localised MPKs contribute to FLS2 signalling. If endosomal MPKs contribute to signalling, there must be proteins present at the same location that are kinase targets of these MPKs and should have been identified in my LE/MVB proteomics. I, therefore, assessed my combined LE/MVB proteome for MPK3, 4 and 6 kinase target proteins that contribute to defence responses.

6.1.1 Candidate MPK3, 4 and 6 targets have been identified in *A.thaliana*

Several studies have identified numerous potential MPK3, 4 and 6 kinase targets utilising diverse approaches. Methods to identify MPK targets have followed three broad strategies: 1). identification of MPK interaction partners, 2). identification of specific motifs phosphorylated by MPK3 and 6, and 3). identification of peptides/proteins phosphorylated by specific MPKs. The first strategy is exemplified by Mukhtar *et al.*, who utilised an extensive library of *A.thaliana* coding sequences as well as pathogen effectors in yeast two hybrid interaction studies to identify candidate MPK interactors (Mukhtar *et al.* 2011). This approach should identify any proteins associating with MPKs, including kinase targets and regulatory proteins. A similar approach was also used to identify rice MPK targets (Singh *et al.* 2012).

Using the second approach, a conserved sequence (L/P-P/X-S-P-R/K) was identified as the targeting sequence of MPK3 and 6. One of the putative MPK3/6 targets was confirmed (At1g80180.1) with this approach (Sörensson *et al.* 2012). The third approach was used in two different ways to identify targets of MPK3, 4 and 6 in *A. thaliana*. Popescu *et al* incubated an array of 3840 *A. thaliana* proteins with 10 different recombinant MPKs, activated by two different MKKs, and radio labelled ³³P-γ-ATP to identify 570 putative MPK

substrates (Popescu *et al.* 2009). This study identified several transcription factors including the SA responsive WRKY DNA-binding protein 62 (WRKY62) as a target of MPK6 (Popescu *et al.* 2009). While Hoehwarter and colleagues inducibly expressed a constitutively active *N. tabacum* variant of *ntMEK2*, known as *ntMEK2^{DD}* (Hoehwarter *et al.* 2013). This *ntMEK2* variant has two amino acid substitutions in the activation loop (S and T to D) and constitutively phosphorylates MPK3 and MPK6 *in vivo*. Following expression of *MEK2^{DD}* in *A. thaliana* phosphopeptides were enriched and identified with LC-MS/MS to identify 141 candidate MPK3 and 6 substrates (Hoehwarter *et al.* 2013). These candidates include a cytoskeleton regulatory protein Villin 3 (VLN3) (Hoehwarter *et al.* 2013). Villin 3 is a member of a protein family that regulates actin filament dynamics by severing or bundling actin depending on the cytosolic conditions, which will be expanded in section 6.3.3. All of these techniques help elucidate the role of MPKs in signalling and these datasets are useful tools with which to identify potential targets of MPKs.

Whilst these datasets are useful as indicators, they are not conclusive lists. As with the proteomic data presented in this thesis they are starting points for further analysis. Confidence on whether a protein is an MPK target can be improved by combining phosphoproteomic data with the data from the studies listed above.

6.1.2 Extensive phospho-proteomic data has been obtained following flg22 elicitation

The approaches discussed above are limited in that they can only define which proteins can be phosphorylated by MPKs. Other information about localisation or level of phosphorylation following a stimulus are needed to decipher the location at which the interaction occurs and after which stimuli are they phosphorylated. Two landmark phospho-proteomic studies following flg22 treatment focused on the PM (Benschop *et al.* 2007, Nühse *et al.* 2007). Interestingly a number of endomembrane regulators were identified as phosphorylated after flg22 treatment including the SNAREs SYP121 and SYP122 (Benschop *et al.* 2007) and the

dynamamin like protein DRP2a (Nühse *et al.* 2007). A more recent study of phospho-proteomic changes following flg22 treatment assessed a crude extract of proteins from plant cell culture (Rayapuram *et al.* 2014). Rayapuram *et al.* also identify endomembrane regulators, including the actin cytoskeleton regulator VLN3, as more phosphorylated after flg22 treatment. Comparisons between phosphoproteomic datasets after flg22 treatment and MPK kinase targets will give a higher confidence dataset of MPK kinase targets that are phosphorylated after flg22 treatment. The combination of data from studies identifying putative MPK targets and from phospho-changes after flg22 treatment provides two powerful tools with which to identify endosomal MPK targets when compared to my proteomic data.

6.1.3 Objectives

My main objective is to identify credible MPK targets in my LE/MVB proteome dataset. I therefore compared my LE/MVB proteome to the candidate MPK kinase target lists (Popescu *et al.* 2009, Mukhtar *et al.* 2011, Sörensson *et al.* 2012, Hoehenwarter *et al.* 2013). This provided a candidate list of endosomal MPK targets to be tested for defects in defence signalling and to be compared other to phospho-proteomic studies after PAMP treatment.

6.2 Results

6.2.1 Identification of putative endosome localised MPK targets

In order to identify targets of endosome localised MPKs, I utilised four studies to create a candidate list of MPK3, 4 or 6 targets (Popescu *et al.* 2009, Mukhtar *et al.* 2011, Sörensson *et al.* 2012, Hoehenwarter *et al.* 2013). This combined candidate list was then compared to the combined LE/MVB proteomes (Section 4.2.8) and the intersection is the pool of potential kinase targets for LE/MVB localised MPKs. This led to the identification of 16 candidate proteins (Table 6.1). I obtained 30 different lines with independent tDNA insertions in 15 genes encoding the candidate proteins, from NASC (<http://arabidopsis.info/>The European Arabidopsis Stock Centre). In addition, VLN3 is one candidate that has been studied and is

partially redundant with VLN2. Therefore, I obtained published tDNA insertion lines with no detectable transcripts of *vln2*, *vln3* and the double mutant cross of *vln2* and *vln3* (Khurana et al. 2010, Bao et al. 2012). Seven of these lines did not germinate leaving 26 lines in total

Short name	GFP						RFP						Path assays		Phospho data	Reference
	Col- 0	YFP- ARA5/RAB2a	YFP- RAB3f	YFP- ARA7/RABF2b	Col- 0	ARA6/RABF1- RFP	ARA7/RABF2b- RFP	ARA7/RABF2b-FLS2-GFP	PIR screen	Susceptibility	Kinase					
CCCI	0	17	0	0	0	0	5	2	X	-	MPK3/6	Popescu et al. 2013				
PESI	0	0	0	0	0	0	0	2	-	-	MPK3/4	Popescu et al. 2009				
Molecular chaperone Hsp40/DnaJ family protein	0	0	2	0	0	0	0	8	-	-	MPK4	Popescu et al. 2009				
UDP-glucose 6-dehydrogenase family protein	3	0	2	0	3	5	3	21	-	-	MPK3/6	Hoehenwarter et al. 2013				
KING1	0	0	0	0	4	0	0	15	-	-	MPK3/6	Sorenson et al. 2013				
EF3C	0	14	17	16	3	9	25	53	X	-	MPK3	Popescu et al. 2009				
VLN3	0	0	5	0	0	0	0	9	-	X	MPK3/6	Hoehenwarter et al. 2013				
transducin family protein / WD-40 repeat family protein	0	29	27	27	8	31	44	129	-	-	MPK3/6	Hoehenwarter et al. 2013				
ALDH3f1	2	0	0	0	2	2	13	30	X	-	MPK6	Popescu et al. 2009				
ACT-like protein tyrosine kinase family protein	0	0	2	0	0	0	0	2	-	-	MPK3/6	Hoehenwarter et al. 2013				
SNX2b	0	0	0	0	0	0	0	2	-	-	MPK3/6	Hoehenwarter et al. 2013				
Unknown protein	0	0	0	0	0	0	0	2	-	-	MPK3/6	Hoehenwarter et al. 2013				
HMZ	0	5	3	12	0	2	19	44	-	-	MPK3/6	Hoehenwarter et al. 2013				
EF3B1	3	0	0	2	0	0	2	2	X	-	MPK6	Hoehenwarter et al. 2013				
Insulinsase (peptidase family M16) family protein	0	8	11	10	0	7	9	27	X	-	MPK3/4/6	Popescu et al. 2009				
Guanylate-binding family protein (GTP)	6	0	0	0	2	2	0	4	-	-	MPK3/6	Sorenson et al. 2013				
	6	7	2	5	9	10	6	14	-	X	MPK3/6	Hoehenwarter et al. 2013				

Table 6.1. Candidate endosomal MPK targets. ATG numbers (TAIR10) and protein short names from proteins that were identified as potential MPK targets in the annotated papers and identified in the LE/MVB proteome (Chapter 4) and RFP-RABF2b/ARA7 IPs after flg22 treatment (Chapter 5). Summed spectrum counts are listed over all replicates from all the conditions tested and the potentially phosphorylating kinase. Plants deficient in the indicated candidate proteins were tested for PIR defects or altered susceptibility to *Pto* DC3000. The candidates tested for PIR defects twice are indicated with an X, as are the two candidates that displayed consistent altered susceptibility to *Pto* DC3000.

(including *vln2*, *vln3* and *vln2,3*). These lines were analysed in a pipeline outlined in figure 6.

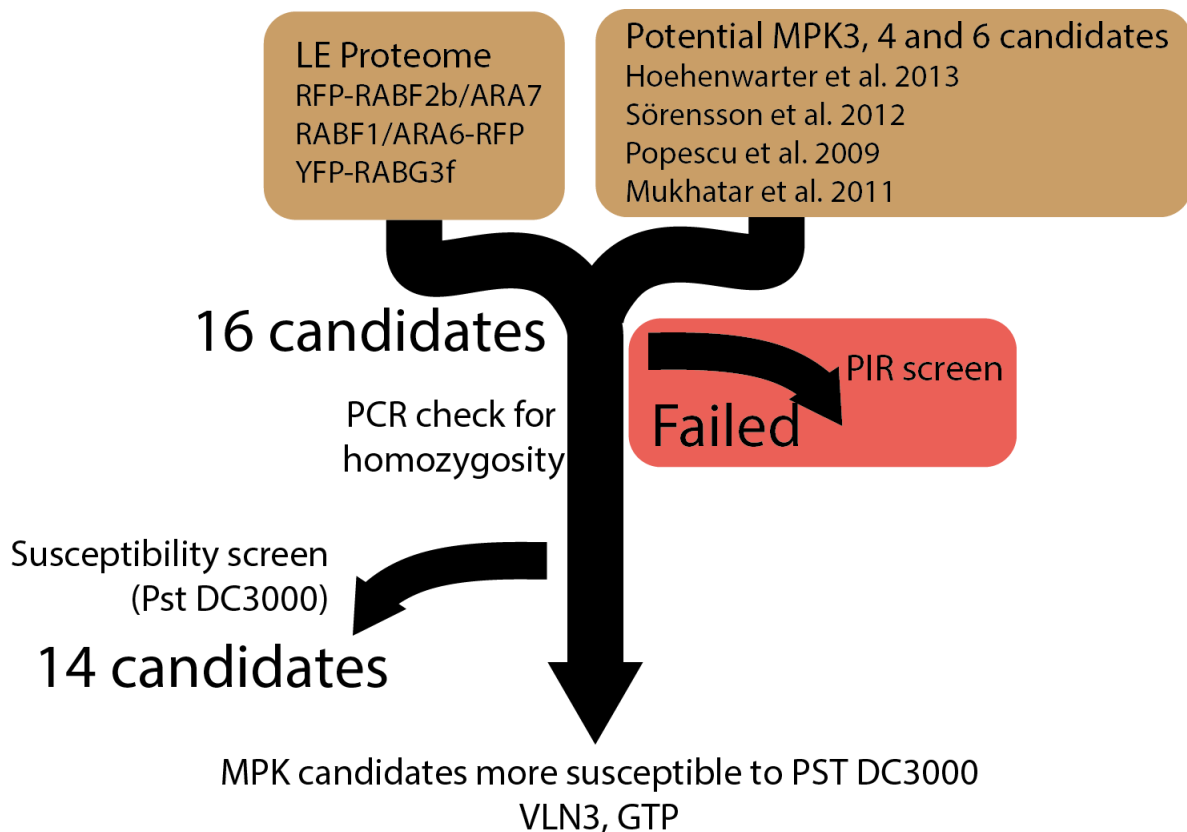


Figure 6.1 Screening pipeline for potential endosomal MPK targets. Endosomal proteins were screened for potential MPK phosphorylation leaving 16 candidates. These candidates were then tested with a PIR screen in seedlings, PCR checked to confirm homozygosity and tested for susceptibility to Pst DC3000 in adult plants.

6.2.2 Screening of tDNA insertion lines for defects in PAMP induced resistance

I confirmed the homozygosity of these tDNA insertion lines with PCR and tested them for defects in PIR by pre-treatment with flg22 before infection with the virulent pathogen *Pto* DC3000 expressing the luciferase operon (LUX) (Figure 6.2a). There are 10 separate lines with a defect in flg22 induced PIR when compared to Col-0. Five of these 10 lines of interest were tested again (Table 6.1). When these experiments were repeated with more seedlings from five of the lines of interest, none of them were significantly different from Col-0 (Figure 6.2b). Therefore it is unlikely that these mutants have a defect in PIR, but the initial observed

deviations are due to high technical variation in these experiments and limited sampling. I therefore did not further test these lines for PIR and used an alternative screening method.

I screened all 23 lines for altered susceptibility to spray inoculation of the virulent pathogen *Pto* DC3000. Mutant lines in two of the tested candidate endosomal MPK targets were altered in susceptibility to the bacterium compared to Col-0 in one replicate. I therefore selected Guanylate binding protein (GTP) and VLN2/VLN3 as candidates to work with further.

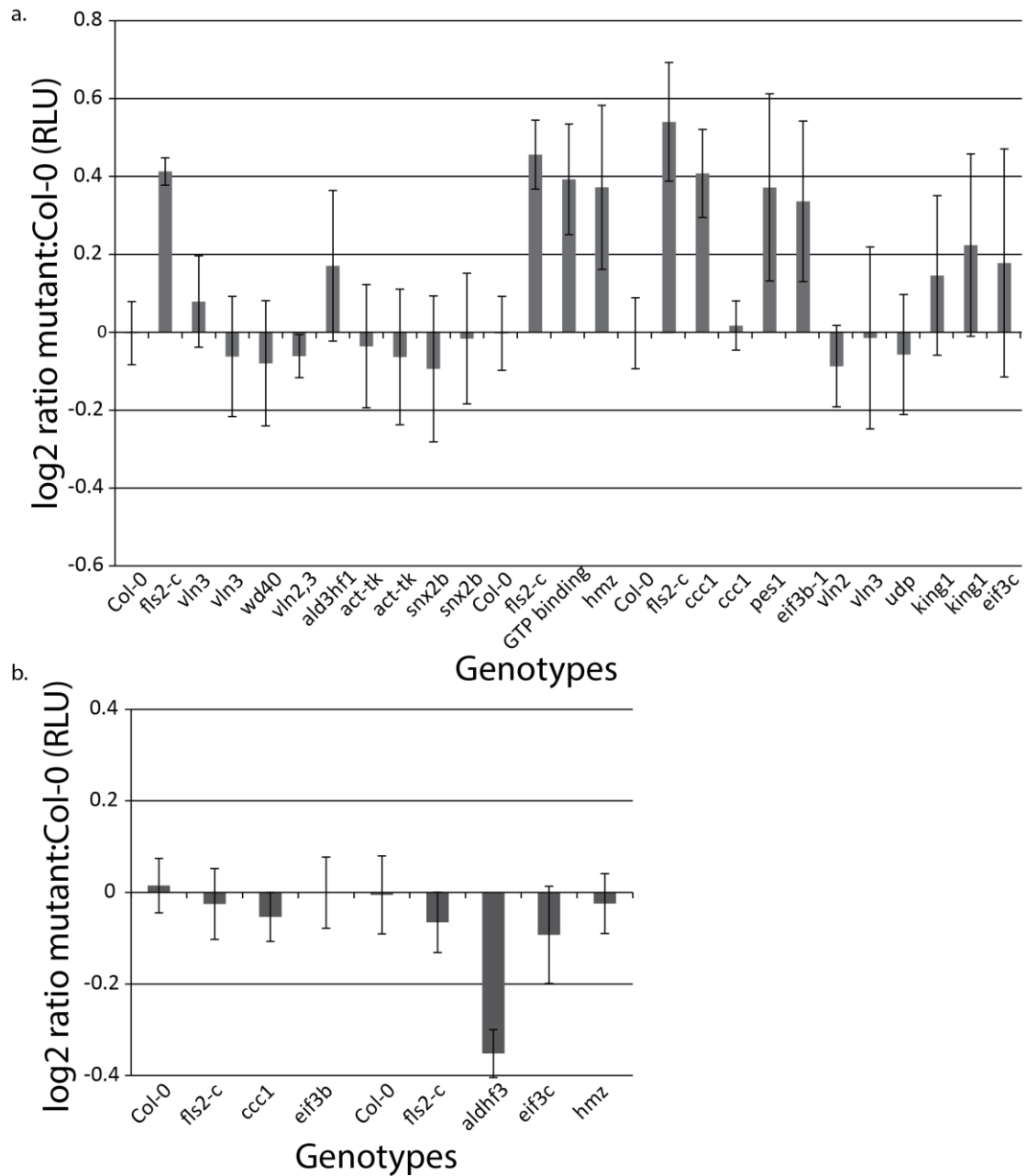


Figure 6.2. High throughput screening of PIR for candidate endosomal MPK targets. Estimated growth of the virulent pathogen *P. syringae* DC3000 expressing the luciferase operon on liquid grown *A. thaliana* after pre-treatment with flg22. Columns represent log₂ ratios of measured luminescence in each genotype to that of Col-0 controls. Error bars represent the standard deviation. a. Initial screening of reported homozygous SALK lines. (n=8 per genotype) b. Secondary screen of SALK lines with confirmed homozygous lines. (n=24 per genotype)

6.2.3 *gtp-1* and *gtp-2* mutants are more resistant to *Pto* DC3000

To preliminarily characterise the *gtp* mutants, I grew these plants under short day conditions. Both mutants appear normal at early stages of growth. By four weeks *gtp-1* is smaller than both Col-0 and *gtp-2* (Figure 6.3a). I repeated the susceptibility assays for *gtp-1* and *gtp-2* tDNA insertion lines and found that *gtp-1* and *gtp-2* alleles are consistently more resistant to spray inoculated *Pto* DC3000 than Col-0 (Figure 6.3b). *gtp-1* displays a stronger resistance phenotype to *gtp-2* suggesting it is a stronger allele than *gtp-2*. This relationship between *gtp-1* and *gtp-2* and their phenotypes is reflected by the growth of both *gtp-1* and *gtp-2*, as *gtp-1* is more stunted than *gtp-2*. One reason for an increased resistance to *Pto* DC3000 is a hyper sensitivity to flg22. Therefore, I tested for an altered flg22 induced ROS burst in *gtp-1* and *gtp-2* mutants (Figure 6.3c). The ROS burst from these mutants was indistinguishable from Col-0. All of these data suggest GTP is involved in the cell's response to pathogenic bacteria downstream of recognition.

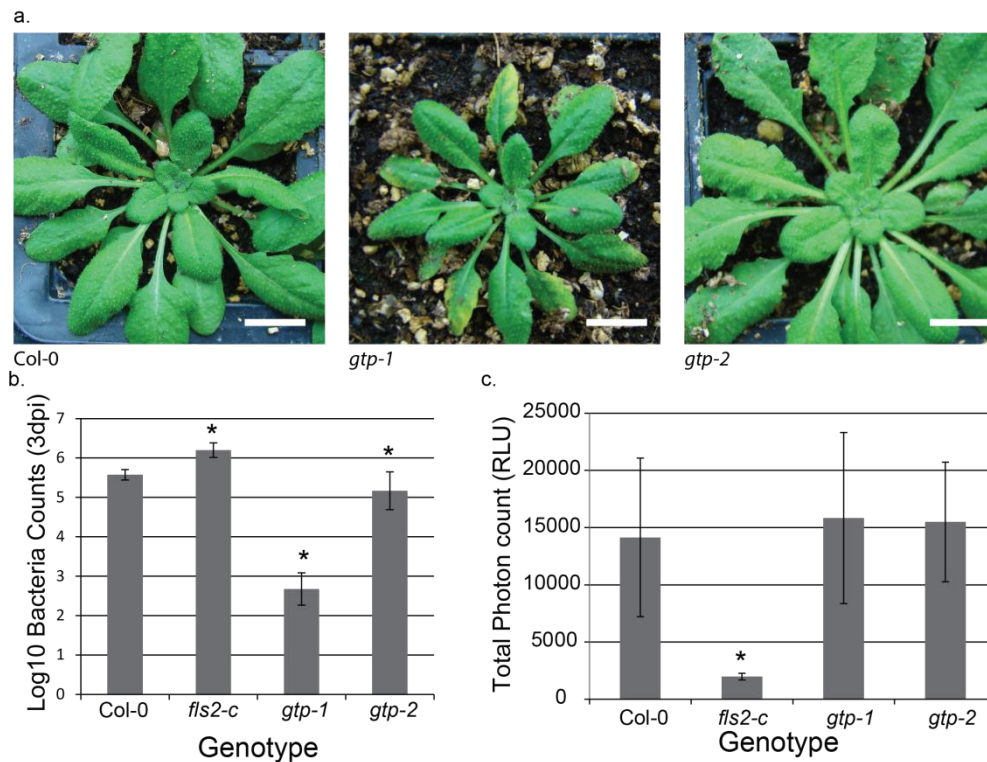


Figure 6.3. Characterisation of phenotype of *gtp* mutants. a. Images of 4 week old plants of the respective genotypes grown on soil in short day conditions. b. Estimation of growth of spray inoculated *P. syringae* DC3000. 4 week old mutants were spray inoculated with the virulent pathogen *P. syringae* DC3000. Columns represent estimated bacterial growth 3 days post infection. Error bars represent the standard deviation. * denotes a significant difference (Student's t test) from Col-0, $p < 0.05$. Graph shows data from 3 biological replicates. c. Oxidative burst triggered by 100 nM flg22 in the indicated genotypes measured with a luminol-based assay as relative light units. Columns represent the average of total photon counts per leaf disc over 40 minutes of flg22 treatment ($n = 16$ for each genotype). Error bars represent the standard deviation. * denotes a significant difference (Student's t test) from Col-0, $p < 0.05$. Graph shows a representative experiment of 3 replicates.

6.2.4 *vln* mutants are more susceptible to *Pto* DC3000

Visual characterisation of the *vln2*, *vln3* and *vln2/3* mutants at eight weeks old confirms the reported phenotypes of these mutants (Figure 6.4a). *vln2* and *vln3* phenotypically resemble Col-0, whereas the *vln2/3* mutants display the reported leaf curling phenotype (van der Honing *et al.* 2012). To further interrogate the role of VLN2 and VLN3 in defence, I analysed

vln2, *vln3* and *vln2/3* mutants for altered susceptibility to *Pto* DC3000. All three mutants were consistently more susceptible to spray inoculated *Pto* DC3000 than Col-0 (Figure 6.4b). Interestingly the phenotypes are not additive, suggesting *VLN2* and *VLN3* act in the same genetic pathway for pathogen defence.

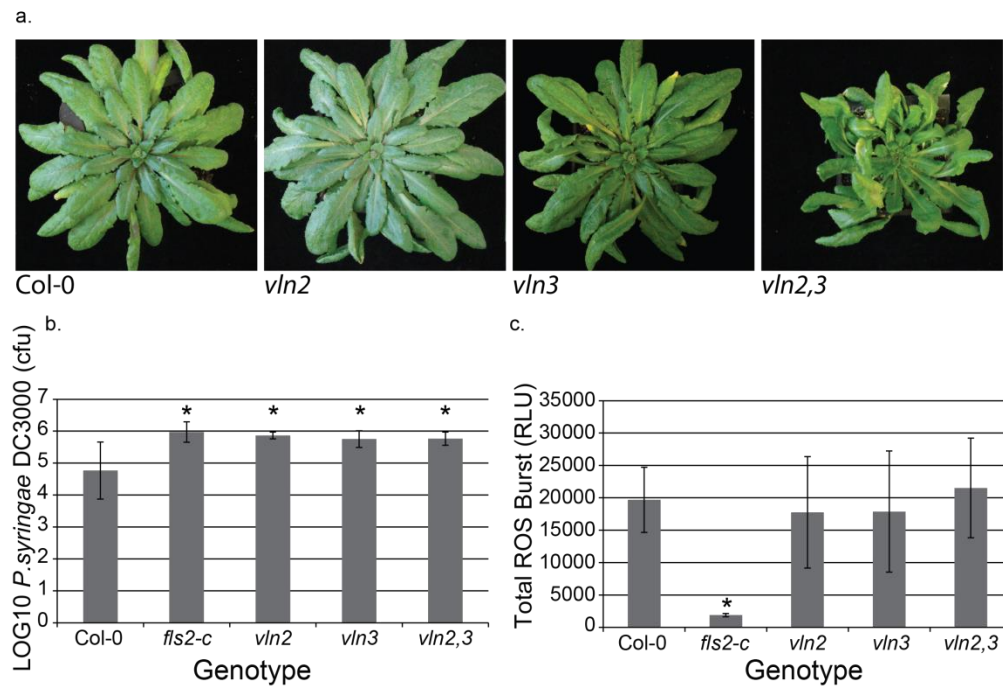


Figure 6.4. Characterisation of phenotype of *vln2*, *vln3* and *vln2,3*. a.

Images of 8 week old plants of the respective genotypes grown on soil in short day conditions. b. Estimation of growth of spray inoculated *P. syringae* DC3000. 4 week old mutants were spray inoculated with the virulent pathogen *P. syringae* DC3000. Columns represent estimated bacterial growth 3 days post infection. Error bars represent the standard deviation. * denotes a significant difference (Student's t test) from Col-0, $p < 0.05$. Graph shows data from 1 representative experiment from 3 biological replicates. c. Oxidative burst triggered by 100 nM flg22 in the indicated genotypes measured with a luminol-based assay as relative light units. Columns represent the average of total photon counts per leaf disc over 40 minutes of flg22 treatment ($n = 16$ for each genotype). Error bars represent the standard deviation. * denotes a significant difference (Student's t test) from Col-0, $p < 0.05$. Graph shows a representative experiment of 3 replicates.

To test whether the enhanced susceptibility phenotype was due to reduced perception of bacterial PAMPs I tested the *vln2*, *vln3* and *vln2/3* mutants for altered ROS burst following flg22 treatment (Figure 6.4b). The mutant lines were indistinguishable from Col-0 demonstrating that the tDNA insertions do not have an unintended effect on the cell's ability to perceive flg22 or respond with a ROS burst.

6.2.5 VLN3 and GTP have experimentally annotated phosphosites

To further assess VLN3 and GTP as kinase targets for endosome localised MPKs I examined their coding sequences for recognised domains and characterised phosphosites (Figure 6.5). VLN3 has three experimentally confirmed phosphosites on serine (S778, S814, S880) residues between the six N terminal gelosin domains and the villin headpiece (Figure 6.5a). These phosphosites have been detected experimentally both before and after JA treatment (Brodersen *et al.* 2006). There is also one additional phosphosite on VLN3 (S812) that was detected following flg22 treatment (Rayapuram *et al.* 2014). Interestingly peptides phosphorylated on S812 and S814 were more abundant compared to un-phosphorylated peptide after flg22 treatment (Rayapuram *et al.* 2014). GTP has two experimentally annotated phosphosites (T814, S815) in between the C-terminal coiled coil domains and the GTP binding domains at the N-terminus (Figure 6.5b). These data supports the hypothesis that GTP and VLN3 are targets of MPKs after flg22 treatment.

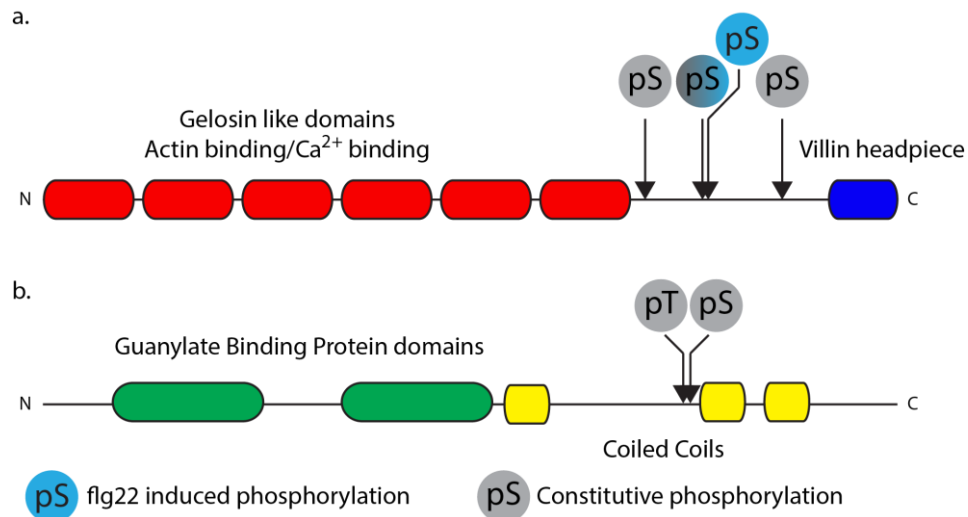


Figure 6.5. Protein structure of MPK phosphorylation candidates. a. VLN3: Gelsolin like domains (PF00597): 28-111; 153-206; 270-237; 412-484; 533-601. Villin headpiece (PF02209): 930-965. Annotated phosphosites on S778, S812, S814, S880 Reiland *et al.* (2009) and Rayapuram *et al.* (2014). Blue coloured phosphosites indicate flg22 inducibility. b. GTP: Guanylate Binding Protein (PF02263): 51-310. Guanylate Binding Protein (PF02841): 314-618. Coiled Coil domains: 632-653, 826-864, 868-889. Annotated phosphosites on T814, S815 Hoehnwarter *et al.* (2013).

6.2.6 VLN3-GFP is not more phosphorylated on serine residues after flg22 treatment

To investigate whether VLN3 is differentially phosphorylated after flg22 treatment, I performed IP of VLN3-GFP in a time course after flg22 treatment and subjected to immunoblot (Figure 6.6). I was able to consistently detect VLN3-GFP after IP of GFP in unelicited and flg22 treated samples and there is no abundance change of the protein. I could detect a signal at the size of VLN3-GFP with the α pS antibody, raised against phosphorylated serine residues. However, there did not appear to be a consistent change in total phosphorylation on all serine residues in VLN3-GFP following flg22 treatment. Interestingly there was a double band present in both blots in IP of VLN3-GFP reminiscent of a phosphorylated protein. These data suggest VLN3-GFP is phosphorylated on serine

residues both before and after flg22 treatment and total serine phosphorylation on the

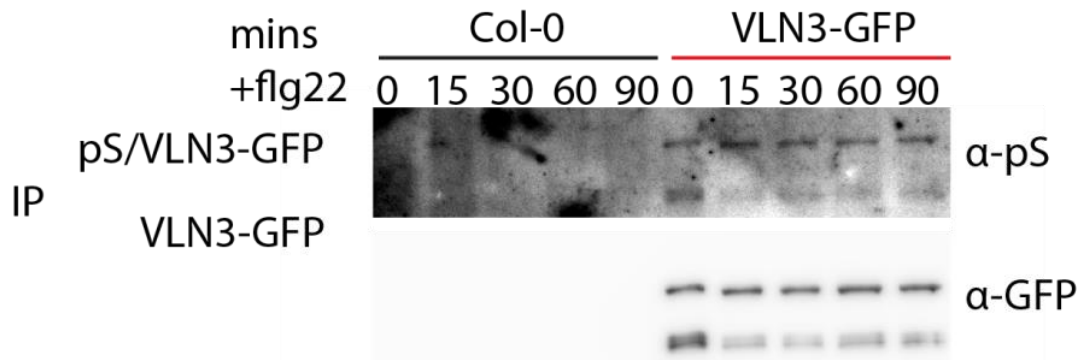


Figure 6.6. Total VLN3-GFP Serine phosphorylation following flg22 treatment is not altered. VLN3-GFP was subjected to IP after flg22 treatment, separated with SDS-PAGE and subjected to immunoblot with α GFP and α pS as indicated. Representative blot of two replicates.

protein did not change following flg22 treatment.

6.3 Discussion

I demonstrated that VLN2, VLN3 are involved and GTP is implicated in the plant's response to bacterial attack, downstream of FLS2 and the ROS burst. My data and published literature also provides circumstantial evidence that VLN3 and GTP are targets of endosomal MPKs following flg22 treatment.

6.3.1 Several putative targets of endosomal MPK are present in RFP-RABF2b/ARA7

Using a combination of knowledge derived from the literature and my proteomic data, I was able to identify 16 candidate targets for endosomal MPKs. Screening for mutants in the genes coding for these candidates allowed me to eliminate 13 targets to leave three potential endosomal MPK targets (VLN2, VLN3 and GTP). These proteins have been identified as potential targets of MPK3/6 (Hoehenwarter *et al.* 2013). When the constitutively active variant of MEKK2 (MEKK2^{DD}) is expressed in *A. thaliana* seedlings phosphopeptides from these proteins are more abundant. Whilst this approach is very powerful, it does not conclusively demonstrate that VLN3 and GTP are direct targets of MPK3/6 as there may be

off target effects, and expression of MKK2^{DD} may cause indirect activation of other kinases. The most likely explanation, however, is that VLN3 and GTP are targets of MPK3 and 6.

It would also be interesting to compare this proteomic dataset to other proteomic or transcriptomic datasets. Identifying endomembrane regulators that are phosphorylated after defence signal activation (flg22 – Benschop *et al.* 2007 or Nuhse *et al.* 2007, RIN4 activation – Elmore *et al.* 2012) would help characterise the mechanisms by which endomembranes are modified during immune responses. Furthermore transcriptome studies could also be used to indicate endomembrane trafficking over the longer term and these comparisons extended to BR mediated responses.

6.3.2 GTP regulates plant defence

GTP is implicated in defence. Both alleles of the *gtp* mutants were more resistant to *Pto* DC3000 than Col-0, and *gtp-1* was more resistant than *gtp-2*. Due to the data discussed in Section 6.2.3 I assumed that *gtp-1* represents a strong allele and *gtp-2* represents a weak allele, probably due to transcript abundance. There is only phenotypic developmental data to support this assumed relationship between the alleles and RT-PCR is essential to validate this assumption.

The function of GTP in plants is unclear but its orthologs have been characterised in other systems. GTP is a homolog of the mammalian Guanlyate binding protein (GBP) family of proteins. These proteins are endomembrane regulators of the dynamin GTPase family, however have been poorly biochemically characterised (Britzen-Laurent *et al.* 2010, Vestal and Jeyaratnam 2011). GBPs are transcriptionally up-regulated by defence signalling through interferon γ and p53 signalling (Kim *et al.* 2011, Yamamoto *et al.* 2012, Zhu *et al.* 2013). Interestingly, human GBPs help protect against intracellular pathogens by recruiting NADPH oxidases, antimicrobial peptides and autophagic machinery to the pathogen infected intracellular compartments (Dupont and Hunter 2012, Yamamoto *et al.* 2012). *A. thaliana*

GTP proteins may fulfil a similar role during biotic interactions. This explanation of their function would, however, conflict with the observed enhanced resistance to bacteria in the *gtp* mutants as a null mutant would be expected to be more susceptible to bacterial infection. The essential next step, however, is to confirm expression levels of *gtp* in these mutants.

There are two most likely explanations for the enhanced resistance phenotype observed in the *gtp* mutants. The first is that GTP is a negative regulator of immune signalling and has a role unlike that of mammalian GBP. GTP may be involved in defence and also be crucial for plant development and so alteration in protein levels results in smaller plants with a reduced inducible immune response. Alternatively GTP protein levels may be monitored by an *R* gene, and interference with the production of the protein results in constitutive defence activation causing a reduced growth phenotype. Arguing against the second hypothesis is that the *gtp* mutants are indistinguishable from Col-0 in terms of PAMP induced ROS burst. Constitutive activation of defence through R protein signalling can result in high SA levels in a plant. SA signalling promotes increased accumulation of FLS2 and RBOHD, so mutants with constitutive SA signalling might be expected to display an enhanced ROS burst upon flg22 treatment, as seen in *acd6* mutants over-accumulating SA (Tateda *et al.* 2014). All of these data are, however, circumstantial and both possibilities need to be tested. Regardless of mode of action GTP is clearly an important player in plant immunity.

6.3.3 VLN3 may regulate the cytoskeleton in response to flg22

VLN3 is another candidate target of endosomal MPK3 and 6. As with GTP the evidence that it is directly phosphorylated by MPK3 and 6 is circumstantial. VLN3 phosphopeptides are more abundant when MEK2^{DD} is over expressed (Hoehenwarter *et al.* 2013) and a VLN3 peptide that is phosphorylated on S812 and S814 is more abundant, relative to unphosphorylated peptide, after flg22 treatment (Rayapuram *et al.* 2014). The data presented in Figure 6.6 (Section 6.2.6) suggests that serine phosphorylation averaged over all VLN3 before and after flg22 treatment is equal. Therefore there must be compensatory de-

phosphorylation of other serine residues (not S812 and S814) after flg22 treatment to maintain the same overall level of serine phosphorylation. The effects of positional phosphorylation on the activity of VLN3 therefore need to be determined. Alternatively, it may be that this experiment technically failed and other antibodies detecting different phosphosites need to be used for testing.

The data presented in Section 6.2.4 demonstrate that mutant *vln2*, *vln3* and the double *vln2,3* mutants are more susceptible to spray inoculated *Pto* DC3000 and that perception of flg22 is not impaired. The function of VLN3 in plants has been fairly well characterised. VLN3-GFP localises to actin filaments in leaf and root epidermal cells (van der Honing *et al.* 2012). However, VLN3's localisation to RABF2b/ARA7 or RABF1/ARA6 positive structures has not been tested. However LE/MVBs move along actin filaments, reviewed Anitei *et al.* (2012), providing ample opportunity for interaction between VLN3 and endosome localised MPKs.

I propose a model of differential VLN3 activity regulated by Ca^{2+} and phosphorylation status following flg22 treatment (Figure 6.7), I will now elaborate on the data behind this model: Human VLN regulates actin in a variety of ways including bundling, capping, severing and disassembling bundles or fibres (Kumar and Khurana 2004, Kumar *et al.* 2004, Kumar *et al.* 2004). The activity of VLN is dependent on Ca^{2+} concentration and phosphostatus (Kumar and Khurana 2004, Kumar *et al.* 2004), although phosphorylation is the primary determinant of VLN severing activity (Kumar and Khurana 2004). There are five Villins in *A. thaliana*, VLN1-5, and they display functional differentiation (Klahre *et al.* 2000). VLN1 is insensitive to Ca^{2+} and does not appear to have any severing or capping ability but only protects actin from depolymerisation by Actin Depolymerising Factor 1 (ADF1) (Huang *et al.* 2005). Conversely VLN3 activity is sensitive to cellular Ca^{2+} levels and can bundle and sever actin filaments. VLN3 bundles actin into filaments at levels of Ca^{2+} below 1 μM into thicker actin cables, but over 1 μM it starts severing actin cables and filaments (Khurana *et al.* 2010).

This makes the activity of VLN3 more like that of human VLN. It may be that the rise in intracellular Ca^{2+} following PAMP perception functions together with endosomal MPK phosphorylation to alter VLN3 activity and trigger actin severing. Whilst VLN3 has been shown to sever actin structures at concentrations of intracellular Ca^{2+} of 1 μM (Khurana *et al.* 2010), intracellular levels of Ca^{2+} following PAMP treatment does not usually reach such high concentrations (Ranf *et al.* 2011). Therefore the relative contributions of

phosphorylation and Ca^{2+} to VLN3 severing activity need to be determined. Currently data on the effects of phosphorylation on any *A. thaliana* VLN is lacking.

The functional observations of the activity of VLN3 accords well with the phenotypic data that *vln2,3* mutants are less bundled, have no actin cables and more small filaments. Furthermore upon flg22 treatment the actin cytoskeleton undergoes disassembly in the first

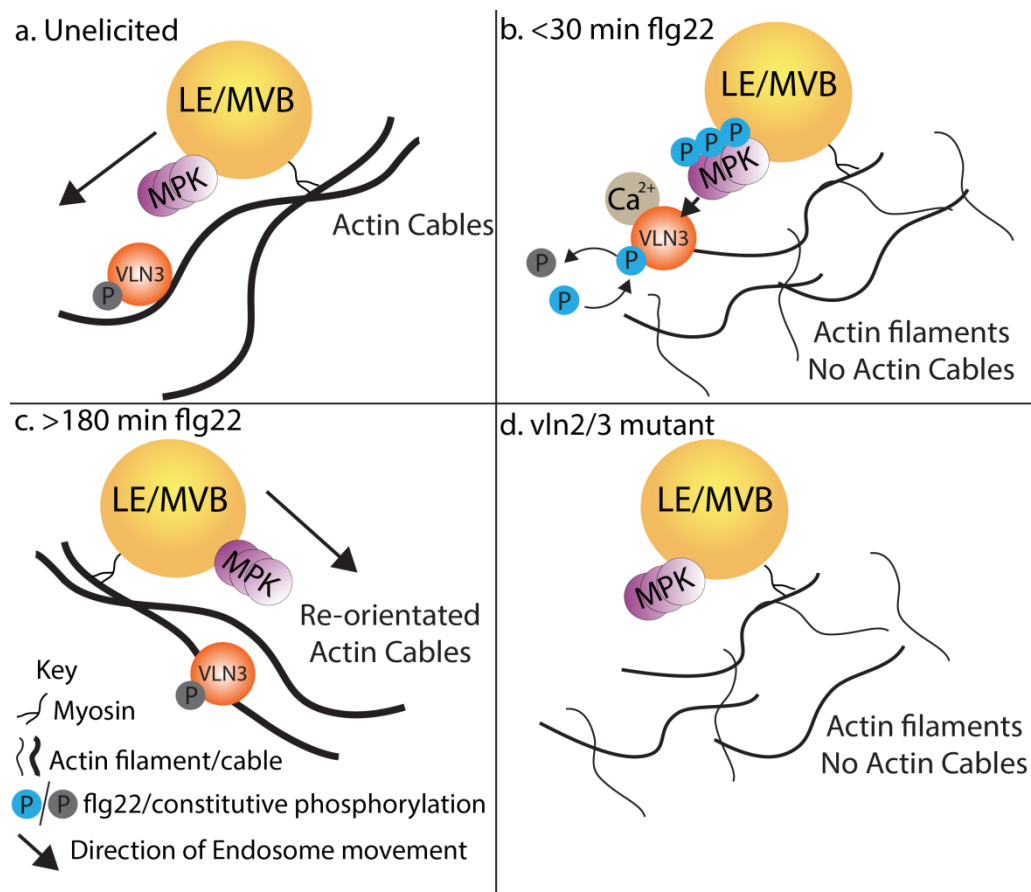


Figure 6.7. Model of VLN3 action following flg22 treatment. a. Before flg22 treatment VLN3 localises to actin filaments and bundles them into actin cables. VLN3 is phosphorylated on S778 and S880. MPKs localised to LE/MVBs, which are trafficked along actin via myosins. b. Upon flg22 treatment an LE/MVB localised MPK cascade is activated and phosphorylates VLN3 on S812 and S814. Phosphorylation and Ca^{2+} binding to VLN3 triggers its severing activity to break actin structures. c. After 3 hours of flg22 treatment VLN3 is dephosphorylated on S812 and S814 and Ca^{2+} is removed and VLN3 now promotes actin bundling and formation of actin cables. d. In the absence of VLN2 and VLN3 actin is not bundled into cables.

three hours following flg22 treatment (Henty-Ridilla *et al.* 2013), phenocopying a *vln2,3* mutant. Then over the next 24 hours the cytoskeleton re-arranges and re-bundles with new polarity (Henty-Ridilla *et al.* 2013). These two pieces of evidence implicate VLN2 and VLN3 in remodelling of the actin cytoskeleton following flg22 treatment. The timing of the rearrangement also implicates a mechanism in addition to Ca^{2+} to trigger the severing function of VLN2 and VLN3. The intracellular Ca^{2+} burst following flg22 treatment is transient and intracellular levels usually return to normal within 20-30 min (Ranf *et al.* 2011). Therefore an additional mechanism is needed to maintain VLN2 and VLN3 severing activity, and this is likely to be via phosphorylation from endosomal MPKs.

The model (Figure 6.6) for the functioning of VLN2 and VLN3 in the cells response to bacteria assumes that VLN2 and VLN3 are more phosphorylated on some residues after flg22 treatment. The relevance of this actin re-orientation following flg22 is still unclear. It is most likely to allow the focal re-localisation of the actin cytoskeleton for polar secretion and the observed re-localisation of organelles following pathogen challenge.

6.3.4 Conclusions and outlook

The data presented here implicates VLN3 and GTP in the defence responses of *A. thaliana* against spray inoculated *Pto* DC3000 and that they are phosphorylated after flg22 treatment. That these two proteins are targets of endosomal MPKs, of course, needs to be confirmed. This data also supports the hypothesis that signalling during flg22 induced responses is transduced from endosomes, but is not conclusive.

These data are promising but the crucial next steps for the *gtp* mutants are to test the expression levels of the transcript in these mutants. Secondly both VLN3 and GTP have been cloned and need to be co-localised to confirm their endosomal localisation. The next step is to confirm the phosphorylation status of these proteins after flg22 treatment and determine whether MPKs are responsible for this phosphorylation. These data combined

would provide strong evidence for phosphorylation of these proteins from endosome localised signalling components.

7 Discussion and Outlook

7.1 Objectives and achievements

The aims of this thesis were:

5. Establish the proteomes of LE/MVBs.
6. Determine LE/MVB proteome changes relevant to FLS2-induced signalling.
7. Investigate endosome localised proteins involved in immune signalling.
8. Examine the relevance of endosome-localised pools of signalling proteins to the overall cellular response to flg22.

I have broadly achieved these aims. Whilst I have not yet obtained conclusive results supporting the latest aim, I have been able to develop a method for enrichment of various endomembrane compartments that is useful to the wider cell biology community and clarifies the involvement of proteins localising to endosomes in the establishment of plant immunity.

The principal contributions presented in this thesis are:

- Development of a method for endomembrane enrichment that is faster and more applicable to different endomembrane compartments than other published methods (Chapter 3).
- Further elucidated the close interaction of RFP-RABF2b/ARA7-labelled LE/MVBs to the TGN compared to RABF1/ARA6-RFP-labelled LE/MVBs (Chapter 4).
- Made a potential link between LE/MVBs and secretion of defence-related flavonols (Chapter 5).
- Revealed that endosomes are locations of defence-activated signalling components (Chapter 5)

- Evidence for endosomal signalling based on roles of the MPK targets VLN3 (cytoskeleton) and GTP (antimicrobial secretion) in anti-bacterial immunity (Chapter 6).

These data have developed our understanding of plant cells and have a variety of implications for disease and cell biology.

7.2 Discussion

7.2.1 Immuno-precipitation advances endomembrane proteomics

Excellent developments have been made in elucidating the proteomes of endomembrane compartments, such as the Golgi and the vacuole, with techniques based on separation through differing biophysical properties, reviewed Parsons *et al.* (2013). We are now beginning to appreciate the functional differentiation between biophysically similar compartments such as the various populations of the TGN or LE/MVBs. Recent reviews end with pleas for more proteomic data to elucidate the differences in endomembrane compartments (Drakakaki and Dandekar 2013, Parsons *et al.* 2013, Bar and Avni 2014). Therefore, the IP technique presented in Chapters 3 and 4 is a very useful tool for the community.

The data presented in Chapters 3 and 4 demonstrates that affinity purification can be applied to biophysically similar endomembrane compartments to assess their functional differences. The method presented requires limited prior knowledge of compartment properties and relies primarily on a single IP step. This can be contrasted with the similar approach of Drakakaki *et al.* (2012) where enrichment of the TGN was required before IP, making my method significantly faster and easier as well as more applicable to other endomembrane compartments. This method is not entirely unique, IP has been used to purify SNARE

complexes and their interactors (Fujiwara *et al.* 2014). However, this is the first study to focus on LE/MVBs and the RAB GTPases that regulate them.

The principle advantages of this IP method is the ability to discriminate between biophysically similar populations of endomembrane compartments and the comparative ease and applicability of IP methods. Only suitable marker proteins, such as those used for microscopic analysis, are required. Furthermore IP provides an attractive complement to co-localisation studies with CLSM, and allows inferences about activation status that is unattainable with microscopy alone (Section 5.2.5). IP-based techniques are not without limitations since definition of the purified material can only be as good as the definition of the marker protein, which may not be entirely straightforward. I was only able to use the markers as they had already been partially characterised with CLSM, Electron microscopy (EM) and centrifugation based proteomic studies (Ueda *et al.* 2004, Konopka *et al.* 2008, Geldner *et al.* 2009). Thus for preliminary characterisation of new systems or organelles, it is necessary to identify and characterize putative marker proteins before the IP-based method can be used.

It is important to emphasise that a diversity of techniques are utilised to characterise the proteome of a compartment. As demonstrated, in Section 4.2.3 and a recent review (Parsons *et al.* 2013), diverse techniques provide a more thorough examination of an organelle than with one technique alone. However, due to the ease and applicability of affinity purification this is a very useful method until new techniques that can combine the unbiased nature of shotgun proteomics and the spatial resolution of microscopy, such as MS imaging (Malmstrom *et al.* 2009), become more widely available.

7.2.2 Proteomic dissection is essential to understand the TGN

The TGN is a complex organelle with very diverse functions. Our understanding of this organelle is primarily based on microscopy studies. As discussed in Sections 4.1.3/7.2.1

these techniques are limited as only a few proteins can be assessed in one experiment. To properly determine relative abundances of TGN proteins in each subdomain of the TGN, thorough quantitative proteomic analysis is needed. The high degree of overlap between the RFP-RABF2b/ARA7 proteome and that of the VHA-A1 proteome (Section 4.2.4) in combination with that of Groen *et al.*(2013) and Drakakaki *et al.*(2012), further implicate a VHA-A1 labelled TGN sub-population or domain in the formation of RFP-RABF2b/ARA7 labelled LE/MVBs. As the RABF1/ARA6-RFP proteome is lacking in TGN markers, RABF1/ARA6-RFP labelled LE/MVBs are unlikely to form from the TGN as ARA7/RABF2b labelled LE/MVBs do. This accords well with observations that RABF1/ARA6-RFP is later on the endocytic route than RFP-RABF2b/ARA7 (Ueda *et al.* 2004) and that RABF1/ARA6-RFP labelled LE/MVBs may form directly from the PM (Ebine *et al.* 2011, Ebine *et al.* 2012). These data, therefore, also contribute to the growing body of evidence of mechanisms underpinning the functional differentiation between LE/MVBs.

Further studies, utilising this IP method specifically focussing on quantifying proteins associating with several different TGN markers such as SYP61/VHA-A1/SYP43/RABA1b/RABA2a/VAMP721, are necessary to better characterise the compartmentalisation within the TGN. These data would allow us to better understand the role of different domains within the TGN and test the model presented in Figure 4.10.

7.2.3 LE/MVBs provide a vehicle through which defence compounds could be secreted

The data from Section 5.2.3 demonstrates that RHM1 is involved in resistance to bacteria potentially through flavonol biosynthesis at LE/MVBs. This observation suggests another defence compound as well as other phenolics and H₂O₂ accumulate in LE/MVBs (Snyder *et al.* 1991, Collins *et al.* 2003, An *et al.* 2006) and the redirection of LE/MVBs to haustoria suggests that these compartments are the route of their secretion (Lu *et al.* 2012, Bozkurt *et*

al. 2014). The combination of these published examples and my data, demonstrates another role for LE/MVBs in pathogen defence.

Furthermore, GTP may also play a role in pathogen defence by recruiting antimicrobial transporters to sites of pathogen detection, based on homology to mammalian proteins (Kim *et al.* 2011, Dupont and Hunter 2012, Yamamoto *et al.* 2012). It is tempting to speculate that GTP regulates recruitment of transporters to load antimicrobials into LE/MVBs or the extrahaustorial matrix after haustorium formation. It would be useful to determine whether GTP can recruit ABC transporters, such as PEN3 (Stein *et al.* 2006), to LE/MVBs as this is the next logical step to test this speculation.

GTP may be guarded by an R protein to explain the stunted growth phenotype. Whilst this needs to be tested, *Pto* DC3000 may produce an effector that targets GTP to inhibit LE/MVB mediated resistance. Overactivation of defence has been described in knock outs of positive PTI regulators such as BAK1 (He *et al.* 2007, Kemmerling *et al.* 2007), BIK1 (Zhang *et al.* 2010) and PMR4 (Nishimura *et al.* 2003). GTP could be guarded by an R gene in a similar manner to MPK4 (Petersen *et al.* 2000), and when knocked out, defence signalling is constitutively triggered.

7.2.4 VLN3 could provide the mechanism by which the cytoskeleton is remodelled following pathogen attack

Whilst it is well established that the cytoskeleton and endomembrane trafficking is altered during defence, the mechanisms by which these are implemented are unknown. Myosins, regulate FLS2 endosome movement and mediate pathogen resistance to fungal pathogens (Yang *et al.* 2014). Furthermore upon pathogen challenge or PAMP treatment the actin cytoskeleton re-models (Henty-Ridilla *et al.* 2013), presumably to regulate the altered endomembrane trafficking. Yet, the mechanism by which actin is regulated upon pathogen

challenge is unknown. Thus, VLN3 is likely to be the link between FLS2 signalling and cytoskeletal remodelling, probably through MPK phosphorylation.

7.2.5 Endosomes function as sites of active signal transduction

The identification of LE/MVB localised MPKs that are activated following flg22 treatment (Section 5.2.5/5.2.6), supports the hypothesis that LE/MVBs act as signalling platforms following flg22 treatment. If these MPKs were signalling then they would have to be localised to the cytosolic face of the LE/MVBs, unlike FLS2 which localises to the intraluminal vesicles (Spallek *et al.* 2013). The alternative explanation for this localisation of active MPKs is that these MPKs are endocytosed with FLS2 to be degraded. This explanation is less likely, however, as MKK2 and MKK5 were identified in LE/MVB IPs before elicitation and additional literature suggests MPKs localise to endosomes constitutively (Müller *et al.* 2010, Gu and Innes 2011). Furthermore, potential MPK targets were also identified in the combined LE/MVB proteome. The next step with this work is to test whether these endosome localised potential MPK targets are phosphorylated by MPKs. It must be confirmed whether VLN3 and GTP are genuine targets of endosomal MPKs. Finally the requirement of the endosome-localised MPK pool in signalling following bacterial attack needs to be assessed.

The identification of a target of flg22-induced MPKs localising to LE/MVBs is not totally novel. Lyst-interacting protein5 (LIP5) is targeted by MPK3 and 6 and localises to RFP-RABF2b/ARA7 labelled LE/MVBs (Wang *et al.* 2014). However, this thesis provides the first evidence of active MPKs localising to LE/MVBs, and it is most likely that endosomal MPKs will phosphorylate their endosome-associated targets. All of these data together argue that endosomes function as sites of signal transduction during bacterial attack. As there are endosome localised MPKs and a protein phosphorylated by MPKs localising to LE/MVBs both before and after flg22 treatment, it is likely that endosomes probably function as sites of signal transduction during bacterial attack.

7.2.6 The plasma membrane is the predominant site of FLS2 signal activation

The data presented in this thesis (Summarised in Section 7.2.4) argues that endosomes are important for localising signalling components in flg22 induced signalling. Certainly, activation of RBOHD and the triggering of the ROS burst occurs at the PM (Kadota *et al.* 2014, Monaghan *et al.* 2014) and is exaggerated when FLS2 endocytosis is inhibited (Smith *et al.* 2014). Furthermore, recent studies have argued that endocytosis of the receptor is not required for the signalling of FLS2 (Smith *et al.* 2014) and for BES1 de-phosphorylation for BRI1 (Irani *et al.* 2012). It has also been concluded that signalling of both of these proteins primarily originates from the PM (Irani *et al.* 2012, Bar and Avni 2014, Smith *et al.* 2014) potentially conflicting with this thesis. Even data supporting endosomal signalling in plants is controversial and has either been contradicted (Geldner *et al.* 2007) or involves prolonged endomembrane trafficking inhibitor treatment, making it difficult to ascribe the observed effects to endocytosis of the receptor only (Sharfman *et al.* 2011).

This subject is even more hotly debated in the animal field by assessing the relative importance of endosomal signalling in EGF perception and EGFR signalling. Numerous studies have demonstrated that interference with receptor endocytosis can either promote or reduce EGF induced MPK activation (Vieira *et al.* 1996, Miaczynska *et al.* 2004, Purvanov *et al.* 2010, Brankatschk *et al.* 2012, Sousa *et al.* 2012). Perhaps the most convincing study was performed by Brankatschk *et al.*(2012). In this study, extensive transcriptional profiling with a series of trafficking mutants after EGF treatment were used to demonstrate that most genes were regulated from the PM, and only a subset were altered only when the receptor was endocytosed properly (Brankatschk *et al.* 2012). Therefore the contribution of endosomal signalling to overall levels of MPK phosphorylation and gene activation appears to be minimal.

7.2.7 Endosomal contribution to signalling

Conversely, endosomes have been shown to be signalling platforms for a variety of signalling cascades induced by receptor kinases including EGFR and now probably for FLS2. APPL is a transcription factor recruited to endosomes in the cell periphery following application of NGF and endocytosis of the activated receptor TrkA in human PC12 cells (Varsano *et al.* 2006). APPL1 then recruits a G-protein regulator and both are trafficked ~5 µm to the perinuclear region of the cell to dissociate and promote TrkA signalling (Lin *et al.* 2006, Varsano *et al.* 2006) by nucleosome remodelling (Miaczynska *et al.* 2004). Similarly, after EGF treatment of HeLa cells, the endocytosed EGFR receptor is trafficked to the perinuclear region with APPL which can then alter transcription (Miaczynska *et al.* 2004). The use of endosomes to transport signalling components is also found in fungi. During *Ustilago maydis* infection of *Zea mays*, endosomes are used to transport Cdk1 related kinase (CRK1), an MPK, from the growing invasive hyphal tip to the nucleus (Bielska *et al.* 2014), demonstrating that endosomes provide a platform for signal transduction.

Endosome localisation is also important for some signalling proteins to reach full activation. The endosome localisation of the EGF-activated MEK-ERK MPKs is necessary for their full levels of phosphorylation (Teis *et al.* 2002, Nada *et al.* 2009). Moreover, full MPK activation can be delayed when endosomes are excluded from the perinuclear region of cells following EGF treatment (Taub *et al.* 2007). It is therefore clear that endosomes do have a function as sites of signal transduction.

The two conflicting views can be reconciled by looking at the specific questions they address. Work by Vieira *et al.* (1996), Miaczynska *et al.* (2004), Taub *et al.* (2007), Purvanov *et al.* (2010), Brankatschk *et al.* (2012), Irani *et al.* (2012), Sousa *et al.* (2012), Smith *et al.* (2014) focuses on whether maximal responses can be activated when endocytosis of the receptor is inhibited. The best studies supporting endosomal signalling assesses whether endosome localisation of signalling components is important for the overall signal

transduction (Miaczynska *et al.* 2004, Lin *et al.* 2006, Varsano *et al.* 2006, Taub *et al.* 2007, Nada *et al.* 2009), therefore testing a slightly different hypothesis. It is therefore important to distinguish between whether the endocytosed receptor activates signalling components from endosomes and whether other (non-receptor) endosome localised proteins contribute to signalling.

7.2.8 Outlook

To further test the role of endosome localised MPKs it will ultimately be necessary to prevent MPK association with endosomes. The mechanism by which MPKs associate with membranes is currently unknown and so selective interference is impossible. Alternatively specific interference of FLS2 endocytosis is essential to determine whether endocytosed FLS2 can contribute to signalling. However, the published methods that alter FLS2 endocytosis have numerous off target effects and so make conclusions based on these data very difficult to interpret. These two pieces of data are crucial to make general conclusions about endosomal signalling but they fall outside of the scope of this thesis.

7.3 Endosomes as sites of signal transduction during bacterial attack

From the data in this thesis, it cannot be concluded as to whether FLS2 is signalling directly from endosomes, and based on the work of Smith *et al.* (2014) and Spallek *et al.* (2013) this is unlikely. However, from my data we can conclude that endosomes act as sites for signal transduction from MPKs, but it is still unclear whether signalling proteins localised to endosomes provide a significant contribution to signalling. I suggest the model in Figure 7.1 as the principal mechanisms by which endosomes could contribute to signalling.

If endosomes act as signalling platforms for some MPKs following flg22 treatment the question arises of why. There are three reasons why signalling from the PM and endosomes

could provide an advantage as a route compared to a PM proteins signalling to cytosolic proteins alone.

1. Endosomes can provide spatial information to a response
2. Signal transduction through protein-protein interaction is more efficient on a membrane than in the cytosol
3. Endosomes allow for the required speed of transport for necessary for the observed speed of signal transduction.

These possibilities will be examined in turn.

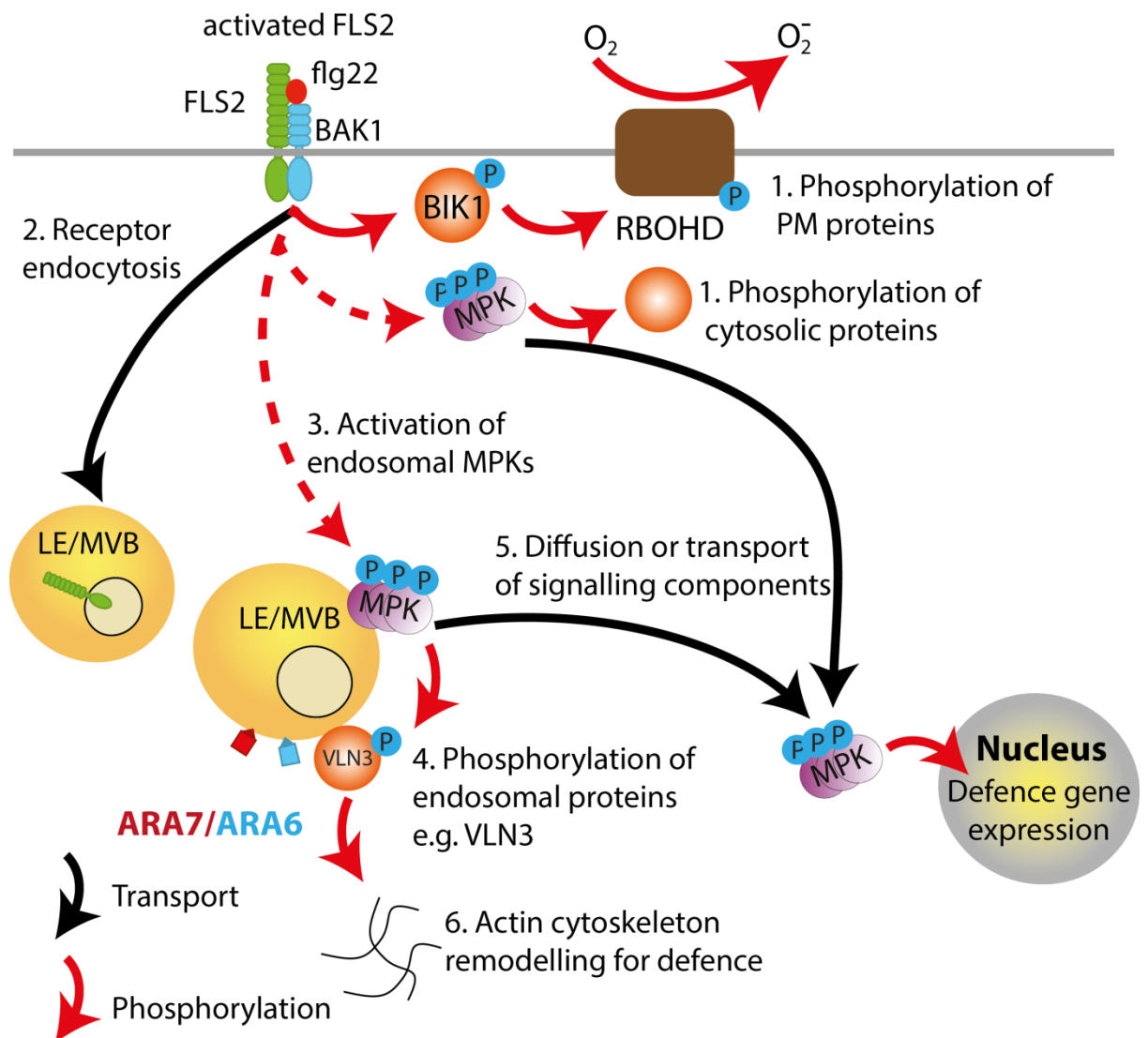


Figure 7.1. Model of the relevance of signalling from endosomes. 1. The FLS2 receptor complex, localised to the PM, triggers signalling through phosphorylation of PM localised proteins such as BIK1 and MPKs. 2. The receptor is endocytosed following activation, ultimately into intraluminal vesicles. 3. MPKs localised to endosomes are activated through an unknown mechanism. 4. Endosome localised proteins such as VLN3, GTP and LIP5 are phosphorylated by endosome localised MPKs. 5. Endosomes provide the mechanism of transport by which endosomes are trafficked to the nucleus. Alternatively the MPKs may diffuse through the cytosol. 6. Phosphorylation of endosome localised VLN3 results in actin cytoskeleton remodelling.

7.3.1 Endosomes could provide spatial information and specificity to flg22 triggered signalling

Positional information from the location of signalling proteins is likely to contribute to defence responses. The three candidate targets of endosomal MPK signalling following flg22 treatment - VLN3, GTP and LIP5 (Wang *et al.* 2014) - require specific localisation within the cell to fulfil their function. To take VLN3 as an example, it needs to interact with the cytoskeleton to fulfil its function of regulating actin (Khurana *et al.* 2010, van der Honing *et al.* 2012). Therefore phosphorylation of VLN3 by MPKs localised to endosomes travelling along actin filaments is supported by the fact that the two components are localised together. It is also tempting to suggest that the direction of endosome movement provides the positional information required to re-orientate the actin cytoskeleton after PAMP perception. Endosomes travelling along the cytoskeleton would constitute an excellent vehicle to modify specific actin filaments and cables as only specific populations of VLN3 would be phosphorylated by MPKs. Furthermore, numerous other endomembrane regulators are phosphorylated after flg22 treatment, such as SYP121 and SYP122 (Benschop *et al.* 2007), potentially targets for other endomembrane localised signalling components. Interestingly SYP121 is involved in penetration resistance to *Bgh* (Assaad *et al.* 2004). This phosphorylation may assist PEN1 in mediating defence related secretion. Spatial localisation of signalling components, such as MPKs, could provide the specificity to ensure specific regulators are phosphorylated.

7.3.2 Mechanistically signalling from endosomes is more efficient than signalling in the cytosol

Recent reviews highlighted that signal transduction from membranes mechanistically is more efficient than from the cytosol (Antonny 2011, Schmick and Bastiaens 2014). When protein-protein interactions are modelled in the cytosol and from membranes it is clear that interactions are favoured when both proteins localise to a membrane. Although protein diffusion is reduced in membranes, proteins are limited to two dimensions of movement so

making protein-protein interactions of proteins localised to membranes more likely (Antonny 2011, Schmick and Bastiaens 2014). Exactly how applicable these modelling data are to FLS2 induced signalling from endosomes is unclear. Scaffold proteins can locally increase the concentrations of proteins to promote interactions and provide a benefit analogous to membrane localisation in terms of protein-protein interaction dynamics.

Whilst the formation of protein complexes is beneficial in terms of promoting protein-protein interactions when all components are able to freely diffuse. It will ultimately reduce the motility of the complex within the cytoplasm as will now be explored.

7.3.3 Endosomes can provide the long range transport for MPKs necessary for flg22 induced signalling

FLS2 signalling complexes localised only to the PM may be able to phosphorylate the same number of MPKs but not all MPKs are equally relevant to signalling. As was suggested in a recent review, a moving signalling platform on endosomes could activate defence responses in the cell faster than from the PM alone (Geldner and Robatzek 2008). Furthermore, as demonstrated in *U. maydis* infection of *Z. mays*, signalling needs to be combined with correct transport to elicit the appropriate response (Bielska *et al.* 2014). Therefore maximal activation of certain signalling proteins can be achieved from the PM by a receptor, but this does not mean that the same strength of signal is transmitted to where it is relevant.

One of the principal assumptions of cellular biochemistry is that proteins freely diffuse within the cell. This assumption, though commonly used, rarely holds up to close scrutiny (Luby-Phelps 2000). If this assumption is not valid, activation of a number of signalling components is insufficient for signalling, but correct intracellular transport is needed as well. The cytoplasm is a crowded environment packed with proteins, nucleic acids and membranes, as so artfully demonstrated in the drawings of Dr Goodsell (Goodsell 2009, Goodsell 2009, Voet and Voet 2009, Goodsell 2010). Estimates of the protein concentration of bacterial cytosol

are as much as 30% (Luby-Phelps 2000, Malmstrom *et al.* 2009). The rates of diffusion of proteins through the cytoplasm are substantially slower than through water. For example, GFP diffuses 10-20 times slower in the cytoplasm than in water and diffusion speed decreases exponentially with object size (Luby-Phelps 2000, Ellis 2001). Therefore proteins, such as MPKs, that signal in multi-protein complexes are likely to move very slowly, if at all in the cytoplasm. Movement of a large signalling complex such as a MPK-MPKK-MPKKK complex by 10 μm presents an almost insurmountable problem by free diffusion as the time required to move these distances would be in the range of 10 min (Luby-Phelps 2000, Bielska *et al.* 2014), probably even more in a plant leaf epidermal cell with the added complication of the large vacuole. Movement of signalling proteins from the cell periphery to their sites of function requires a method of driven transport to initiate the very early transcriptional changes in the observed time frames of <10 min of flg22 treatment (Navarro *et al.* 2004). Cytoplasmic streaming of proteins can generate movement of up to 60 $\mu\text{m/s}$ in some plant and green algae species (Tominaga and Nakano 2012, Henn and Sadot 2014), 5 μm a second, but this would require the protein to have some membrane or cytoskeletal association. Endosomes are, therefore, a likely candidate vehicle by which signals reach the nucleus or other organelles from the PM. These data also reinforce the hypothesis that localisation of signalling proteins is as important as number of signalling proteins activated.

7.3.4 Signalling from the PM, cytosol and endosomes occurs during bacterial attack

Clearly perception of flg22 and activation of immediate responses by FLS2 such as the ROS burst and MPK phosphorylation are activated from the PM and are important to determining signal transduction. In addition signalling proteins certainly localise to the cytosol. In order for signalling proteins to require the necessary distances and to efficiently transduce signals, a cytosolic localisation alone is unlikely. During bacterial attack, it is clear that endosomes are not the sole platform from which MPKs signal. They are the site for signal transduction to LIP5 at least and probably VLN3 and GTP. It is also likely that a mechanism of transport other than diffusion is required to allow MPKs to signal to the nucleus in the observed time

frames, endosomes may fulfil this role. For speed of movement, localisation and efficiency of signalling, endosomes are good candidates for signalling platforms in addition to the PM and cytosol. Thus endosomes probably are sites of signal transduction during bacterial attack.

8 References

Abas, L. and C. Luschnig (2010). "Maximum yields of microsomal-type membranes from small amounts of plant material without requiring ultracentrifugation." Analytical Biochemistry**401**(2): 217-227.

Aebersold, R. and M. Mann (2003). "Mass spectrometry-based proteomics." Nature**422**(6928): 198-207.

Agrios, G. N. (1989). "Plant Pathology (3rd Edition). XVI + 803 S., 265 Abb. San Diego–New York–Berkeley–Boston–London–Sydney–Tokyo–Toronto 1988. Academic Press Inc." Journal of Basic Microbiology**29**(8): 500-500.

Albrecht, C., F. Boutrot, C. Segonzac, B. Schwessinger, S. Gimenez-Ibanez, D. Chinchilla, J. P. Rathjen, S. C. de Vries and C. Zipfel (2011). "Brassinosteroids inhibit pathogen-associated molecular pattern–triggered immune signaling independent of the receptor kinase BAK1." Proceedings of the National Academy of Sciences.

Albrecht, C., F. Boutrot, C. Segonzac, B. Schwessinger, S. Gimenez-Ibanez, D. Chinchilla, J. P. Rathjen, S. C. de Vries and C. Zipfel (2012). "Brassinosteroids inhibit pathogen-associated molecular pattern-triggered immune signaling independent of the receptor kinase BAK1." Proceedings of the National Academy of Sciences of the United States of America**109**(1): 303-308.

Alvim Kamei, C. L., J. Boruc, K. Vandepoele, H. Van den Daele, S. Maes, E. Russinova, D. Inzé and L. De Veylder (2008). "The PRA1 Gene Family in Arabidopsis." Plant Physiology**147**(4): 1735-1749.

An, Q., K. Ehlers, K.-H.Kogel, A. J. E. Van Bel and R. Hüchelhoven (2006). "Multivesicular compartments proliferate in susceptible and resistant MLA12-barley leaves in response to infection by the biotrophic powdery mildew fungus." New Phytologist**172**(3): 563-576.

An, Q., R. Hüchelhoven, K.-H.Kogel and A. J. E. Van Bel (2006). "Multivesicular bodies participate in a cell wall-associated defence response in barley leaves attacked by the pathogenic powdery mildew fungus." Cellular Microbiology**8**(6): 1009-1019.

Anders, N. and G. Jürgens (2008). "Large ARF guanine nucleotide exchange factors in membrane trafficking." Cellular and Molecular Life Sciences**65**(21): 3433-3445.

Anitei, M. and B. Hoflack (2012)."Bridging membrane and cytoskeleton dynamics in the secretory and endocytic pathways." Nat Cell Biol**14**(1): 11-19.

Antonny, B. (2011)."Mechanisms of membrane curvature sensing." Annu Rev Biochem**80**: 101-123.

Arcaro, A. and M. P. Wymann (1993). "Wortmannin is a potent phosphatidylinositol 3-kinase inhibitor: the role of phosphatidylinositol 3,4,5-trisphosphate in neutrophil responses." Biochem J**296 (Pt 2)**: 297-301.

Asai, T., G. Tena, J. Plotnikova, M. R. Willmann, W. L. Chiu, L. Gomez-Gomez, T. Boller, F. M. Ausubel and J. Sheen (2002). "MAP kinase signalling cascade in Arabidopsis innate immunity." Nature**415**(6875): 977-983.

Asami, T., Y. K. Min, N. Nagata, K. Yamagishi, S. Takatsuto, S. Fujioka, N. Murofushi, I. Yamaguchi and S. Yoshida (2000). "Characterization of Brassinazole, a Triazole-Type Brassinosteroid Biosynthesis Inhibitor." Plant Physiology**123**(1): 93-100.

Asaoka, R., T. Uemura, J. Ito, M. Fujimoto, E. Ito, T. Ueda and A. Nakano (2012). "Arabidopsis RABA1 GTPases are involved in transport between the trans-Golgi network and the plasma membrane, and are required for salinity stress tolerance." Plant J.

Assaad, F. F., J. L. Qiu, H. Youngs, D. Ehrhardt, L. Zimmerli, M. Kalde, G. Wanner, S. C. Peck, H. Edwards, K. Ramonell, C. R. Somerville and H. Thordal-Christensen (2004). "The PEN1 syntaxin defines a novel cellular compartment upon fungal attack and is required for the timely assembly of papillae." Molecular Biology of the Cell**15**(11): 5118-5129.

Bader, A. N., E. G. Hofman, J. Voortman, P. M. P. van Bergen en Henegouwen and H. C. Gerritsen (2009). "Homo-FRET Imaging Enables Quantification of Protein Cluster Sizes with Subcellular Resolution." Biophysical Journal**97**(9): 2613-2622.

Balbis, A. and B. I. Posner (2010). "Compartmentalization of EGFR in cellular membranes: Role of membrane rafts." Journal of Cellular Biochemistry**109**(6): 1103-1108.

Bantscheff, M., M. Schirle, G. Sweetman, J. Rick and B. Kuster (2007). "Quantitative mass spectrometry in proteomics: a critical review." Anal Bioanal Chem**389**(4): 1017-1031.

Bao, C., J. Wang, R. Zhang, B. Zhang, H. Zhang, Y. Zhou and S. Huang (2012). "Arabidopsis VILLIN2 and VILLIN3 act redundantly in sclerenchyma development via bundling of actin filaments." Plant J**71**(6): 962-975.

Bar, M. and A. Avni (2014). "Endosomal trafficking and signaling in plant defense responses." Current Opinion in Plant Biology**22**(0): 86-92.

Beck, M., G. Komis, A. Ziemann, D. Menzel and J. Šamaj (2011). "Mitogen-activated protein kinase 4 is involved in the regulation of mitotic and cytokinetic microtubule transitions in Arabidopsis thaliana." New Phytologist**189**(4): 1069-1083.

Beck, M., J. Zhou, C. Faulkner, D. MacLean and S. Robatzek (2012). "Spatio-Temporal Cellular Dynamics of the Arabidopsis Flagellin Receptor Reveal Activation Status-Dependent Endosomal Sorting." The Plant Cell Online.

Bednarek, P., M. Piślewska-Bednarek, A. Svatoš, B. Schneider, J. Doubský, M. Mansurova, M. Humphry, C. Consonni, R. Panstruga, A. Sanchez-Vallet, A. Molina and P. Schulze-Lefert (2009). "A Glucosinolate Metabolism Pathway in Living Plant Cells Mediates Broad-Spectrum Antifungal Defense." Science**323**(5910): 101-106.

Belkhadir, Y., A. Durbak, M. Wierzba, R. J. Schmitz, A. Aguirre, R. Michel, S. Rowe, S. Fujioka and F. E. Tax (2010). "Intragenic suppression of a trafficking-defective brassinosteroid receptor mutant in Arabidopsis." Genetics**185**(4): 1283-1296.

Belkhadir, Y., Y. Jaillais, P. Epple, E. Balsemão-Pires, J. L. Dangl and J. Chory (2011). "Brassinosteroids modulate the efficiency of plant immune responses to microbe-associated molecular patterns." Proceedings of the National Academy of Sciences.

Benschop, J. J., S. Mohammed, M. O'Flaherty, A. J. R. Heck, M. Slijper and F. L. H. Menke (2007). "Quantitative Phosphoproteomics of Early Elicitor Signaling in Arabidopsis." Molecular & Cellular Proteomics**6**(7): 1198-1214.

Berg, M., A. Parbel, H. Pettersen, D. Fenyö and L. Björkesten (2006). "Reproducibility of LC-MS-based protein identification." Journal of Experimental Botany**57**(7): 1509-1514.

Bielska, E., Y. Higuchi, M. Schuster, N. Steinberg, S. Kilaru, N. J. Talbot and G. Steinberg (2014). "Long-distance endosome trafficking drives fungal effector production during plant infection." Nat Commun**5**.

Bleckmann, A., S. Weidtkamp-Peters, C. A. M. Seidel and R. Simon (2010). "Stem Cell Signaling in Arabidopsis Requires CRN to Localize CLV2 to the Plasma Membrane." Plant Physiol.**152**(1): 166-176.

Böhlenius, H., S. M. Mørch, D. Godfrey, M. E. Nielsen and H. Thordal-Christensen (2010). "The Multivesicular Body-Localized GTPase ARFA1b/1c Is Important for Callose Deposition and ROR2 Syntaxin-Dependent Preinvasive Basal Defense in Barley." The Plant Cell Online**22**(11): 3831-3844.

Bondarenko, P. V., D. Chelius and T. A. Shaler (2002). "Identification and relative quantitation of protein mixtures by enzymatic digestion followed by capillary reversed-phase liquid chromatography-tandem mass spectrometry." Anal Chem**74**(18): 4741-4749.

Bonifacino, J. S. and A. Hierro (2011). "Transport according to GARP: receiving retrograde cargo at the trans-Golgi network." Trends in Cell Biology**21**(3): 159-167.

Bottanelli, F., D. C. Gershlick and J. Denecke (2012). "Evidence for Sequential Action of Rab5 and Rab7 GTPases in Prevacuolar Organelle Partitioning." Traffic**13**(2): 338-354.

Boutté, Y., K. Jonsson, H. E. McFarlane, E. Johnson, D. Gendre, R. Swarup, J. Friml, L. Samuels, S. Robert and R. P. Bhalerao (2013). "ECHIDNA-mediated post-Golgi trafficking of auxin carriers for differential cell elongation." Proceedings of the National Academy of Sciences**110**(40): 16259-16264.

Bozkurt, T. O., K. Belhaj, Y. F. Dagdas, A. Chaparro-Garcia, C.-H. Wu, L. M. Cano and S. Kamoun (2014). "Rerouting of plant late endocytic trafficking towards a pathogen interface." Traffic: n/a-n/a.

Bozkurt, T. O., S. Schornack, J. Win, T. Shindo, M. Ilyas, R. Oliva, L. M. Cano, A. M. E. Jones, E. Huitema, R. A. L. van der Hoorn and S. Kamoun (2011). "Phytophthora infestans

effector AVRblb2 prevents secretion of a plant immune protease at the haustorial interface." Proceedings of the National Academy of Sciences**108**(51): 20832-20837.

Brader, G., A. Djamei, M. Teige, E. T. Palva and H. Hirt (2007). "The MAP Kinase Kinase MKK2 Affects Disease Resistance in Arabidopsis." Molecular Plant-Microbe Interactions**20**(5): 589-596.

Brankatschk, B., S. P. Wichert, S. D. Johnson, O. Schaad, M. J. Rossner and J. Gruenberg (2012). "Regulation of the EGF Transcriptional Response by Endocytic Sorting." Sci. Signal.**5**(215): ra21-.

Britzen-Laurent, N., M. Bauer, V. Berton, N. Fischer, A. Syguda, S. Reipschläger, E. Naschberger, C. Herrmann and M. Stürzl (2010). "Intracellular Trafficking of Guanylate-Binding Proteins Is Regulated by Heterodimerization in a Hierarchical Manner." PLoS ONE**5**(12): e14246.

Brodersen, P., M. Petersen, H. Bjorn Nielsen, S. Zhu, M. A. Newman, K. M. Shokat, S. Rietz, J. Parker and J. Mundy (2006). "Arabidopsis MAP kinase 4 regulates salicylic acid- and jasmonic acid/ethylene-dependent responses via EDS1 and PAD4." Plant J**47**(4): 532-546.

Brux, A., T. Y. Liu, M. Krebs, Y. D. Stierhof, J. U. Lohmann, O. Miersch, C. Wasternack and K. Schumacher (2008). "Reduced V-ATPase activity in the trans-Golgi network causes oxylipin-dependent hypocotyl growth Inhibition in Arabidopsis." Plant Cell**20**(4): 1088-1100.

Bücherl, C. A., G. W. van Esse, A. Kruis, J. Luchtenberg, A. H. Westphal, J. Aker, A. van Hoek, C. Albrecht, J. W. Borst and S. C. de Vries (2013). "Visualization of BRI1 and BAK1(SERK3) Membrane Receptor Heterooligomers during Brassinosteroid Signaling." Plant Physiology**162**(4): 1911-1925.

Butenko, M. A., M. Wildhagen, M. Albert, A. Jehle, H. Kalbacher, R. B. Aalen and G. Felix (2014). "Tools and Strategies to Match Peptide-Ligand Receptor Pairs." Plant Cell**26**(5): 1838-1847.

Cai, C., J. L. Henty-Ridilla, D. B. Szymanski and C. J. Staiger (2014). "Arabidopsis Myosin XI: A Motor Rules the Tracks." Plant Physiology.

Cai, H., Y. Zhang, M. Pypaert, L. Walker and S. Ferro-Novick (2005). "Mutants in trs120 disrupt traffic from the early endosome to the late Golgi." The Journal of Cell Biology**171**(5): 823-833.

Campbell, R. E., O. Tour, A. E. Palmer, P. A. Steinbach, G. S. Baird, D. A. Zacharias and R. Y. Tsien (2002). "A monomeric red fluorescent protein." Proceedings of the National Academy of Sciences**99**(12): 7877-7882.

Carter, C., S. Pan, J. Zouhar, E. L. Avila, T. Girke and N. V. Raikhel (2004). "The Vegetative Vacuole Proteome of Arabidopsis thaliana Reveals Predicted and Unexpected Proteins." The Plant Cell Online**16**(12): 3285-3303.

Castle, J. D. (2001). Purification of Organelles from Mammalian Cells. Current Protocols in Protein Science, John Wiley & Sons, Inc.

Cespedes, C. L., J. R. Salazar, A. Ariza-Castolo, L. Yamaguchi, J. G. Avila, P. Aqueveque, I. Kubo and J. Alarcon (2014). "Biopesticides from plants: Calceolaria integrifolia s.l." Environ Res**132**: 391-406.

Chen, C. Z. and R. N. Collins (2005). Analysis and Properties of the Yeast YIP1 Family of Ypt-Interacting Proteins. Methods in Enzymology. C. J. D. William E. Balch and H. Alan, Academic Press. **Volume 403**: 333-339.

Chen, S., P. Lang, D. Chronis, S. Zhang, W. S. De Jong, M. G. Mitchum and X. Wang (2014). "In planta processing and glycosylation of a nematode CLE effector and its interaction with a host CLV2-like receptor to promote parasitism." Plant Physiology.

Chen, X., N. G. Irani and J. Friml (2011). "Clathrin-mediated endocytosis: the gateway into plant cells." Current Opinion in Plant Biology**14**(6): 674-682.

Cheng, F.-y., K. Blackburn, Y.-m. Lin, M. B. Goshe and J. D. Williamson (2008). "Absolute Protein Quantification by LC/MSE for Global Analysis of Salicylic Acid-Induced Plant Protein Secretion Responses." Journal of Proteome Research**8**(1): 82-93.

Chinchilla, D., C. Zipfel, S. Robatzek, B. Kemmerling, T. Nurnberger, J. D. G. Jones, G. Felix and T. Boller (2007). "A flagellin-induced complex of the receptor FLS2 and BAK1 initiates plant defence." Nature**448**(7152): 497-500.

Choi, H., B. Larsen, Z.-Y. Lin, A. Breitskreutz, D. Mellacheruvu, D. Fermin, Z. S. Qin, M. Tyers, A.-C. Gingras and A. I. Nesvizhskii (2011). "SAINT: probabilistic scoring of affinity purification-mass spectrometry data." Nat Meth**8**(1): 70-73.

Choi, S.-w., T. Tamaki, K. Ebine, T. Uemura, T. Ueda and A. Nakano (2013). "RABA Members Act in Distinct Steps of Subcellular Trafficking of the FLAGELLIN SENSING2 Receptor." The Plant Cell Online.

Chow, C.-M., H. Neto, C. Foucart and I. Moore (2008). "Rab-A2 and Rab-A3 GTPases Define a trans-Golgi Endosomal Membrane Domain in Arabidopsis That Contributes Substantially to the Cell Plate." The Plant Cell Online**20**(1): 101-123.

Christoforidis, S., H. M. McBride, R. D. Burgoyne and M. Zerial (1999). "The Rab5 effector EEA1 is a core component of endosome docking." Nature**397**(6720): 621-625.

Clark, S. E., M. P. Running and E. M. Meyerowitz (1995). "CLAVATA3 is a specific regulator of shoot and floral meristem development affecting the same processes as CLAVATA1." Development**121**(7): 2057-2067.

Clay, N. K., A. M. Adio, C. Denoux, G. Jander and F. M. Ausubel (2009). "Glucosinolate metabolites required for an Arabidopsis innate immune response." Science**323**(5910): 95-101.

Clouse, S. D., M. Langford and T. C. McMorris (1996). "A Brassinosteroid-Insensitive Mutant in Arabidopsis thaliana Exhibits Multiple Defects in Growth and Development." Plant Physiology**111**(3): 671-678.

Collins, N. C., H. Thordal-Christensen, V. Lipka, S. Bau, E. Kombrink, J.-L. Qiu, R. Huckelhoven, M. Stein, A. Freialdenhoven, S. C. Somerville and P. Schulze-Lefert (2003). "SNARE-protein-mediated disease resistance at the plant cell wall." Nature**425**(6961): 973-977.

Conchon, S., X. Cao, C. Barlowe and H. R. Pelham (1999). "Got1p and Sft2p: membrane proteins involved in traffic to the Golgi complex." The EMBO journal**18**(14): 3934-3946.

CristinaRodriguez, M., M. Petersen and J. Mundy (2010). "Mitogen-Activated Protein Kinase Signaling in Plants." Annual Review of Plant Biology**61**(1): 621-649.

Cui, Y., Q. Zhao, C. Gao, Y. Ding, Y. Zeng, T. Ueda, A. Nakano and L. Jiang (2014). "Activation of the Rab7 GTPase by the MON1-CCZ1 Complex Is Essential for PVC-to-Vacuole Trafficking and Plant Growth in Arabidopsis." The Plant Cell Online.

Dallner, G. (1974). "Isolation of rough and smooth microsomes--general." Methods Enzymol**31**: 191-201.

De Duve, C. (1971). "Tissue fractionation. Past and present." J Cell Biol**50**(1): 20d-55d.

de Lima, P. F., C. A. Colombo, A. F. Chiorato, L. F. Yamaguchi, M. J. Kato and S. A. Carbonell (2014). "Occurrence of Isoflavonoids in Brazilian Common Bean Germplasm (*Phaseolus vulgaris* L.)." J Agric Food Chem**62**(40): 9699-9704.

Deal, R. B. and S. Henikoff (2011). "The INTACT method for cell type-specific gene expression and chromatin profiling in Arabidopsis thaliana." Nat. Protocols**6**(1): 56-68.

Dettmer, J., A. Hong-Hermesdorf, Y.-D. Stierhof and K. Schumacher (2006). "Vacuolar H⁺-ATPase Activity Is Required for Endocytic and Secretory Trafficking in Arabidopsis." Plant Cell**18**(3): 715-730.

Diet, A., B. Link, G. J. Seifert, B. Schellenberg, U. Wagner, M. Pauly, W.-D. Reiter and C. Ringli (2006). "The Arabidopsis Root Hair Cell Wall Formation Mutant *lrx1* Is Suppressed by Mutations in the RHM1 Gene Encoding a UDP-I-Rhamnose Synthase." The Plant Cell Online**18**(7): 1630-1641.

Dodds, P. N. and J. P. Rathjen (2010). "Plant immunity: towards an integrated view of plant-pathogen interactions." Nat Rev Genet**11**(8): 539-548.

Drakakaki, G. and A. Dandekar (2013). "Protein secretion: how many secretory routes does a plant cell have?" Plant Sci**203-204**: 74-78.

Drakakaki, G., W. van de Ven, S. Pan, Y. Miao, J. Wang, N. F. Keinath, B. Weatherly, L. Jiang, K. Schumacher, G. Hicks and N. Raikhel (2012). "Isolation and proteomic analysis of the SYP61 compartment reveal its role in exocytic trafficking in Arabidopsis." Cell Res**22**(2): 413-424.

Duan, Q., D. Kita, C. Li, A. Y. Cheung and H.-M.Wu (2010). "FERONIA receptor-like kinase regulates RHO GTPase signaling of root hair development." Proceedings of the National Academy of Sciences of the United States of America**107**(41): 17821-17826.

Dunkley, T. P. J., S. Hester, I. P. Shadforth, J. Runions, T. Weimar, S. L. Hanton, J. L. Griffin, C. Bessant, F. Brandizzi, C. Hawes, R. B. Watson, P. Dupree and K. S. Lilley (2006). "Mapping the Arabidopsis organelle proteome." Proceedings of the National Academy of Sciences**103**(17): 6518-6523.

Dunkley, T. P. J., R. Watson, J. L. Griffin, P. Dupree and K. S. Lilley (2004). "Localization of Organelle Proteins by Isotope Tagging (LOPIT)." Molecular & Cellular Proteomics**3**(11): 1128-1134.

Dupont, Christopher D. and Christopher A. Hunter (2012). "Guanylate-Binding Proteins: Niche Recruiters for Antimicrobial Effectors." Immunity**37**(2): 191-193.

Ebine, K., M. Fujimoto, Y. Okatani, T. Nishiyama, T. Goh, E. Ito, T. Dainobu, A. Nishitani, T. Uemura, M. H. Sato, H. Thordal-Christensen, N. Tsutsumi, A. Nakano and T. Ueda (2011). "A membrane trafficking pathway regulated by the plant-specific RAB GTPase ARA6." Nat Cell Biol**13**(7): 853-859.

Ebine, K., N. Miyakawa, M. Fujimoto, T. Uemura, A. Nakano and T. Ueda (2012). "Endosomal trafficking pathway regulated by ARA6, a RAB5 GTPase unique to plants." Small GTPases**3**(1): 23-27.

Ebine, K., T. Uemura, A. Nakano and T. Ueda (2012). "Flowering Time Modulation by a Vacuolar SNARE via *FLOWERING LOCUS C* in *Arabidopsis thaliana*." PLoS ONE**7**(7): e42239.

Ellinger, D., M. Naumann, C. Falter, C. Zwikowics, T. Jamrow, C. Manisseri, S. C. Somerville and C. A. Voigt (2013). "Elevated early callose deposition results in complete penetration resistance to powdery mildew in Arabidopsis." Plant Physiol**161**(3): 1433-1444.

Ellis, R. J. (2001). "Macromolecular crowding: obvious but underappreciated." Trends Biochem Sci**26**(10): 597-604.

Elmore, J. M., J. Liu, B. Smith, B. Phinney and G. Coaker (2012). "Quantitative proteomics reveals dynamic changes in the plasma membrane proteome during Arabidopsis immune signaling." Molecular & Cellular Proteomics.

Escobar-Restrepo, J.-M., N. Huck, S. Kessler, V. Gagliardini, J. Gheyselinck, W.-C. Yang and U. Grossniklaus (2007). "The FERONIA Receptor-like Kinase Mediates Male-Female Interactions During Pollen Tube Reception." Science**317**(5838): 656-660.

Eubel, H., J. Heazlewood and A. H. Millar (2007). Isolation and Subfractionation of Plant Mitochondria for Proteomic Analysis. Plant Proteomics. H. Thiellement, M. Zivy, C. Damerval and V. Méchin, Humana Press. **355**: 49-62.

Eubel, H., E. H. Meyer, N. L. Taylor, J. D. Bussell, N. O'Toole, J. L. Heazlewood, I. Castleden, I. D. Small, S. M. Smith and A. H. Millar (2008). "Novel Proteins, Putative Membrane Transporters, and an Integrated Metabolic Network Are Revealed by Quantitative Proteomic Analysis of Arabidopsis Cell Culture Peroxisomes." Plant Physiology**148**(4): 1809-1829.

Felix, G., J. D. Duran, S. Volko and T. Boller (1999). "Plants have a sensitive perception system for the most conserved domain of bacterial flagellin." The Plant Journal**18**(3): 265-276.

Feraru, E., M. I. Feraru, R. Asaoka, T. Paciorek, R. De Rycke, H. Tanaka, A. Nakano and J. Friml (2012). "BEX5/RabA1b Regulates trans-Golgi Network-to-Plasma Membrane Protein Trafficking in Arabidopsis." The Plant Cell Online**24**(7): 3074-3086.

Foster, L. J., C. L. de Hoog, Y. Zhang, Y. Zhang, X. Xie, V. K. Mootha and M. Mann (2006). "A Mammalian Organelle Map by Protein Correlation Profiling." Cell**125**(1): 187-199.

Fujiwara, M., T. Uemura, K. Ebine, Y. Nishimori, T. Ueda, A. Nakano, M. H. Sato and Y. Fukao (2014). "Interactomics of Qa-SNARE in Arabidopsis thaliana." Plant and Cell Physiology.

Gadeyne, A., C. Sánchez-Rodríguez, S. Vanneste, S. Di Rubbo, H. Zauber, K. Vanneste, J. Van Leene, N. De Winne, D. Eeckhout, G. Persiau, E. Van De Slijke, B. Cannoot, L. Vercruyssen, Jonathan R. Mayers, M. Adamowski, U. Kania, M. Ehrlich, A. Schweighofer, T.

Ketelaar, S. Maere, Sebastian Y. Bednarek, J. Friml, K. Gevaert, E. Witters, E. Russinova, S. Persson, G. De Jaeger and D. Van Damme (2014). "The TPLATE Adaptor Complex Drives Clathrin-Mediated Endocytosis in Plants." Cell**156**(4): 691-704.

Gao, C., M. Luo, Q. Zhao, R. Yang, Y. Cui, Y. Zeng, J. Xia and L. Jiang (2014). "A Unique Plant ESCRT Component, FREE1, Regulates Multivesicular Body Protein Sorting and Plant Growth." Curr Biol**24**(21): 2556-2563.

Gao, M., J. Liu, D. Bi, Z. Zhang, F. Cheng, S. Chen and Y. Zhang (2008). "MEKK1, MKK1/MKK2 and MPK4 function together in a mitogen-activated protein kinase cascade to regulate innate immunity in plants." Cell Res**18**(12): 1190-1198.

Geldner, N., N. Anders, H. Wolters, J. Keicher, W. Kornberger, P. Muller, A. Delbarre, T. Ueda, A. Nakano and G. Jürgens (2003). "The Arabidopsis GNOM ARF-GEF Mediates Endosomal Recycling, Auxin Transport, and Auxin-Dependent Plant Growth." Cell**112**(2): 219-230.

Geldner, N., V. Déneraud-Tendon, D. L. Hyman, U. Mayer, Y.-D. Stierhof and J. Chory (2009). "Rapid, combinatorial analysis of membrane compartments in intact plants with a multicolor marker set." The Plant Journal**59**(1): 169-178.

Geldner, N., D. L. Hyman, X. Wang, K. Schumacher and J. Chory (2007). "Endosomal signaling of plant steroid receptor kinase BRI1." Genes & Development**21**(13): 1598-1602.

Geldner, N. and S. Robatzek (2008). "Plant receptors go endosomal: A moving view on signal transduction." Plant Physiology**147**(4): 1565-1574.

Gendre, D., K. Jonsson, Y. Boutte and R. P. Bhalerao (2014). "Journey to the cell surface-the central role of the trans-Golgi network in plants." Protoplasma.

Gendre, D., H. E. McFarlane, E. Johnson, G. Mouille, A. Sjödin, J. Oh, G. Levesque-Tremblay, Y. Watanabe, L. Samuels and R. P. Bhalerao (2013). "Trans-Golgi Network Localized ECHIDNA/Ypt Interacting Protein Complex Is Required for the Secretion of Cell Wall Polysaccharides in Arabidopsis." The Plant Cell Online.

Gendre, D., J. Oh, Y. Boutté, J. G. Best, L. Samuels, R. Nilsson, T. Uemura, A. Marchant, M. J. Bennett, M. Grebe and R. P. Bhalerao (2011). "Conserved Arabidopsis ECHIDNA protein

mediates trans-Golgi-network trafficking and cell elongation." Proceedings of the National Academy of Sciences.

Goh, T., W. Uchida, S. Arakawa, E. Ito, T. Dainobu, K. Ebine, M. Takeuchi, K. Sato, T. Ueda and A. Nakano (2007). "VPS9a, the Common Activator for Two Distinct Types of Rab5 GTPases, Is Essential for the Development of Arabidopsis thaliana." The Plant Cell Online**19**(11): 3504-3515.

Gómez-Gómez, L., Z. Bauer and T. Boller (2001). "Both the Extracellular Leucine-Rich Repeat Domain and the Kinase Activity of FLS2 Are Required for Flagellin Binding and Signaling in Arabidopsis." The Plant Cell Online**13**(5): 1155-1163.

Gómez-Gómez, L. and T. Boller (2000). "FLS2: An LRR Receptor-like Kinase Involved in the Perception of the Bacterial Elicitor Flagellin in Arabidopsis." Molecular Cell**5**(6): 1003-1011.

Goodsell, D. S. (2009). "Escherichia coli." Biochemistry and Molecular Biology Education**37**(6): 325-332.

Goodsell, D. S. (2009). "Neuromuscular synapse." Biochemistry and Molecular Biology Education**37**(4): 204-210.

Goodsell, D. S. (2010). "Mitochondrion." Biochemistry and Molecular Biology Education**38**(3): 134-140.

Grefen, C., N. Donald, K. Hashimoto, J. Kudla, K. Schumacher and M. R. Blatt (2010). "A ubiquitin-10 promoter-based vector set for fluorescent protein tagging facilitates temporal stability and native protein distribution in transient and stable expression studies." The Plant Journal**64**(2): 355-365.

Groen, A. J. and K. S. Lilley (2010). "Proteomics of total membranes and subcellular membranes." Expert Review of Proteomics**7**(6): 867-878.

Groen, A. J., G. Sancho-Andres, L. M. Breckels, L. Gatto, F. Aniento and K. S. Lilley (2014). "Identification of trans-golgi network proteins in Arabidopsis thaliana root tissue." J Proteome Res**13**(2): 763-776.

Groen, A. J., G. Sancho-Andrés, L. M. Breckels, L. Gatto, F. Aniento and K. S. Lilley (2013). "Identification of Trans-Golgi Network Proteins in Arabidopsis thaliana Root Tissue." Journal of Proteome Research**13**(2): 763-776.

Gruhler, A., W. X. Schulze, R. Matthiesen, M. Mann and O. N. Jensen (2005). "Stable isotope labeling of Arabidopsis thaliana cells and quantitative proteomics by mass spectrometry." Mol Cell Proteomics**4**(11): 1697-1709.

Gu, Y. and R. W. Innes (2011). "The KEEP ON GOING Protein of Arabidopsis Recruits the ENHANCED DISEASE RESISTANCE1 Protein to Trans-Golgi Network/Early Endosome Vesicles." Plant Physiology**155**(4): 1827-1838.

Gygi, S. P., B. Rist, S. A. Gerber, F. Turecek, M. H. Gelb and R. Aebersold (1999). "Quantitative analysis of complex protein mixtures using isotope-coded affinity tags." Nat Biotechnol**17**(10): 994-999.

Haeweker, H., S. Rips, H. Koiwa, S. Salomon, Y. Saijo, D. Chinchilla, S. Robatzek and A. von Schaewen (2010). "Pattern Recognition Receptors Require N-Glycosylation to Mediate Plant Immunity." Journal of Biological Chemistry**285**(7): 4629-4636.

Hardham, A., D. Takemoto and R. White (2008). "Rapid and dynamic subcellular reorganization following mechanical stimulation of Arabidopsis epidermal cells mimics responses to fungal and oomycete attack." BMC Plant Biology**8**(1): 63.

Hatsugai, N. and I. Hara-Nishimura (2010). "Two vacuole-mediated defense strategies in plants." Plant Signal Behav**5**(12): 1568-1570.

Hatsugai, N., S. Iwasaki, K. Tamura, M. Kondo, K. Fuji, K. Ogasawara, M. Nishimura and I. Hara-Nishimura (2009). "A novel membrane fusion-mediated plant immunity against bacterial pathogens." Genes Dev**23**(21): 2496-2506.

Haweker, H., S. Rips, H. Koiwa, S. Salomon, Y. Saijo, D. Chinchilla, S. Robatzek and A. von Schaewen (2010). "Pattern Recognition Receptors Require N-Glycosylation to Mediate Plant Immunity." Journal of Biological Chemistry**285**(7): 4629-4636.

He, K., X. Gou, T. Yuan, H. Lin, T. Asami, S. Yoshida, S. D. Russell and J. Li (2007). "BAK1 and BKK1 Regulate Brassinosteroid-Dependent Growth and Brassinosteroid-Independent Cell-Death Pathways." Current Biology**17**(13): 1109-1115.

Heese, A., D. R. Hann, S. Gimenez-Ibanez, A. M. E. Jones, K. He, J. Li, J. I. Schroeder, S. C. Peck and J. P. Rathjen (2007). "The receptor-like kinase SERK3/BAK1 is a central regulator of innate immunity in plants." Proceedings of the National Academy of Sciences of the United States of America**104**(29): 12217-12222.

Hemsley, P. A., T. Weimar, K. S. Lilley, P. Dupree and C. S. Grierson (2013). "A proteomic approach identifies many novel palmitoylated proteins in Arabidopsis." New Phytologist**197**(3): 805-814.

Henn, A. and E. Sadot (2014). "The unique enzymatic and mechanistic properties of plant myosins." Curr Opin Plant Biol**22C**: 65-70.

Henty-Ridilla, J. L., M. Shimono, J. Li, J. H. Chang, B. Day and C. J. Staiger (2013). "The Plant Actin Cytoskeleton Responds to Signals from Microbe-Associated Molecular Patterns." PLoS Pathog**9**(4): e1003290.

Higaki, T., T. Kurusu, S. Hasezawa and K. Kuchitsu (2011). "Dynamic intracellular reorganization of cytoskeletons and the vacuole in defense responses and hypersensitive cell death in plants." Journal of Plant Research**124**(3): 315-324.

Hoehenwarter, W., M. Thomas, E. Nukarinen, V. Egelhofer, H. Röhrig, W. Weckwerth, U. Conrath and G. J. M. Beckers (2013). "Identification of Novel in vivo MAP Kinase Substrates in Arabidopsis thaliana Through Use of Tandem Metal Oxide Affinity Chromatography." Molecular & Cellular Proteomics**12**(2): 369-380.

Hong, Z., H. Jin, T. Tzfira and J. Li (2008). "Multiple mechanism-mediated retention of a defective brassinosteroid receptor in the endoplasmic reticulum of Arabidopsis." Plant Cell**20**(12): 3418-3429.

Hornig-Do, H.-T., G. Günther, M. Bust, P. Lehnartz, A. Bosio and R. J. Wiesner (2009). "Isolation of functional pure mitochondria by superparamagnetic microbeads." Analytical Biochemistry**389**(1): 1-5.

Hothorn, M., Y. Belkhadir, M. Dreux, T. Dabi, J. P. Noel, I. A. Wilson and J. Chory (2011). "Structural basis of steroid hormone perception by the receptor kinase BRI1." Nature**474**(7352): 467-471.

Hu, Q., R. J. Noll, H. Li, A. Makarov, M. Hardman and R. Graham Cooks (2005). "The Orbitrap: a new mass spectrometer." J Mass Spectrom**40**(4): 430-443.

Huang, S., R. C. Robinson, L. Y. Gao, T. Matsumoto, A. Brunet, L. Blanchoin and C. J. Staiger (2005). "Arabidopsis VILLIN1 Generates Actin Filament Cables That Are Resistant to Depolymerization." The Plant Cell Online**17**(2): 486-501.

Ichimura, K., C. Casais, S. C. Peck, K. Shinozaki and K. Shirasu (2006). "MEKK1 Is Required for MPK4 Activation and Regulates Tissue-specific and Temperature-dependent Cell Death in Arabidopsis." Journal of Biological Chemistry**281**(48): 36969-36976.

Irani, N. G., S. Di Rubbo, E. Mylle, J. Van den Begin, J. Schneider-Pizoń, J. Hniliková, M. Šiša, D. Buyst, J. Vilarrasa-Blasi, A.-M. Szatmári, D. Van Damme, K. Mishev, M.-C. Codreanu, L. Kohout, M. Strnad, A. I. Caño-Delgado, J. Friml, A. Madder and E. Russinova (2012). "Fluorescent castasterone reveals BRI1 signaling from the plasma membrane." Nat Chem Biol**8**(6): 583-589.

Irani, N. G. and E. Russinova (2009). "Receptor endocytosis and signaling in plants." Current Opinion in Plant Biology**12**(6): 653-659.

Ito, J., T. S. Batth, C. J. Petzold, A. M. Redding-Johanson, A. Mukhopadhyay, R. Verboom, E. H. Meyer, A. H. Millar and J. L. Heazlewood (2010). "Analysis of the Arabidopsis Cytosolic Proteome Highlights Subcellular Partitioning of Central Plant Metabolism." Journal of Proteome Research**10**(4): 1571-1582.

Jacobs, A. K., V. Lipka, R. A. Burton, R. Panstruga, N. Strizhov, P. Schulze-Lefert and G. B. Fincher (2003). "An Arabidopsis Callose Synthase, GSL5, Is Required for Wound and Papillary Callose Formation." Plant Cell**15**(11): 2503-2513.

Jaquinod, M., F. Villiers, S. Kieffer-Jaquinod, V. Hugouvieux, C. Bruley, J. Garin and J. Bourguignon (2007). "A Proteomics Dissection of Arabidopsis thaliana Vacuoles Isolated from Cell Culture." Molecular & Cellular Proteomics**6**(3): 394-412.

Jones, J. D. G. and J. L. Dangl (2006). "The plant immune system." Nature**444**(7117): 323-329.

Kadota, Y., J. Sklenar, P. Derbyshire, L. Stransfeld, S. Asai, V. Ntoukakis, Jonathan D. Jones, K. Shirasu, F. Menke, A. Jones and C. Zipfel (2014). "Direct Regulation of the NADPH Oxidase RBOHD by the PRR-Associated Kinase BIK1 during Plant Immunity." Molecular Cell**54**(1): 43-55.

Kalde, M., T. S. Nuhse, K. Findlay and S. C. Peck (2007). "The syntaxin SYP132 contributes to plant resistance against bacteria and secretion of pathogenesis-related protein 1." Proc Natl Acad Sci U S A**104**(28): 11850-11855.

Kang, B. H. (2011). "Shrinkage and fragmentation of the trans-Golgi network in non-meristematic plant cells." Plant Signal Behav**6**(6): 884-886.

Kang, B. H., E. Nielsen, M. L. Preuss, D. Mastrorade and L. A. Staehelin (2011). "Electron tomography of RabA4b- and PI-4Kbeta1-labeled trans Golgi network compartments in Arabidopsis." Traffic**12**(3): 313-329.

Kano, F., S. Yamauchi, Y. Yoshida, M. Watanabe-Takahashi, K. Nishikawa, N. Nakamura and M. Murata (2009). "Yip1A regulates the COPI-independent retrograde transport from the Golgi complex to the ER." Journal of Cell Science**122**(13): 2218-2227.

Kayes, J. M. and S. E. Clark (1998). "CLAVATA2, a regulator of meristem and organ development in Arabidopsis." Development**125**(19): 3843-3851.

Keinath, N. F., S. Kierszniowska, J. Lorek, G. Bourdais, S. A. Kessler, H. Shimosato-Asano, U. Grossniklaus, W. X. Schulze, S. Robatzek and R. Panstruga (2010). "PAMP (Pathogen-associated Molecular Pattern)-induced Changes in Plasma Membrane Compartmentalization Reveal Novel Components of Plant Immunity." Journal of Biological Chemistry**285**(50): 39140-39149.

Kemmerling, B., A. Schwedt, P. Rodriguez, S. Mazzotta, M. Frank, S. A. Qamar, T. Mengiste, S. Betsuyaku, J. E. Parker, C. Müssig, B. P. H. J. Thomma, C. Albrecht, S. C. de Vries, H. Hirt and T. Nürnberger (2007). "The BRI1-Associated Kinase 1, BAK1, Has a

Brassinolide-Independent Role in Plant Cell-Death Control." Current Biology**17**(13): 1116-1122.

Ketelaar, T. (2013). "The actin cytoskeleton in root hairs: all is fine at the tip." Curr Opin Plant Biol**16**(6): 749-756.

Khurana, P., J. L. Henty, S. Huang, A. M. Staiger, L. Blanchoin and C. J. Staiger (2010). "Arabidopsis VILLIN1 and VILLIN3 have overlapping and distinct activities in actin bundle formation and turnover." Plant Cell**22**(8): 2727-2748.

Kim, B. H., A. R. Shenoy, P. Kumar, R. Das, S. Tiwari and J. D. MacMicking (2011). "A family of IFN-gamma-inducible 65-kD GTPases protects against bacterial infection." Science**332**(6030): 717-721.

Kirkpatrick, D. S., S. A. Gerber and S. P. Gygi (2005). "The absolute quantification strategy: a general procedure for the quantification of proteins and post-translational modifications." Methods**35**(3): 265-273.

Klahre, U., E. Friederich, B. Kost, D. Louvard and N.-H.Chua (2000). "Villin-Like Actin-Binding Proteins Are Expressed Ubiquitously in Arabidopsis." Plant Physiology**122**(1): 35-48.

Kleffmann, T., D. Russenberger, A. von Zychlinski, W. Christopher, K. Sjölander, W. Grissem and S. Baginsky (2004). "The Arabidopsis thaliana Chloroplast Proteome Reveals Pathway Abundance and Novel Protein Functions." Current Biology**14**(5): 354-362.

Konopka, C. A., S. K. Backues and S. Y. Bednarek (2008). "Dynamics of Arabidopsis Dynamin-Related Protein 1C and a Clathrin Light Chain at the Plasma Membrane." The Plant Cell Online**20**(5): 1363-1380.

Korbei, B., J. Moulinier-Anzola, L. De-Araujo, D. Lucyshyn, K. Retzer, Muhammad A. Khan and C. Luschnig (2013). "Arabidopsis TOL Proteins Act as Gatekeepers for Vacuolar Sorting of PIN2 Plasma Membrane Protein." Current Biology**23**(24): 2500-2505.

Koumandou, V. L., J. Dacks, R. Coulson and M. Field (2007). "Control systems for membrane fusion in the ancestral eukaryote; evolution of tethering complexes and SM proteins." BMC Evolutionary Biology**7**(1): 29.

Kuhn, B. M., M. Geisler, L. Bigler and C. Ringli (2011). "Flavonols accumulate asymmetrically and affect auxin transport in Arabidopsis." Plant Physiol**156**(2): 585-595.

Kumar, N. and S. Khurana (2004). "Identification of a Functional Switch for Actin Severing by Cytoskeletal Proteins." Journal of Biological Chemistry**279**(24): 24915-24918.

Kumar, N., A. Tomar, A. L. Parrill and S. Khurana (2004). "Functional Dissection and Molecular Characterization of Calcium-sensitive Actin-capping and Actin-depolymerizing Sites in Villin." Journal of Biological Chemistry**279**(43): 45036-45046.

Kumar, N., P. Zhao, A. Tomar, C. A. Galea and S. Khurana (2004). "Association of Villin with Phosphatidylinositol 4,5-Bisphosphate Regulates the Actin Cytoskeleton." Journal of Biological Chemistry**279**(4): 3096-3110.

Kwon, C., C. Neu, S. Pajonk, H. S. Yun, U. Lipka, M. Humphry, S. Bau, M. Straus, M. Kwaaitaal, H. Rampelt, F. E. Kasmi, G. Jurgens, J. Parker, R. Panstruga, V. Lipka and P. Schulze-Lefert (2008). "Co-option of a default secretory pathway for plant immune responses." Nature**451**(7180): 835-840.

Lachmann, J., C. Ungermann and S. Engelbrecht-Vandré (2011). "Rab GTPases and tethering in the yeast endocytic pathway." Small GTPases**2**(3): 182-186.

Latijnhouwers, M., T. Gillespie, P. Boevink, V. Kriechbaumer, C. Hawes and C. M. Carvalho (2007). "Localization and domain characterization of Arabidopsis golgin candidates." Journal of Experimental Botany**58**(15-16): 4373-4386.

Latijnhouwers, M., C. Hawes and C. Carvalho (2005). "Holding it all together? Candidate proteins for the plant Golgi matrix." Current Opinion in Plant Biology**8**(6): 632-639.

Lawrence, G., C. C. Brown, B. A. Flood, S. Karunakaran, M. Cabrera, M. Nordmann, C. Ungermann and R. A. Fratti (2014). "Dynamic association of the PI3P-interacting Mon1-Ccz1 GEF with vacuoles is controlled through its phosphorylation by the type 1 casein kinase Yck3." Molecular Biology of the Cell**25**(10): 1608-1619.

Lee, G.-J., E. J. Sohn, M. H. Lee and I. Hwang (2004). "The Arabidopsis Rab5 Homologs Rha1 and Ara7 Localize to the Prevacuolar Compartment." Plant and Cell Physiology**45**(9): 1211-1220.

Li, J. (2003). "Brassinosteroids signal through two receptor-like kinases." Current Opinion in Plant Biology**6**(5): 494-499.

Li, J., J. Wen, K. A. Lease, J. T. Doke, F. E. Tax and J. C. Walker (2002). "BAK1, an Arabidopsis LRR Receptor-like Protein Kinase, Interacts with BRI1 and Modulates Brassinosteroid Signaling." Cell**110**(2): 213-222.

Li, J. M. and J. Chory (1997). "A putative leucine-rich repeat receptor kinase involved in brassinosteroid signal transduction." Cell**90**(5): 929-938.

Lin, D. C., C. Quevedo, N. E. Brewer, A. Bell, J. R. Testa, M. L. Grimes, F. D. Miller and D. R. Kaplan (2006). "APPL1 Associates with TrkA and GIPC1 and Is Required for Nerve Growth Factor-Mediated Signal Transduction." Molecular and Cellular Biology**26**(23): 8928-8941.

Lipka, V., J. Dittgen, P. Bednarek, R. Bhat, M. Wiermer, M. Stein, J. Landtag, W. Brandt, S. Rosahl, D. Scheel, F. Llorente, A. Molina, J. Parker, S. Somerville and P. Schulze-Lefert (2005). "Pre- and Postinvasion Defenses Both Contribute to Nonhost Resistance in Arabidopsis." Science**310**(5751): 1180-1183.

Liu, T., Z. Liu, C. Song, Y. Hu, Z. Han, J. She, F. Fan, J. Wang, C. Jin, J. Chang, J. M. Zhou and J. Chai (2012). "Chitin-induced dimerization activates a plant immune receptor." Science**336**(6085): 1160-1164.

Lorente-Rodríguez, A., M. Heidtman and C. Barlowe (2009). "Multicopy suppressor analysis of thermosensitive YIP1 alleles implicates GOT1 in transport from the ER." Journal of Cell Science**122**(10): 1540-1550.

Lozano-Duran, R., A. P. Macho, F. Boutrot, C. Segonzac, I. E. Somssich and C. Zipfel (2013). "The transcriptional regulator BZR1 mediates trade-off between plant innate immunity and growth." Elife**2**: e00983.

Lu, D., W. Lin, X. Gao, S. Wu, C. Cheng, J. Avila, A. Heese, T. P. Devarenne, P. He and L. Shan (2011). "Direct Ubiquitination of Pattern Recognition Receptor FLS2 Attenuates Plant Innate Immunity." Science**332**(6036): 1439-1442.

Lu, D., S. Wu, X. Gao, Y. Zhang, L. Shan and P. He (2010). "A receptor-like cytoplasmic kinase, BIK1, associates with a flagellin receptor complex to initiate plant innate immunity." Proceedings of the National Academy of Sciences**107**(1): 496-501.

Lu, Y.-J., S. Schornack, T. Spallek, N. Geldner, J. Chory, S. Schellmann, K. Schumacher, S. Kamoun and S. Robatzek (2012). "Patterns of plant subcellular responses to successful oomycete infections reveal differences in host cell reprogramming and endocytic trafficking." Cellular Microbiology: no-no.

Luby-Phelps, K. (2000). "Cytoarchitecture and physical properties of cytoplasm: volume, viscosity, diffusion, intracellular surface area." Int Rev Cytol**192**: 189-221.

Luna, E., V. Pastor, J. Robert, V. Flors, B. Mauch-Mani and J. Ton (2011). "Callose deposition: a multifaceted plant defense response." Mol Plant Microbe Interact**24**(2): 183-193.

Lund, A. and A. Fuglsang (2012). Purification of Plant Plasma Membranes by Two-Phase Partitioning and Measurement of H⁺ Pumping. Plant Salt Tolerance. S. Shabala and T. A. Cuin, Humana Press. **913**: 217-223.

Mackey, D., Y. Belkhadir, J. M. Alonso, J. R. Ecker and J. L. Dangl (2003). "Arabidopsis RIN4 is a target of the type III virulence effector AvrRpt2 and modulates RPS2-mediated resistance." Cell**112**(3): 379-389.

Malmstrom, J., M. Beck, A. Schmidt, V. Lange, E. W. Deutsch and R. Aebersold (2009). "Proteome-wide cellular protein concentrations of the human pathogen *Leptospira interrogans*." Nature**460**(7256): 762-765.

Markgraf, D. F., K. Peplowska and C. Ungermann (2007). "Rab cascades and tethering factors in the endomembrane system." FEBS Letters**581**(11): 2125-2130.

Masclaux, F. G., J. P. Galaud and R. Pont-Lezica (2005). "The riddle of the plant vacuolar sorting receptors." Protoplasma**226**(3-4): 103-108.

Matsushima, R., Y. Hayashi, M. Kondo, T. Shimada, M. Nishimura and I. Hara-Nishimura (2002). "An Endoplasmic Reticulum-Derived Structure That Is Induced under Stress Conditions in Arabidopsis." Plant Physiology**130**(4): 1807-1814.

Mayer, U., G. Buttner and G. Jurgens (1993). "APICAL-BASAL PATTERN-FORMATION IN THE ARABIDOPSIS EMBRYO - STUDIES ON THE ROLE OF THE GNOM GENE." Development**117**(1): 149-162.

McBride, H. M., V. Rybin, C. Murphy, A. Giner, R. Teasdale and M. Zerial (1999). "Oligomeric complexes link Rab5 effectors with NSF and drive membrane fusion via interactions between EEA1 and syntaxin 13." Cell**98**(3): 377-386.

Mészáros, T., A. Helfer, E. Hatzimasoura, Z. Magyar, L. Serazetdinova, G. Rios, V. Bardóczy, M. Teige, C. Koncz, S. Peck and L. Bögre (2006). "The Arabidopsis MAP kinase kinase MKK1 participates in defence responses to the bacterial elicitor flagellin." The Plant Journal**48**(4): 485-498.

Meyer, D., S. Pajonk, C. Micali, R. O'Connell and P. Schulze-Lefert (2009). "Extracellular transport and integration of plant secretory proteins into pathogen-induced cell wall compartments." The Plant Journal**57**(6): 986-999.

Miaczynska, M., S. Christoforidis, A. Giner, A. Shevchenko, S. Uttenweiler-Joseph, B. Habermann, M. Wilm, R. G. Parton and M. Zerial (2004). "APPL Proteins Link Rab5 to Nuclear Signal Transduction via an Endosomal Compartment." Cell**116**(3): 445-456.

Miller, V. J. and D. Ungar (2012). "Re'COG'nition at the Golgi." Traffic**13**(7): 891-897.

Misumi, Y., Y. Misumi, K. Miki, A. Takatsuki, G. Tamura and Y. Ikehara (1986). "Novel blockade by brefeldin A of intracellular transport of secretory proteins in cultured rat hepatocytes." Journal of Biological Chemistry**261**(24): 11398-11403.

Mogensen, T. H. (2009). "Pathogen recognition and inflammatory signaling in innate immune defenses." Clin Microbiol Rev**22**(2): 240-273, Table of Contents.

Monaghan, J., S. Matschi, O. Shorinola, H. Rovenich, A. Matei, C. Segonzac, Frederikke G. Malinovsky, John P. Rathjen, D. MacLean, T. Romeis and C. Zipfel (2014). "The Calcium-Dependent Protein Kinase CPK28 Buffers Plant Immunity and Regulates BIK1 Turnover." Cell Host & Microbe**16**(5): 605-615.

Monaghan, J. and C. Zipfel (2012). "Plant pattern recognition receptor complexes at the plasma membrane." Current Opinion in Plant Biology**15**(4): 349-357.

Morciano, M., J. Burré, C. Corvey, M. Karas, H. Zimmermann and W. Volkandt (2005). "Immunoisolation of two synaptic vesicle pools from synaptosomes: a proteomics analysis." Journal of Neurochemistry**95**(6): 1732-1745.

Mukhtar, M. S., A.-R. Carvunis, M. Dreze, P. Epple, J. Steinbrenner, J. Moore, M. Tasan, M. Galli, T. Hao, M. T. Nishimura, S. J. Pevzner, S. E. Donovan, L. Ghamsari, B. Santhanam, V. Romero, M. M. Poulin, F. Gebreab, B. J. Gutierrez, S. Tam, D. Monachello, M. Boxem, C. J. Harbort, N. McDonald, L. Gai, H. Chen, Y. He, E. U. E. Consortium, J. Vandenhoute, F. P. Roth, D. E. Hill, J. R. Ecker, M. Vidal, J. Beynon, P. Braun and J. L. Dangl (2011). "Independently Evolved Virulence Effectors Converge onto Hubs in a Plant Immune System Network." Science**333**(6042): 596-601.

Müller, J., M. Beck, U. Mettbach, G. Komis, G. Hause, D. Menzel and J. Šamaj (2010). "Arabidopsis MPK6 is involved in cell division plane control during early root development, and localizes to the pre-prophase band, phragmoplast, trans-Golgi network and plasma membrane." The Plant Journal**61**(2): 234-248.

Mysore, K. S. and C. M. Ryu (2004). "Nonhost resistance: how much do we know?" Trends Plant Sci**9**(2): 97-104.

Nada, S., A. Hondo, A. Kasai, M. Koike, K. Saito, Y. Uchiyama and M. Okada (2009). The novel lipid raft adaptor p18 controls endosome dynamics by anchoring the MEK–ERK pathway to late endosomes.

Nakagami, H., H. Soukupová, A. Schikora, V. Zárský and H. Hirt (2006). "A Mitogen-activated Protein Kinase Kinase Kinase Mediates Reactive Oxygen Species Homeostasis in Arabidopsis." Journal of Biological Chemistry**281**(50): 38697-38704.

Nam, K. H. and J. Li (2002). "BRI1/BAK1, a Receptor Kinase Pair Mediating Brassinosteroid Signaling." Cell**110**(2): 203-212.

Naramoto, S., M. S. Otegui, N. Kutsuna, R. de Rycke, T. Dainobu, M. Karampelias, M. Fujimoto, E. Feraru, D. Miki, H. Fukuda, A. Nakano and J. Friml (2014). "Insights into the localization and function of the membrane trafficking regulator GNOM ARF-GEF at the Golgi apparatus in Arabidopsis." Plant Cell**26**(7): 3062-3076.

Navarro, L., C. Zipfel, O. Rowland, I. Keller, S. Robatzek, T. Boller and J. D. G. Jones (2004). "The transcriptional innate immune response to flg22: interplay and overlap with Avr gene-dependent defense responses and bacterial pathogenesis." Plant Physiology**135**(2): 1113-1128.

Nekrasov, V., J. Li, M. Batoux, M. Roux, Z.-H. Chu, S. Lacombe, A. Rougon, P. Bittel, M. Kiss-Papp, D. Chinchilla, H. P. van Esse, L. Jorda, B. Schwessinger, V. Nicaise, B. P. H. J. Thomma, A. Molina, J. D. G. Jones and C. Zipfel (2009). "Control of the pattern-recognition receptor EFR by an ER protein complex in plant immunity." Embo Journal**28**(21): 3428-3438.

Nielsen, E., A. Y. Cheung and T. Ueda (2008). "The Regulatory RAB and ARF GTPases for Vesicular Trafficking." Plant Physiology**147**(4): 1516-1526.

Nielsen, M. E., A. Feechan, H. Böhlenius, T. Ueda and H. Thordal-Christensen (2012). "Arabidopsis ARF-GTP exchange factor, GNOM, mediates transport required for innate immunity and focal accumulation of syntaxin PEN1." Proceedings of the National Academy of Sciences**109**(28): 11443-11448.

Nikolovski, N., D. Rubtsov, M. P. Segura, G. P. Miles, T. J. Stevens, T. P. J. Dunkley, S. Munro, K. S. Lilley and P. Dupree (2012). "Putative glycosyltransferases and other plant Golgi apparatus proteins are revealed by LOPIT proteomics." Plant Physiology.

Nishimura, M. T., M. Stein, B. H. Hou, J. P. Vogel, H. Edwards and S. C. Somerville (2003). "Loss of a callose synthase results in salicylic acid-dependent disease resistance." Science**301**(5635): 969-972.

Nomura, K., S. DebRoy, Y. H. Lee, N. Pumplin, J. Jones and S. Y. He (2006). "A Bacterial Virulence Protein Suppresses Host Innate Immunity to Cause Plant Disease." Science**313**(5784): 220-223.

Nomura, K., C. Mecey, Y.-N. Lee, L. A. Imboden, J. H. Chang and S. Y. He (2011). "Effector-triggered immunity blocks pathogen degradation of an immunity-associated vesicle traffic regulator in Arabidopsis." Proceedings of the National Academy of Sciences**108**(26): 10774-10779.

Nühse, T. S., A. R. Bottrill, A. M. E. Jones and S. C. Peck (2007). "Quantitative phosphoproteomic analysis of plasma membrane proteins reveals regulatory mechanisms of plant innate immune responses." The Plant Journal**51**(5): 931-940.

Old, W. M., K. Meyer-Arendt, L. Aveline-Wolf, K. G. Pierce, A. Mendoza, J. R. Sevinsky, K. A. Resing and N. G. Ahn (2005). "Comparison of Label-free Methods for Quantifying Human Proteins by Shotgun Proteomics." Molecular & Cellular Proteomics**4**(10): 1487-1502.

Ong, S. E., B. Blagoev, I. Kratchmarova, D. B. Kristensen, H. Steen, A. Pandey and M. Mann (2002). "Stable isotope labeling by amino acids in cell culture, SILAC, as a simple and accurate approach to expression proteomics." Mol Cell Proteomics**1**(5): 376-386.

Ostertag, M., J. Stammler, D. Douchkov, R. Eichmann and R. Hüchelhoven (2013). "The conserved oligomeric Golgi complex is involved in penetration resistance of barley to the barley powdery mildew fungus." Molecular Plant Pathology**14**(3): 230-240.

Parsons, H. T., K. Christiansen, B. Knierim, A. Carroll, J. Ito, T. S. Batth, A. M. Smith-Moritz, S. Morrison, P. McInerney, M. Z. Hadi, M. Auer, A. Mukhopadhyay, C. J. Petzold, H. V. Scheller, D. Loqué and J. L. Heazlewood (2012). "Isolation and Proteomic Characterization of the Arabidopsis Golgi Defines Functional and Novel Components Involved in Plant Cell Wall Biosynthesis." Plant Physiology**159**(1): 12-26.

Parsons, H. T., G. Drakakaki and J. L. Heazlewood (2013). "Proteomic dissection of the Arabidopsis Golgi and trans-Golgi network." Frontiers in Plant Science**3**.

Parsons, H. T., G. Drakakaki and J. L. Heazlewood (2013). "Proteomic dissection of the Arabidopsis Golgi and trans-Golgi network." Front Plant Sci**3**: 298.

Pečenková, T., M. Hála, I. Kulich, D. Kocourková, E. Drdová, M. Fendrych, H. Toupalová and V. Žárský (2011). "The role for the exocyst complex subunits Exo70B2 and Exo70H1 in the plant-pathogen interaction." Journal of Experimental Botany**62**(6): 2107-2116.

Peplowska, K., D. F. Markgraf, C. W. Ostrowicz, G. Bange and C. Ungermann (2007). "The CORVET Tethering Complex Interacts with the Yeast Rab5 Homolog Vps21 and Is Involved in Endo-Lysosomal Biogenesis." Developmental Cell**12**(5): 739-750.

Perkins, D. N., D. J. Pappin, D. M. Creasy and J. S. Cottrell (1999). "Probability-based protein identification by searching sequence databases using mass spectrometry data." Electrophoresis**20**(18): 3551-3567.

Petersen, M., P. Brodersen, H. Naested, E. Andreasson, U. Lindhart, B. Johansen, H. B. Nielsen, M. Lacy, M. J. Austin, J. E. Parker, S. B. Sharma, D. F. Klessig, R. Martienssen, O. Mattsson, A. B. Jensen and J. Mundy (2000). "Arabidopsis map kinase 4 negatively regulates systemic acquired resistance." Cell**103**(7): 1111-1120.

Pinheiro, H., M. Samalova, N. Geldner, J. Chory, A. Martinez and I. Moore (2009). "Genetic evidence that the higher plant Rab-D1 and Rab-D2 GTPases exhibit distinct but overlapping interactions in the early secretory pathway." Journal of Cell Science**122**(20): 3749-3758.

Popescu, S. C., G. V. Popescu, S. Bachan, Z. Zhang, M. Gerstein, M. Snyder and S. P. Dinesh-Kumar (2009). "MAPK target networks in Arabidopsis thaliana revealed using functional protein microarrays." Genes & Development**23**(1): 80-92.

Poultney, C. S., R. A. Gutiérrez, M. S. Katari, M. L. Gifford, W. B. Paley, G. M. Coruzzi and D. E. Shasha (2007). "Sungear: interactive visualization and functional analysis of genomic datasets." Bioinformatics**23**(2): 259-261.

Purvanov, V., A. Koval and V. L. Katanaev (2010). "A Direct and Functional Interaction Between Go and Rab5 During G Protein-Coupled Receptor Signaling." Sci. Signal.**3**(136): ra65-.

Qi, X., M. Kaneda, J. Chen, A. Geitmann and H. Zheng (2011). "A specific role for Arabidopsis TRAPP II in post-Golgi trafficking that is crucial for cytokinesis and cell polarity." The Plant Journal**68**(2): 234-248.

Qi, X. and H. Zheng (2011). "Arabidopsis TRAPP II is functionally linked to Rab-A, but not Rab-D in polar protein trafficking in trans-Golgi network." Plant Signal Behav**6**(11): 1679-1683.

Raikhel, N. and G. Hicks (2007). "Signaling from plant endosomes: compartments with something to say!" Genes & Development**21**(13): 1578-1580.

Ranf, S., L. Eschen-Lippold, P. Pecher, J. Lee and D. Scheel (2011). "Interplay between calcium signalling and early signalling elements during defence responses to microbe- or damage-associated molecular patterns." The Plant Journal: no-no.

Ranf, S., L. Eschen-Lippold, P. Pecher, J. Lee and D. Scheel (2011). "Interplay between calcium signalling and early signalling elements during defence responses to microbe- or damage-associated molecular patterns." Plant J**68**(1): 100-113.

Rappsilber, J., U. Ryder, A. I. Lamond and M. Mann (2002). "Large-scale proteomic analysis of the human spliceosome." Genome Res**12**(8): 1231-1245.

Rayapuram, N., L. Bonhomme, J. Bigeard, K. Haddadou, C. Przybylski, H. Hirt and D. Pflieger (2014). "Identification of Novel PAMP-Triggered Phosphorylation and Dephosphorylation Events in Arabidopsis thaliana by Quantitative Phosphoproteomic Analysis." Journal of Proteome Research**13**(4): 2137-2151.

Reiter, W.-D. and G. Vanzin (2001). "Molecular genetics of nucleotide sugar interconversion pathways in plants." Plant Molecular Biology**47**(1-2): 95-113.

Richter, S., U. Voß and G. Jürgens (2009). "Post-Golgi Traffic in Plants." Traffic**10**(7): 819-828.

Ridley, B. L., M. A. O'Neill and D. Mohnen (2001). "Pectins: structure, biosynthesis, and oligogalacturonide-related signaling." Phytochemistry**57**(6): 929-967.

Ringli, C., L. Bigler, B. M. Kuhn, R.-M. Leiber, A. Diet, D. Santelia, B. Frey, S. Pollmann and M. Klein (2008). "The Modified Flavonol Glycosylation Profile in the Arabidopsis rol1 Mutants Results in Alterations in Plant Growth and Cell Shape Formation." The Plant Cell Online**20**(6): 1470-1481.

Robatzek, S., D. Chinchilla and T. Boller (2006). "Ligand-induced endocytosis of the pattern recognition receptor FLS2 in Arabidopsis." Genes & Development**20**(5): 537-542.

Robert, S., S. N. Chary, G. Drakakaki, S. Li, Z. Yang, N. V. Raikhel and G. R. Hicks (2008). "Endosidin1 defines a compartment involved in endocytosis of the brassinosteroid receptor BRI1 and the auxin transporters PIN2 and AUX1." Proceedings of the National Academy of Sciences**105**(24): 8464-8469.

Robinson, D. G., M.-C.Herranz, J. Bubeck, R. Pepperkok and C. Ritzenthaler (2007). "Membrane Dynamics in the Early Secretory Pathway." Critical Reviews in Plant Sciences **26**(4): 199-225.

Ross, P. L., Y. N. Huang, J. N. Marchese, B. Williamson, K. Parker, S. Hattan, N. Khainovski, S. Pillai, S. Dey, S. Daniels, S. Purkayastha, P. Juhasz, S. Martin, M. Bartlett-Jones, F. He, A. Jacobson and D. J. Pappin (2004). "Multiplexed protein quantitation in *Saccharomyces cerevisiae* using amine-reactive isobaric tagging reagents." Mol Cell Proteomics **3**(12): 1154-1169.

Roux, M., B. Schwessinger, C. Albrecht, D. Chinchilla, A. Jones, N. Holton, F. G. Malinovsky, M. Tör, S. de Vries and C. Zipfel (2011). "The Arabidopsis Leucine-Rich Repeat Receptor-Like Kinases BAK1/SERK3 and BKK1/SERK4 Are Required for Innate Immunity to Hemibiotrophic and Biotrophic Pathogens." The Plant Cell Online.

Russell, M. R. and K. S. Lilley (2012). "Pipeline to assess the greatest source of technical variance in quantitative proteomics using metabolic labelling." J Proteomics **77**: 441-454.

Russinova, E., J. W. Borst, M. Kwaaitaal, A. Cano-Delgado, Y. H. Yin, J. Chory and S. C. de Vries (2004). "Heterodimerization and endocytosis of Arabidopsis brassinosteroid receptors BRI1 and AtSERK3 (BAK1)." Plant Cell **16**(12): 3216-3229.

Rutherford, S. and I. Moore (2002). "The Arabidopsis Rab GTPase family: another enigma variation." Current Opinion in Plant Biology **5**(6): 518-528.

Sadowski, P. G., A. J. Groen, P. Dupree and K. S. Lilley (2008). "Sub-cellular localization of membrane proteins." PROTEOMICS **8**(19): 3991-4011.

Saijo, Y. (2010). "ER quality control of immune receptors and regulators in plants." Cellular Microbiology **12**(6): 716-724.

Saijo, Y., N. Tintor, X. Lu, P. Rauf, K. Pajerowska-Mukhtar, H. Haeweker, X. Dong, S. Robatzek and P. Schulze-Lefert (2009). "Receptor quality control in the endoplasmic reticulum for plant innate immunity." Embo Journal **28**(21): 3439-3449.

Saito, C. and T. Ueda (2009).Chapter 4 Functions of RAB and SNARE Proteins in Plant Life.International Review of Cell and Molecular Biology. W. J. Kwang, Academic Press.

Volume 274: 183-233.

Sanderfoot, A. A., F. F. Assaad and N. V. Raikhel (2000)."The Arabidopsis Genome.An Abundance of Soluble N-Ethylmaleimide-Sensitive Factor Adaptor Protein Receptors."Plant Physiology**124**(4): 1558-1569.

Schellmann, S. and P. Pimpl (2009). "Coats of endosomal protein sorting: retromer and ESCRT." Current Opinion in Plant Biology**12**(6): 670-676.

Scheuring, D., C. Viotti, F. Krüger, F. Künzl, S. Sturm, J. Bubeck, S. Hillmer, L. Frigerio, D. G. Robinson, P. Pimpl and K. Schumacher (2011). "Multivesicular Bodies Mature from the Trans-Golgi Network/Early Endosome in Arabidopsis." The Plant Cell Online.

Schindler, J. and H. G. Nothwang (2006). "Aqueous polymer two-phase systems: Effective tools for plasma membrane proteomics." PROTEOMICS**6**(20): 5409-5417.

Schmick, M. and Philippe I. H. Bastiaens (2014)."The Interdependence of Membrane Shape and Cellular Signal Processing."Cell**156**(6): 1132-1138.

Schmidt, U. G., A. Endler, S. Schelbert, A. Brunner, M. Schnell, H. E. Neuhaus, D. Marty-Mazars, F. Marty, S. Baginsky and E. Martinoia (2007). "Novel Tonoplast Transporters Identified Using a Proteomic Approach with Vacuoles Isolated from Cauliflower Buds." Plant Physiology**145**(1): 216-229.

Schulze, B., T. Mentzel, A. K. Jehle, K. Mueller, S. Beeler, T. Boller, G. Felix and D. Chinchilla (2010). "Rapid Heteromerization and Phosphorylation of Ligand-activated Plant Transmembrane Receptors and Their Associated Kinase BAK1."Journal of Biological Chemistry**285**(13): 9444-9451.

Schwessinger, B., M. Roux, Y. Kadota, V. Ntoukakis, J. Sklenar, A. Jones and C. Zipfel (2011)."Phosphorylation-Dependent Differential Regulation of Plant Growth, Cell Death, and Innate Immunity by the Regulatory Receptor-Like Kinase BAK1."PLoS Genet**7**(4): e1002046.

Searle, B. C. (2010). "Scaffold: A bioinformatic tool for validating MS/MS-based proteomic studies." PROTEOMICS**10**(6): 1265-1269.

Segonzac, C. and C. Zipfel (2011). "Activation of plant pattern-recognition receptors by bacteria." Current Opinion in Microbiology**14**(1): 54-61.

Shahriari, M., K. Richter, C. Keshavaiah, A. Sabovljevic, M. Huelskamp and S. Schellmann (2011). "The Arabidopsis ESCRT protein-protein interaction network." Plant Molecular Biology**76**(1-2): 85-96.

Sharfman, M., M. Bar, M. Ehrlich, S. Schuster, S. Melech-Bonfil, R. Ezer, G. Sessa and A. Avni (2011). "Endosomal signaling of the tomato leucine rich repeat receptor-like protein LeEix2." The Plant Journal: no-no.

She, J., Z. Han, T. W. Kim, J. Wang, W. Cheng, J. Chang, S. Shi, J. Wang, M. Yang, Z. Y. Wang and J. Chai (2011). "Structural insight into brassinosteroid perception by BR11." Nature**474**(7352): 472-476.

Shiu, S.-H. and A. B. Bleeker (2001). "Receptor-like kinases from Arabidopsis form a monophyletic gene family related to animal receptor kinases." Proceedings of the National Academy of Sciences**98**(19): 10763-10768.

Singh, R., M. O. Lee, J. E. Lee, J. Choi, J. H. Park, E. H. Kim, R. H. Yoo, J. I. Cho, J. S. Jeon, R. Rakwal, G. K. Agrawal, J. S. Moon and N. S. Jwa (2012). "Rice mitogen-activated protein kinase interactome analysis using the yeast two-hybrid system." Plant Physiol**160**(1): 477-487.

Sivars, U., D. Aivazian and S. R. Pfeffer (2003). "Yip3 catalyses the dissociation of endosomal Rab-GDI complexes." Nature**425**(6960): 856-859.

Smertenko, A. and V. E. Franklin-Tong (2011). "Organisation and regulation of the cytoskeleton in plant programmed cell death." Cell Death Differ**18**(8): 1263-1270.

Smith, J. M., D. J. Salamango, M. E. Leslie, C. A. Collins and A. Heese (2014). "Sensitivity to Flg22 is modulated by ligand-induced degradation and de novo synthesis of the endogenous flagellin-receptor FLAGELLIN-SENSING2." Plant Physiol**164**(1): 440-454.

Snyder, B. A., B. Leite, J. Hipskind, L. G. Butler and R. L. Nicholson (1991). "Accumulation of sorghum phytoalexins induced by *Colletotrichum graminicola* at the infection site." Physiological and Molecular Plant Pathology**39**(6): 463-470.

Sörensson, C., M. Lenman, J. Veide-Vilg, S. Schopper, T. Ljungdahl, M. Grøtli, M. J. Tamás, S. C. Peck and E. Andreasson (2012). "Determination of primary sequence specificity of Arabidopsis MAPKs MPK3 and MPK6 leads to identification of new substrates." Biochemical Journal**446**(2): 271-278.

Sousa, L. P., I. Lax, H. Shen, S. M. Ferguson, P. D. Camilli and J. Schlessinger (2012). "Suppression of EGFR endocytosis by dynamin depletion reveals that EGFR signaling occurs primarily at the plasma membrane." Proceedings of the National Academy of Sciences**109**(12): 4419-4424.

Spallek, T., M. Beck, S. Ben Khaled, S. Salomon, G. Bourdais, S. Schellmann and S. Robatzek (2013). "ESCRT-I Mediates FLS2 Endosomal Sorting and Plant Immunity." PLoS Genet**9**(12): e1004035.

Staehelein, L. A. and B.-H.Kang (2008). "Nanoscale Architecture of Endoplasmic Reticulum Export Sites and of Golgi Membranes as Determined by Electron Tomography." Plant Physiology**147**(4): 1454-1468.

Staiger, C. J., M. B. Sheahan, P. Khurana, X. Wang, D. W. McCurdy and L. Blanchoin (2009). "Actin filament dynamics are dominated by rapid growth and severing activity in the Arabidopsis cortical array." The Journal of Cell Biology**184**(2): 269-280.

Steen, H. and M. Mann (2004). "The abc's (and xyz's) of peptide sequencing." Nat Rev Mol Cell Biol**5**(9): 699-711.

Stegmann, M., R. G. Anderson, K. Ichimura, T. Pecenkova, P. Reuter, V. Žárský, J. M. McDowell, K. Shirasu and M. Trujillo (2012). "The Ubiquitin Ligase PUB22 Targets a Subunit of the Exocyst Complex Required for PAMP-Triggered Responses in Arabidopsis." The Plant Cell Online**24**(11): 4703-4716.

Stein, M., J. Dittgen, C. Sanchez-Rodriguez, B. H. Hou, A. Molina, P. Schulze-Lefert, V. Lipka and S. Somerville (2006). "Arabidopsis PEN3/PDR8, an ATP binding cassette transporter, contributes to nonhost resistance to inappropriate pathogens that enter by direct penetration." Plant Cell**18**(3): 731-746.

Steuble, M., B. Gerrits, A. Ludwig, J. M. Mateos, T.-M. Diep, M. Tagaya, A. Stephan, P. Schätzle, B. Kunz, P. Streit and P. Sonderegger (2010). "Molecular characterization of a trafficking organelle: Dissecting the axonal paths of calyntenin-1 transport vesicles." PROTEOMICS**10**(21): 3775-3788.

Su, S.-H., M. C. Suarez-Rodriguez and P. Krysan (2007). "Genetic interaction and phenotypic analysis of the Arabidopsis MAP kinase pathway mutations mekk1 and mpk4 suggests signaling pathway complexity." FEBS Letters**581**(17): 3171-3177.

Su, W., Y. Liu, Y. Xia, Z. Hong and J. Li (2011). "Conserved endoplasmic reticulum-associated degradation system to eliminate mutated receptor-like kinases in Arabidopsis." Proc Natl Acad Sci U S A**108**(2): 870-875.

Suarez-Rodriguez, M. C., L. Adams-Phillips, Y. Liu, H. Wang, S.-H. Su, P. J. Jester, S. Zhang, A. F. Bent and P. J. Krysan (2007). "MEKK1 Is Required for flg22-Induced MPK4 Activation in Arabidopsis Plants." Plant Physiology**143**(2): 661-669.

Tang, W., Z. Deng and Z.-Y. Wang (2010). "Proteomics shed light on the brassinosteroid signaling mechanisms." Current Opinion in Plant Biology**13**(1): 27-33.

Tang, W., T. W. Kim, J. A. Oses-Prieto, Y. Sun, Z. Deng, S. Zhu, R. Wang, A. L. Burlingame and Z. Y. Wang (2008). "BSKs mediate signal transduction from the receptor kinase BRI1 in Arabidopsis." Science**321**(5888): 557-560.

Tateda, C., Z. Zhang, J. Shrestha, J. Jelenska, D. Chinchilla and J. T. Greenberg (2014). "Salicylic Acid Regulates Arabidopsis Microbial Pattern Receptor Kinase Levels and Signaling." The Plant Cell Online.

Taub, N., D. Teis, H. L. Ebner, M. W. Hess and L. A. Huber (2007). "Late endosomal traffic of the epidermal growth factor receptor ensures spatial and temporal fidelity of mitogen-activated protein kinase signalling." Molecular Biology of the Cell**18**(12): 4698-4710.

Teis, D., W. Wunderlich and L. A. Huber (2002). "Localization of the MP1-MAPK Scaffold Complex to Endosomes Is Mediated by p14 and Required for Signal Transduction." Developmental Cell**3**(6): 803-814.

Thellmann, M., K. Rybak, K. Thiele, G. Wanner and F. F. Assaad (2010). "Tethering Factors Required for Cytokinesis in Arabidopsis." Plant Physiology**154**(2): 720-732.

Tominaga, M. and A. Nakano (2012). "Plant-Specific Myosin XI, a Molecular Perspective." Front Plant Sci**3**: 211.

Toth, R., C. Gerding-Reimers, M. J. Deeks, S. Menninger, R. M. Gallegos, I. A. Tonaco, K. Hubel, P. J. Hussey, H. Waldmann and G. Coupland (2012). "Prieurianin/endosidin 1 is an actin-stabilizing small molecule identified from a chemical genetic screen for circadian clock effectors in Arabidopsis thaliana." Plant J**71**(2): 338-352.

Treutter, D. (2006). "Significance of flavonoids in plant resistance: a review." Environmental Chemistry Letters**4**(3): 147-157.

Tsien, R. Y. (1998). "THE GREEN FLUORESCENT PROTEIN." Annual Review of Biochemistry**67**(1): 509-544.

Ueda, T., N. Matsuda, T. Anai, H. Tsukaya, H. Uchimiya and A. Nakano (1996). "An Arabidopsis gene isolated by a novel method for detecting genetic interaction in yeast encodes the GDP dissociation inhibitor of Ara4 GTPase." Plant Cell**8**(11): 2079-2091.

Ueda, T., T. Uemura, M. H. Sato and A. Nakano (2004). "Functional differentiation of endosomes in Arabidopsis cells." Plant J**40**(5): 783-789.

Ueda, T., T. Uemura, M. H. Sato and A. Nakano (2004). "Functional differentiation of endosomes in Arabidopsis cells." The Plant Journal**40**(5): 783-789.

Ueda, T., M. Yamaguchi, H. Uchimiya and A. Nakano (2001). "Ara6, a plant-unique novel type Rab GTPase, functions in the endocytic pathway of Arabidopsis thaliana." EMBO J**20**(17): 4730-4741.

Uemura, T., Y. Suda, T. Ueda and A. Nakano (2014). "Dynamic Behavior of the trans-Golgi Network in Root Tissues of Arabidopsis Revealed by Super-Resolution Live Imaging." Plant and Cell Physiology**55**(4): 694-703.

Uemura, T. and T. Ueda (2014). "Plant vacuolar trafficking driven by RAB and SNARE proteins." Current Opinion in Plant Biology**22**(0): 116-121.

Uemura, T., T. Ueda, R. L. Ohniwa, A. Nakano, K. Takeyasu and M. H. Sato (2004). "Systematic analysis of SNARE molecules in Arabidopsis: Dissection of the post-Golgi network in plant cells." Cell Structure and Function**29**(2): 49-65.

Underwood, W. and S. C. Somerville (2013). "Perception of conserved pathogen elicitors at the plasma membrane leads to relocalization of the Arabidopsis PEN3 transporter." Proceedings of the National Academy of Sciences**110**(30): 12492-12497.

van der Honing, H. S., H. Kieft, A. M. C. Emons and T. Ketelaar (2012). "Arabidopsis VILLIN2 and VILLIN3 Are Required for the Generation of Thick Actin Filament Bundles and for Directional Organ Growth." Plant Physiology**158**(3): 1426-1438.

Varsano, T., M.-Q. Dong, I. Niesman, H. Gacula, X. Lou, T. Ma, J. R. Testa, J. R. Yates and M. G. Farquhar (2006). "GIPC Is Recruited by APPL to Peripheral TrkA Endosomes and Regulates TrkA Trafficking and Signaling." Molecular and Cellular Biology**26**(23): 8942-8952.

Vernoud, V., A. C. Horton, Z. Yang and E. Nielsen (2003). "Analysis of the Small GTPase Gene Superfamily of Arabidopsis." Plant Physiology**131**(3): 1191-1208.

Vestal, D. J. and J. A. Jeyaratnam (2011). "The guanylate-binding proteins: emerging insights into the biochemical properties and functions of this family of large interferon-induced guanosine triphosphatase." J Interferon Cytokine Res**31**(1): 89-97.

Vieira, A. V., C. Lamaze and S. L. Schmid (1996). "Control of EGF receptor signaling by clathrin-mediated endocytosis." Science**274**(5295): 2086-2089.

Viotti, C., J. Bubeck, Y.-D. Stierhof, M. Krebs, M. Langhans, W. van den Berg, W. van Dongen, S. Richter, N. Geldner, J. Takano, G. Jürgens, S. C. de Vries, D. G. Robinson and K. Schumacher (2010). "Endocytic and Secretory Traffic in Arabidopsis Merge in the Trans-Golgi Network/Early Endosome, an Independent and Highly Dynamic Organelle." The Plant Cell Online**22**(4): 1344-1357.

Voet, J. G. and D. Voet (2009). "Communication through illustration: The work of David Goodsell." Biochemistry and Molecular Biology Education**37**(4): 203-203.

Voigt, C. A. (2014). "Callose-mediated resistance to pathogenic intruders in plant defense-related papillae." Frontiers in Plant Science**5**.

Wang, D. and X. Dong (2011). "A Highway for War and Peace: The Secretory Pathway in Plant-Microbe Interactions." Molecular Plant**4**(4): 581-587.

Wang, D., N. D. Weaver, M. Kesarwani and X. Dong (2005). "Induction of Protein Secretory Pathway Is Required for Systemic Acquired Resistance." Science**308**(5724): 1036-1040.

Wang, F., Y. Shang, B. Fan, J. Q. Yu and Z. Chen (2014). "Arabidopsis LIP5, a positive regulator of multivesicular body biogenesis, is a critical target of pathogen-responsive MAPK cascade in plant basal defense." PLoS Pathog**10**(7): e1004243.

Watanabe, S., T. L. Shimada, K. Hiruma and Y. Takano (2013). "Pathogen Infection Trial Increases the Secretion of Proteins Localized in the Endoplasmic Reticulum Body of Arabidopsis." Plant Physiology**163**(2): 659-664.

Whyte, J. R. C. and S. Munro (2002). "Vesicle tethering complexes in membrane traffic." Journal of Cell Science**115**(13): 2627-2637.

Widell, S., T. Lundborg and C. Larsson (1982). "Plasma Membranes from Oats Prepared by Partition in an Aqueous Polymer Two-Phase System: On the Use of Light-Induced Cytochrome b Reduction as a Marker for the Plasma Membrane." Plant Physiology**70**(5): 1429-1435.

Wolf-Yadlin, A., S. Hautaniemi, D. A. Lauffenburger and F. M. White (2007). "Multiple reaction monitoring for robust quantitative proteomic analysis of cellular signaling networks." Proc Natl Acad Sci U S A**104**(14): 5860-5865.

Yamamoto, M., M. Okuyama, Ji S. Ma, T. Kimura, N. Kamiyama, H. Saiga, J. Ohshima, M. Sasai, H. Kayama, T. Okamoto, David C. S. Huang, D. Soldati-Favre, K. Horie, J. Takeda and K. Takeda (2012). "A Cluster of Interferon- γ -Inducible p65 GTPases Plays a Critical Role in Host Defense against *Toxoplasma gondii*." Immunity**37**(2): 302-313.

Yang, L., L. Qin, G. Liu, V. V. Peremyslov, V. V. Dolja and Y. Wei (2014). "Myosins XI modulate host cellular responses and penetration resistance to fungal pathogens." Proceedings of the National Academy of Sciences.

Yun, H. S., M. Kwaaitaal, N. Kato, C. Yi, S. Park, M. H. Sato, P. Schulze-Lefert and C. Kwon (2013). "Requirement of vesicle-associated membrane protein 721 and 722 for sustained growth during immune responses in Arabidopsis." Mol Cells**35**(6): 481-488.

Yun, H. S., C. Yi, H. Kwon and C. Kwon (2013). "Model for regulation of VAMP721/722-mediated secretion: growth vs. stress responses." Plant Signal Behav**8**(11): e27116.

Žárský, V., F. Cvrčková, F. Bischoff and K. Palme (1997). "At-GDI1 from Arabidopsis thaliana encodes a rab-specific GDP dissociation inhibitor that complements the sec19 mutation of Saccharomyces cerevisiae." FEBS Letters**403**(3): 303-308.

Zhang, J., W. Li, T. Xiang, Z. Liu, K. Laluk, X. Ding, Y. Zou, M. Gao, X. Zhang, S. Chen, T. Mengiste, Y. Zhang and J.-M. Zhou (2010). "Receptor-like Cytoplasmic Kinases Integrate Signaling from Multiple Plant Immune Receptors and Are Targeted by a Pseudomonas syringae Effector." Cell Host & Microbe**7**(4): 290-301.

Zhang, L., X. e. Wang, X. Peng, Y. Wei, R. Cao, Z. Liu, J. Xiong, X. Ying, P. Chen and S. Liang (2006). "Immunoaffinity Purification of Plasma Membrane with Secondary Antibody Superparamagnetic Beads for Proteomic Analysis." Journal of Proteome Research**6**(1): 34-43.

Zhang, Y., C.-M. Liu, A.-M. C. Emons and T. Ketelaar (2010). "The Plant Exocyst." Journal of Integrative Plant Biology**52**(2): 138-146.

Zhu, Z., J. Wei, Z. Shi, Y. Yang, D. Shao, B. Li, X. Wang and Z. Ma (2013). "Identification of human guanylate-binding protein 1 gene (hGBP1) as a direct transcriptional target gene of p53." Biochemical and Biophysical Research Communications**436**(2): 204-211.

Zipfel, C., S. Robatzek, L. Navarro, E. J. Oakeley, J. D. G. Jones, G. Felix and T. Boller (2004). "Bacterial disease resistance in Arabidopsis through flagellin perception." Nature**428**(6984): 764-767.

Zouhar, J., E. Rojo and D. C. Bassham (2009). "AtVPS45 Is a Positive Regulator of the SYP41/SYP61/VTI12 SNARE Complex Involved in Trafficking of Vacuolar Cargo." Plant Physiology**149**(4): 1668-1678.